GLASS GIANTS

Mass-optimized massive cast glass slab

Maria Iro Stefanaki

June, 2020

Student: Maria Iro Stefanaki | 4950402

First mentor: Dr. Faidra Oikonomopoulou
Structural Mechanics and Design

Second mentor: Dr. Serdar Asut
Design Informatics

External Examiner: Ir. Edward Verbree

Abstract

The current thesis aims to explore the potential of producing large-scale structural cast glass elements with the help of 3d printed sand moulds.
Until now, mostly small blocks from structural cast glass have been generated in the building industry, revealing a research gap regarding massive components. Apart from the size, the unlimited shape potentials of cast glass have hardly been explored so far. This is because glass casting can be a very challenging process when it comes to the solidification of the material which needs to be completed under specific program settings. If the glass component contains elements of quite different cross sections, or a very thick element in which the outer layers are annealed much earlier than the inner ones, stress concentrations may appear and a thermal shock can crack the elements due to different temperatures. Except from the brittleness of the body during the annealing process, it can take months, even years for a large-scale element to be completed, because of the full controllable conditions under which the annealing process takes place. In addition, the mould types that are currently used for cast glass components present several restrictions such as the manufacturing costs, the accuracy or the sizing.

For investigating all previous challenges, an existing glass slab in the Acropolis museum, in Athens, was chosen to embody the research goals. The slab is located on top of archeological discoveries making the need for transparency necessary. The current slab consists of float glass panes with a concrete substructure which severely restrains the viewing. The thesis aim is to develop a free-form monolithic slab exclusively from cast glass without the need of external substructure, feasible to be safely produced with the appropriate sand mould.

In order to address the above demands, the topology optimization method was introduced. Several algorithms of topology optimization have been developed. A compliance-based optimization was demonstrated as the most appropriate for the specific project. During this topology optimization process, the algorithm, after dividing the given body into specific segments according to the predetermined mesh size, structurally analyses and validates it.
Afterwards, the algorithm classifies each element as important and non-important, depending on the contribution they have in the stiffness retaining of the entire body. The non-contributing elements are removed, creating voids and producing a lightweight perforated body that according to the previous challenges fits perfectly for the cast glass slab production.

Obtained from the literature framework, the main principles that the design follows gravitate towards the structural, cast glass and manufacturing requirements. The external applied load, in addition to the allowable structural values were calculated. The importance for a flat upper surface, where a safety float glass layer of a permitted deformation should be laminated, was established. Regarding the cast glass demands, it is necessary to acquire a design with smooth surfaces, round edges and uniform distributed material throughout the entire model. For the current project, the optimized slab is decided to mainly consist of borosilicate glass. Last but not least, due to the sand moulds requirements, the model should not contain any elements of less than 4mm. A slab separation is crucial for transportation reasons.

After the definition of the main design principles that the final product should respect, the design development was conducted with the combination of three methods: topology optimization, manual design and structural validation. The final result of the optimized slab successfully fulfills the preset design criteria, as the obtained structure presents 55.2% less mass than the solid version that was initially designed to replace the existing slab in the museum. In addition, a more efficient material distribution in the optimized model renders the slab more compatible for the cast glass annealing process.

The result of the topology optimization technique was a quite complex geometry which is not that effective to be produced in the conventional moulds that are currently available for cast glass applications. Therefore, a new technique needed to be explored, which follows the 3d printing evolution in the building industry. The 3d printed sand moulds are already established for applications of steel and concrete products. However, in terms of glass, apart from the conventional sand moulds that already exist

in the art field, the printed sand moulds have just started gaining enough recognition in the building environment.

The 3d printed sand moulds are recommended to accommodate the fabrication part of this project, since they can produce any customization and irregularity that the optimized slab contains. The main restriction is the limited available sizing that the commercial printers provide. As a solution to this problem, the separation of the large-scale mould into smaller segments was studied, as well as the development of the connecting system of these parts. The entire fabrication technique, from the moulds printing method, to the assembly components and glass melting was investigated.

Finally, the transportation and integration of the slab into the building was explored, concluding with structural solutions that respect the museum and the assembly order that the slab can be attached on it.

Acknowledgments

As this project is finishing, I am realizing that this master program comes to an end. Two intense years, full of experiences, that feels like a lifetime but at the same time as only a couple of months.

For this thesis I would like to firstly thanks my mentors. My first mentor Faidra Oikonomopoulou, was there since the very beginning of this project "bombing" me with her fascinating ideas, her deep knowledge and sharpness, motivated me to dive into the glass world and love it eventually.

I am glad that I had Serdar Asut as my second mentor. He was supporting the whole thesis journey, giving me the freedom that I needed and at the same time highlighting with his constructive feedback the most important aspects.

I would also like to thank Jackson Jewett, whose solid advices, regarding the topology optimization, helped this thesis to move forward.

Special thanks to Ivneet Bhatia and Wilfried Damen, who transferred their valuable findings and experience from their last year similar projects, through their reports and our actual communication.

I would like to thank my parents, Dimitra and Manolis. I wouldn't be here without their support, encourage and their belief on me, even when I lost my self-belief. Also, my sister, Vicky, who is always supportive and proud of her little sister.

Also special thanks to my boyfriend, Vassilis, who was next to me throughout this difficult journey, very supportive and patient in every outbreak. Thank you for reading the whole report!

Finally, I would like to thank my friends, Grammatiki, with whom we were sharing the heavy glass concerns and anxieties, Kiana, Q and Steph for making the hard time of the thesis brighter and sharing our common thesis fears and stress.

Table of contents

1. Introduction

Although glass is one of the oldest artificial building materials, only recently it has gained more attention concerning structural functions, while it finds more and more applications in the building field and generally in industry. This evolution is facilitated due to the development of cast glass and 3d printing techniques which can provide more complex geometries than the 2d floating glass which was dominated until some years ago.

Transparency, durability, compression strength higher than most structural materials and recyclability are just some advantages of glass that architecture could greatly profit from. However, limitations in cast glass still restrict the usage of giant monolithic structural components in architecture and require further research and development in order to extend the boundaries of glass (Oikonomopoulou et al. 2018).

This thesis identifies the problems and restrictions of producing massive structural cast glass components in architecture and studies methods, techniques and examples to solve them through topology optimization. A case-study project of a current glass slab with metal structure will be used to apply these techniques and lead the way to more transparent, total glass monolithic slabs in a more efficient, sustainable and less expensive production.

2. Research Framework

The chapter sets the research framework on which the thesis objective is focused. More specifically, after the demonstrated research gap reveals the problem statement, several research questions arise. Then, the detailed strategy for answering the questions during the entire thesis are set.

2.1. Background: current large-scale applications of cast glass

Although in architecture cast glass is currently making its first steps, in fields like astronomy, nuclear power and art, extensive monolithic cast glass applications are already well established. An overview of such examples could provide reasoned knowledge related to the potentials, the challenges and the solutions of cast glass components of those fields that can be transferred and used in architectural applications.

The greatest cast glass components that exist are the giant telescope mirror blanks, which are used in astronomy. Through many years of several attempts trying to reach very large spans with these multi-ton parabolic-shaped mirrors, engineers managed to produce a giant glass mirror of 8.4 m diameter by using a honeycomb structure. With thinner blank and supportive ribs, these mirrors were stiffer, weighing less and annealed faster and safer without the temperature fluctuations of a solid blank (Oikonomopoulou et al. 2018).
The above massive application of cast glass will be extensively described in Chapter 4.1.5, along with smaller scale applications in architecture because of the great interest that presents from the optimization point of view.

Another more recent application of cast glass is the monolithic lead glass blocks which are used in radiation-shields. These massive pieces weighing several tones consist of glass as the main ingredient and high lead or other similar elements content. Lead glass blocks are mainly used in nuclear and medical field in viewing windows, medical diagnostic rooms and laboratories where the protection from radiation as well as the excellent visual clarity are significant (Corning, 2018).

In the art field, a lot of artists have explored cast glass potentials in their artwork. Some of them have created considerably big and some complex shaped sculptures like projects of Karen La Monte, Roni Horn and David Ruth. Karen La Monte created her human-scale glass sculptures by fragmenting the models into smaller pieces and casting the glass in plaster moulds. (Corning Museum of Glass, 2008) The major monolithic cast glass artwork is the "Pink Tons" by Roni Horn, a solid cube-shaped sculpture weighing 4.5 t. Sizeable internal cracks can be observed in the sculpture, which created probably through a thermal shock during the annealing process (Oikonomopoulou et al. 2018).

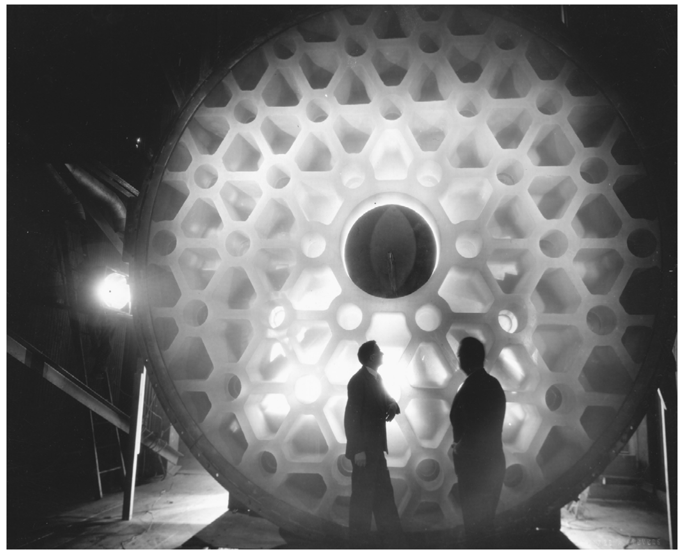

Figure 1: The honeycomb structure in Hale's giant telescope (Corning Museum of Glass, 1999).

Figure 2: The cracked solid artwork of Roni Horn, Pink Ton. Source: https://www.tate.org.uk/

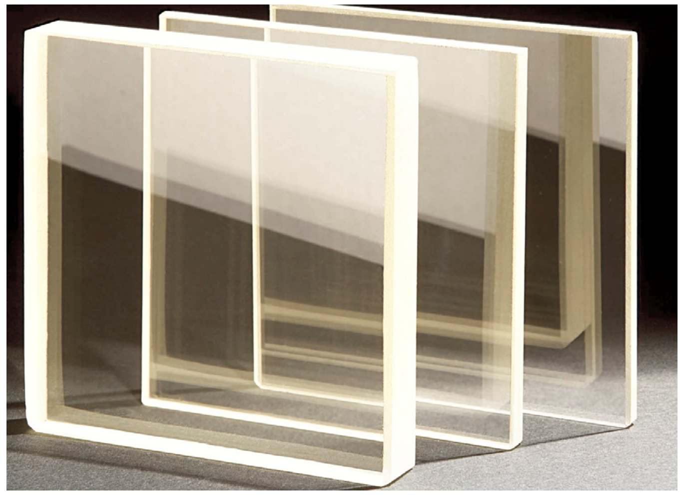

Figure 3: Thick lead glass block for radiation shielding. Source: https://www.corning.com/

2.2. Problem statement

Through a careful observation of the aforementioned massive examples of cast glass, one could deduce some of the main challenges due to which cast glass is rarely used in architecture and even less when it comes to large-scale projects or shapes more complex than a simple block. In case structural properties are required, the undertaking is even harder. A glass component, in order to be structurally sufficient and stiff enough, has to be thicker to address the compressive stress.

The above examples show that one of the biggest problem glass designers and producers have to cope with is the annealing procedure of the massive components. This cooling process, which will be further described in a later chapter, is very critical and time-consuming because cracks can occur during it in case of improper anneal. Very thick solid components make the annealing process harder since the outer layers cool faster than the inner ones having as a result thermal shock of the glass (Oikonomopoulou et al. 2018).

Another problem that arises from the previous applications is the weight of the solid monolithic pieces of glass. Large amounts of glass, especially in cases of structural components, can make a monolithic piece extremely heavy, weighing a lot of tones, which renders transportation and handling very difficult in the building context. Additionally, the quantity of the material that will be used in such case makes the component unsustainable and financially unaffordable.

In terms of manufacturing, the production of large-scale glass pieces with complex shapes had restricted potentials, particularly for the building industry where the cost and time efficiency can be extra limitations rather than in science field. Expensive metal and graphite moulds or inaccurate disposable ones were the most common fabrication techniques for cast glass, although inappropriate methods for massive pieces or intriguing geometries. The potential of a new promising technique using 3d-printed sand moulds needs to be explored in large dimensioned monolithic cast glass component.

The sizing limits, the fragmentation of the ideal full size mould into realistic dimensions, according to the 3d printer and the connectivity of the smaller pieces will be searched in the thesis.

A topology optimization of a massive solid piece could generate a light-weight, self-supported and quicker produced component. In terms of an objective function, through topology optimization, stiffness of the component is preserved while a complex rib-based geometry with reduced volume is created. The rib-based geometry will also help with a uniform mass distribution, which in combination with the voids that will be introduced, it will reduce the annealing time and the dangers of cracks during annealing process.

2.3. Research question

Therefore, the main objective of the thesis is to explore the possibility of reducing the annealing time and the weight of a monolithic structural piece from cast glass through optimizing its topology and investigate the suitable fabrication methods.

The principal question that arises is:

What are the potential and the limitations of using Topology Optimization as a design tool and 3d printed sand moulds as a manufacturing method to produce massive structural cast glass components of reduced annealing time and volume?

While also some research sub questions come of:

- Which is the objective function for a topology optimization (TO) of a cast glass slab?
- Which design constrains derive from casting glass and manufacturing process for a massive cast glass slab?
- How can a monolithic massive cast glass slab be fabricated with 3d sand moulds? How can smaller pieces of moulds be assembled in order to produce one giant piece of cast glass?
- How this optimized glass slab will be integrated into the building? (connections, details etc)

2.4. Relevance

Glass is one of architects favorite material because the transparency that provides can find plenty applications in buildings. Structural designers on the other hand are suspicious regarding the use of glass in load-bearing elements due to the restricted thickness of floating glass which is prone to buckling and the limited size and shape of cast glass elements, important factors for structural components.

Topology optimization of a massive component can reduce the weight, thus size is no longer a constraint. Additionally, the annealing time problem can be overcome if voids are spread throughout the component's body creating elements with uniform thickness.

Therefore, exploring cast glass potentials through computational methods to create a topology optimized product that could be implemented in plenty similar cases leads architecture in a future beyond conservative techniques and points of view. Another goal of this thesis is to reduce the material consumption of such solid glass components which establish a sustainability research, a quiet sensitive issue nowadays.

2.5. Methodology-time planning

The methodology that will be followed until the end of this thesis, as it is described in the flowchart of the following pages, consists of a strategy which focuses on three main phases, the research from the literature, the design development and the fabrication with the detailing part. Throughout the whole journey of completing this thesis, the initial methodology was followed, enlightening the desired path in every step.

To begin with, the first steps of the research and the literature study were conducted in such way that a deeper understanding of the main aspects of the topic could lead to the best determination of the problems and the goal of the thesis, the main core of it.
After searching the current large-scale cast glass applications, the problem statement arose having as a result the forming of the research question and sub-questions.
The next step in order to start the journey of answering that question was consisted of a long period of extended research towards four different directions: the exploration of the case study, the cast glass theory, the topology optimization theory and the research regarding the available moulds.

After the research framework was set and deeply investigated, the design criteria for the TO were established and an initial structural validation led to a size optimization of the slab. Before starting the topology optimization, a shape optimization was conducted by trials of different designs, inspired from the literature and tested with computer simulations.

Regarding the topology optimization, the procedure consisted of a constant rotation among topology optimization in Ansys, manual redesigning and structural validation until obtaining the final result. The iterations were lasting as long as the mesh size could become smaller and give a finer geometry.
After the final geometry was tested in an overall structural behavior, the post processing of the geometry gave a smoother and more uniform final result.

The optimization period was inherited by the fabrication phase, during which the moulds for the entire slab were extensively designed as well as the assembly sequence for the glass casting. The connection of the two slabs was solved and tested along with the detailed drawings for the integration of the slabs in the building. Finally, after summing up all findings and results, the overall conclusions were shaped.

The complete procedure is also illustrated in the time-planning that follows, where one could notice a more detailed description of the thesis tasks and the time period they span throughout the academic calendar.

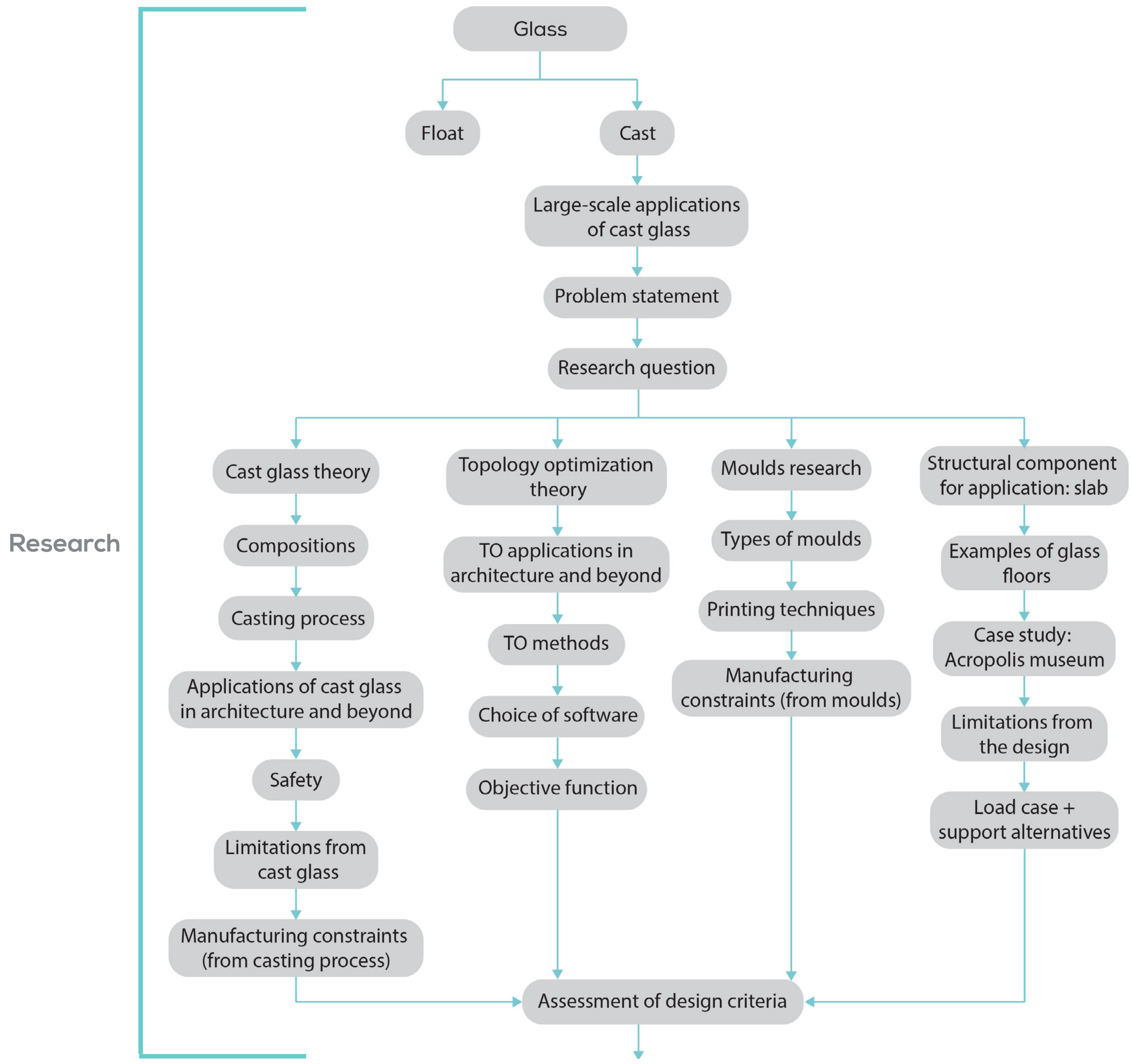

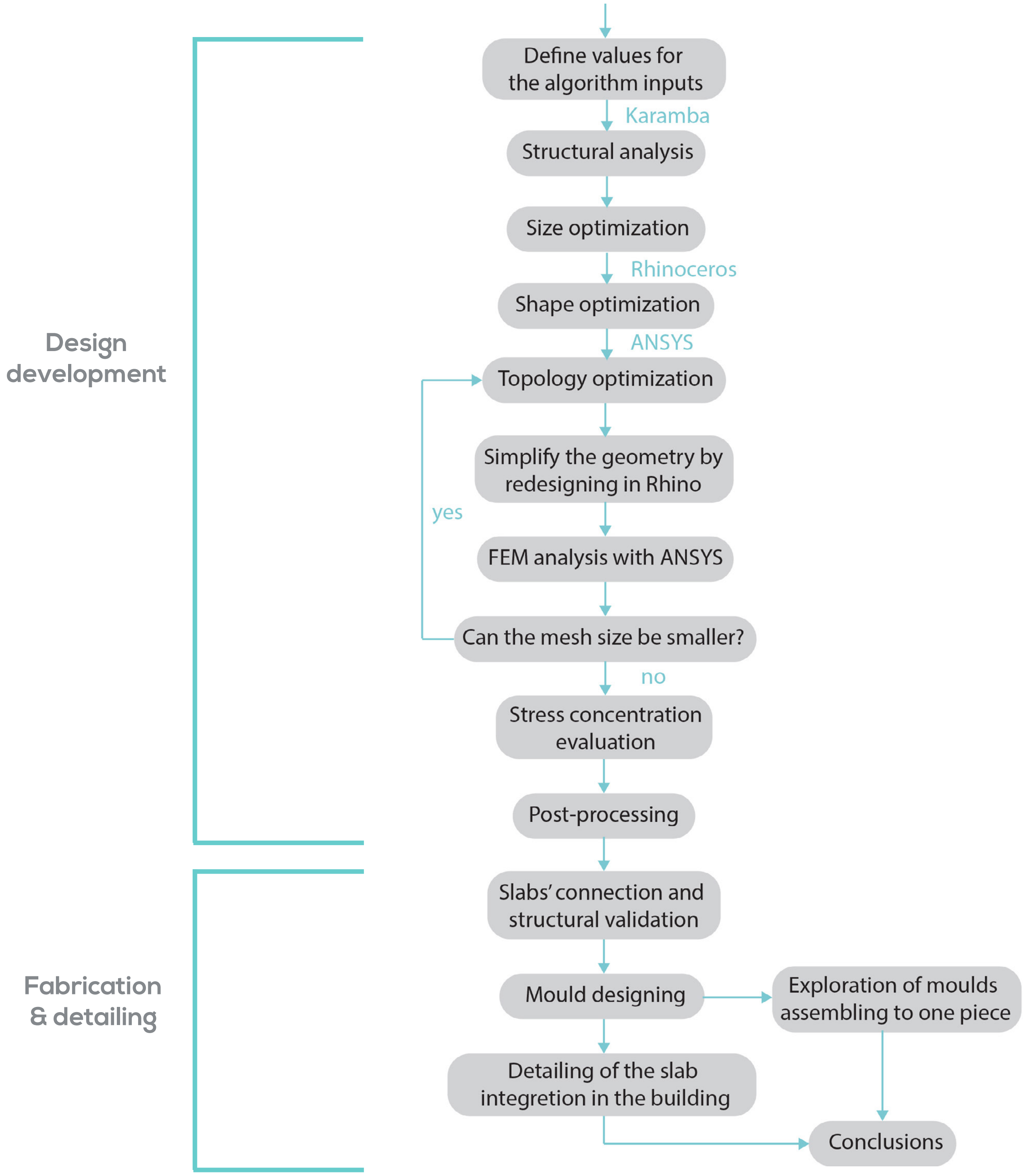

Design development
Define values for the algorithm inputs
Karamba
Structural analysis
Size optimization
Rhinoceros
Shape optimization
ANSYS
Topology optimization
Simplify the geometry by redesigning in Rhino
yes
FEM analysis with ANSYS
Can the mesh size be smaller?
no
Stress concentration evaluation
Post-processing
Fabrication & detailing
Slabs' connection and structural validation
Mould designing
Exploration of moulds assembling to one piece
Detailing of the slab integretion in the building
Conclusions

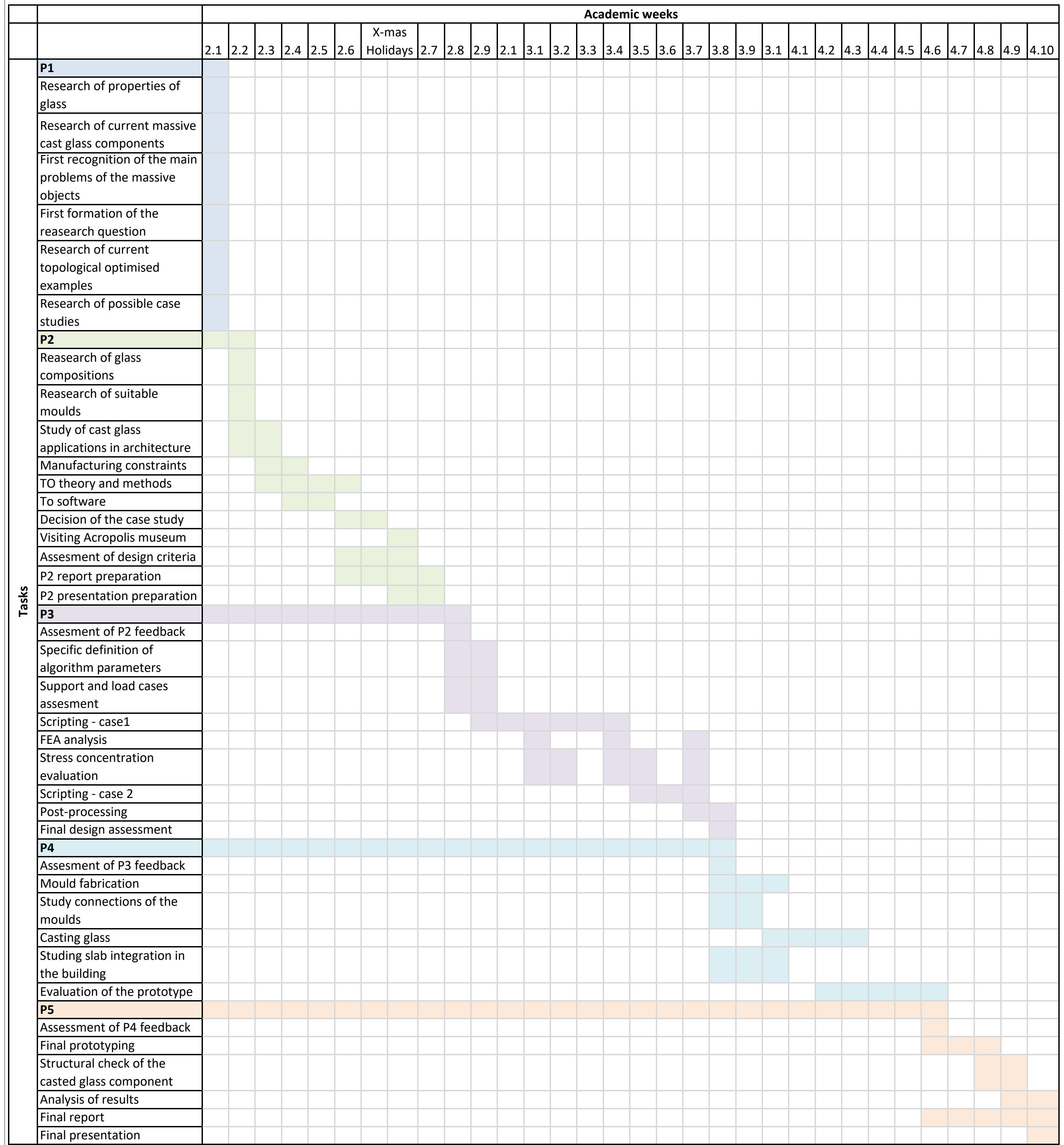

Academic weeks
2.1 2.2 2.3 2.4 2.5 2.6 X-mas Holidays 2.7 2.8 2.9 2.1 3.1 3.2 3.3 3.4 3.5 3.6 3.7 3.8 3.9 3.1 4.1 4.2 4.3 4.4 4.5 4.6 4.7 4.8 4.9 4.10
Tasks
P1
Research of properties of glass
Research of current massive cast glass components
First recognition of the main problems of the massive objects
First formation of the reasearch question
Research of current topological optimised examples
Research of possible case studies
P2
Reasearch of glass compositions
Reasearch of suitable moulds
Study of cast glass applications in architecture
Manufacturing constraints
TO theory and methods
To software
Decision of the case study
Visiting Acropolis museum
Assesment of design criteria
P2 report preparation
P2 presentation preparation
P3
Assesment of P2 feedback
Specific definition of algorithm parameters
Support and load cases assesment
Scripting - case1
FEA analysis
Stress concentration evaluation
Scripting - case 2
Post-processing
Final design assessment
P4
Assesment of P3 feedback
Mould fabrication
Study connections of the moulds
Casting glass
Studing slab integration in the building
Evaluation of the prototype
P5
Assessment of P4 feedback
Final prototyping
Structural check of the casted glass component
Analysis of results
Final report
Final presentation

3. Case study

Slabs are currently one of the main points of focus when it comes to glass structures. The implementation of the research objective will be embodied through a float glass floor in the Acropolis Museum of Athens.

Figure 4: Glass geodesic dome with steel substructure (Wurm, J., 2007).

Figure 5: The great court at the British museum. Foster + Partners (Source: https://divisare.com)

Figure 6: Louvre's pyramid from a glass-steel structure . (Source: Bengtsson A., https://www.flickr.com/)

Regarding the case study on which the thesis will focus, a compressive structure was important to be chosen as a result of the higher compressive strength that glass presents associated with the lower tensile strength. The most appropriate structures which were firstly considered are slabs, arches, domes or beams. Already plenty of glass structures have been realized, with the majority of which employing other materials as steel or concrete as supporting structure, like the structures of the right images.
However, most of them use the 2-dimensional float glass without taking advantage of the shape and size freedom that cast glass offers. Only a few constructions have managed to create self-supported elements completely out of cast glass such as the Crystal House and the Atocha Memorial which are further described in Chapter 4.1.4.

Additionally to the structural properties of glass, the importance of transparency was a determinant factor for choosing the case study of this thesis. In architecture, glass floors are employed quite frequently when significant points of interest cannot be seen. In museums, glass floors are placed on top of archaeological discoveries for extra and panoramic observation. Glass floors can also be encountered in skyscrapers, where the view of a city or sea is highlighted. Architectural concepts in plenty buildings require transparency of the floor such as museums, bridges, very high buildings and more, in order to create a sense of hovering in the users.

However, until now most of these floors are supported by structural steel grid or concrete beams, elements which eliminate and fragment the view. There are also some cases with glass laminated beams supporting the glass floor, providing a fully glass overview but with optical distraction due to connections or the distinction of different elements. Therefore, according to the topic of the thesis the aim is to investigate a monolithic cast glass slab above important sights without additional substructure or connections from other materials in order to provide the observation of entire view avoiding any obstacle.

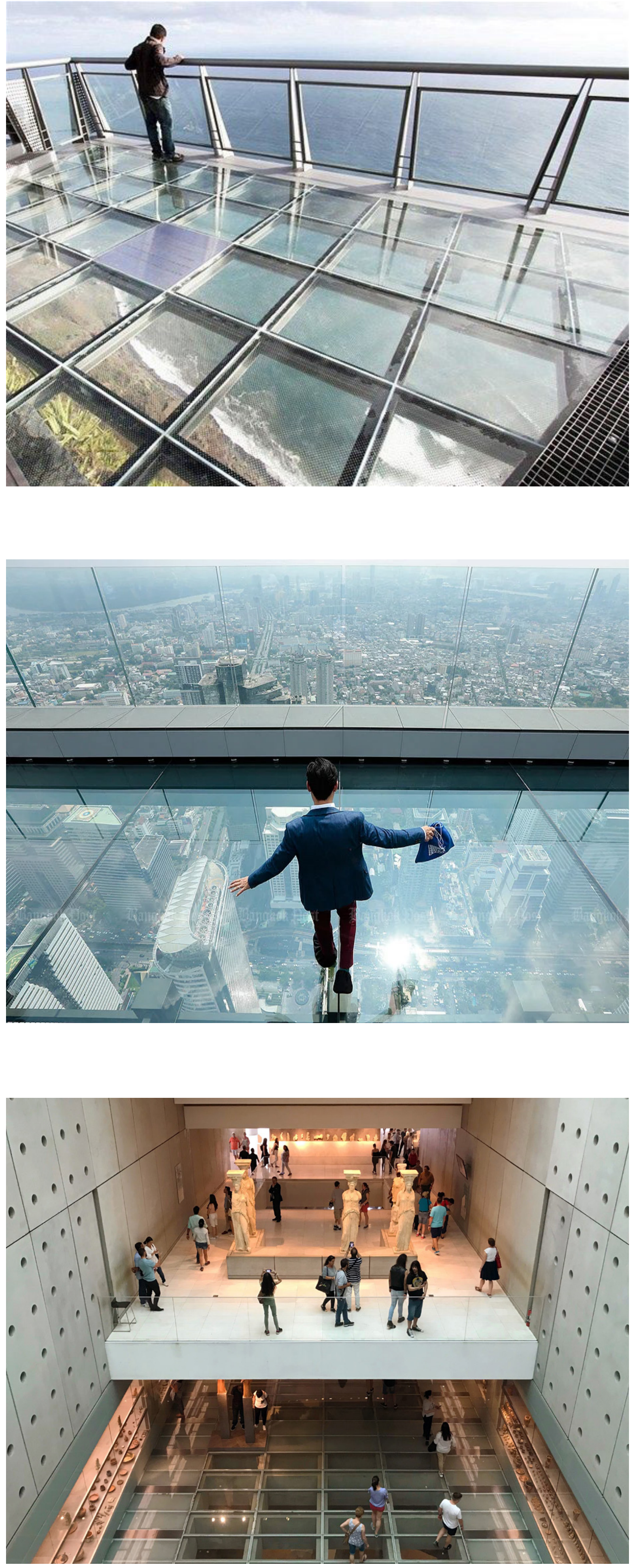

Figure 7: Realized glass floors as possible case studies.

3.1. Examples of glass slabs

Due to the mainly two dimensional nature of the float glass, from which glass slabs currently consist of, an extra substructure is vital in order to prevent the bending of the slender sheets. However, a heavy but stiff enough substructure can cause a considerable deflection of the whole slab. Although there are some existing solutions with lightweight structural systems as mentioned below, a cast glass slab with reduced material due to optimization in the cross section according to the anticipated stresses can be a desired solution.

Steel or concrete substructure

Nowadays most glass floors are realized with steel or concrete substructure supporting several float glass sheets. That way, architects need to compromise the full transparency and restrict viewing as well as their designing freedom in terms of shape potentials or highlighting important points of interest through design.

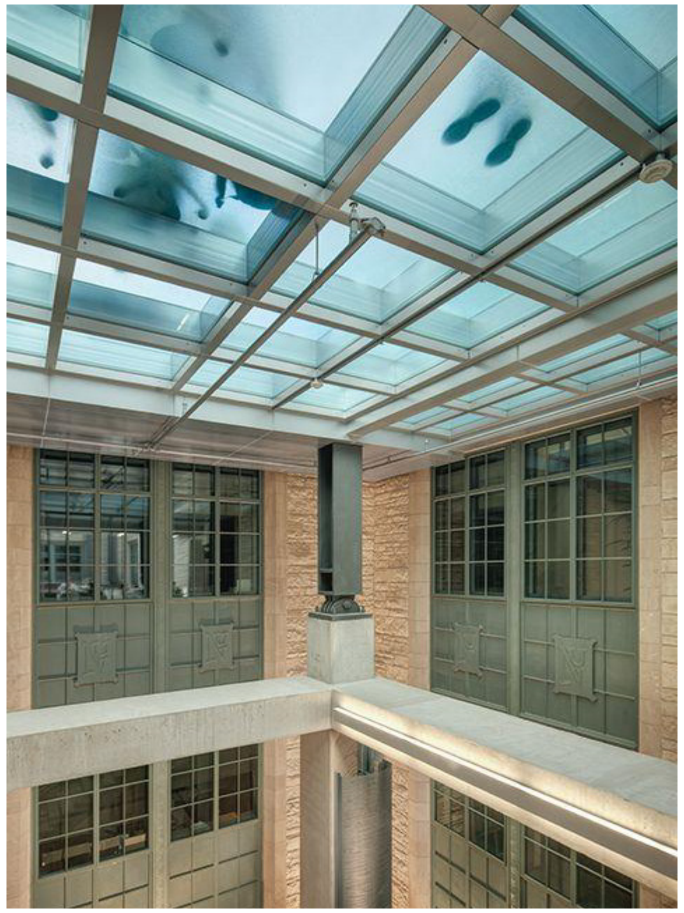

Figure 8: Usual form of glass floor with steel substructure. (Photos courtesy: Technical Glass Products)

Laminated glass beams and fins

Another approach regarding a glass floor, more sensitive to optical clarity, is laminated glass pieces supported by laminated glass beams and fins. A representative example of this category is the glass roof on the refectory of the student residence of the Technical University of Dresden, as Figure 9 shows.

It is a hierarchical load-bearing structure with continuous principal beams spanning 5.75 m maximum distance and consisting of four-leaves laminated panels. Secondary beams are interrupted from the main ones spanning the distance of the insulating glass panels on top, 1.45 m. Principal and secondary beams are both composed of four 12 mm fully tempered and heat soaked glass leaves and PVB 1.5 mm interlayer. The external glass layers serve safety reasons for the inner load-bearing ones. The connection of the two categories of beams is realized with steel node connectors which are adjusted with gasket strips in order the contact of steel and glass surfaces to be avoided (Wurm, J., 2007).

In this case, steel is not possible to be avoided completely while a dense substructure from glass beams is disturbing the architect's intention for transparency and freely handling the allocation of the optical obstacles.

Figure 9: The planar load-bearing structure of the glass roof at the TU Dresden. (Wurm, J., 2007)

Another remarkable example of this category is the completely made of glass Apple Store by EOC Engineers, in New York. The pavilion was first constructed with 105 glass panels, in

2006. However, after request for refurbishment in 2011, the architect Bohlin Cywinski Jackson together with the engineers decided to make use of the new technologies and innovations that had been developed since the previous construction. They managed to reduce the glass panels to 15 and consequently reducing the connections of elements. Also a new connection type, embedded to the laminated elements was introduced (Cruz, 2016).

Figure 10: The fully transparent Apple Cube in New York. (Source: https://www.eocengineers.com/)

Glass sandwich panels

Glass sandwich panels are also a usual solution for glass floors. However, there are examples using materials such as steel or GFRP in order to fill the cavity layer enhancing the stiffness of the component but at the same time sacrificing the transparency.

It has to be clarified that the examples in Figure 11 use on purpose these materials to generate semi-transparent slabs for insulating and sun-shading reasons, without having transparency as an important parameter for the design.

Figure 11: Sandwich glass slabs with GFRP and steel filling (Wurm, J., 2007).

In a thesis of TU Delft, Building Technology track, by Dimitris Vitalis, 2017, a completely transparent sandwich panel was designed located in Athens Acropolis museum.

The aim of the thesis was to replace the substructure of an existing glass floor with a sandwich panel consisting only glass, increasing the transparency and the architectural interest.

The panel consists of two glass panes connected with glass spacers. Several different sizes and shapes of spacers were tested through numerical models, while the distribution of them in the panel surface was studied and derived from parametric design. Seven small- scale models with different types of spacers were constructed and tested through 4-point bending tests.
The final design was an optimized core topology of the sandwich panel regarding the most suitable for the case study structural performance of each configuration and the aesthetical requirements, as presented below.

Later, the object of the thesis was further developed, constructed and tested with Dr. Faidra Oikonomopoulou leading design and development, while Prof. Ir. Rob Nijsse and associate professor Dr. Ir. Fred Veer led the construction stage. In the experiment, a panel consisting of two laminated heat strengthened glass sheets with glass tube spacers was tested. The distribution and the cross section of the tubes were optimized by Arup in a way of spreading the shear forces equally. The full model of 1.5 x 6 m was fabricated with the tubes secured with UV curing glue and tested by 40 students in several load combinations with successful results. After the testing, the panel was displayed at the Glasstec conference in Dusseldorf.

Figure 13: The tested sandwich slab successfully carried the load of 40 students in multiple load cases. (Source: www.bouttudelft.nl/)

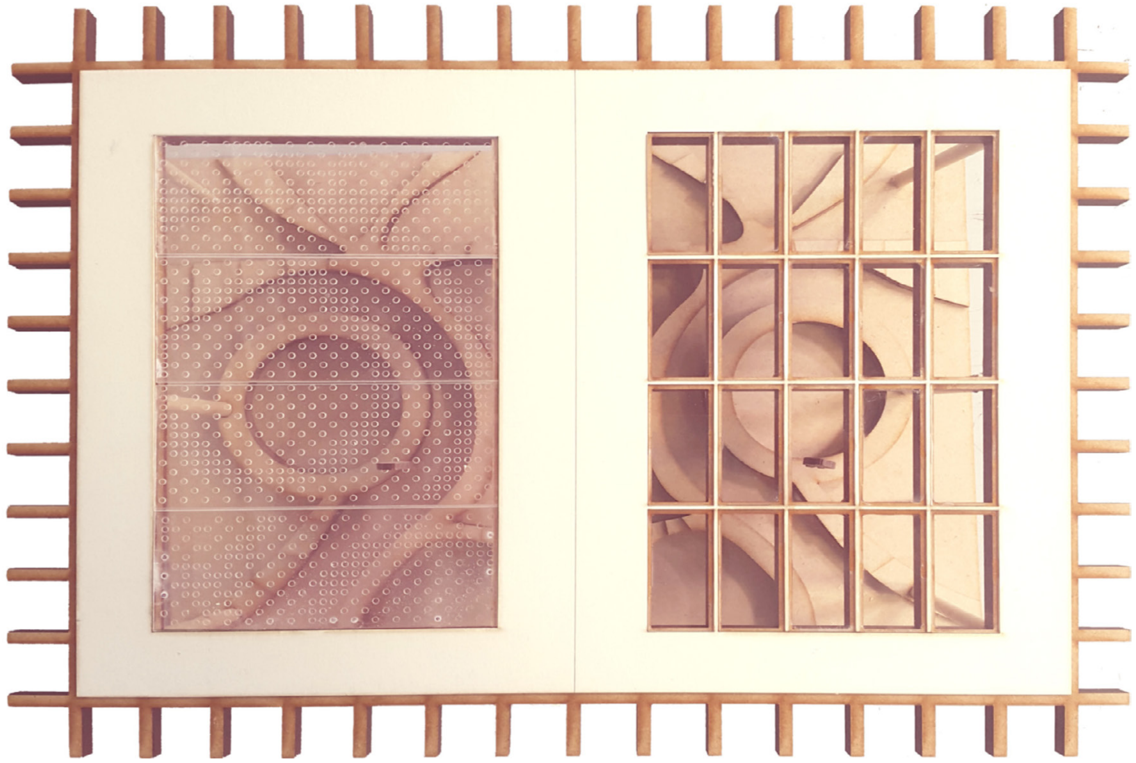

Figure 12: The comparison between the existing glass floor with the steel substructure (right) with the glass sandwich panel of the adapted distribution of the spacers (Vitalis, D., 2017).

3.2. Selection of case study: Acropolis museum

After the above thoughts and research on current glass floor examples, the case of the Acropolis museum arose as a suitable case study for the thesis goals, since it already contains several glass floors.

The building was designed by the Bernard Tschumi Architects. Since the completion of its construction in 2007, it constitutes one of the most important museum buildings in Europe and a significant landmark for the city of Athens.

The museum floats over archeological excavations that were found on site, a fact that strongly influenced the design of the building. Glass floors are integrated in several points of the museum, allowing the visitors to observe the important ancient findings which existed in that area of Athens. In addition, the glass floors enhance the lighting effect into the building.

Nevertheless, these glass slabs consist of float glass sheets with steel frames and are supported by a typical dense grid of concrete beams.

The goal of the thesis regarding the aforementioned case study is to explore the potential of generating a slab exclusively from glass which can increase the optical clarity of the significant sights. At the same time, the proposed slab is aimed at remaining adequately stiff to resist the applied loads while presenting a more light-weight, easy-handling and sustainable structure than the current one.

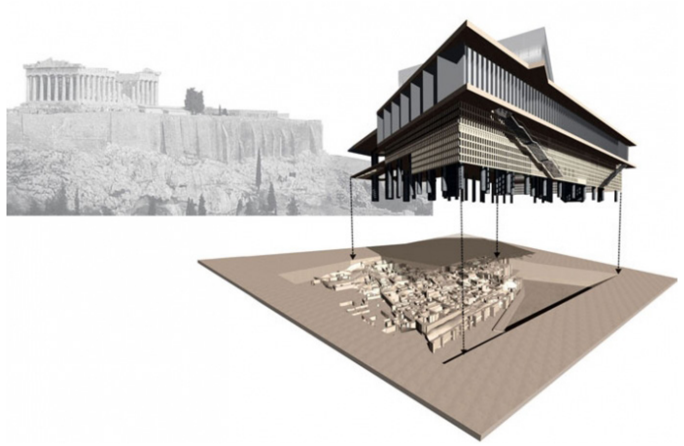

Figure 15: The museum lies on top of important archeological discoveries from ancient Athens. (Source: https://www.yatzer.com)

Figure 14: The main entrance of the museum. (Source: https://www.athensopentour.com)

3.3. Drawings

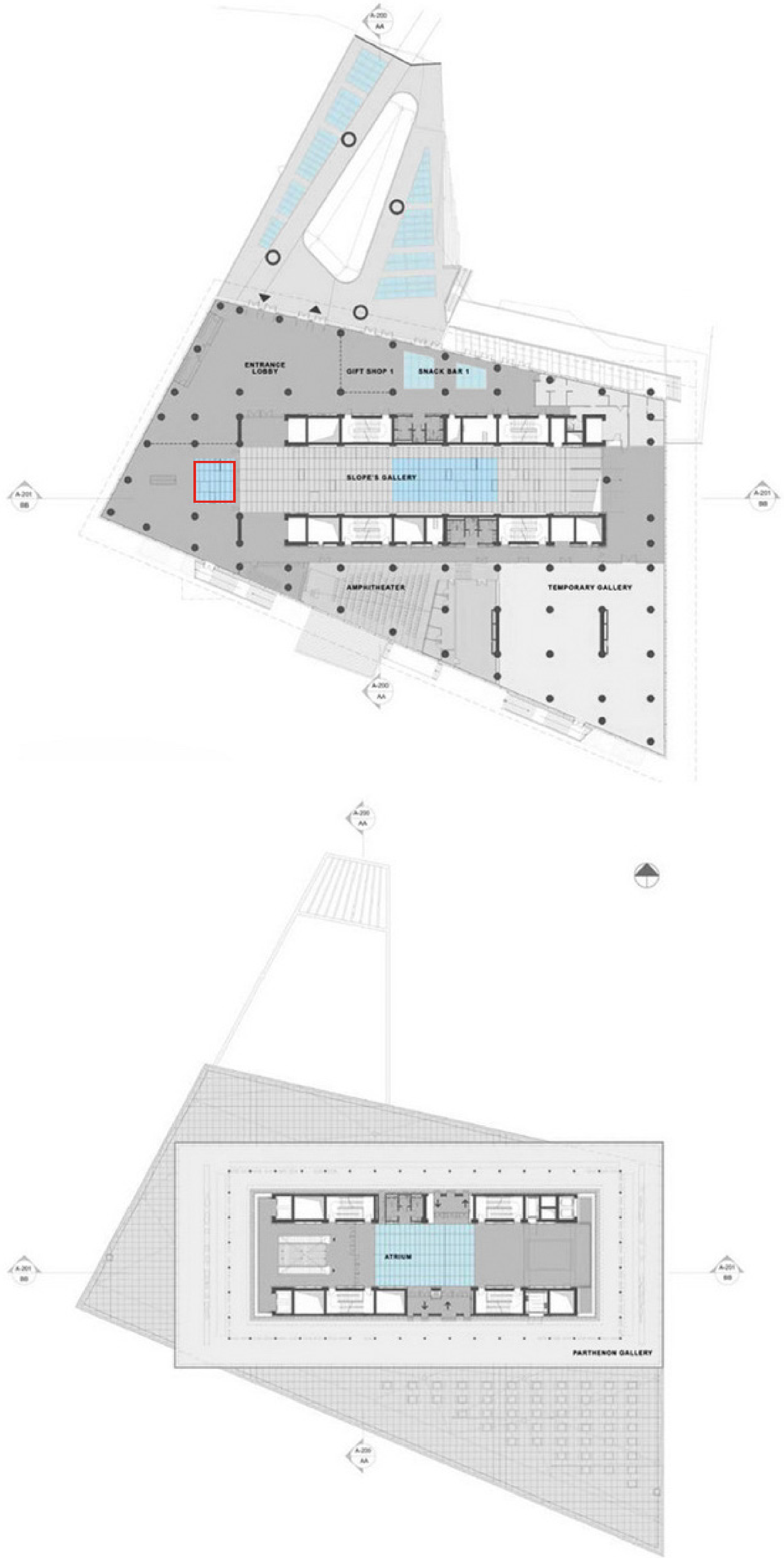

Figure 16: All the glass floors on the building. The chosen slab is highlighted. (Source: https://www.archilovers.com)

As already mentioned, several glass floors exist in the building, aiming to panoramic observation of the archeological discoveries underneath the museum. That is why most of them are located on the ground floor as presented in the floor plans of Figure 16. There is also a great glass floor on the third floor which brings plenty of sunlight into the building.

In the transversal section below (Figure 17) two of the main glass floors above the ancient discoveries can be seen. The left one acts as a bracing for the two columns, among which it is supported. The structural importance of the floor can be demonstrated by the thickness of the concrete beams that support it, 90 cm high.

In the thesis, one of the glass floors is chosen to implement the investigation for the replacement of the steel/concrete supported glass slab with a completely cast glass optimized floor. The right floor which is located in the entrance of the museum was selected as a slab with better structural location. The chosen floor is 7x6.2m and is illustrated in the section and floor plan of Figure 20.

In case of successful results, through the thesis investigation, the attempt can be replicated in the rest glass floors of the museum. That way, the museum could increase the optical clarity of its exhibits and bring more light into the building, through a more architecturally interesting and environmentally friendly construction.

Figure 18: The glass floor which lies on top of the caryatids from an underneath view. The concrete beams are so thick that one cannot recognize the glass slab from a lateral view. (Source: https://www.thisisathens.org/)

Figure 19: One of the glass floors allowing a restricted view towards the archeological excavations. (Source: https://www.yatzer.com)

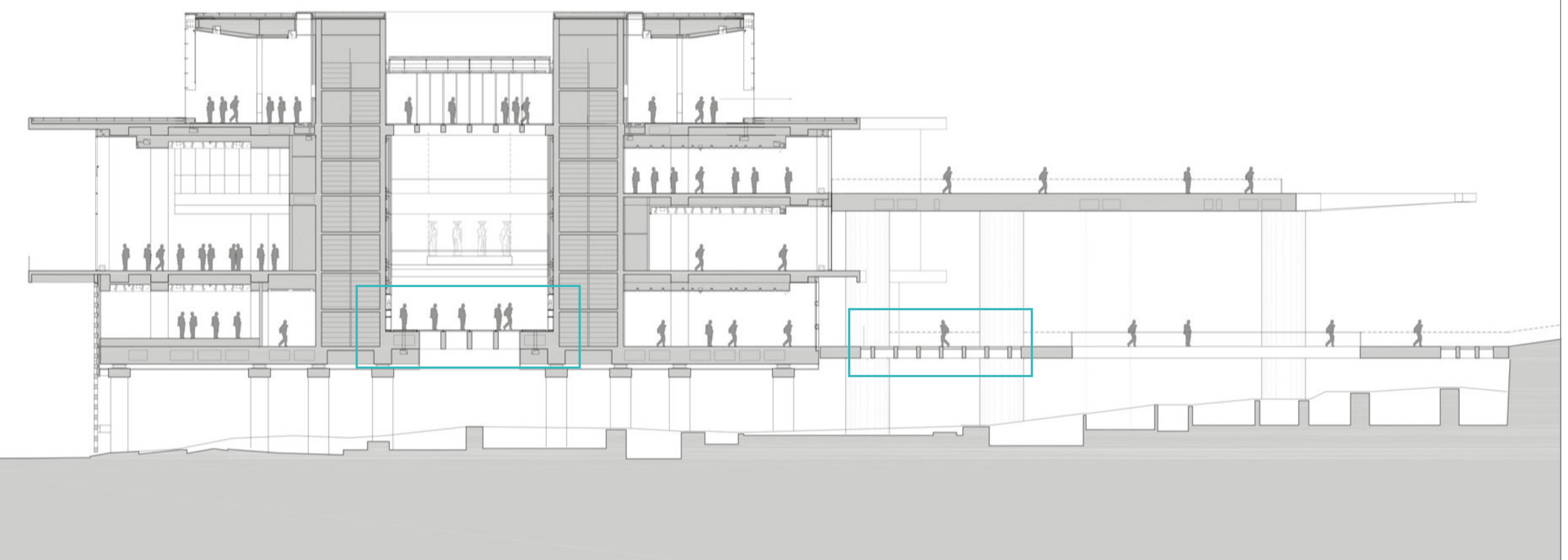

Figure 17: Section of the museum in which two of the glass floors are illustrated. Source: municipality of Athens obtained from Vitalis, D, 2017.

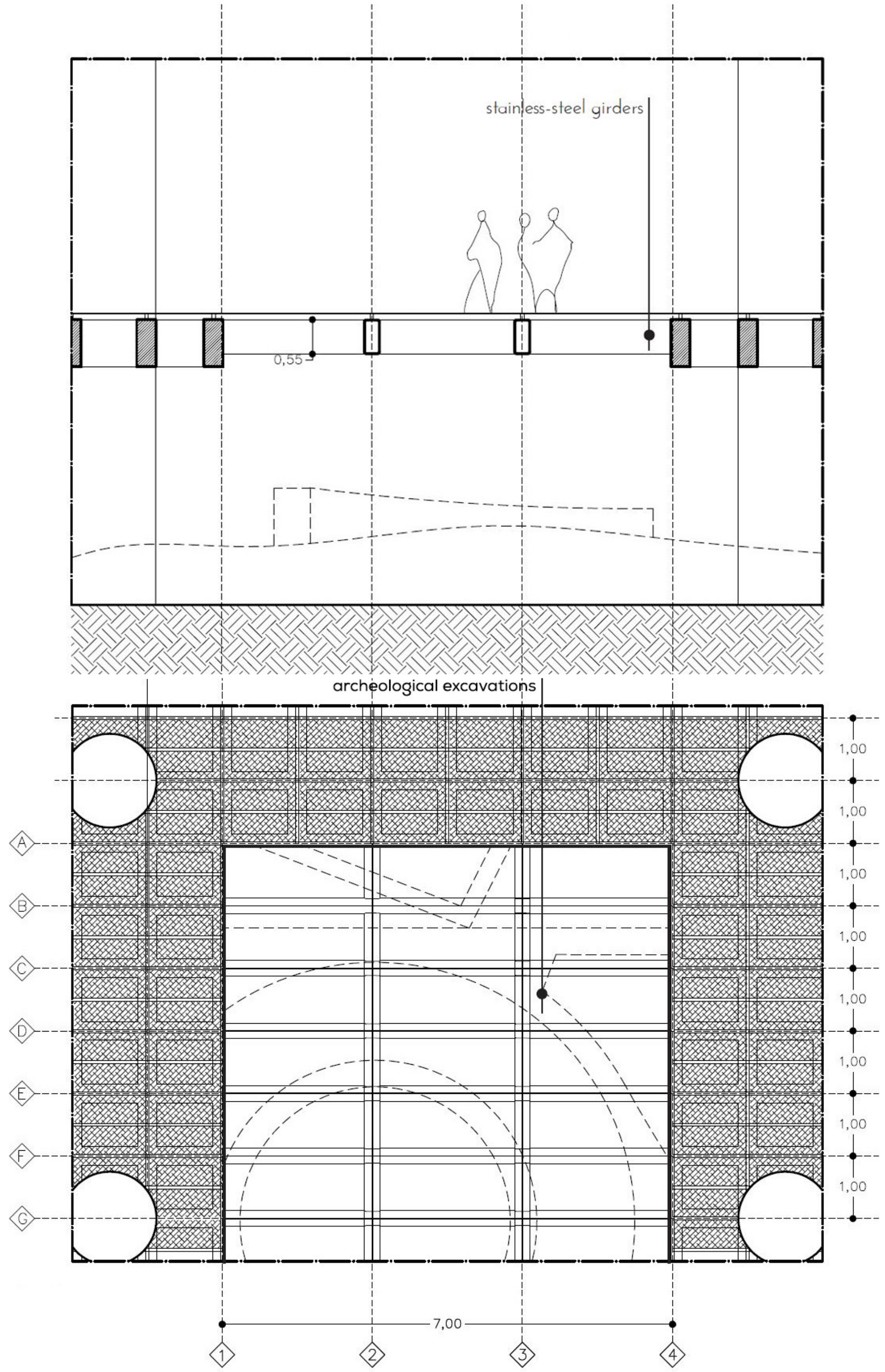

Figure 20: The section and the floor plan of the selected glass slab (Vitalis, D, 2017).

3.4. Load case - boundary conditions

As it is derived from the literature, in similar optimized planar components, two load combinations should be tested in order to demonstrate the stiffness adequacy. One will consist of dead load in addition with a distributed live load and in the other the dead load will be combined with live load in one side for an asymmetrical case.

However, during the form finding part only the first combination of the distributed load together with a safety factor will be considered in order to have a uniform result in terms of geometry. After finding the optimized topology for the form of the slab, several structural analyses should run in order to check if the slab can resist asymmetrical live load. Following the FEA analysis an amplification of some critical elements with extra material might be necessary (Liew et al. 2017).

Since the tested element is a slab, deflection is the primary structural property that should remain unharmed during the optimization. Therefore, stress concentrations will be checked as a secondary parameter but ULS or SLS will not be tested.

Regarding the support conditions during the optimization, multiple cases with different kind and location of supports should be tested. In case of designing a shallow vault on the bottom of the slab to reduce the tensile stresses of the element, the supports should be placed on the corners and fix the arching bottom preventing horizontal thrusts. Therefore, the sufficient stiffness will be developed and internal compression stresses will be activated (Liew et al. 2017).

From Eurocode 1, the slab is classified in C3 category regarding the live load that has to accommodate, which refers to buildings with moving crowds such as museums and exhibition rooms. Although Vitalis, 2017, had considered the same slab to the C5 category due to the standing people for sightseeing, it is an over-estimation since the slab is in the entrance of the main room and the crowds will not stand on top for more than few minutes each.

For the simulations, the worst case scenario of 5 kN/m2 was considered, while a safety factor γ_M=1.5 was included in th calculations. Thus:

$$L=7.5kN/m^2$$

Table 6.1 – Categories of use

Category	Specific use	Example
A	Areas for domestic and residential activities	Rooms in residential buildings and houses; bedrooms and wards in hospitals; bedrooms in hotels and hostels kitchens and toilets.
B	Office areas	
C	Areas where people may congregate (with the exception of areas defined under category A, B and D [1)])	**C1**: Areas with tables, etc e.g. areas in schools, cafes, restaurants, dining halls, reading rooms, receptions **C2**: Areas with fixed seats, e.g. areas in churches, theatres or cinemas, conference rooms, lecture halls, assembly halls, waiting rooms, railway waiting rooms. **C3**: Areas without obstacles for moving people, e.g. areas in museums, exhibition rooms, etc. and access areas in public and administration buildings, hotels, hospitals, railway station forecourts **C4**:Areas with possible physical activities, e.g. dance halls, gymnastic rooms, stages . **C5**:Areas susceptible to large crowds, e.g. in buildings for public events like concert halls, sports halls including stands, terraces and access areas and railway platforms.
D	Shopping areas	**D1**: Areas in general retail shops **D2**: Areas in department stores.

[1)] Attention is drawn to 6.3.1.1(2), in particular for C4 and C5. See EN 1990 when dynamic effects need to be considered. For Category E, see Table 6.3

NOTE 1. Depending on their anticipated uses, areas likely to be categorised as C2, C3, C4 may be categorised as C5 by decision of the client and/or National annex.

Table 6.2 – Imposed loads on floors, balconies and stairs in buildings

Categories of loaded areas	q_k [kN/m^2]	Q_k [kN]
Category A		
- Floors	1,5 to 2,0	2,0 to 3,0
- Stairs	2,0 to 4,0	2,0 to 4,0
- Balconies	2,5 to 4,0	2,0 to 3,0
Category B	2,0 to 3,0	1, 5 to 4,5
Category C		
- C1	2,0 to 3,0	3,0 to 4,0
- C2	3,0 to 4,0	2,5 to 7,0 (4,0)
- C3	3,0 to 5,0	4,0 to 7,0
- C4	4,5 to 5,0	3,5 to 7,0
- C5	5,0 to 7,5	3,5 to 4,5
Category D		
-D1	4,0 to 5,0	3,5 to 7,0 (4,0)
-D2	4,0 to 5,0	3,5 to 7,0

NOTE: Where a range is given in this table, the value may be set by the National annex. The recommended values, intended for separate application, are underlined. q_k is intended for the determination of general effects and Q_k for local effects. The National annex may define different conditions of use of this Table.

Figure 21: Eurocode 1: Imposed loads on floors. (Source: https://eurocodes.jrc.ec.europa.eu)

3.5. Limitations from the design

One of the main structural properties of glass is the by far different behavior of the material against compression and tension. The compressive strength is to a great extent higher than the tensile one.

According to the literature review, a usual technique of reducing the tensile stresses of a planar slab is to introduce an arched surface on the bottom side of the element. In that technique ribs or diaphragms transmit the loads to the vault and then to the supports, while stiffening the structure (Liew et al. 2017).

The possibility of adopting that technique in this project or not will be examined during the design development.

Regarding the topside of the slab, it is significant to be planar and voids should be avoided in order to provide a pleasant and safe walk on it. These parameters should be included in the optimization process.

Depending on the size of the slab and the structural simulations that will be run, the generation of a fragmented or monolithic slab should be considered from transportation and manufacturing point of view.

Finally, another problem that could be encountered through the thesis is the reflection that one could detect in the glass floors of the building. Due to the natural and technical lighting of the museum, the reflection of them into the glass makes the observation of the discovered sight even harder.

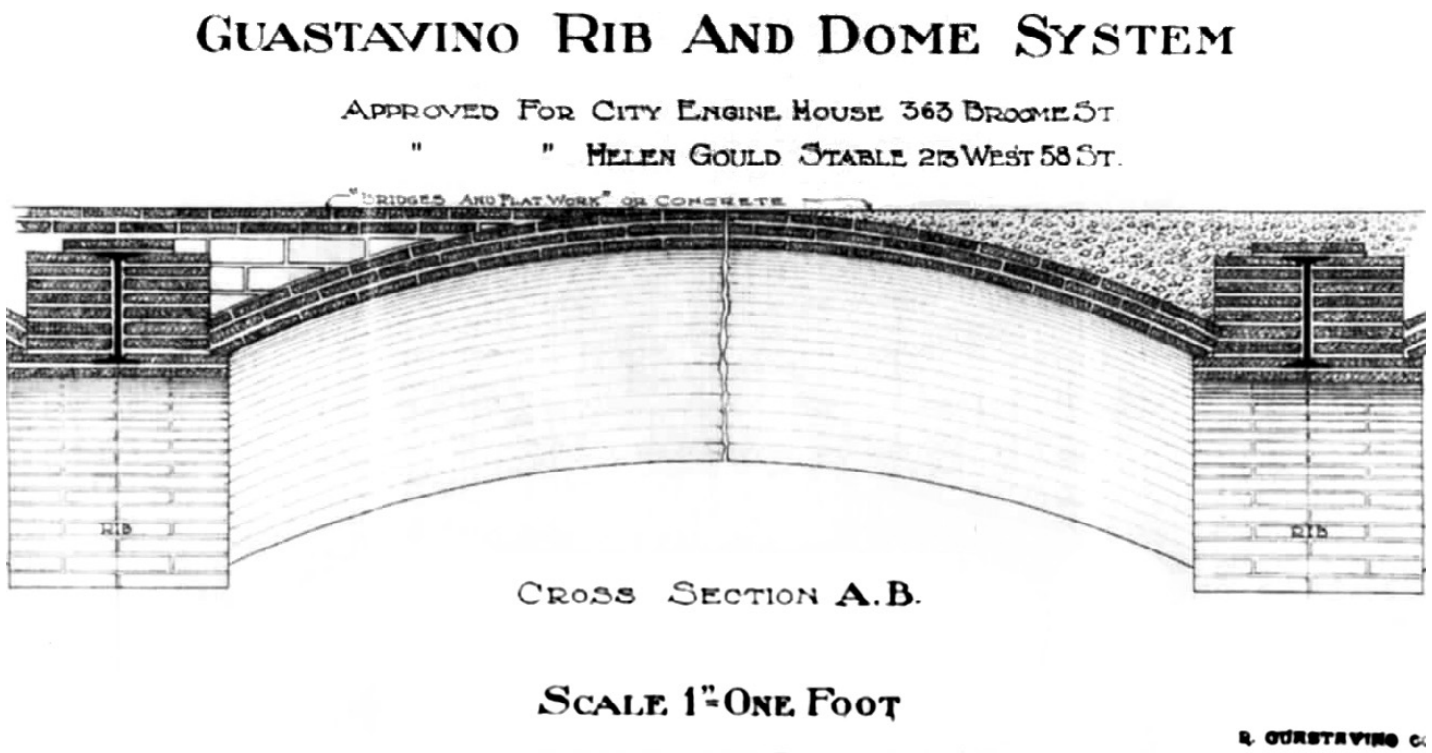

Figure 22: Guastavino rib and dome system, New York, 1902 (Liew et al. 2017).

4. Literature study

In this chapter, the theoretical foundation of the three main pillars, cast glass theory, fabrication research-moulds and topology optimization theory, will be established.

4.1. Cast glass theory

Transparency and brittleness are the most well-known properties of glass and the first thoughts of someone regarding that material. The majority of glass applications are defined by the above properties.
However, glass is way more than that. It is actually a strong material, the structural performance of which is only recently further explored (Oikonomopoulou, F., 2019).

4.1.1. Properties of glass

Starting clearly as a façade element, which was the main use of glass until the last decades, nowadays it tends to be compared with giants of construction, like steel and concrete.
Although glass was considered as a brittle material, passing from the 2-dimensional floating glass to 3d cast glass led brittleness to an obsolete statement.

The table in next page shows the most important mechanical and thermal properties of soda-lime glass and compares them with the respective ones of steel, softwood and concrete. The great compression strength can overtake concrete's corresponding value and in some occasions even steel's. Thus, it is demonstrated why glass is a good solution as a load-bearing material in compression structures.

While glass passes from liquid form to solid, a microstructure with many microscopic flaws and irregularities is generated, aborting the desired compact form. When tensile stresses act on these grooves, stress concentrations will appear in the crack root and will propagate it after the maximum stress exceeds a critical value. The crack spreads remarkably fast from one edge to another (Wurm, J., 2007).

Currently, the actual strength of solid cast glass components for structural applications cannot be precisely determined. According to the assumption that the highest the volume of the cast glass object, the higher amount of randomly distributed flaws, the bending strength of a massive cast glass element is expected to be comparable but scarcely lower than the respective strength of float glass (Oikonomopoulou et al. 2018).

Therefore, extra attention should be paid on the safety precautions for a giant cast glass piece as the object of this thesis.

In terms of sustainability, glass is a recyclable material when it is pured from extra adhesives and other materials that cannot be separated and can be recycled endlessly without losing its quality (Nijsse, R., 2003). It is also a non-corrodible material, thus it requires less or no maintenance cost.

	Steel S 235	Softwood S 10	Concrete C20/25	Glass Soda-lime glass
Density ρ [kN/m³]	78.5	6	22	25
Modulus of elasticity E [kN/cm²]	21000	1100	2900	7000 (like aluminum)
Tensile strength $f_{t,k}$ [MPa]	240 (yield strength)	14	2.2	45
Elongation at break ε [%]	25	0.7	-	0.006-0.17
Compressive strength $f_{c,k}$ [MPa]	235	II 17-26 ⊥ 4-6	20	approx. 500
Limiting tensile stress σ_{Rd}	21.8	0.9	(~0.1)	1.2/1.8
Safety factor γ	γ_M = 1.1	γ_M = 1.3	1.8	2.5
Breaking length σ/ρ [m]	2800	1500	(45)	480/720
Thermal conductivity [W/m*K]	75	II 0.5 ⊥ 0.2	1.6	1
Thermal shock resistance ΔT [1/K]	-	-	-	40
Coefficient of thermal expansion α_T [1/K]	$12 * 10^{-6}$	II $5 * 10^{-6}$ ⊥ $35 * 10^{-6}$	$10 * 10^{-6}$	$9 * 10^{-6}$ 60 K ≈0.5 mm

Table 1: A comparison between several thermal and mechanical properties of soda lime glass and other structural materials (Wurm, J., 2007).

4.1.2. Compositions

The most important types of glasses depending on the compositions of them and the elements that are consisted of are six.
In the table below, the six families of glass are shown as well as the respective compositions, most usual applications and main observations regarding their chemical and mechanical behavior.

Glass type	Approximate composition	Observations	Typical applications
Soda-lime (window glass)	73% SiO_2 17% Na_2O 5% CaO 4% MgO 1% Al_2O_3	_Durable. _Least expensive type of glass. _Poor thermal resistance. _Unacceptable resistance to strong alkalis.	Window panes Bottles Façade glass
Borosilicate	80% SiO_2 13% B_2O_3 4% Na_2O 2.3% Al_2O_3 0.1% K_2O	_Good thermal shock and chemical resistance. _More expensive than soda-lime and lead glass.	Laboratory glassware Household ovenware Lightbulbs Large telescope mirrors
Lead silicate	63% SiO_2 21% PbO 7.6% Na_2O 6% K_2O 0.3% CaO 0.2% MgO 0.2% B_2O_3 0.6% Al_2O_3	_Second least expensive type of glass. _Softer glass compared to other types. _Easy to coldwork. _Poor thermal properties. _Good electrical insulating properties.	Artistic ware Neon-sign tubes Na2O Television screens Absorption of Xrays (when PbO % is high)
Aluminosilicate	57% SiO_2 20.5% Al_2O_3 12% MgO 1% Na_2O 5.5% CaO	_Very good thermal shock and chemical resistance. _High manufacturing cost.	Mobile phone screens fiber glass High temperature thermometers Combustion tubes
Fused-silica	99.5% SiO_2	_Highest thermal shock and chemical resistance. _Comparatively high melting point. _Difficult to work with. _High production cost.	Outer windows on space vehicles Astronomical telescopes
96% silica	96% SiO_2 3% B_2O_3	_Very good thermal shock and chemical resistance. _Meticulous manufacturing process and high production cost.	Furnace sight glasses outer windows on space vehicles

Table 2: The most common glass types which its chemical compositions, properties and typical applications (Oikonomopoulou et al. 2018).

Due to their better performance under lower melting temperatures and the reduced manufacturing costs, soda-lime and borosilicate glass are the most preferable types for cast glass applications in structures (Oikonomopoulou, F., 2019).

However, soda-lime glass presents a higher thermal expansion coefficient which has as a result the annealing process and thus the manufacturing time to last longer than components from borosilicate glass. A comparison between the annealing times of the bigger brick from borosilicate glass used in the Atocha Memorial and of the smaller Crystal Houses soda-lime brick demonstrates the above state (Oikonomopoulou et al. 2017).

Therefore, borosilicate glass seems to be appropriate for the requirements of an optimized cast glass slab, since it presents an adequate thermal shock performance and it is affordable. Borosilicate's low thermal expansion coefficient leads to less annealing time which is crucial for such a large-scale element.

Additionally, it does not present difficulties or high cost on fabrication and manufacturing, important factor since the fabrication of a topology optimized component can generate quite complex geometries. This type of glass has already been used in large-scale products which demonstrates it as the most suitable glass for the massive slab that will be investigated.

	Atocha Memorial	Crystal Houses
Type of glass	borosilicate	soda-lime
Dimensions	70x200x300 mm	65x210x210 mm
Weight	8.4 kg	7.2 kg
Thermal expansion coefficient	$3.2–4x10^{-6}/K$	$9.1–9.5x10^{-6}/K$
Annealing time	**20 h**	**36–38 h**
Mould type	high precision press mould	high precision open mould

Table 3: A comparison between features of two different cast glass bricks affecting the manufacturing time (Goppert, K, et al, 2008 and Oikonomopoulou et al. 2017).

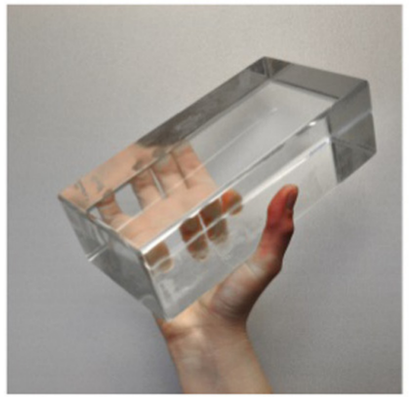

Figure 23: Left: Cast glass block used in Atocha Memorial. Right: Cast glass brick employed in the Crystal Houses (Oikonomopoulou et al. 2018).

4.1.3. Casting process-Annealing procedure

Cast glass production differs by far from float glass panes. There are two kind of casting glass methods, a primary **(melt-quenching)** and a secondary process **(kiln-casting)**. The main difference can be found in the initial form of glass before casting. During the primary casting, glass is in a hot fully liquid state directly derived from its raw ingredients, while in the secondary one, glass is already consisted of solid pieces like sheets, grains etc, has to be re-heated and then it can flow and shaped according to the mould. Therefore, the temperatures that are obtained in the secondary process are lower than the primary one (Oikonomopoulou et al. 2018).

Another critical difference between the two casting techniques is the required equipment for each one. During the secondary casting, since the temperatures are lower, only one kiln is involved for the melting of the glass pieces into the moulds and the later stage of annealing process. However, in the primary casting, the glass is firstly formed from its ingredients under very high temperatures in one furnace, where is also poured into the mould and then it is transferred to another furnace to anneal (Oikonomopoulou et al. 2018).

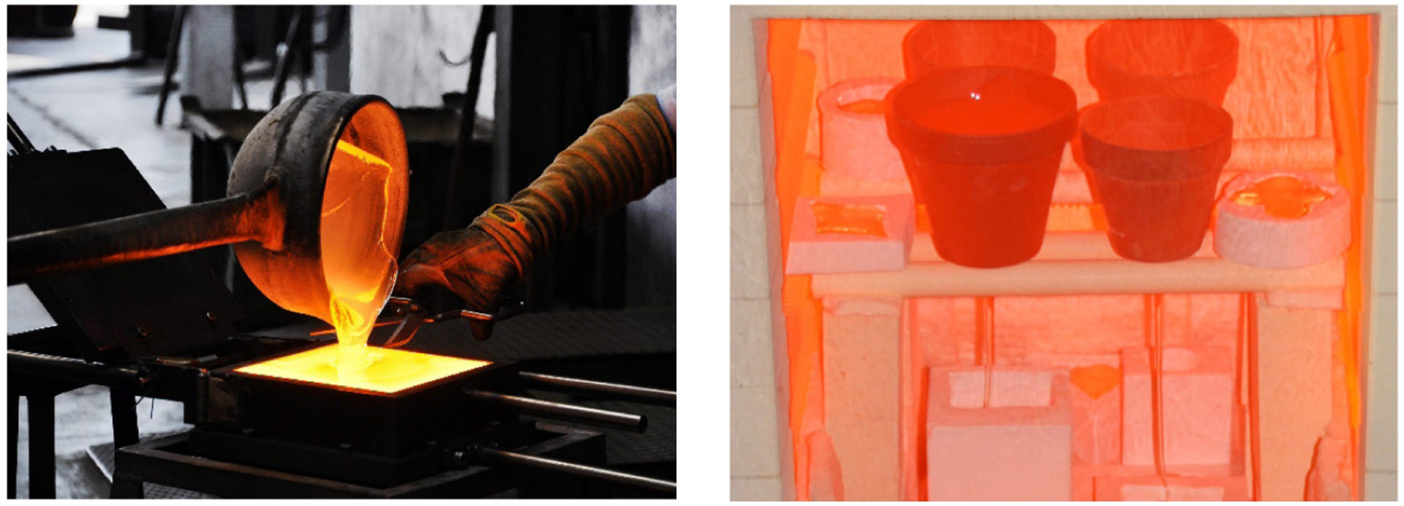

Figure 24: Illustration of the primary (left) and secondary (right) casting method of glass (Oikonomopoulou et al. 2018).

For the production of a cast glass element five main phases are necessary. In each of them, the duration and the temperature change vary. All the critical temperature points during the annealing process are illustrated in the representative for ideal conditions graph of Figure 25.

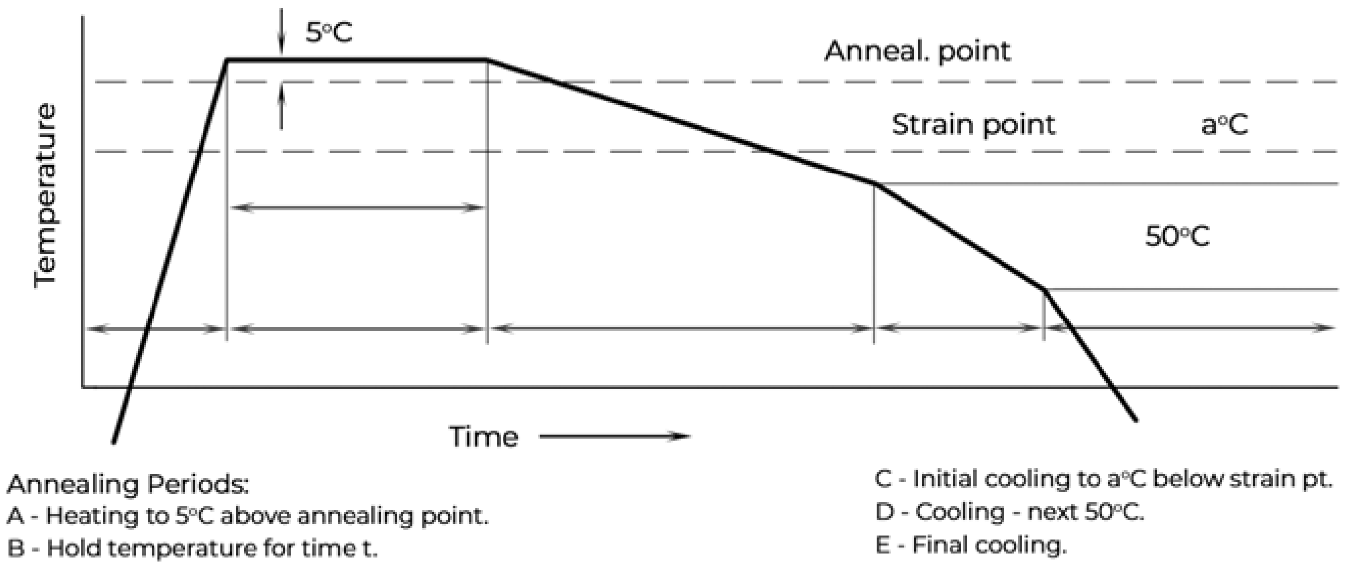

Figure 25: Diagram describing the commercial annealing - ordinary ware of a glass component under ideal conditions (Shand and Armistead, 1958).

The common point of both casting procedures is the annealing process. Three main stages can be highlighted during the annealing of the casted glass after the mould is filled. First is the softening point, under which the glass temperature is rapidly cooled down for a few degrees. The rapid cooling aims to cancel crystal molecular arrangement of melting and due to the lower viscosity any induced thermal stress can be relaxed. Under the softening point, glass is able now to retain its shape without deforming due to its weight. The next important stage is close to the strain point while possible strains are eliminated and internal stresses are prevented if the rate of cooling is adequately slow. When the temperature falls lower than the strain point any existing stresses can be considered permanent. The final drop of temperature can be realized a bit faster but still low enough to prevent thermal shocks (Oikonomopoulou et al. 2018).

Although the required heat transfer for the annealing process can be theoretically calculated, for large-scale components it has to be practically determined, since it depends on plenty of factors such as shape, size, geometry, mass distribution and even furnace features.

4.1.4. Current applications of cast glass in architecture and beyond

Some important applications of cast glass of large-scales in other industries or with smaller components in architecture will be analyzed further in this chapter.

Telescope mirrors

Astronomers started using ground reflecting telescopes with metal mirrors since 17th century but since metal reached its limits soon, they were replaced by glass mirrors, trying to enlarge them as much as they could (Corning Museum of Glass, 1999).
Until mid 1930's, telescope mirrors were produced as solid components. After managing only 2.5 m of spanning with solid blanks and annealing time of 12 months, engineers tried an optimized geometry for the blank. In 1936, in Mt. Palomar Observatory a 5m glass blank with honeycomb geometry was released by Corning for the Hale telescope. It was double the size of the larger solid blank, however, the annealing time was 2 months less than that.
The new blank, which consisted of Pyrex glass allowing less expansion and contraction of the mirror, so less distortion, was adequate stiff due to the rib structure that was created around the hexagonal cores.

Using the same optimized structure, Corning was able to produce the same 2.4m blank in only 3 months with an 80% weight reduction. However, a time-consuming post-processing period was demanded in order desired accuracy to be obtained (Oikonomopoulou et al. 2018).

In a later stage, spin-casting, a new technique to produce giant monolithic telescope mirrors was introduced. In the Giant Magellan Telescope the seven blanks using the spin-casting method combined with the honeycomb structure are the biggest monolithic cast glass components nowadays. Their diameter reach the 8.4m each, while through the spinning technique during which the glass is casted in a mould placed in a rotating furnace, the annealing time is reduced in 3 months as well as the weight. These blanks consist of E6 borosilicate glass by Ohara, which proved to expand and contract less as its low thermal expansion coefficient verifies, requires lower temperatures to melt, flows easier and it is more affordable comparing to Pyrex (Oikonomopoulou et al. 2018).

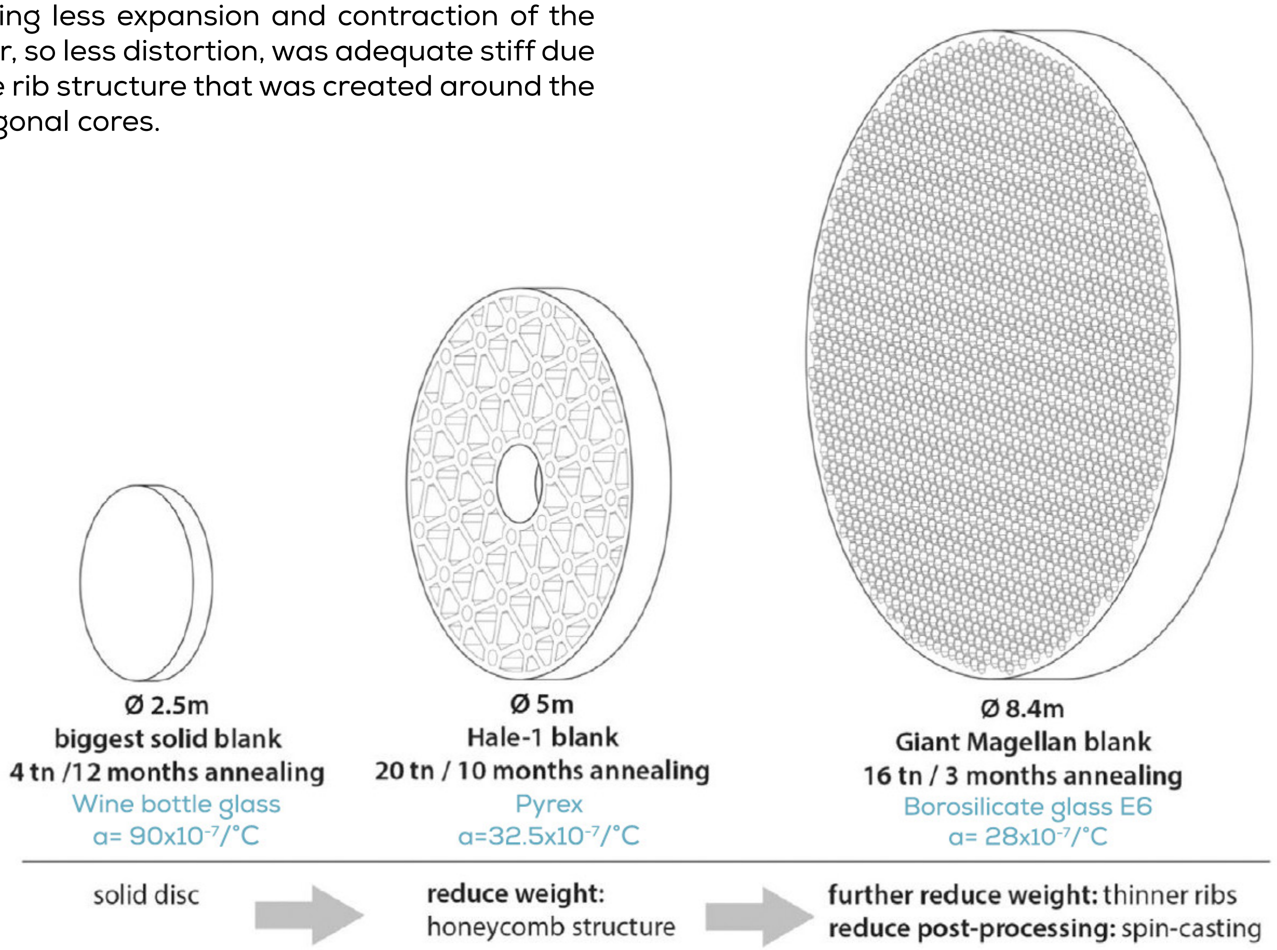

Figure 26: Cast glass telescope mirrors' evolution (Oikonomopoulou, F., et al. 2018).

Art field

Regarding the art field, Roni Horn's massive solid glass blocks, which is described in Chapter 2.1, is not the only large scale solid artwork from cast glass in moulds.

Another considerable more precision demanding relevant piece of art is the block on the Denis Altar, in France, designed by the artist Vladimir Zbynovsky and fabricated by Corning Specialty Glass. It is an element from Corning 7056 optical glass of around 1.4 t and dimensions 1.42x1.42x0.28m, as illustrated in Figure 27.

The real challenge of the project was the perfect fitting of the glass casted element with the surface of the underneath supporting stone. The fabrication process was divided in several stages. Firstly, a rectangular glass block was produced in a metal mould covered with a refractory non-stick sheet, with every side flat. The annealing time of the element was around 1 month. Then the rough surface of the rock was imprinted on the glass. To do so, at room temperature, a plaster mould with the required pattern was loaded on the glass under 500kg. The glass was slowly reheated then to 690 °C, its softening point, until the pattern to be completely imprinted. That stages last for one month as well as the last phase of cooling again down to room temperature (Oikonomopoulou et al. 2018).

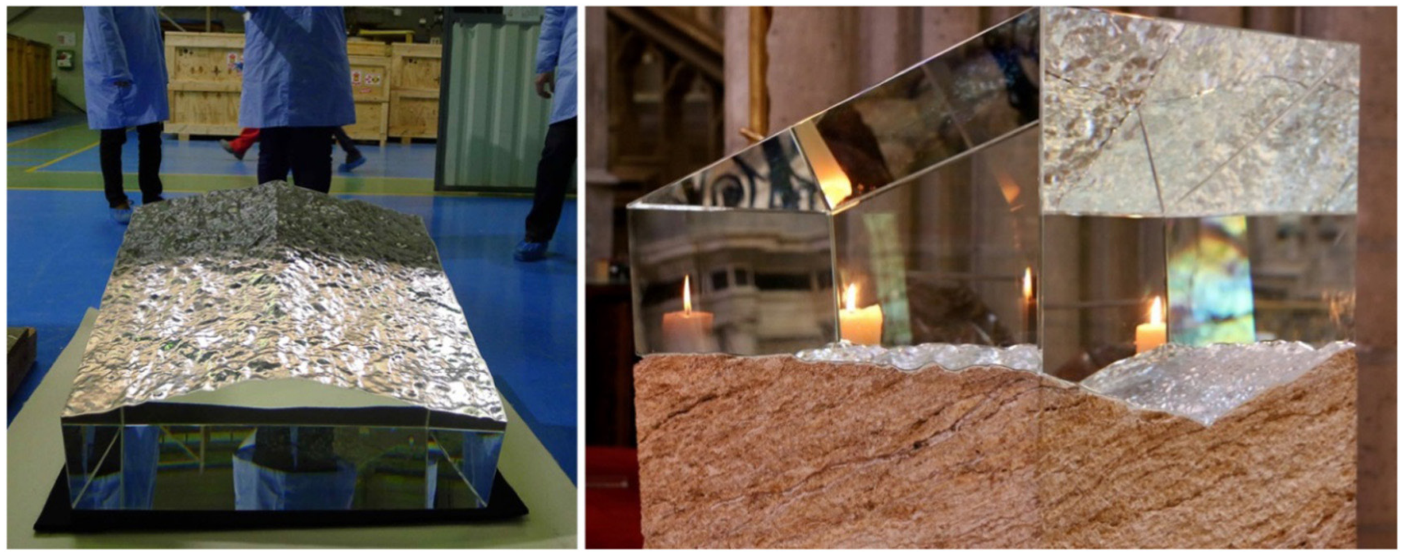

Figure 27: The casting face and the final result of the artwork. Image credits: Thierry Dannoux.

Facades with cast glass blocks

The following examples are the most characteristic realized applications of structural cast glass components in architecture: The Atocha Memorial in Madrid, the Crystal Houses in Amsterdam, the Crown Fountain in Chicago and the Optical House in Hiroshima. The projects use exclusively cast glass blocks of similar small volume and connecting elements in their self-supported facades to provide transparency and daylight to the inside.

The Atocha Memorial | Crystal Houses | Crown Fountain | The Optical House

Figure 28: Architectural projects with facades consist of structural cast glass bricks (Oikonomopoulou, F., et al. 2018)..

A further description of the Crystal Houses' façade from MVRDV Architects is introduced here, since it is a project which extends the limits of cast glass structures obtaining the highest visual clarity. The façade of a former townhouse was refurbished employing more than 6500 solid cast soda-lime glass bricks of 65x210x210 mm dimensions. The intention of the architects was to implement the traditional architecture with the brick patterns in the new design by introducing transparency (Oikonomopoulou, F., et al. 2017).

To achieve the highest unobstructed transparency, any kind of substructure or metal connectors should not be implemented. Therefore, the bricks in the self-supported 10x12 m façade are connected with a layer of a colorless UV-curing adhesive. The high-stiffness and the appropriate thickness of the bonding adhesive layer, which was obtained after experimental work in

prototypes, had as a result the uniform behavior of the whole façade, brick and adhesive, as one rigid element. On account of this, a perfect matching of the elements and the layer of the adhesive should be obtained.

Therefore, the inevitable shrinkage of the glass during its annealing time followed a longer post-processing with CNC-cutting (Oikonomopoulou, F., et al. 2017).

The buckling of the load-bearing glass structure could be overcome due to the size of the brick and the solidity of them, depending on the high compressive strength of the glass, 300-420MPa by Granta Design Limited (2015). Also, for the lateral forces, four buttresses were added from the inner part of the façade by interlaced glass bricks (Oikonomopoulou, F., et al. 2017).

Topologically optimized cast glass nodes

This is a research which was conducted in a thesis context of Building Technology track, in TU Delft. The study investigates the potential of using topology optimization as a designing tool for a cast glass node. The nodes comprise a redesign of the current connections in a grid shell on the Singapore University of Technology and Design.

The proposal of the thesis was a new hybrid structure with glass cylindrical beams, cast glass optimized nodes, metal wires and metal elements for the connections of the beams and the node. The presence of metal was important in the construction due to the high tensile stresses that concentrate in a node. For the final geometry several iterations of the topology optimization algorithm ran through Ansys software.

One of the optimized nodes was casted and connected with the metal elements and the glass beams which were derived from the study. For the fabrication, two types of moulds with two different types of glass were investigated. For the first attempt, 3d printed sand moulds were fabricated using lead glass.
The second alternative was produced with lost-wax cast with use of recycled art glass pieces. However, since the second method is a slower process and requires intense labor, the sand moulds method is proposed (Damen, W., 2019).

As for the results of the research, two different node sizes were studied. One smaller, lightweight node and one heavier for a larger grid shell alternative. The light one weights 2.7 kg, 70% lighter than the solid unoptimized initial node and with an estimated annealing time of 4 hours. On the other hand, the bigger node weighing 5.4 kg and the annealing process was expected to last 16 hours (Damen, W., 2019).

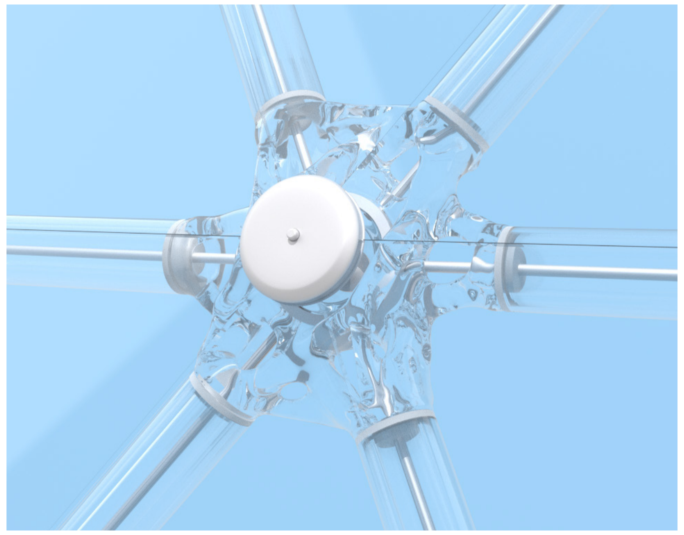

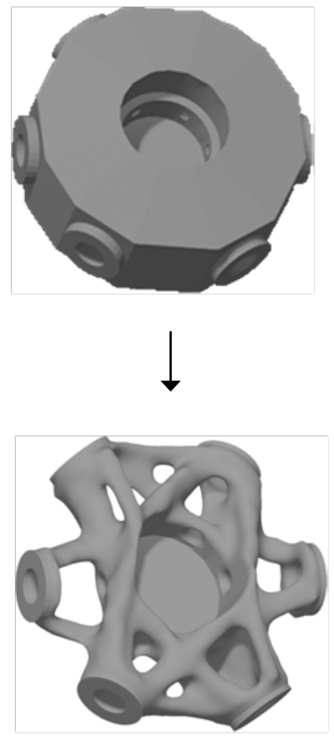

Figure 29: Optimized cast glass grid shell node. Before and after (Damen, W., 2019).

Topologically optimized cast glass column

Another useful master thesis of Building Technology track, TU delft, is the research regarding the exploration of using 3d printed sand mould for the fabrication of a cast glass topologically optimized column from I. Bhatia, 2019. The studied column is located in the Kolumba Museum of Cologne, by the architect Peter Zumthor.

Although the research started with a first attempt of optimizing a linear column, soon it was clear that the removal of any part of the geometry in a straight column would interrupt and destroy the stress line continuity. Therefore, for better results and for eliminating the amount of columns, a triangular one was optimized.
After finding the most appropriate shape for the column, with 6m height and around 8m maximum width, Ansys software was used for the optimization. Several iterations led to the final result that Figure 30 illustrates. The final model was weighing around 4.4 t and had a mass retention of 75%of the original geometry (Bhatia, I., S., 2019).

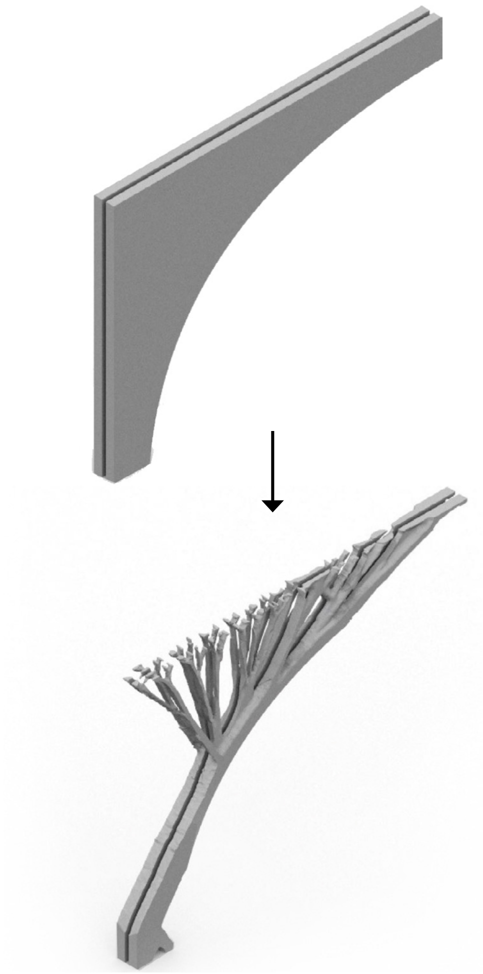

Figure 30: Optimized cast glass column from Bhatia, I., S., 2019.

For the manufacturing part of the physical model, plenty attempts including different type of moulds, binder systems and casting processes of samples were firstly conducted. After concluding the most suitable features for the fabrication, 3 sections from the optimized column where chosen and prototyped in different scales (Bhatia, I., S., 2019).

To sum up, in the following table all the important information from the previous cast glass examples are collected. A comparison between the glass and mould types that were used, the dimensioning of the components and the complexity of their shape, the required annealing time and possible software used for optimization is presented.

	Application				
	G. Magellan Telescope mirror	Art field: Denis Altar block	Crystal House	TO glass nodes	TO glass column
Type of glass	E6 borosilicate glass	Corning 7056 optical glass	Soda-lime glass	Borosilicate glass	Borosilicate glass
Glass element size	8.4m diameter	1.42x1.42x0.2 8m	65x210x210m m	-	6m height 8m max width
Weight	16 t	1.4 t	7.2 kg	2.7 kg	4.4 t
Annealing time	3 months	1 month	36-38 h	4 h	-
Unit repetition	No	No	Yes	No	No
Mould type	Disposable	Disposable	Permanent open steel moulds	3d printed sand mould	3d printed sand mould
Form complexity	Moderate	Moderate	Low	High	High
TO software	-	-	-	ANSYS	ANSYS
Current condition	Realized	Realized	Realized	Research	Research

Table 4: Comparison between important features of the aforementioned cast glass applications as an outcome of all the above examples.

4.1.5. Safety

Until now safety strategies have been mostly applied on float glass components. These strategies are either tempering the glass sheet, which means adding compressive stresses on the surfaces of the panes before the end of the floating process, or employ lamination of multiple sheets together, in order to maintain structural stiffness with sacrificial extra layers.

In terms of safety in cast glass components, the most popular strategy is a fragmentation of the entire geometry. Crystal houses are a relevant example, where instead of a monolithic structural cast glass façade, the geometry was split into smaller bricks which are able to isolate a possible crack and prevent it from spreading through the entire wall. In such case, the component is able to resist crack propagation, until the replacement of the destroyed piece.

Since the aim of this thesis is to investigate large monolithic pieces, the above safety strategy cannot be implemented. In contrast, one or two sheets of float glass can be added on top of the slab to protect the monolithic optimized component from failure, following the lamination principles.

As an extra design constraint of the slab, it is important to take into account the deflection of the sacrificial layers when validating the shape and the openings (holes) of the optimized slab.

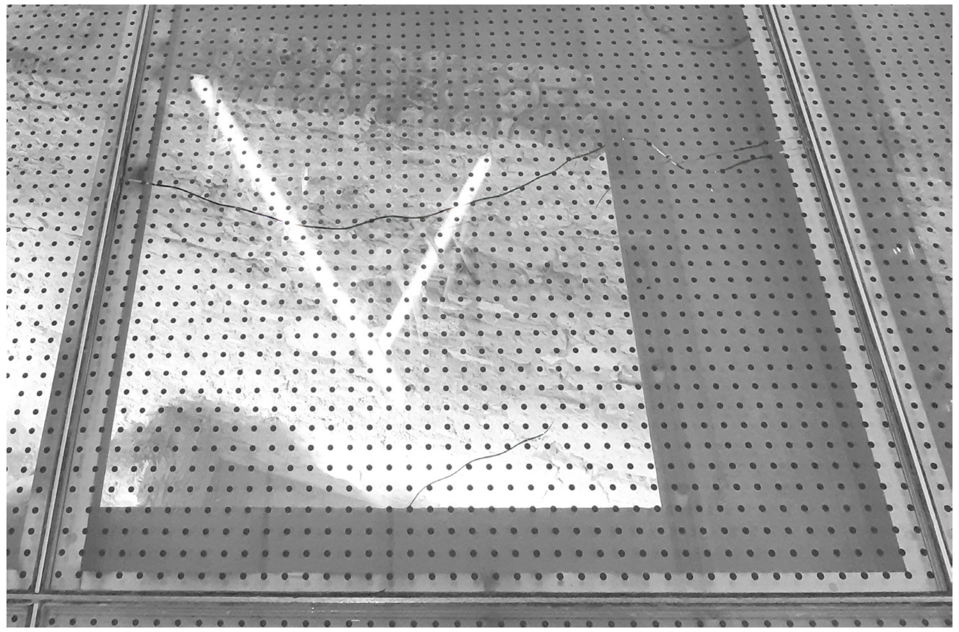

Figure 31: Fully functional glass floor with a big crack on the sacrificial layer, Acropolis Museum. (personal archive)

4.1.6. Limitations from cast glass

After experimentations with cast glass and multiple shapes and geometries, it is demonstrated that a mass reduction of the glass component, can greatly shorten the annealing time since there is less material to cool. Creating voids and rearrange the geometry with rib-elements provide with more surfaces and less inner mass, therefore the required heat for temperature reduction can flow better. In that way, large temperature fluctuations inside the volume of the component can be avoided, reducing the possibility for thermal shock.

In addition, internal stresses and high hydrostatic pressure can be generated during the annealing process. Regarding the design of the component, sharp edges and corners sticking out of it should be avoided, since the annealing of them will last much less than the thicker solid parts. The temperature difference of these elements can cause inhomogeneous shrinkage which lead to dangerous internal stresses release. Thus, smoothen elements with rounded edges are preferred.

Another important factor when someone designs a glass element is the equal distribution of the material throughout the entire mass of the object. That way the internal stresses can be also minimized. Therefore, by designing the glass component with a uniform mass and thickness of its parts, the annealing time and the thread of cracks will be greatly reduced (Oikonomopoulou, F., et al. 2018).

Finally, a flat even upper surface is crucial in order to accommodate the lamination of the safety float glass sheets.

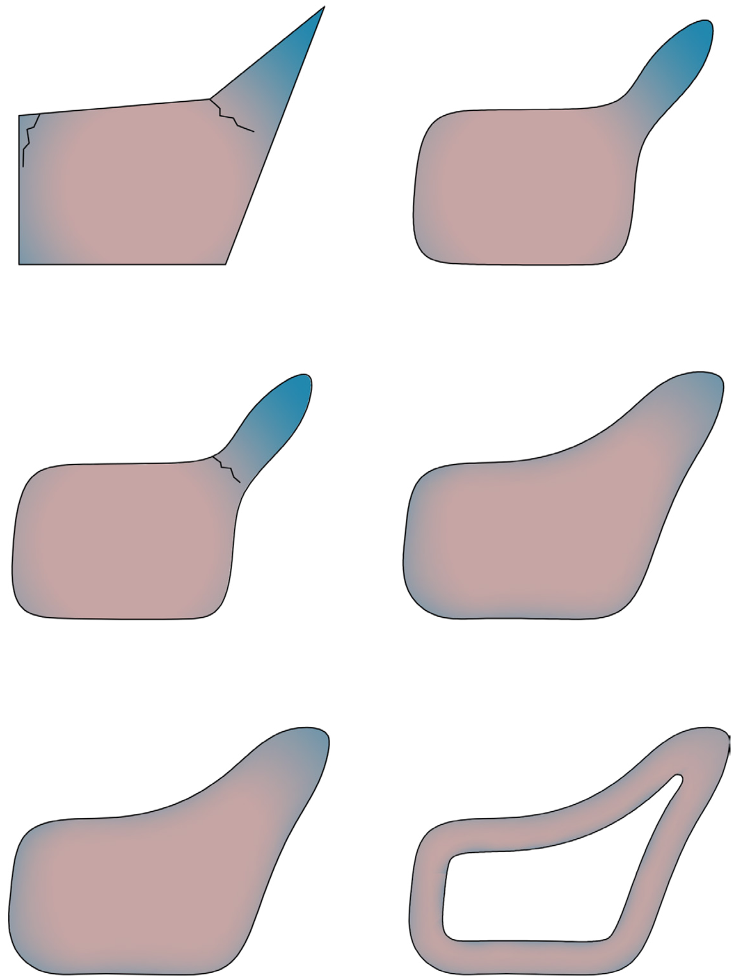

Figure 32: Avoidance of sharp corners-edges and unequal mass distribution can lead to an efficient design with less temperature differences.

4.1.7. Manufacturing constraints from casting

Cast glass, since it does not contain any solid particles when it is fully melted, in contrast with concrete, is able to flow and fill even quite small parts of a mould. However, unlike metal which is more watery, glass as considerably more viscous takes longer to fill a complex geometry mould. Thus, it is important to keep it completely liquefied in high temperatures for sufficient time in order to settle adequately (Oikonomopoulou, F., et al. 2018).

During the optimization process or if it is not possible during the post-processing, very narrow paths for the glass should be eliminated since reaching them can be hard for the material or increase the production time. Another important point is the removal of very thin elements on the component. Otherwise, while removing the moulds of the final product, those elements are possible to break.

Another important aspect that needs to be taken into account while manufacturing cast glass is the upthrust which can be very high when the glass melts and flows into the mould.

4.1.8. Discussion

To sum up, as architects' interest in transparency is constantly growing, new techniques require further development in order to efficiently serve these desires. Glass, therefore, has to be studied in depth, starting from its properties, mechanical and thermal, which make it a very competitive material nowadays, since the attention for a structural material with ultimate transparency is increased.

The recyclability of glass, the high compressive performance, the corrosion resistance, the low energy consumption and the infinite shape potential that additive manufacturing can allow are some of glass advantages apart from transparency.

On the other hand, problems like the meticulous and time-consuming annealing process have to be under further development according to realized solution such as the honeycomb structure of the telescope mirrors.

In this thesis, where the topological optimization approach will be explored, borosilicate glass has been chosen as the most appropriate solution. The reason is that it presents a sufficient thermal shock performance and it is affordable. It has already been used in large-scale components such as the Giant Magellan Telescope and it proved to require less annealing time than the soda-lime glass, the second possible choice.

In a slab located in a public building with thousands of people visiting it every day, the safety factor is important to be considered. The most common safety solutions that have been developed until now are not suitable for the current design assignment. Therefore, a lamination from float glass inspired solution will be implemented by laminating one or two glass panes on top of the optimized cast glass slab in order to restrain any possible crack propagation and maintain the main geometry structurally sufficient.

Finally, during the TO on a later stage, criteria regarding smooth surfaces, rounded edges, elements of equal material distribution and avoidance of narrow paths or very thin elements are obtained from this chapter.

4.2. Fabrication research - Moulds

An important aspect of projects from cast glass is the selection of the appropriate mould in which the molten glass will be poured. A research regarding conventional types, techniques and materials of moulds in addition with the recently developed additive manufacturing possibilities and accomplishments is displayed in the following sub-chapters.

The most appropriate type for this project's mould along with the specific manufacturing technique, the current applications and the limitations that will contribute to form the final design criteria are analyzed as well.

4.2.1. Types of moulds

The main commercial categories of moulds regarding cast glass are the disposable, the permanent and the lately developed and attention gained in cast glass field, 3d printed sand moulds. The choice of the suitable mould can be a result of multiple factors such as the precision demands, the manufacturing costs, the production volume and the shape of the desired geometry.

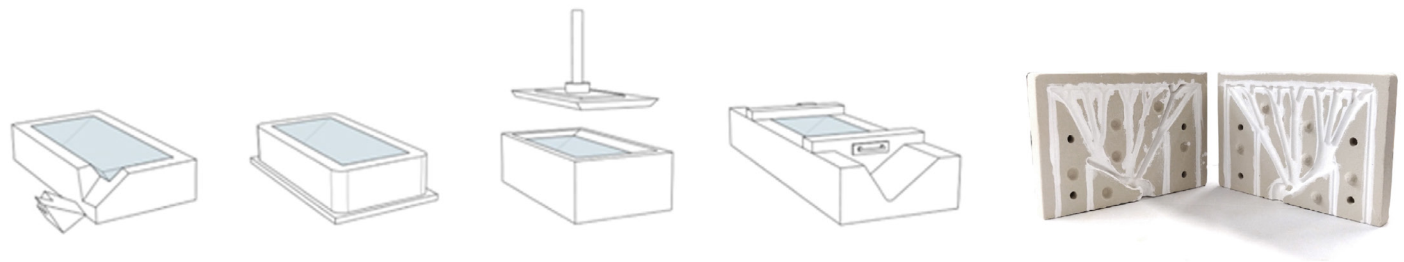

Figure 33: Most popular conventional mould types and the 3d printing sand mould. (Oikonomopoulou et al. 2018), (Bhatia, I., S., 2019)

As it is shown in Table 5, the most common materials for the **disposable moulds** are silica plaster or alumina-silica fiber. Although this type of mould has significant low manufacturing costs, it is designed to produce one object each time since it gets destroyed after the use. Therefore, it is recommended for a single component production or a small batch of castings. Due to their manufacturing techniques, disposable moulds can provide geometries of poor accuracy and low complexity. It is appropriate for glass casting as it can resist high temperatures, although melt-quenching is not suggested for these brittle moulds (Oikonomopoulou et al. 2018).

The **permanent moulds** are usually composed of metal, stainless steel or graphite and can be either fixed or adjustable to produce objects with similar yet slightly different shape or size. The accuracy of this type can reach high levels, increasing the manufacturing costs significantly. Thus, the permanent moulds are the optimum choice for a big production of components of the same or similar shape.
Due to the robustness of these moulds' materials, it is preferably to be used under the melt-quenching process for time-efficiency, which is intensified thanks to the quite smooth and transparent surface of the final product with minimum post-processing requirements (Oikonomopoulou et al. 2018).

A novel technique in the construction industry which is further explored and developed due to the complexity requirements of parametric design and topology optimization geometries are the **3d printed sand moulds**. These sand moulds have quite low manufacturing costs while it is possible to reuse the material after completing the production of one object, leading to a very sustainable production technique. The glass casting in such moulds is still under research for the building industry, however, it is a promising technique in which if the appropriate binder and coatings are applied, could lead to qualitative glass surface with low post processing demands (Oikonomopoulou et al. 2020).

According to the comparison of all the respective factors in Table 5, for the design-task of the thesis, **3d printed sand moulds** are chosen. The high precision in addition with the fast and economic production and the compatibility with the complex shapes lead to a clear choice over the rest. Geometries derived from topology optimization are one of a kind, customized designs depending on different sizing, boundary conditions and loading that cannot easily implemented. Thus, a mass production of such geometries, where metal moulds could be preferred, is not recommended.

	Permanent moulds	Disposable moulds	3d printed sand moulds
Reusability	Permanent	Disposable	Disposable
Material	Steel/Stainless steel or Graphite	Silica Plaster or Alumina-silica fiber	Sand
Accuracy	High	Low	**High**
Manufacturing Costs	High	Low	**Low**
Adjustability	Can be adjustable	Not adjustable	Not adjustable
Post-processing	Low	High	Depend on binder and coating chosen
Applicability	Repetitive geometries	Custom-made objects (field of art)	Complex geometries
Observations	Complexity of the shape increase the costs	Intense labor	Quick + no need for supports

Table 5: Information for the three possible moulds for cast glass derived from Oikonomopoulou et al. 2018 and Bhatia, I., S., 2019.

4.2.2. Realized applications of 3d printed sand moulds

Until recently, sand moulds were a well-established fabrication technique for metal casting in aerospace and mechanical manufacturing industries. With the evolution of additive manufacturing, the idea of the conventional sand moulds combined with the flexibility of casting various materials of any shape appealed to the building industry and especially to architects, who appreciate the most the geometrical freedom.

Except from the art field, where custom conventional sand moulds of low accuracy are already used, there is almost no current application of sand moulds for cast glass elements. Some explorations of 3d printed sand moulds for steel or concrete elements are presented below along with experimental academic prototypes for glass casting.

Topologically optimized metal node from Arup

Arup's research team conducted an investigation of designing a lightweight metal node through topology optimization while exploring the potential of producing it with the use of 3d printing sand moulds. The project is extensively presented in Chapter 4.3.3 regarding the designing techniques, however, the pioneering use of the sand mould method combined with traditional metal casting could not absent from this unit.

After using different techniques for producing the extremely complex final shape of the node, such as direct metal printing , they ended up trying casting in printed sand moulds in collaboration with the 3Dealise company (Galjaard, S., et al, 2015).

In order to obtain such a complicated and organic geometry that the topology optimization resulted, they had to use cores to accommodate the undercuts. To overcome this difficulty, the research team decided to slice up the mould in smaller pieces, making this way every part of the mould accessible. In Figure 34, pieces of the printed sand mould can be seen along with the holes of the interlocking system between them for accurate positioning.

During this research project, Arup's team is highlighting the speed of the production such a technique accommodates, the reusability of the material which contribute to a sustainable building future and the minimization of the manufacturing costs. On the other hand, as a main constraint of the 3d printing technique, the limited dimensioning of the printers' building platforms is referred (Niehe, P, 2017).

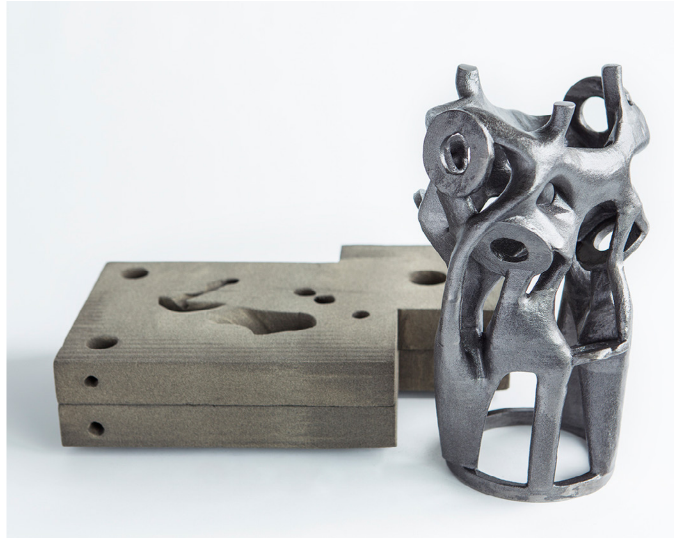

Figure 34: The 3d printed sand mould for the metal topology optimized node from Arup. (@Davidfotografie)

Topologically Optimized Concrete Slabs ETH

As the project is further described in Chapter 4.3.3 from the topological optimization point of view, it is worth mentioning here as another application of 3d printed sand moulds exploring a state-of-the-art fabrication technique.

The project was conducted in order to explore two topology optimization methods and a novel fabrication technique of 3D print stay-in-place formwork (PSPF) for concrete. The investigation was occasioned by the limited sizing of large-scale digital fabrication infrastructure and the availability of using suitable materials for structural applications, such as reinforced concrete.

After the printing of the sand formwork and post-processing the surfaces (Figure 35) by cleaning and strengthening the mould with epoxy resin, the research team placed it into a 3d printed container with a protective layer of unconsolidated sand in between. In a next step, the reinforced with 10mm long steel fibers concrete was casted into the mould (Jipa et al., 2016).

The principles of the final slab are based on the precision and the infinite possibilities of shape that topology optimization requires, such as on the structural strength that the reinforced concrete provides leading to an innovative fabrication method which deserves further investigation.

Figure 35: Post-processing of the 3d printed sand mould contained in a closed 3d printed box (Jipa et al., 2016).

Figure 36: Casting the fiber-reinforced concrete into the sand formwork (Jipa et al., 2016).

RISE Glas research on 3d printed sand moulds for cast glass, Sweden

RISE research institutes of Sweden and Flygt, E conducted a preliminary study in order to explore the possibilities of 3d printed sand moulds for glass casting. The research objective is the potential of a fast, high-accurate and with low manufacturing costs fabrication method for customized cast glass components, which can be directly obtained from the CAD files.

The research team tested various binders to solidify the sand such as Furan, Phenol and several coatings applied with brush or spray aiming to the smoother surface result on the glass. They wanted to achieve elements with minimum post-processing demands.
An attempt for strengthening the glass element with the use of an activator in the mould was conducted as well. Further investigation is expected for a similar technique that can obtain stronger glass elements without compromising the transparency (Flygt, 2018).

Figure 37: The molten glass is poured into moulds of different binders treated with different coatings. (Flygt, 2018)

Figure 38: A completed test with round smooth edges and the mark of the binder type (Flygt, 2018).

Academic experiments on cast glass components, TU Delft

In a previous chapter, two master theses in TU Delft, at 2019, in which cast glass applications were investigated, were mentioned. In these projects, the fabrication technique was based on casting in 3d printed sand moulds. As a part of the prototyping phase, the potential of the printed sand moulds was explored physically with experimenting and solving aspects such as the appropriate binder and coating material, along with the geometry constraints and requirements of the mould designing.

More specifically, a cast glass node and a cast glass column were studied from Damen, W., 2019 and Bhatia, I., S., 2019 respectively. Both projects were prototyped with the contribution of ExOne company, where the sliced sand moulds in Figures 39 and 40 were printed, whilst different binder materials and treatment of several coatings were examined. Afterwards, various experiments regarding glass casting were conducted in the Glass Lab of TU Delft through the kiln-casting method.

For the final moulds, CHP and Anorganic binder materials for the sand mould were tested, the surfaces were treated with Crystal Cast coating as it was the optimum outcome from the first experiments and lead glass was used for the kiln-casting, since it presents a lower melting temperature.

As this research concluded, regarding the composition of the printed sand mould, the Anorganic binder is demonstrated as the most promising out of the rest commercial materials for the glass casting procedure, since the mould retains its strength during the high temperatures of kiln-casting. In order to obtain the smooth, glossy and fully transparent surface that is expected from such glass components, further research of the appropriate coating is necessary (Oikonomopoulou et al. 2020).

The aforementioned theses are the first experiments of glass casting in 3d printed sand moulds concerning the building environment. Thanks to all advantages of this kind of moulds and fabrication process, the attempt needs to be further developed towards large-scale applications, easier demoulding and better quality results with less post-processing.

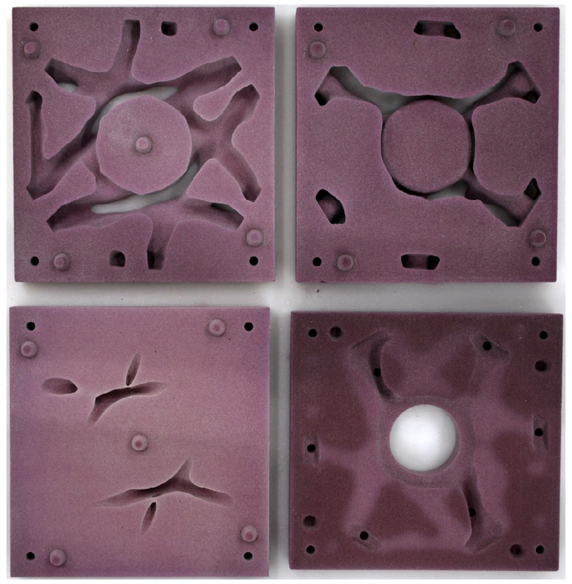

Figure 39: Prototyping of optimized cast glass node with use of 3d printed sand mould (Damen, W., 2019).

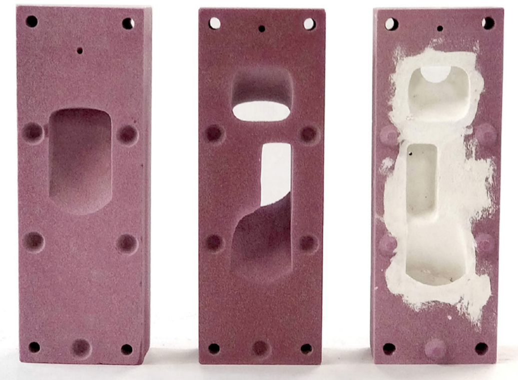

Figure 40: Prototyping of optimized cast glass column through 3d printed sand mould (Bhatia, I., S., 2019).

4.2.3. Printing technique

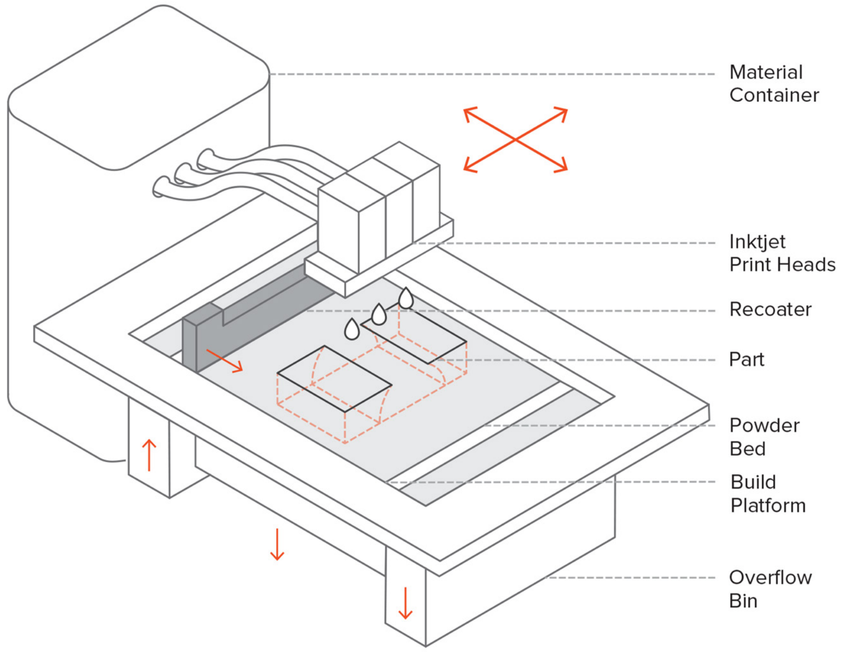

Figure 41: Graphical illustration of how the 3d printing machine works. (Source: https://www.3dnatives.com/)

Binder jetting is the additive manufacturing technique behind 3d printed sand moulds. During this process, as it is illustrated in Figure 42, after loading the printer with the digital data, the system starts by applying a thin layer of the required particle material, in this case sand, in a build platform. Then, the selected liquid binder agent is dropped in the sand bed from the high performance print head wherever the solid object is to be built. The building platform is afterwards lowered to receive the next sand layer and the binding drops. This procedure carries on until the whole object is built by adding the solidified geometry layer by layer among the loose sand.

When the process is completed, the dry unbounded sand is removed revealing the required component. For the above removal, all areas with loose sand must be approachable and not completely closed. The removed sand can be fully reused for more objects.

Currently, the biggest sand printed machine can provide a building platform of 4 x 2 x 1 m by Voxeljet company. Since the designed slab will be 7 x 6.2 m the mould needs to be printed in pieces and an assembly strategy is required afterwards.

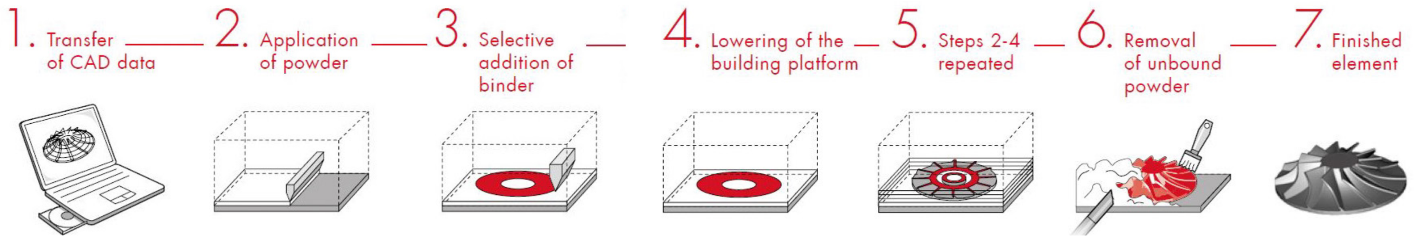

Figure 42: Printing stages of a 3d printed sand mould. (Source: https://www.voxeljet.com/)

4.2.4. Manufacturing constraints from moulds

Except from the manufacturing constraints related to the casting process that were mentioned in Chapter 4.1.7, various restrains emerge from the manufacturing of the mould in first place. These requirements need to be taken into account during the mould designing, while they slightly influence the design criteria during the topology optimization process.

The constraints that arise from the 3d printing of the sand moulds, Figure 44, are very similar to the ones that are already established from the conventional sand casting, as it is shown in Figure 43.

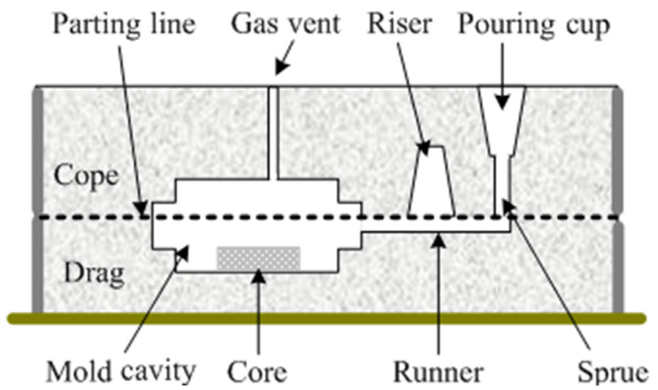

Figure 43: Requirements of conventional sand casting technique (https://www.substech.com/)

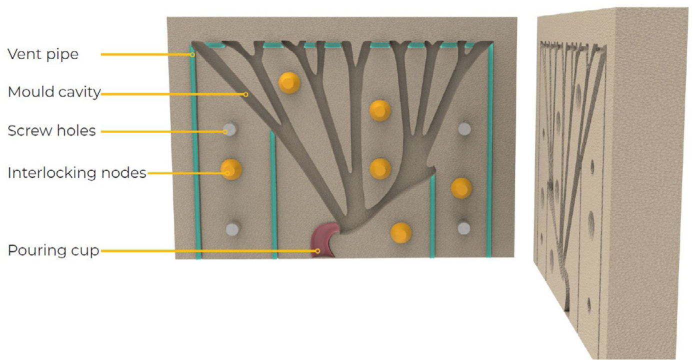

Figure 44: Requirements of 3d printed sand moulds (Bhatia, I., S., 2019).

First of all, every part of the mould needs to be accessible, in order to remove easily the unconsolidated sand after the printing is complete and to apply the coating in every surface that will contact the glass. For that reason, it is important to cut the mould up in slices depending each time on the casting geometry. Connecting solutions are necessary for the slices combination, such as the interlocking nodes and the holes for screwing that Bhatia, I., S., (2019) used.

As in the conventional sand casting, in the 3d printing fabrication a pouring cup need to be implemented in the sand mould as well as small pipes for the air release to avoid bubbles into the casted element. An inlet channel through which the molten glass enters the mould cavity might also be important, always depending on the desired geometry. A riser part which can provide with extra material the casting while it is shrinking could be useful when cast glass is fabricated into 3d printed sand moulds, although it requires extra post processing for removing any leftover material there.

Due to the high levels of hydrostatic pressure that glass can exert to the mould while melting, it is highly recommended to strengthen the walls of the mould in every direction in order to avoid failure. For that reason, the printing companies advise a minimum wall thickness of each element and therefore the minimum distance between two paths, of 3-4 mm for aluminum, 6 mm for cast steel and 8 mm for steel. There are no current guidelines for printed sand moulds for glass casting. By comparing the young's modulus E of the glass and the above materials, we could accept a wall of 3-4 mm for cast glass elements.

4.3. Topology optimization

As already mentioned, in order to solve to problems of the meticulous and time-consuming annealing process as well as reducing the weight and the material quantity, topology optimization should be introduced.

First of all, since in many examples from the literature for optimizing similar components, different types of structural optimization are used, it is important first to clarify them. Apart from the definitions, all three optimization types are clearly distinguished in Figure 45 graphically.

There are three categories of structural optimization, size, shape and topology. We talk about **size** optimization when the designed domain of the object remains unchanged but the thickness and the size of the elements' cross section can be adjusted according to the requirements.
On the other hand, a shape optimization is the process of changing the boundaries of an object's **shape** but not the topology. This means that new voids cannot be created during the shape optimization.
Finally, when an object is topologically optimized, the **topological** layout can be changed as desired, new holes can be opened and the number of the elements that constitute the object can also be altered (Bendsoe, M.P., Sigmund, O., 2003).

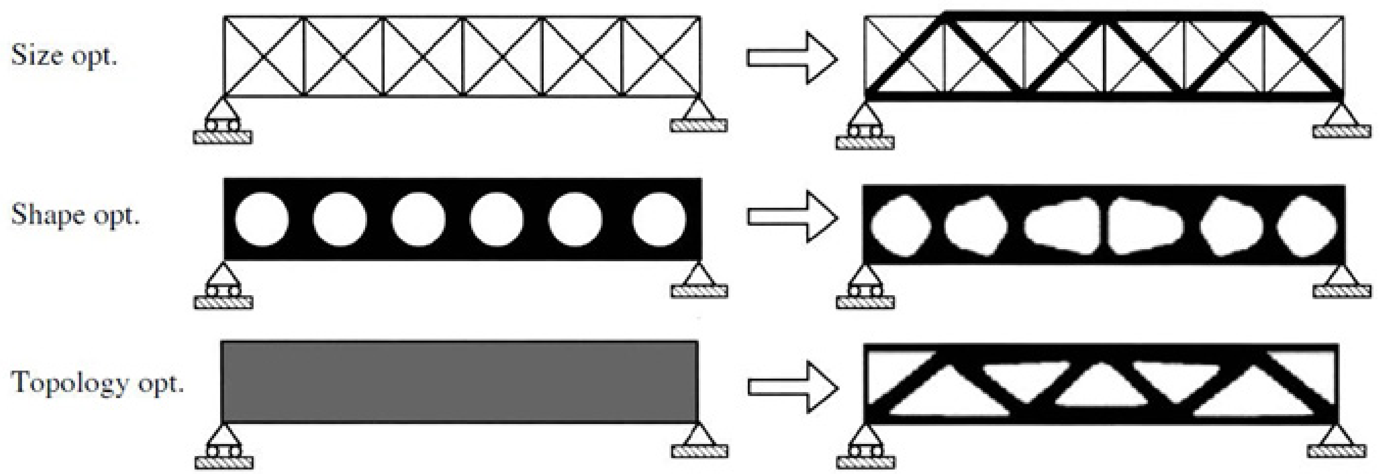

Figure 45: Comparison between size, shape and topology optimization (Gebisa, A. W., Lemu, H.G., 2017).

For a deeper understanding of the theory behind optimization, a definition for the general meaning of topology should be mentioned. As topology, dictionaries describe the mathematical study of the properties of an object which despite deformations, twisting and stretching of it, they resist. However, gluing and tearing are actions that are not included since they will change the properties, and therefore the topology.

According to Beghini, L.L, et al, 2014, in topology optimization, the optimal layout of the material for a given design domain and specific boundary conditions is tried to be obtained with regard to an objective function. Topology optimization (TO) is also described by Autodesk as the reveal of the most efficient design which is obtained by the algorithmic process through a setup of criteria and constrains, usually aiming to a material reduction.

From a mathematical point of view, TO can be described from the following representation. It basically consists of one function and two variables. The objective function (f) is used to classify the design, while according to each different design option, it gives back a value which demonstrates the design performance. Since most of the times the optimization goal is to solve a minimization problem, the aim of the function is a smaller number.

The x is the design variable which indicates a function or a vector describing the design. It can be used as a parameter which is probably changing during the optimization, representing the geometry or the material properties.
Finally, y is the state variable which concerns the structural performance of the design. It is the function or vector that can represent according to the optimizing strategy, the displacement, stress, strain, compliance or force.
The two variables constitute the constraints which need to be respected from the function (f) while it is minimizing.

$$(\boldsymbol{SO})\begin{cases}\text{minimize } f\,(x\,,y) \text{ with respect to } x \text{ and } y\\ \text{subject to }\begin{cases}\text{behavorial constraint on } y\\ \text{design constraints on } x\\ \text{equilibrium constraint.}\end{cases}\end{cases}$$

(Christensen & Klarbring, 2009)

4.3.1. TO methods

In order to conduct a topology optimization, several methods have been developed. According to Lundgren J. and Palmqvist C, 2012 the most popular methods could be the following:

• Homogenization
• SIMP: Solid Isotropic Microstructure with Penalization
• (B)ESO: (Bi-directional) Evolutionary Structural Optimization
• Level set

Homogenization method

During the homogenization method, which is often used in composite materials, the geometry is redesigned into linear elastic structure integrating infinite, in terms of size and quantity, unit cells. These cells consist of material and voids or two different materials whose densities vary according to the objective function. By defining the varying material densities taking value from 0 to 1 in the design domain, the shape is optimized. However, there are elements which in terms of the design variable are not 0 or 1, but intermediate. These elements are presented as grey areas and are really hard to be translated into a physical structure. The all solid elements (black) are filled with material and the only voids (white) are just deleted (Bendsoe, M.P., Sigmund, O., 2003).

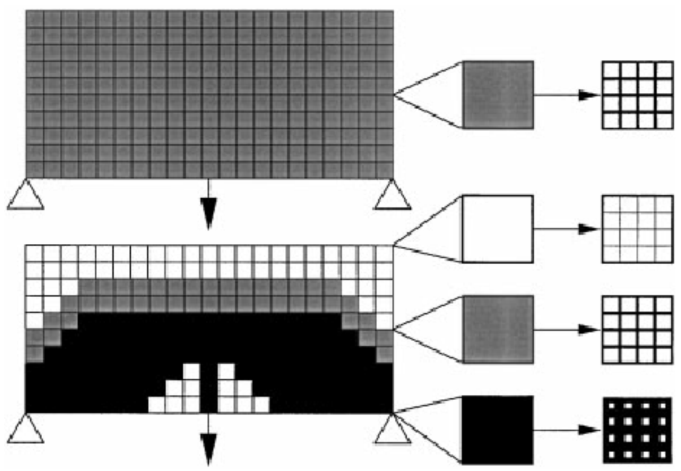

Figure 46: The initial and final phase of the homogenization method. Up is before optimization and at the bottom the black (solid), grey (intermediate) and white (void) elements can be recognized. (Belblidia, F., Bulman, S. 2002)

SIMP method

In SIMP method, the design variable is defined from a pseudo material density which again range between 0, 1. The density represents the stiffness each element has and as in homogenization method, 0 means delete and 1 means high stiffness, which is translated as solid. Although there are intermediate values as well, the grey areas, a penalization factor is introduced in order to classify them and force them to receive one of the two values, 0 or 1.

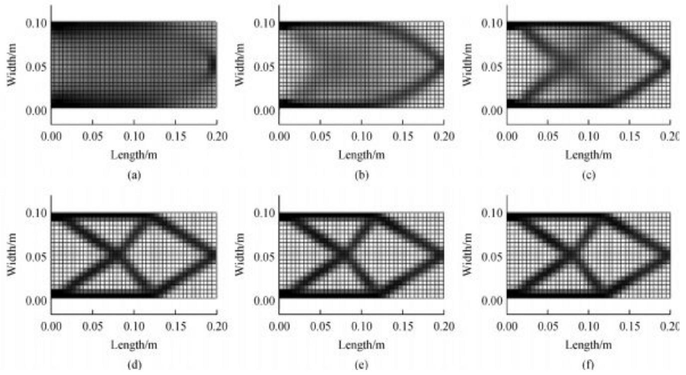

Figure 47: Multiple iteration with the SIMP method. It is obvious how the intermediate, grey areas are eliminated due to the penalization factor. (Liu, X., et al., 2011)

(B)ESO method

In the Evolutionary Structural Optimization, the strategy is to eliminate in every iteration the less contributing elements. The objective function in ESO can be either stress based or stiffness and displacement (compliance) based.

In case stress-based optimization, whenever an element is detected with a ratio of its stress value by the maximum stress of the whole model less than a predetermined value, it is removed. The iterations continue until no ratios below that value can be found. Although this method has no intermediate element values, is either black or white, the final results based on the stress constraints can lead to an inadequately stiff model. Therefore, a stiffness-displacement based optimization was developed. In this case, elements with the least strain are eliminated (Lundgren J. and Palmqvist C, 2012).

Furthermore, another development of this method is the Bi-directional addition. The main difference with ESO is that here it is possible to both add and remove elements according to their contribution in the total structure. The classification for each element includes a FEA assessment. Solid elements, as well as voids, are evaluated according to their ratios and can be removed or refilled respectively (Huang, Xie, 2010).

Comparing to the first two methods mentioned, (B)ESO is more efficient from a manufacturing point of view, since it does not include the intermediate zones. However, it requires more iterations and also there are claims that (B)ESO encounters risk regarding sub-optimal results.

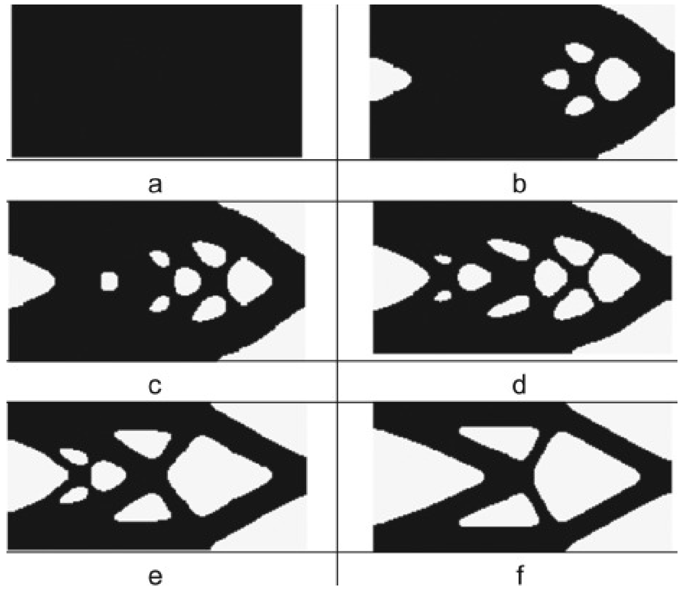

Figure 48: BESO method: the elements' straight elimination and the absence of the intermediate grey zones can be observed (Zhao, F., 2014).

Level set method

The level set method is a combination of shape and topology optimization, since it forms new topologies but with shape optimization principles, therefore, by moving and changing the boundary lines/surfaces on the design domain in every iteration. Initially, series of randomly placed voids are included in the design. According to the stress performance of the material at the boundaries of the voids, material can be added if it presents lower stress value than a preset percentage of the initial maximum stress of the whole model, or removed if it is higher.

During the several iterations, the randomly placed voids are gradually moved in more optimum positions. They can be merged together or completely disappeared, this way changing the number of holes, thus, the topology of the model. Adding more voids from the beginning hardly will affect the final result, however, the required iterations until a steady outcome will be less (Wang, M.Y., et al, 2003).

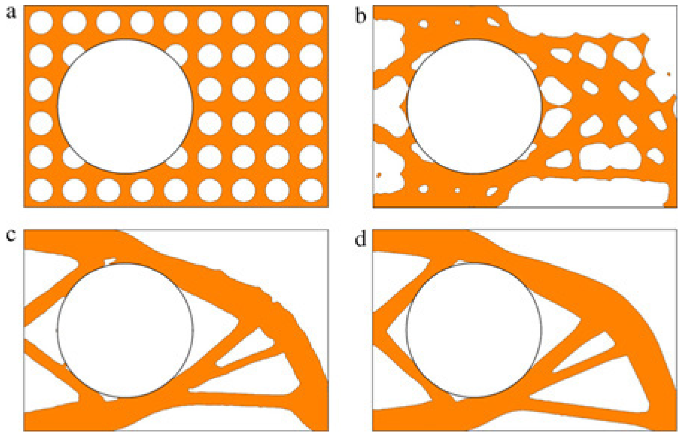

Figure 49: Level set method: the shifting of the voids' location and shapes until the final optimized result can be noticed in the image (Cai, S., Zhang, W., 2015).

4.3.2. Objective function

An important classification for the topology optimization derives from the structural constraints. A TO can be based on stresses, which usually refer to the Von Mises stresses, or compliance. The choice of the appropriate structural constraint has to take into account the type of the material and the boundary conditions of the optimizing component. Since topology optimization in glass components is a bright new approach, the selection of the structural constraints that will be respected during the optimization is a critical point.

Von Mises stresses based TO is a more suitable approach for optimization in ductile materials, such as steel. The main restriction comes from the simplification of Von Mises stress in one critical value per element. This means that compressive and tensile forces are no longer distinguished in Mises stress value. In brittle materials, such as glass and concrete, tension and compression strengths are considerably different. Therefore, a Von Mises based optimization could result in a misleading and dangerous outcome for a component out of glass, as the case of this thesis (Hailu et al, 2017).

That is why a **principle** stresses based TO should be introduced. Due to that optimization, different objectives for compression and tension stresses could be set, while the critical tensile stresses can be located. However, since principal stresses are based on the reference plane of each element, in a procedure like TO during which the design object is constantly changing, defining these stresses every time would be extremely hard and time-consuming. Therefore, this TO strategy is yet to be developed, although it has already been implemented as an academic research of 2D projects by Jewett and Carstensen, 2019.

When it comes to brittle material, though, **compliance** based topology optimization is the most appropriate. During this approach, a desired goal, usually volume minimization is tried to be achieved with respect to the compliance (strain/displacement) or the stiffness constraint of the initial design. In addition, since the objective of this thesis is a slab, the persistence of the displacement under the allowable limits is the most critical parameter. However, the main disadvantage of compliance based TO is the lack of stress concentrations and location consideration. Therefore, a FEM analysis to check the principle stresses and locate the possible peak stresses is necessary.

In Hailu et al, 2017, a comparison in compliance based and Von Mises stress based TO is conducted, in an experiment where both strategies are used under SIMP algorithmic methodology. The comparison outcome can be observed in Table 6. The results are the outcomes of multiple models subjected to the two TO approaches.

	Compliance based TO	Von Mises stresses based TO
Material compatibility	Brittle	Ductile
Desired goal	Volume minimization	Weight minimization
Form complexity	High	Moderate
Maximum stresses	High	Low
Maximum compliance	Low	Moderate
Post processing	High	Low
Variations of the results	High	Low
Challenges	Unable to consider stress concentrations	Singularity phenomenon and local nature of the stresses

Table 6: Comparison of the compliance and stress based TO derived from Hailu et al, 2017.

4.3.3. TO applications in architecture and beyond

Arup's steel node

One of the most famous topology optimization on the building environment is the steel node optimized by Arup, in 2015. The necessity for optimization and additive manufacturing of such geometries was tested in a project for a shopping street in Hague, when almost 1600 different shaped tensegrity nodes were required. Therefore, in order to reduce time, cost and material, TO was introduced.

The goal of the project was to produce one novel kind of node with reduced weight but with the same structural capacity as the conservative one. Two attempts for optimization of the node were conducted as Figure 50 illustrates. For the optimization, the OptiStruct software (Altair Optistruct v11) was used, with optimization and FEM features to be integrated. After the design domain and the boundary conditions, such as loads, supports and material properties, were set, the design objective was also established as the minimum weight of the total structure. The design objective had to respect the Von Mises stresses as the structural constraints (Galjaard, S., et al, 2015).

After several iterations and a smoothing post-processing and production preparation, the final model was fabricated with the help of 3d printed sand moulds as already described in Chapter 4.2.2.

The final model which is illustrated bellow, in Figure 50, weights 75% less than the initial node, with half its height. The new node is capable of support the same tensile forces in the same connections but can reduce the weight of the entire structure to more than 40% comparing to the initial design (Galjaard, S., et al, 2015).

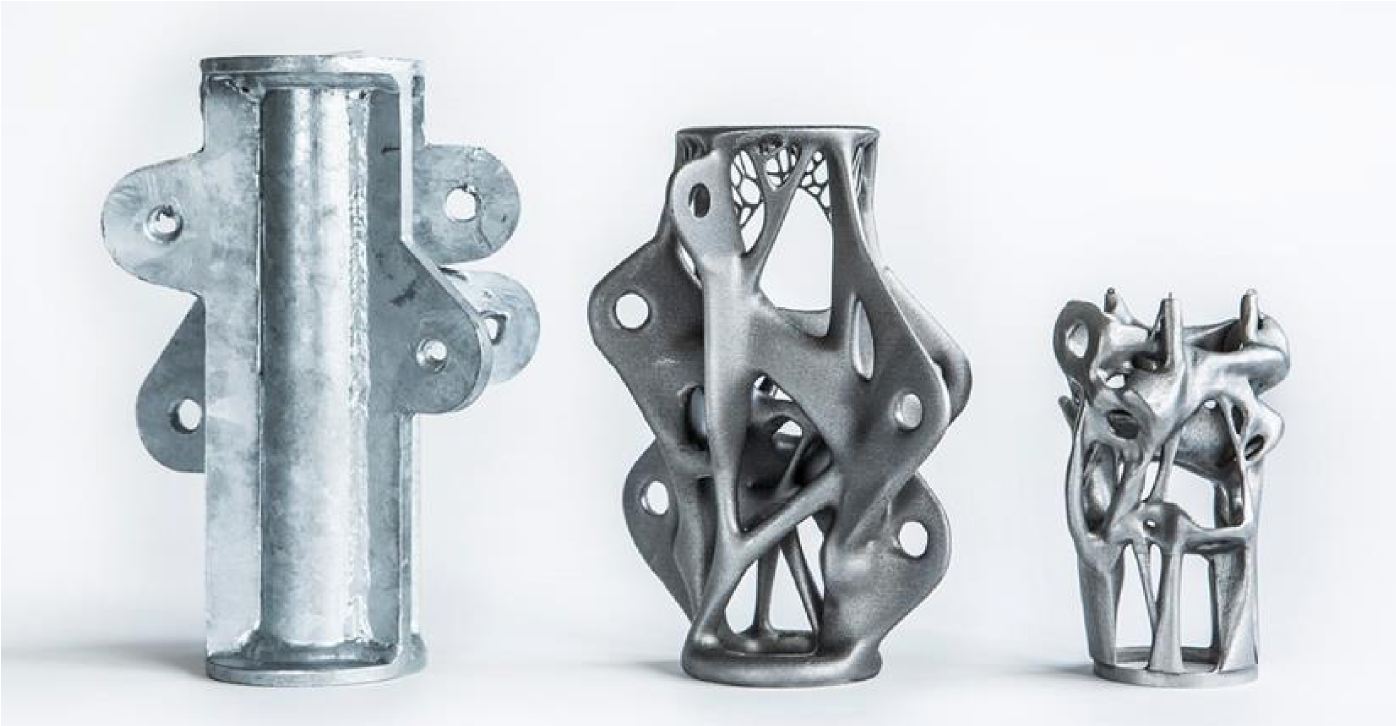

Figure 50: The evolution of the node from the unoptimized (left) to the final lightweight optimized result (right). (https://www.arup.com/), (Davidfotografie)

Optimized concrete slabs-ETH

In the department of Digital Building Technologies, of the ETH Zurich, several topology optimized components have been researched. Many of these components constitute optimized concrete slabs. Two of them will be described in this chapter.

The first project by Jipa et al., 2016 consist of two cases with different optimizing approaches. In case A the slab was optimized employing Millipede software, the Rhinoceros/Grasshopper plug in, which uses the homogenization method in addition with a mesh subdivision process. For the second alternative, the SIMP method of the Simulia ABAQUS software was tested. Except from the different optimization method, different design constraints were set for the two cases (Jipa et al., 2016).

Both design objectives were converged in material reduction but the first case would also aim to minimize the deformations under a uniform surface load while second case's goal was a stress minimization. Another difference was the supports set in each case. In prototype A, three fixed supports were tested in the middle of the surface, as illustrated in Figure 51, while prototype B was supported by 4 simple corner supports (Figure 52).

Both prototypes, after post-processing according to manufacturing constraints, were fabricated with Binder Jet 3D Printing and sand formworks, while the casted concrete was reinforced with 2.75% of 10mm long steel fibers (Jipa et al., 2016).

The weight minimizations of both slabs are estimated around 70% less than a similar solid slab. However, due to the different boundary conditions, algorithm methods and software that were applied to the two cases, the final results are totally different.

Figure 51: Prototype A: The 3-points fixed supported topologically optimized concrete slab (Jipa et al., 2016).

Figure 52: Prototype B: The 4-points simple supported topologically optimized concrete slab (Jipa et al., 2016).

Optimized concrete slabs-ETH

The next example of the concrete slabs research in ETH Zurich is from Liew A.,et al 2017, Philippe's Block Research group. In this project, a concrete prototype floor system is tested in order to be implemented in the NEST-HiLo research and innovation unit later. The project is not the most representative topology optimization example, since it mostly uses form finding and shape optimization approaches, however, it is worth to be mentioned as an alternative solution of optimization problems.

As glass, concrete has also a considerable higher compressive than tensile strength. Therefore, another design strategy was followed for creating a compression only structure. As shown in Figure 53, a rib-stiffened shallow vaulted slab system was introduced. The designed slab contains fixed supports in the four corners.

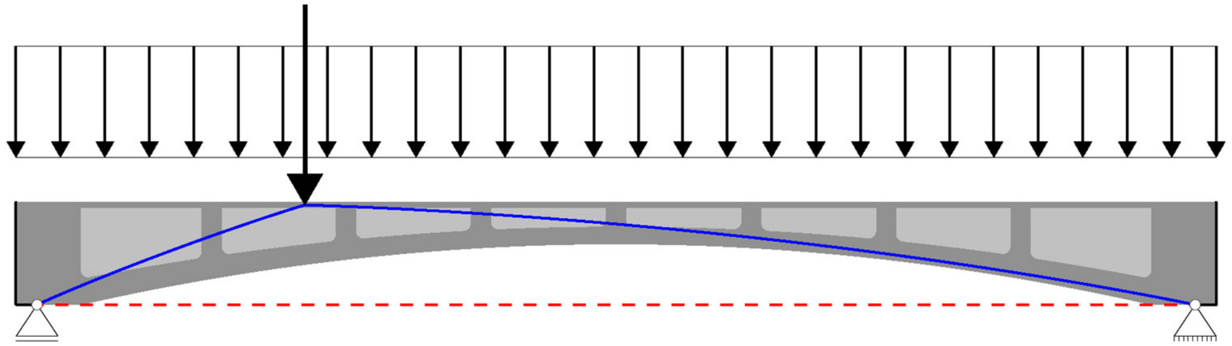

Figure 53: The rib-stiffened floor with shallow vaulted bottom-side and the two kinds of load that carries (Rippmann et al, 2018).

Aiming to a better structural performance with a lower material quantity, RhinoVAULT software was used for the form finding, ensure a funicular structure. After the drawing of a rib network according to the forces flow, a shape optimization was conducted to the obtained elements. Finally, FEA solver was used to check stress concentrations or high deflections, optimizing at the same time the size of the elements.

The final result, as it is shown on Figure 54, from the hybrid form finding procedure was fabricated with an EPS foam and timber mould, with the help of CNC milling and wire-cutting techniques, and tested under several load cases (Liew A., et al 2017).

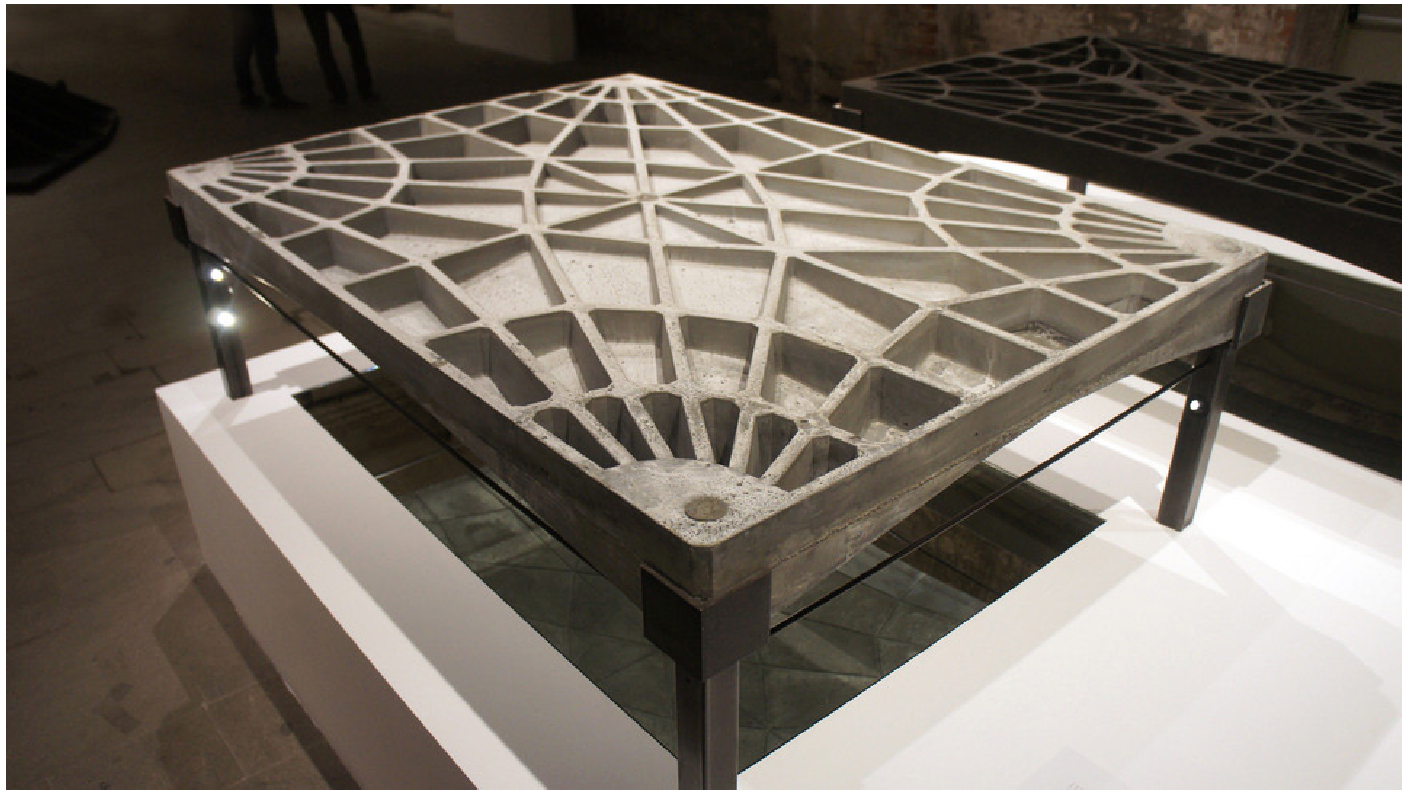

Figure 54: The final prototyped slab in exhibition. (https://block.arch.ethz.ch/, by Nick Krouwel)

Autodesk/JPL interplanetary lander

The last example of TO which will be mentioned does not belong in the building field. It is a testing prototype for the potential of Generative Design software from Autodesk, in 2019.

The project was a collaboration of Autodesk and NASA Jet Propulsion Lab aiming to the design and fabrication of an interplanetary lander module. The function of the module is to safely bring scientific equipment to extraterrestrial areas. Therefore, weight reduction is crucial since that mean decrease of the required fuels.

For the optimization with the Generative Design, an algorithm of a level set method is used. A significant feature apart from the weight minimization is the manufacturing constraints of the chosen material, since in the final prototype several fabrication techniques have been tested. More specifically, the main body of the module was cast in a 3d printed mould from sand, the optimized legs produced with CNC-milling and any extra smaller components were 3d-printed with metal.
Regarding the initial aim, the final optimized module was weighing around 35% less than the conventional one.

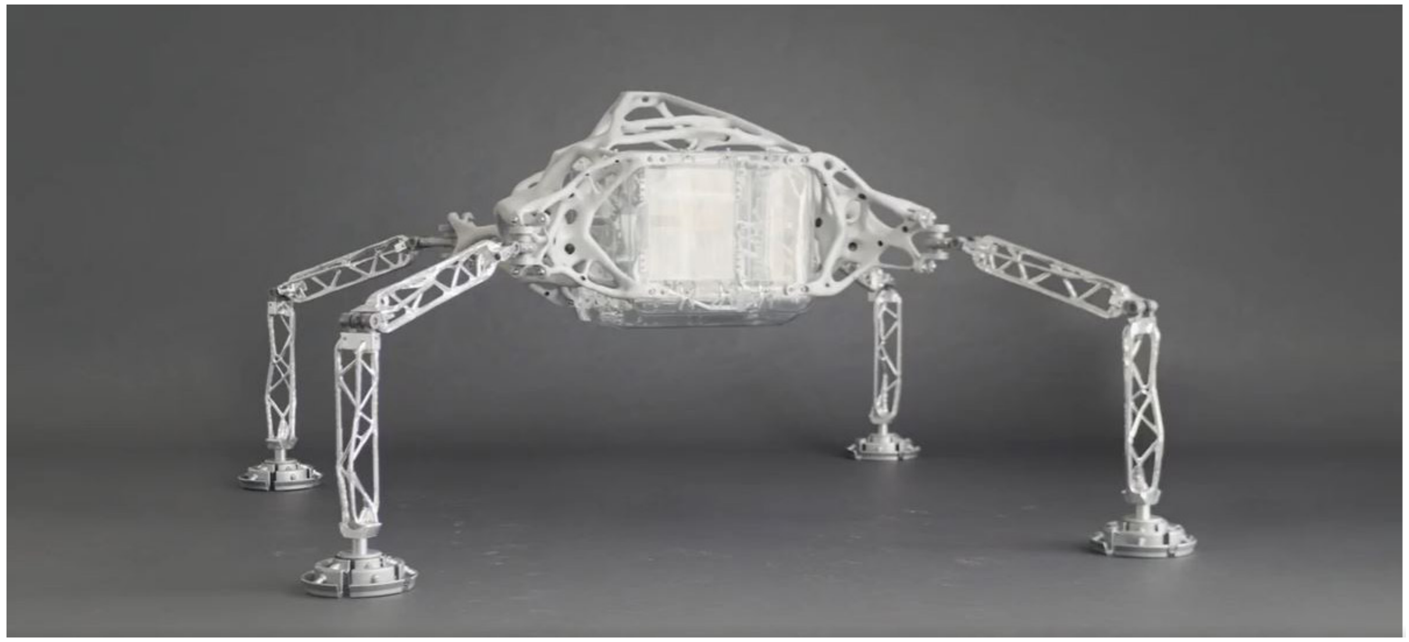

Figure 55: The optimized JPL interplanetary lander. (Source: https://www.autodesk.com)

A comparison table summarizes the most significant aspects of all previous examples as it is shown in Table 7. The list of the topology optimized applications should also contain the two research projects of TU Delft, which were described in Chapter 4.1.4.

	Arup's steel node	Optimized concrete slab- Jipa et al. Case A	Optimized concrete slab- Jipa et al. Case B	Optimized concrete slab- Liew et al.	JPL interplanetary lander	Optimized node-TU Delft	Optimized column-TU Delft
TO algorithm	-	homogenization method + mesh subdivision	SIMP method	-	Level set method	SIMP method	SIMP method
Material	Cast steel	Reinforced Concrete	Reinforced Concrete	Concrete	Metal	Cast glass	Cast glass
Structural constraint	Von Mises stresses	Compliance	Stress	-	-	Compliance	Compliance
Mass reduction	75%	70%	70%	-	35%	70%	75%
Software	Altair Optistruct v11	Millipede	Simulia ABAQUS	RhinoVAULT + FEA solver	Generative Design	ANSYS	ANSYS
Fabrication method	3d printed sand moulds	Binder Jet 3D Printing and sand formworks	Binder Jet 3D Printing and sand formworks	EPS foam and timber mould, with the help of CNC milling	1. 3d printed sand moulds 2. CNC-milling	3d printed sand mould	3d printed sand mould

Table 7: Comparison of the important aspects of some relative TO application in the building industry.

4.3.4. Suitable software

Plenty of suitable software for topology optimization have been developed the last years. The commercial software programs described below are selected as the most often used in the building environment and they are all freely accessible with an academic license.

Millipede

Millipede is a Rhinoceros/Grasshopper plug-in which uses the **homogenization method** as an algorithm approach. The software has very fast results using linear elastic system and can be combined with Galapagos, another Grasshopper plug-in, to solve generic form finding problems. The design domain and an expected density are given as the design variable. Although it is a software with very fast results, the provided options are limited.

Ameba

Another Grasshopper plug-in with more possibilities comparing to Millipede is Ameba. This program uses the **BESO method** suitable for a topological optimization. Options like importing specific material properties and plenty possibilities of boundary conditions are provided here. The design objective here is the minimization of the volume but as the respected constraint, options such as the Von Mises stresses or the displacement are both available.

The software use cloud computing, meaning that the calculations are realized online, which allows faster results. An important advantage is that mesh smoothing and re-meshing tools are included in Ameba workflow.

ANSYS

A program with very extensive and well-developed possibilities is ANSYS. It uses **SIMP method** for TO, while plenty of options regarding the material properties, the optimization desired results and structural as well as manufacturing constraints can be precisely set. The software provides both stress-based, according to Von Mises stresses, and compliance-based topology optimization.

An extra benefit of ANSYS is the FEA solver which implements. This means that in case the structural constraint is displacement, the stresses can be checked directly in ANSYS if the optimization has also been conducted there. Finally, there are tools in ANSYS suitable for the smoothing post-processing after the optimization.

Autodesk Fusion 360

Another software using **SIMP methodology** is the Fusion 360 from Autodesk. The package of Fusion 360 constitutes a compilation of several existing Autodesk software. It also includes FEA tool for a structural check analysis after the TO and is compatible with both stress and compliance structural constraints. Cloud computing is also employed in this software for faster results, as well as a wide broad material library.

Other Autodesk tools can continue the process after the TO with smoothing post-processing providing organic shapes, significant for glass demands.

Autodesk Generative Design

The Generative Design, which is also provided from Autodesk, has been released and tested recently. It uses level set method and it offers a powerful cloud computing. Due to its new approach it can provide with multiple design solutions, giving the opportunity to the designers to choose the one that is closer to their desires (cost, aesthetics). It offers plenty possibilities regarding the design parameters (cost, production time, etc) and it takes into account the manufacturing constraints since the beginning.

The software choice depends on the objective function that is defined from the case study. A slab topology optimization requires control of deflection under a preset limit. The main goal is to minimize the volume of the slab under compliance constrains.

As already mentioned, a regular restriction of compliance-based optimization is the necessity of further post-processing with FEA software in order to check and smoothen up stress concentrations that might occur.

4.3.5. Discussion

To conclude, topology optimization is a process during which the most efficient design layout can be obtained after determining the suitable presets of boundary conditions, design domain, material, desired goal of the design objective along with the structural and manufacturing constraints. Plenty of software providing TO have been developed the last years, using algorithms according to one of the four different TO methods.

Depending on the material and the boundary conditions of each case, stress based or compliance based TO can be chosen. In our case, since this thesis is about the topology optimization of a glass slab, compliance based optimization is chosen. Models from brittle materials such as glass, which present a much lower tensile than compressive strength should not be optimized under Von-mises stress based optimization. The single value that is taken into account for both tensile and compressive stresses can be misleading and generate dangerous results. Since the principle stresses based optimization is not sufficiently developed yet, compliance optimization which respects the stiffness of the glass model in combination with FEA analysis to track the elaboration of tensile stresses can be the best option here. Also, the most critical value for a slab is the displacement, which is the constraint that will be respected during the TO.

According to all the above, for the TO of this thesis, the exploration starts with Ameba, the Grasshopper plug-in, in order to obtain a fast idea of the final result. However, no reliable results were obtained due to license limitations. As a next step, ANSYS is used for a more advanced outcome in addition with the integrated FEA solver which is vital for the compliance based TO and the post-processing tools for the manufacturing preparation.

4.4. Research Conclusion

In this chapter an attempt to sum up the overall knowledge gained from the entire literature study regarding glass casting, moulds and topology optimization will be displayed.

Cast Glass

To start with, an important outcome from the literature is that glass, which presents a considerably high compressive strength, can be transformed from a 2d brittle cladding to a robust 3d structural material, if casted. With cast glass, any desired size or shape that the accessible fabrication technique is able to produce can be available, whilst the buckling effect of the float glass is tackled.
The most critical point of producing cast glass elements is the meticulous and time consuming annealing process. The annealing procedure is a very important treatment of the product which needs to be totally controlled and demands specific design principles in order to be completed successfully and on time.
More specifically, a uniform and even mass distribution of the cast glass element is necessary. This way, failure due to thermal shock between thicker and thinner elements with temperature difference can be avoided, while a smooth surface with round edges will minimize the stress concentrations making the element less brittle. A smooth gradient of thickness between adjacent elements can be acceptable as well.

Currently, cast glass has restricted application in architecture as a structural material. The realized implementations in buildings concern elements of small dimensioning, in brick size, which consist self-loading facades.
Larger applications of cast glass can be found in astronomy, with the telescope mirror blanks, and in the art field with various glass artworks.

Therefore, cast glass is worth to be used more in the building environment by exploiting its full potential of structural and aesthetic capacity. As a next step in building industry, larger, more complicated, transparent, durable, recyclable and beautiful structures from cast glass need to be produced.

Moulds

Regarding the mould findings, after researching on the available fabrication methods of cast glass elements, the 3d printed sand moulds were chosen as the most appropriate method for a unique monolithic large-scale project, with the complexity that a topology optimization result is characterized.

Until now, 3d printed sand moulds scarcely appear in the architecture field, with mostly steel and concrete castings. Although casting glass into pressed sand moulds are already a common technique in the art field, in the building industry it is still an unexplored path.

Sand is one of the most appropriate materials to accommodate the tremendous temperature demands of cast glass. It is a natural, cheap and easily accessible material which, in combination with the suitable strong and effortlessly removable binder, can be the optimum method for a large-scale element from cast glass. In addition, due to 3d printing advantages any type of geometry can be obtained, even the most complex ones. In combination with the binder jetting technique's characteristics, support structures are not necessary, making the mould production even more easy.

The constraints of the prior method can slightly affect the designing method but need to be carefully taken into account while designing the mould, in order to provide the desirable result.

Topology optimization

Plenty definitions for the topology optimization method exist, from the mathematical point of view till the engineering design techniques. The main common point which proceeds from all those is that through topology optimization the material layout of an object is redistributed in the most optimum way aiming to minimization of the response variable, with respect to the preset constraints.

Throughout the last decade, several software accommodating one out of the four most common algorithms have been developed with great results in the automotive, aerospace and mechanical fields and recently some few results in the building industry.

According to the techniques that are developed regarding topology optimization of structural elements, the main structural constraint can be either the Von Mises stress or the compliance. Since the task of the current thesis is a TO cast glass slab the compliance based optimization is the most appropriate. This decision arose from two reasons: the glass behavior towards tensile and compressive stress is completely different, therefore the single Von Mises stress value would be insufficient here, additionally with the importance of the deflection validation when it comes to a slab structure.

Armed with all this obtained knowledge in the three basic columns of interest for this project, the thesis can be successfully led to most practical paths, on which the research findings are applied.

5. Design development

After establishing the design criteria that arose from the literature review, the design development phase, consisting of a combination of topology optimization, structural analysis and manual redesign, leads to the final design.

5.1. Design criteria

The main design criteria derived from the literature review focus on three different aspects of the project: the structural, the cast glass and the manufacturing demands. The establishment of these criteria will set the given parameters, the constraint which will be respected and the desired goal of the topology optimization which follows. Any principle that is not possible to be implemented in the optimization process is introduced in a later stage.

- Structural
  - Live load **5 kN/m²**
  - Max deflection L/250 = **24.8 mm**
  - Tensile stress limit **17.5 MPa**
  - Mass minimization
  - Compliance-based TO
  - Maximum voids' area **A = 1.17 m²** and max span = **1.65 m**
- Cast glass
  - Uniform mass distribution
  - Smooth surfaces/round edges
  - Borosilicate glass
- Manufacturing
  - No narrower paths than **4mm**
  - Slab separation for the transportation
  - Flat upper face for the safety sheets lamination

Structural performance constraints

From the structural point of view, the main points that will guide the design development phase start from the assessment of the load condition of the slab and the definition of the limits on crucial structural values that the final product cannot exceed.

The main load condition on the slab derives from the live load that a component like that, in a public building, will carry. The live load on the slab was estimated on Chapter 3.4. according to the Eurocode 1, Category 3, for areas in museums. The guideline provides with a range of 3-5 kN/m² imposed load. By taking the worst case scenario of 5 kN/m² and applying, in addition, a safety factor of γ_M=1.5, the load that was actually applied in the model was **7.5 kN/m²**.

Regarding the limits of the crucial structural values, deformation is the most characteristic parameter when it comes to slabs structural validation. The allowable deformation that the slab is not supposed to exceed was determined according to Eurocode 1 as span/250.

$$d_{max} = 6200 \text{ mm}/250 = \mathbf{24.8\ mm}$$

For the safety of the construction, an extra layer of float glass has been decided to be laminated on top of the cast glass slab. The float glass operates as the sacrificial layer which protects the optimized slab from failure. According to the topology optimization concept, several holes, of various dimensions, appear in the entire slab while the redundant material is removed. Extra attention needs to be paid in order to evaluate the stiffness of the float glass layer placed above these holes. It was decided that two panes of 4 mm float glass will be used. For the assessment of that layer's deflection, the same guideline of span/250 is followed, with span referring to the hole's longest length.

After a numerical calculation in Karamba, Appendix B, two main principles regarding the voids' sizing arose so that the deflection of the float glass existing on top does not exceed the allowable limit. The obtained principles refer to a maximum span of **1.65 m** and an area of **1.17 m²**. A void is classified as inappropriate only in case it exceeds both these values.

Apart from the specific structural values, it is important here to mention the structural constraint on which the topology optimization will be relied. As already have been explained, the optimization method that will be followed is **compliance-based**. This means that, the stiff-ness of the model along with the deflection of the slab need to be kept under the allowable limit. Since the stress concentrations cannot be controlled during the optimization process, it is crucial to evaluate them after each optimization by testing with FEA analysis. Regarding the cal-culation of the tensile stress limit was conducted in accordance to DIN 18008, the German struc-tural design guidelines for glass constructions. Although there are no official standards for cast glass constructions, in this case, it is considered behaving under tensile stress similarly with the annealed float glass. Therefore, the required limit came out from the formula of the annealed glass tensile strength R_d:

$$\mathbf{R_{d\ float}} = \frac{k_{mod} * k_c * f_k}{\gamma_m}$$

The values of the formula derived from Table 8, using the values for the float glass case of a horizontal component with the impact of live load. Therefore, the tensile stress limit which obtained is 17.5 MPa.

$$R_{d\ float} = \frac{0.70 * 1.0 * 45}{1.8} = \mathbf{17.5\ MPa}$$

Symbol	Description	Value	
γ_m	Partial safety factor of resistance of the material	**1.8**	Float Glass
		1.5	HTG / FTG
f_k	Characteristic value of tensile strength	**45 MPa**	Float Glass
		70 MPa	HTG
		120 MPa	FTG
k_c	Coefficient for consideration the type of construction	**1.8**	Only for floatvertical glasswith circumferential linear support.
		1.0	HSG / FTG/ Float Glass horizontal² or without circumferential linear support.
k_{mod}	Coefficient for consideration of the load duration of **annealed** float glass	**0.25**	For permanent load (self-weight)
		0.40	For medium load (e.g. snow, thermal expansion)
		0.70	For short loads (e.g. wind, blast impact)

Table 8: Important values for defining the tensile strength of float, heat strengthened or fully tempered glass structures.

Cast glass constraints

As for the requirements due to the material, the most important aspect that it is vital to be under consideration in that phase is the an-nealing process limitations. During the design development a model with uniform distributed mass throughout its body, with elements of sim-ilar cross section and round edges needs to be created.

From the findings of the literature review, the borosilicate glass was chosen due to its low thermal expansion coefficient which results in a decreased annealing time comparing to the second most suitable candidate, soda lime glass. The successful paradigm of the Giant Magellan blank, the biggest cast glass piece in the world, which consists of borosilicate glass, demonstrates its compatibility with large-scale elements, as the studied slab.

For the following digital simulations, borosilicate-KG33 is used due to its low thermal expansion coefficient, high tensile strength and low costs among the rest types of borosilicate glass. The most important properties of the chosen material can be seen in the Table 9 below and in Appendix A.

	Unit	KG33
Density	Kg/m^3	2200-2250
Young's modulus	GPa	61-65
Tensile strength	MPa	28.6-31.6
Compressive strength	MPa	286-316
Poisson's ratio	-	0.19-0.2
Thermal expansion coefficient	μstrain/°C	3.13-3.26

Table 9: Mechanical and thermal properties of the chosen material-KG33 (CES Edupack, 2019).

Manufacturing constraints

Regarding the requirements of the manufacturing process that affect the design development, elements with a cross section or distance with the adjacent ones less than 4 mm cannot be accepted, since they are prone to breakage during demoulding or the glass will not be able to flow inside them.

Another manufacturing demand concerns the lamination of the safety float glass on the upper face of the slab which is crucial to retain a sufficient flat surface so that the sacrificial layer to be rigidly connected.

Finally, the feasibility of the element transportation and assembly is a factor that needs to be taken into account as well. After research for the maximum dimensioning of vehicles inside a Greek city, it came out that the maximum allowable truck can reach a size of 2.55*12*3-3.2

m net storage volume. Thus, the slab has to be separated in two pieces as Figure 56 illustrates. The initial thoughts for the project were focused on creating a challenging large scale monolithic cast glass element, experimenting on the design through TO and testing it. Therefore, because of transportation feasibility reasons the slab was decided to be split in the minimum possible number of pieces.

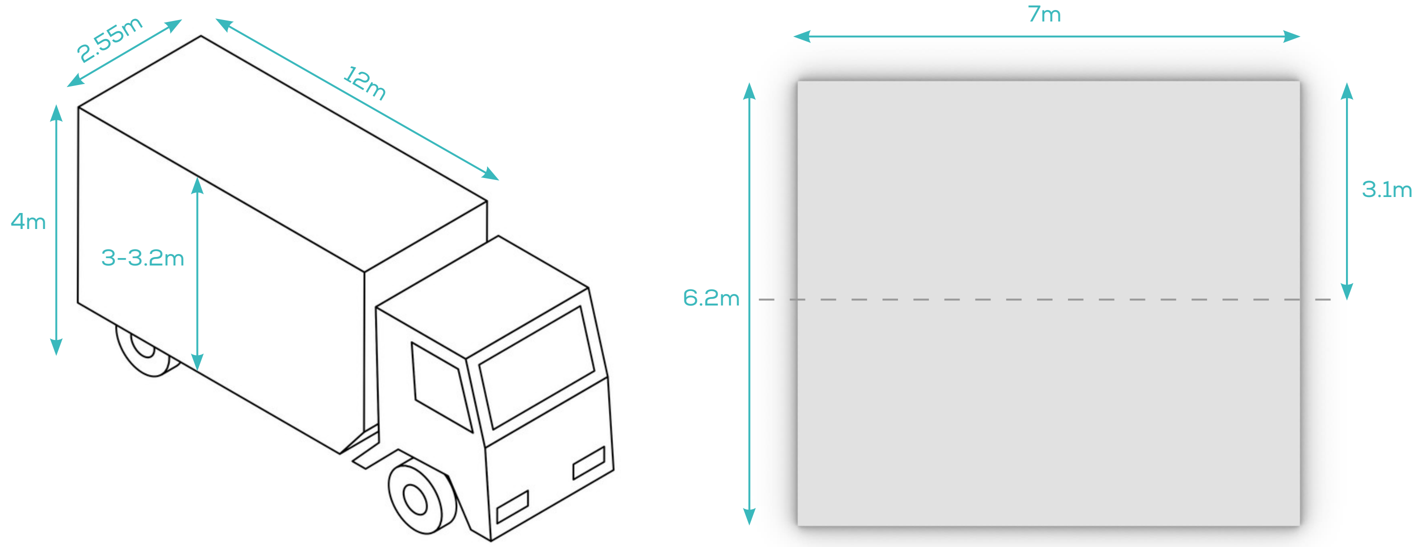

Figure 56: Left: Maximum allowable dimensions of a truck on Greek roads. Right: The necessary separation of the slab for a feasible transportation.

Optimization goal

As for the desired goal from the design development process, a lightweight geometry with the optimum material distribution regarding the compliance retention is expected. The mass reduction of the model, the numerical goal of the optimization, is discovered during the optimization process with trials of gradual decrease until the model stops responding to the preset requirements or exceeds the limits. According to the literature framework, the topology optimized projects in the building industry present a range of 35-75% mass minimization. The current thesis aims to a mass reduction within these limits.

The optimized model needs to serve an acceptable structural performance as well as the cast glass and manufacturing requirements.

5.2. Structural analysis - Size optimization

To begin with, an initial model which would be the base for the optimization and any other design technique had to be established. Right now the existing slab that is studied, consists of a float glass and a steel substructure construction. A solid model from cast glass of 6.2*7.0*0.2 m was designed and structurally analyzed in Karamba, a Grasshopper plug-in. The thickness of the slab, which was set at 20 cm as a maximum value, was aimed to be optimized through decreasing trials in relation with the deflection limit.

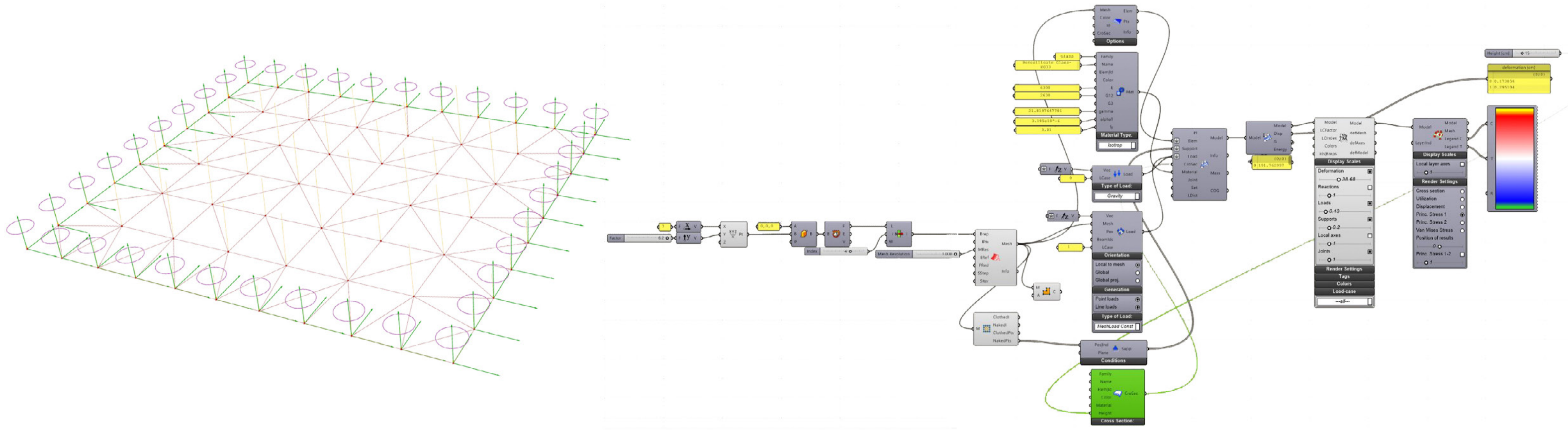

Figure 57: The script of the structural analysis for the whole slab in Karamba.

Two different support conditions were tested while the optimum size of the slab was specified. In case A, the slabs are supported on the four corners, while, in case B, circumferential linear supports are applied. In both cases, a fixed movement in the direction of x,y,z axes is provided, while the rotation around x and y axis is free.

The same analysis was conducted for the whole 7.0*6.2 m slab and for the half slab 7.0*3.1 m, according to the separation from the previous chapter. The main difference between entire and half slab here is that on the half slab there are only 3 edges supported, since the forth one will be connected with the other half piece.

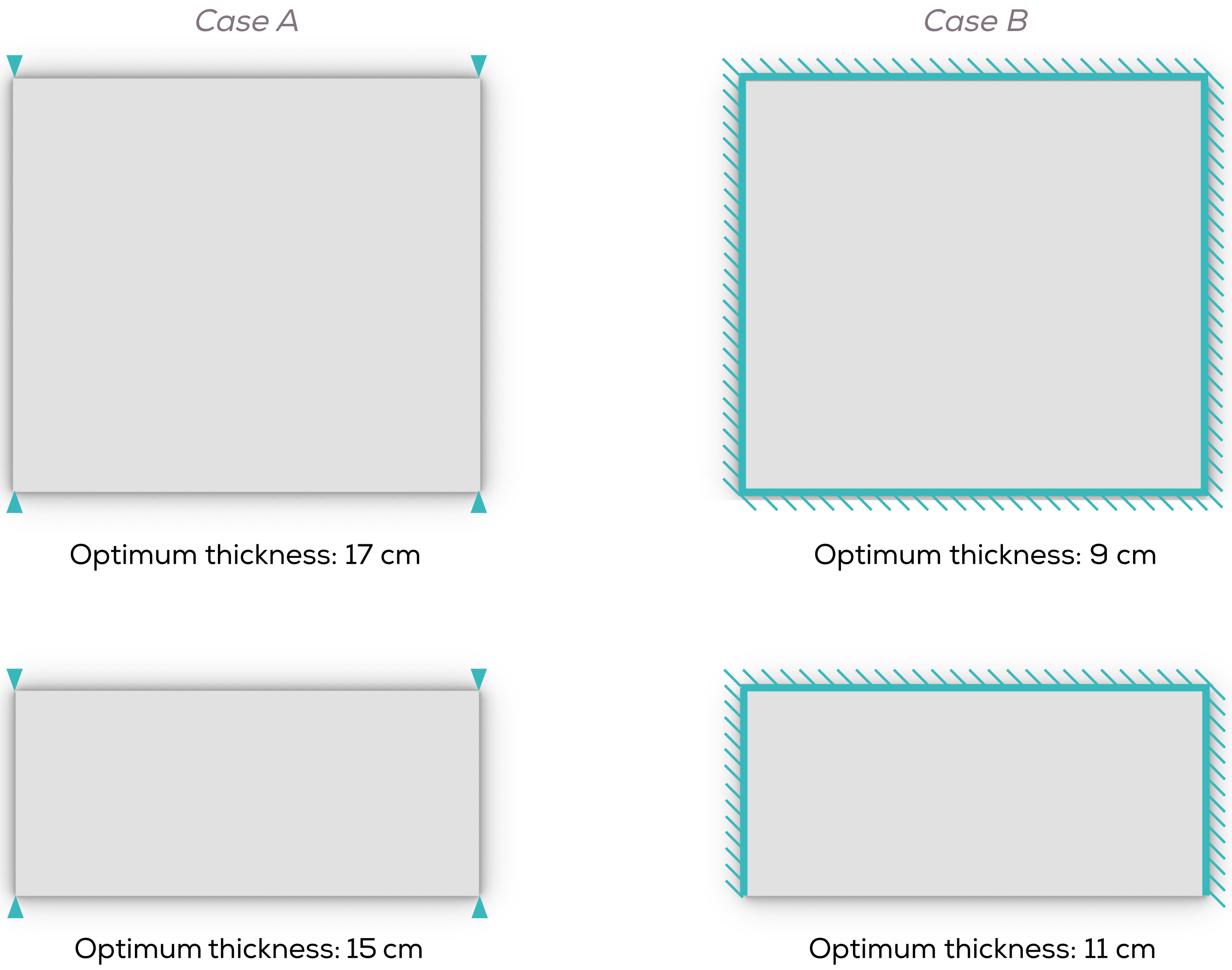

Figure 58: The two different support conditions applied and tested in whole (up) and half (down) slab.

As Figure 58 shows, a different optimum thickness arose from the analysis for each case, with a range of 9-17 cm. It is obvious that the case B, with the linear supported slabs, has the most preferable results, since less material leads to a lightweight, sustainable and with shorter and safer annealing time structure.
Therefore, the choice of the slab's thickness, which is used on later stages, is based on these results.

5.3. Shape optimization

As it is already mentioned in Chapter 3.5., glass, which presents 10 times higher compressive strength than its tensile, has better structural behavior in mostly-compression structures. In a slab, where the upper surface is crucial to be flat, a classic technique is to create a vault at the bottom of it, which, like the catenary arch, minimizes the tensile stresses. Therefore, the next step of the design development stage was to discover the optimum shape of the slab towards the above vaulted technique.

Although from the previous size optimization, the thickness of the half slab with the linear supports can be 11 cm, for the curved models, this value was considered as an approximate average of the thickness range. Therefore, 17.5 cm was set the maximum thickness and 8.5 cm the minimum.

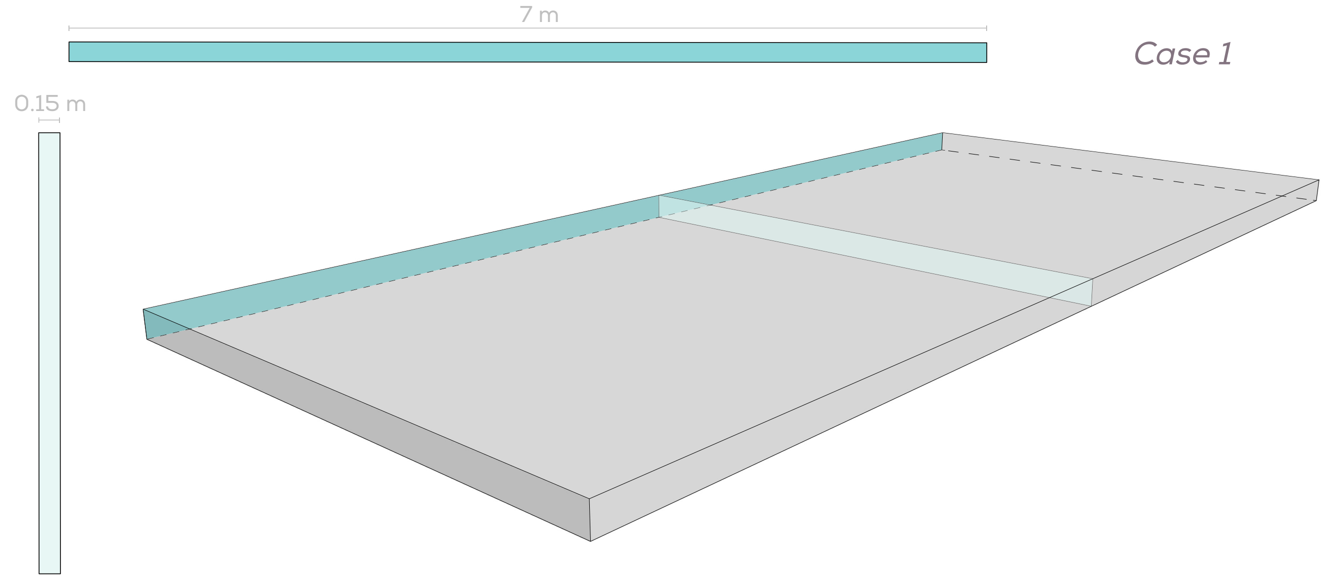

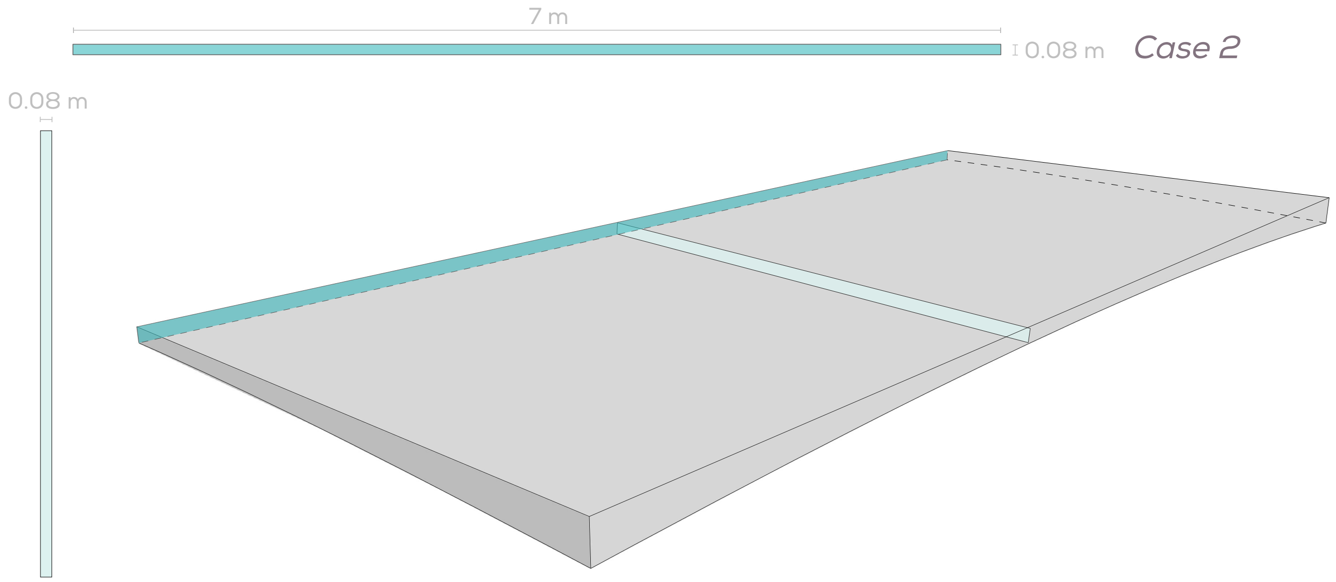

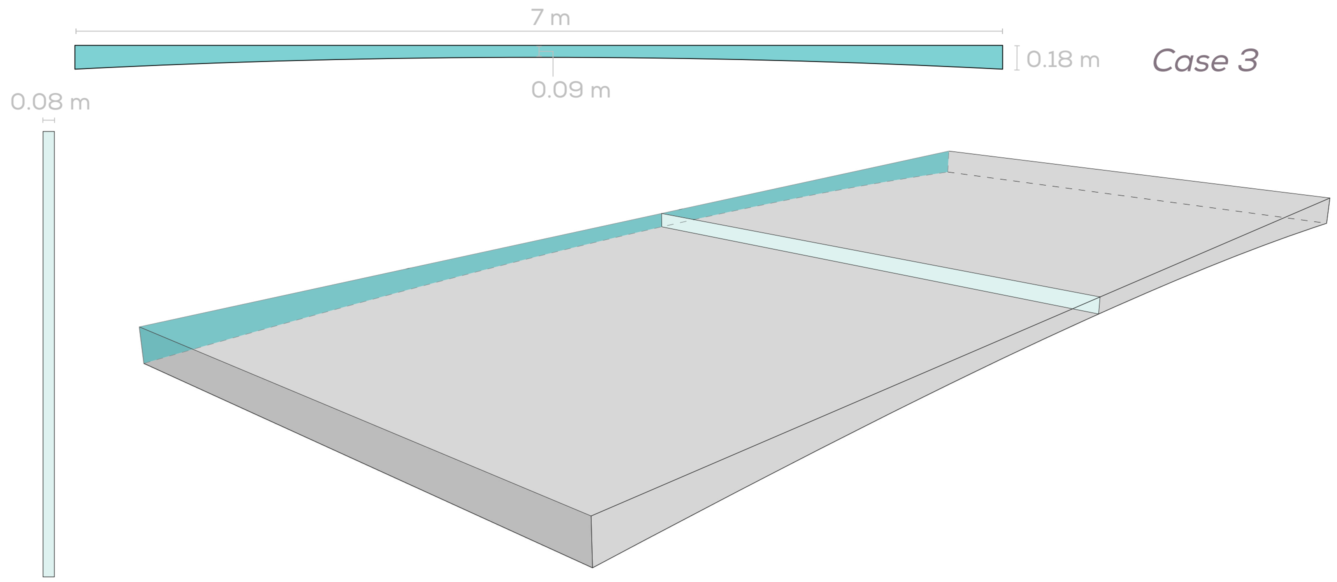

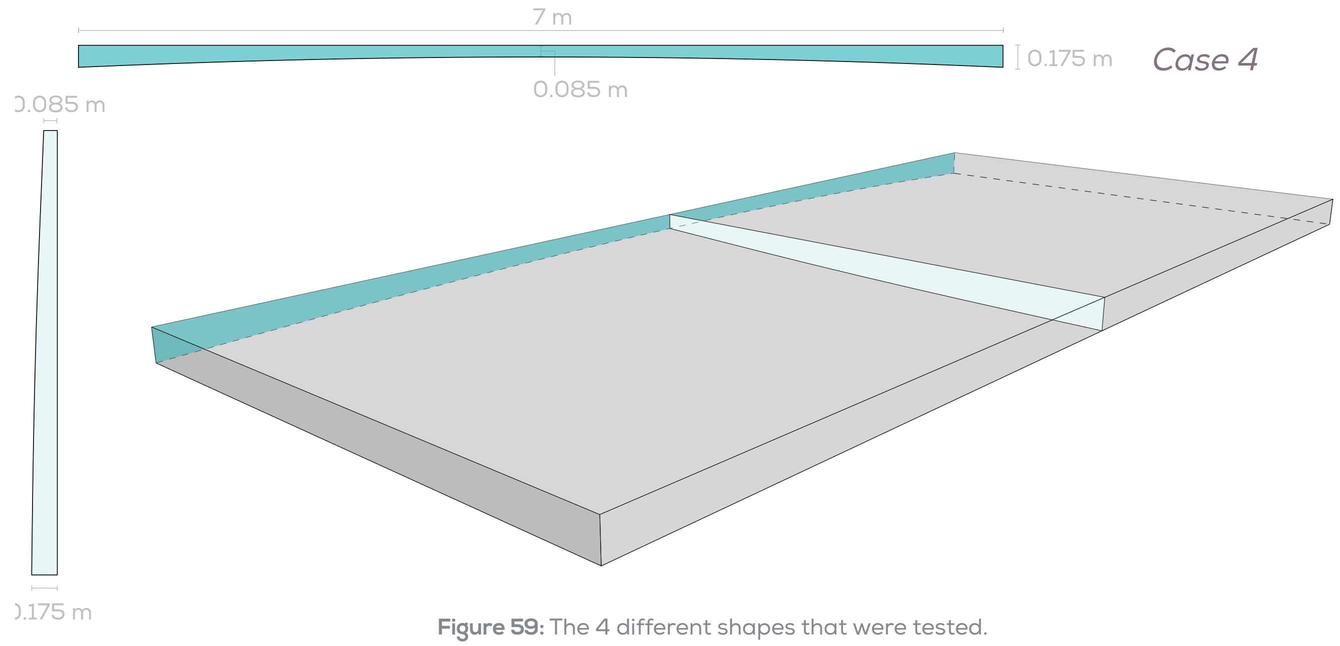

Figure 59: The 4 different shapes that were tested.

As Figure 59 illustrates, three alternative shapes were designed and tested with ANSYS relative to their mass, the total deformation and the maximum tensile and compressive stresses. Even though the design differences are slight in such big scale, the affect of the geometry in the structural behavior of each is considerable. The results of the analysis are displayed on the Table 10, in comparison with the first orthogonal design.

For the determination of the optimum shape, a dynamic relaxation method through Kangaroo, Grasshopper plug-in, was conducted. The first shape, a double curved geometry, evolved

from fixing the corner points of the flat mesh and splitting the slab. Although this alternative provides with a significantly more lightweight model, it presents an overall lower structural behavior.
The next shape, a one-sided curved slab, which derived from fixing the two facing edges, shows a slightly lower tensile stress, the most critical value for this optimization.

Finally, by fixing all surrounding edges and releasing the rest of the mesh, a geometry with only the middle face curved emerged. All structural values from ANSYS simulation, present a significant improvement in comparison with the initial simple design. Therefore, the fourth alternative design will be used for all the following steps.

	Units	Case 1	Case 2	Case 3	Case 4
Mass	kg	7465	4659	5793	7421
Total deformation	mm	2.246	8.892	3.766	1.905
Max tensile stress	MPa	10.856	19.632	9.129	6.100
Max compressive stress	MPa	-10.867	-18.973	-11.673	-7.205

Table 10: A comparison of the structural evaluation of each different shape.

5.4. Topology optimization

After the optimum size and shape of the model was obtained and structurally evaluated, the topology optimization, from which the final design of the slab emerged, started. As the initial methodology designates, the optimization would start with use of Ameba software, a Grasshopper plug-in, in order to obtain a faster first impression of the results due to the familiar Grasshopper environment and the simplicity of the software. In that way, the draft results of Ameba with the restricted availability of inputs could be compared, for research purposes, with the advanced results of Ansys. Unfortunately, due to license limitation no results could be obtained for 3d geometry, thus, the optimization was decided to be conducted in Ansys.

To begin with, since the slab consists of two pieces with identical boundary conditions and load exposure, both pieces will have the same result out of the optimization process. Therefore, for facilitating the computing procedure, only the one piece was used for the optimization, expecting a final symmetrical overall result.

The first step was to import the material properties, as they were presented in Table 9, Chapter 5.1. As the diagrams in Figure 60 display, the model obtained from the shape optimization is simply supported with hinged linear supports on three edges, allowing only free rotation around x,y axes. The live load q = 7.5 kN/m², here

F = 7.5 kN/m² * 3.1 m * 7 m = **162.75 kN**

and the dead load were applied on the top surface of the slab.

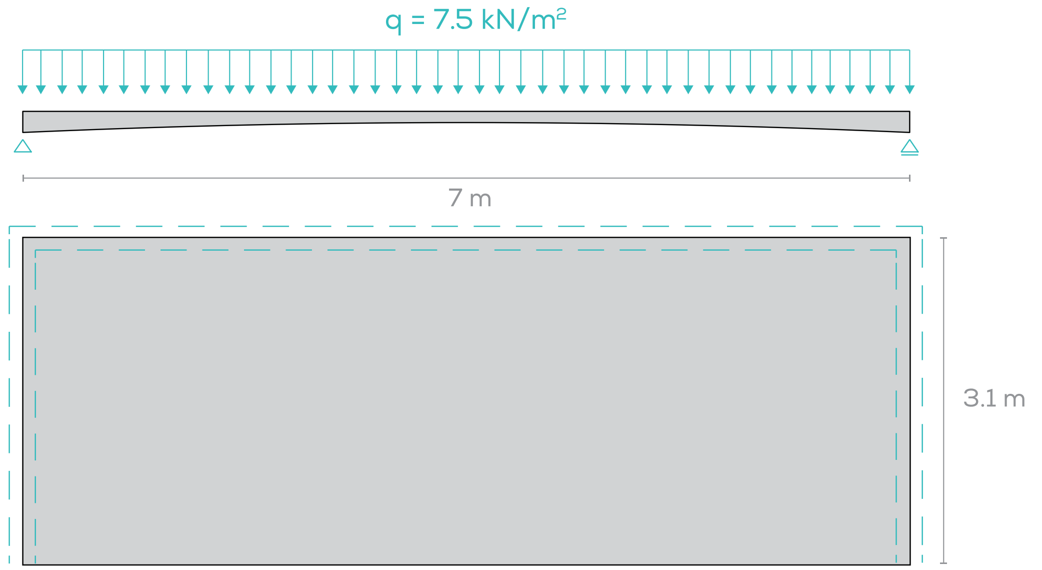

Figure 60: 2d diagrams showing the supports of the slab and the uniformly distributed live load.

Another important aspect that should be taken into account during importing the preset design criteria in Ansys were the voids' principals. Unfortunately, this parameter could not be included in the optimization phase. The only relative control was the min and max elements sizing which was unable to contain information regarding the area and span of a hole. Therefore, the retaining of the voids' restrictions as well as the check of the deflection and tensile stresses limits was being conducted after each optimization manually.

After setting the boundary conditions, loads, material properties and the desired goal of the mass reduction, the geometry meshing generation needs to be completed before starting the optimization. That stage was one of the most intriguing parts of the whole process. Due to educational license of the software, numerical limitations allows a specific number of nodes and elements in a project.

It was realized soon after several experiments with the software that as long as the mesh size remains big, the optimization generates coarse results by removing large size elements. That way a fine optimized model with smooth uniform distributed results of small elements removed wherever they do not contribute in its structural performance cannot be created. Therefore, the meshing size needs to be as small as the academic license allows.

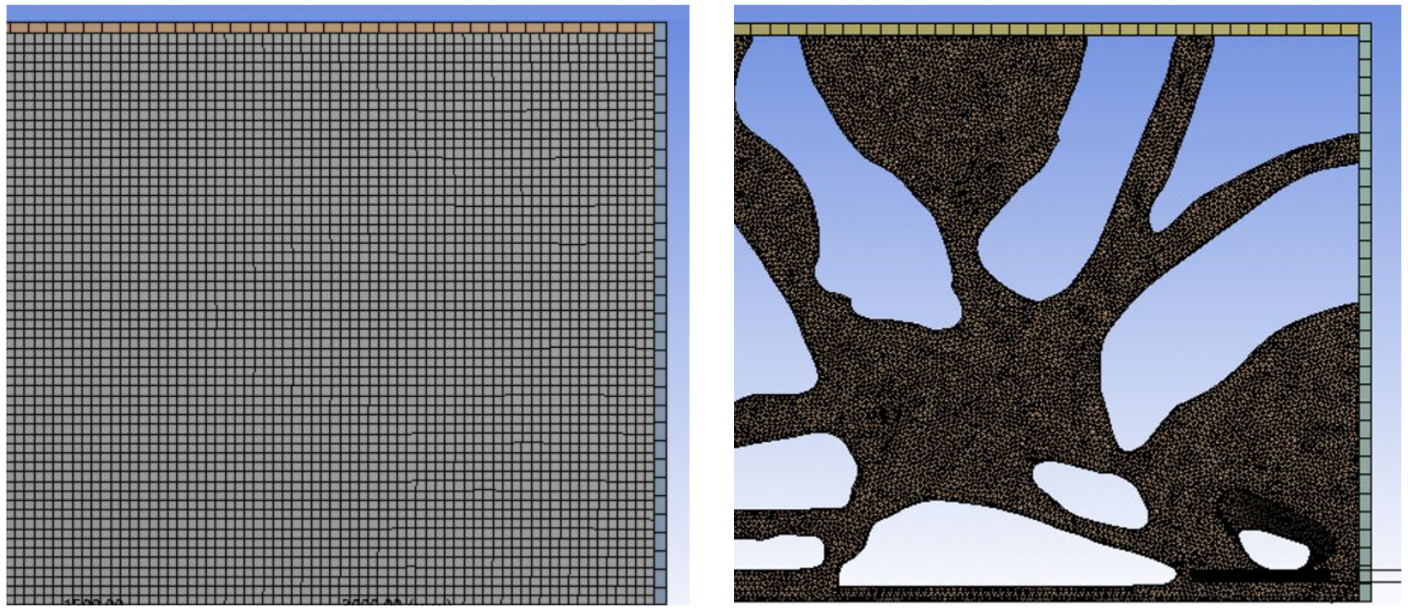

Figure 61: Meshing of the initial model with 52mm size vs meshing of the last optimization model with mesh size 14mm. Coarse meshing in contrast with fine.

In an attempt to overcome the software limitation for meshing, it was decided to perform various optimizations instead of a single one, in which the meshing size would be decreased gradually. The fact that in each step the mass would be further reduced, allowed an even smaller mesh size, since there was less material and therefore less elements and nodes. The optimization phase completes when the mesh size cannot be further decreased.

In Figure 62, the first results of four optimizations are displayed, in combination with the mesh size, the percentage of mass reduction and the critical structural values of each which can be found on Table 11. After each optimization in ANSYS Workbench, the obtained geometry was a rough model with plenty irregularities and open surfaces which rendered it impossible to be further used and analyzed in ANSYS. The meshing of such geometry was extremely time-consuming, if it was able to be completed. In order to overcome these difficulties, a new method of post-treatment for the acquired results was introduced.

The model was being converted in a merged solid body at Spaceclaim, exported to a .3dm file and then, in Rhinocheros, with the use of several designing tools, such as duplicate face border, Boolean, drape, etc, the geometry was being regenerated in a simpler, normalized form in accordance with the main principles of the coarse model, ready to be imported in ANSYS. Before the beginning of the next optimization, the redesigned model was structurally analyzed on order to check for stress concentrations.

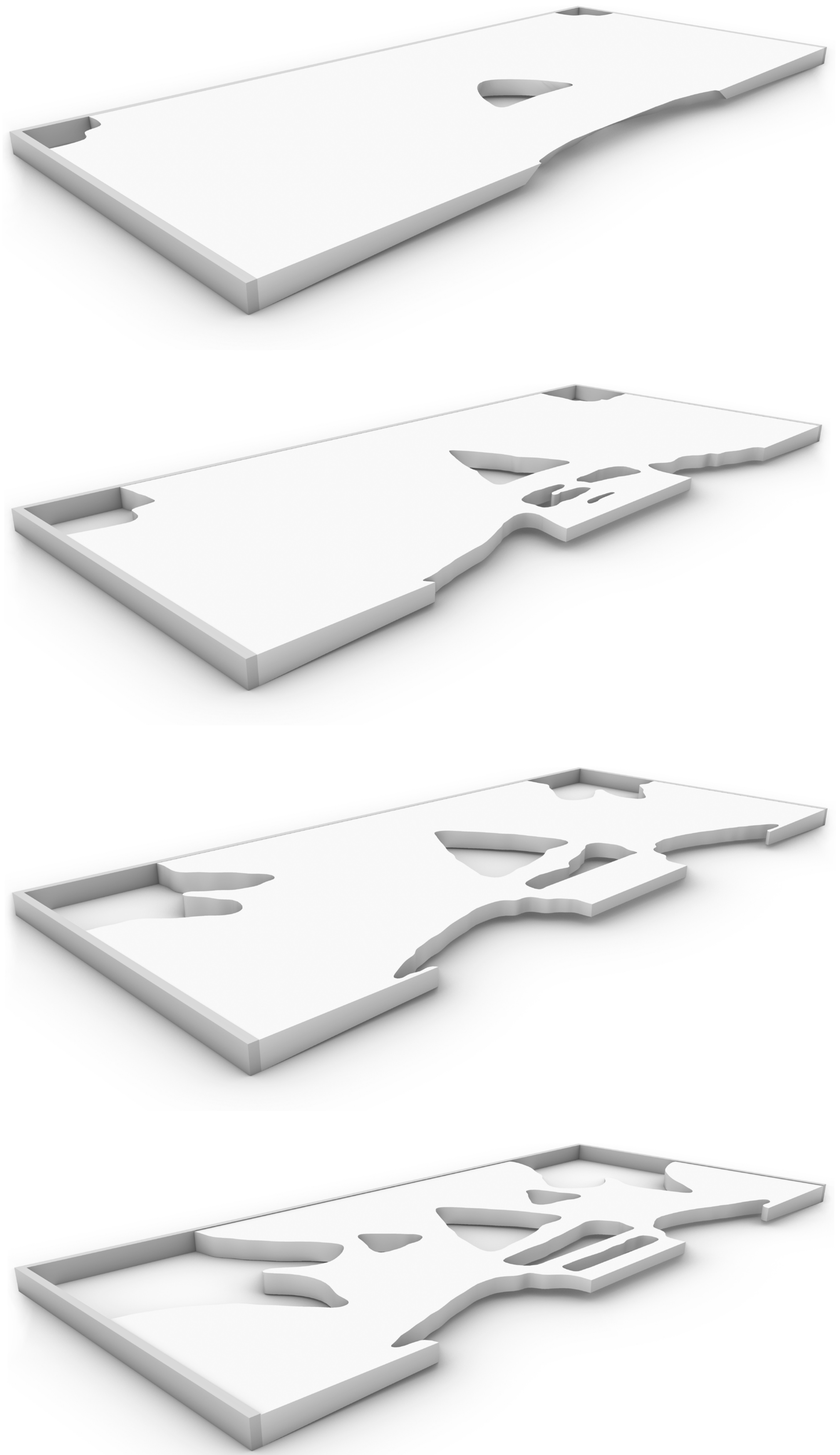

Figure 62: The first four optimizations' results until the concerning increase of the corner cavities.

	Units	Opt0	Opt1	Opt2	Opt3	Opt4	Opt4 alternative
Mesh size	mm	52	44	25	22	19	21
Mass reduction	-	-	6%	12%	26.5%	42.6%	36.2%
Total deformation	mm	1.905	1.719	1.878	2.099	2.545	2.374
Max tensile stress	MPa	6.100	5.875	5.734	5.815	6.709	9.650
Max compressive stress	MPa	-7.205	6.902	-6.475	-6.397	-7.455	-11.750

Table 11: Assessment table of all optimizations with valid results that were conducted.

Regarding the numerical results, in each optimization the mass reduction was almost double the reduction of the previous one, aiming to reach gradually a low mass value almost half of the initial one. On the first three optimizations, there was actually an improvement on all critical structural values, proving that over-designed structures can bring worse results.

On the fourth optimization a slight increase was presented while an undesired enlargement of the corner voids was noticed. Since the corner areas are closer to two-sides support, it is rational to require less material, however, the generated holes were exceeded the preset restrictions, both area and span limits. To demonstrate the unsuitability of these holes a structural simulation including the top float glass panes was conducted, as Figure 63 illustrates.

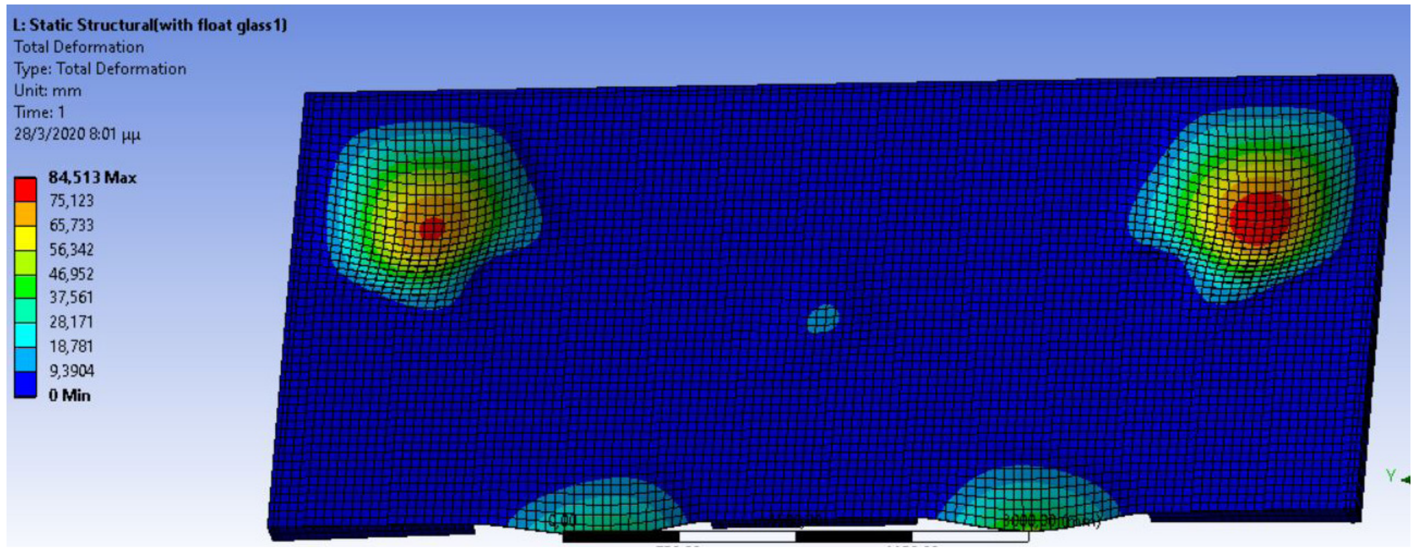

Figure 63: The total deflection of the float glass layers.

Indeed, the deflection limit for these holes was 10,3 mm, as obtained from the Karamba script, way less than the simulation in Ansys showed.

Therefore, addition of extra elements to minimize the holes was essential. Figure 64 displays the additional elements that were implemented in the model of the fourth optimization. As it was expected since the mass increased the mesh size of the new model rose again. Nevertheless, the deflection of the new model was demonstrated less than the allowable limit (Figure 65).

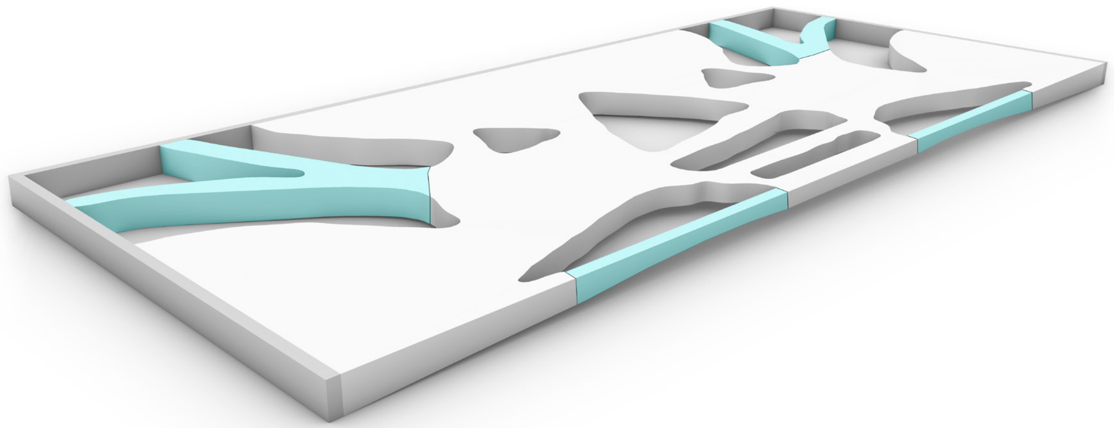

Figure 64: The additional elements minimizing the voids opening.

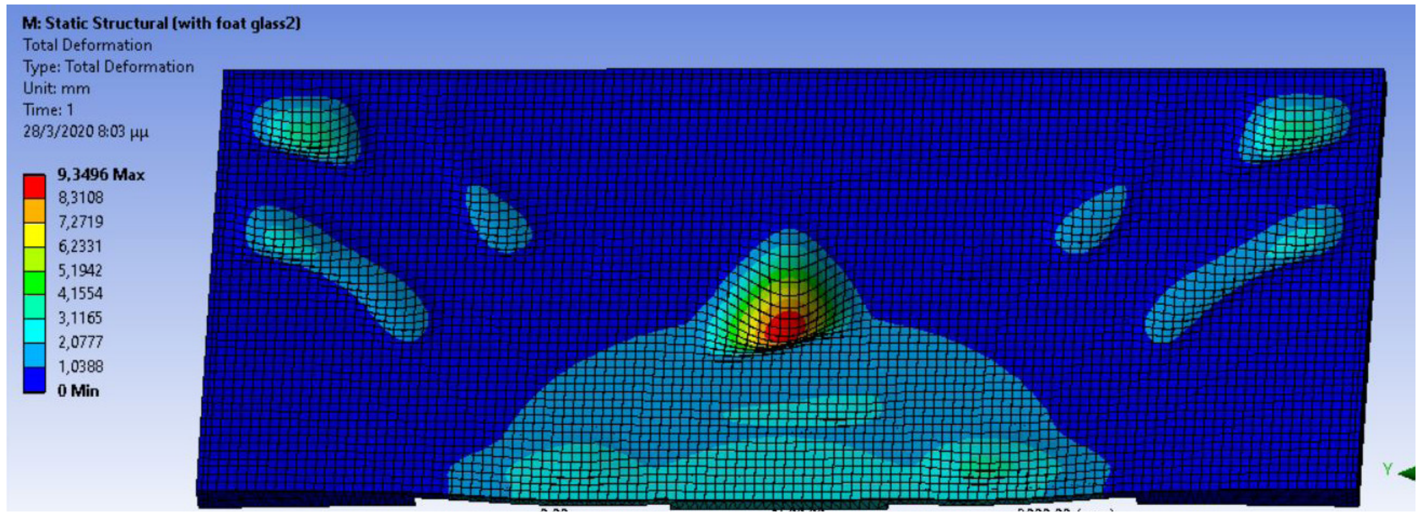

Figure 65: The decreased deflection of the float glass after the additional elements.

As a general notice regarding topology optimization in ANSYS, the algorithm of this software, based on the SIMP method, is not able to refill the model. Unlike the BESO algorithm, SIMP cannot add elements that can positively contribute in the model's overall structural performance, only removes those with the smaller contribution.
During the optimization process, there may be elements in the model which should not be removed, despite the fact that they do not con-

tribute on the structural stiffness of the body. Such elements can be the ones in Figure 64 or the faces between the two slabs where a connection needs more material to exist. The only way to secure the retaining of these elements is to include them or their faces in the exclusion region of the optimization.

At that point, in order to further minimize the mesh size, for a more uniform distribution of the mass throughout the slab, the model was divided in half. Focusing only in the one half of the slab would provide a model with less elements and nodes that would not exceed the license limitations. A remote rotation around x and y axis was introduced on the split edge in order to simulate the structural behavior of the complete slab. Since each half body ended up with identical boundary conditions, geometries and load application, the final 7*3.1 m slab will be the merging of the two symmetric pieces.
In that way, the half slab was able to be further optimized three more times as long as the meshing size could still decrease. The last results are shown in Figure 67 and Table 12.

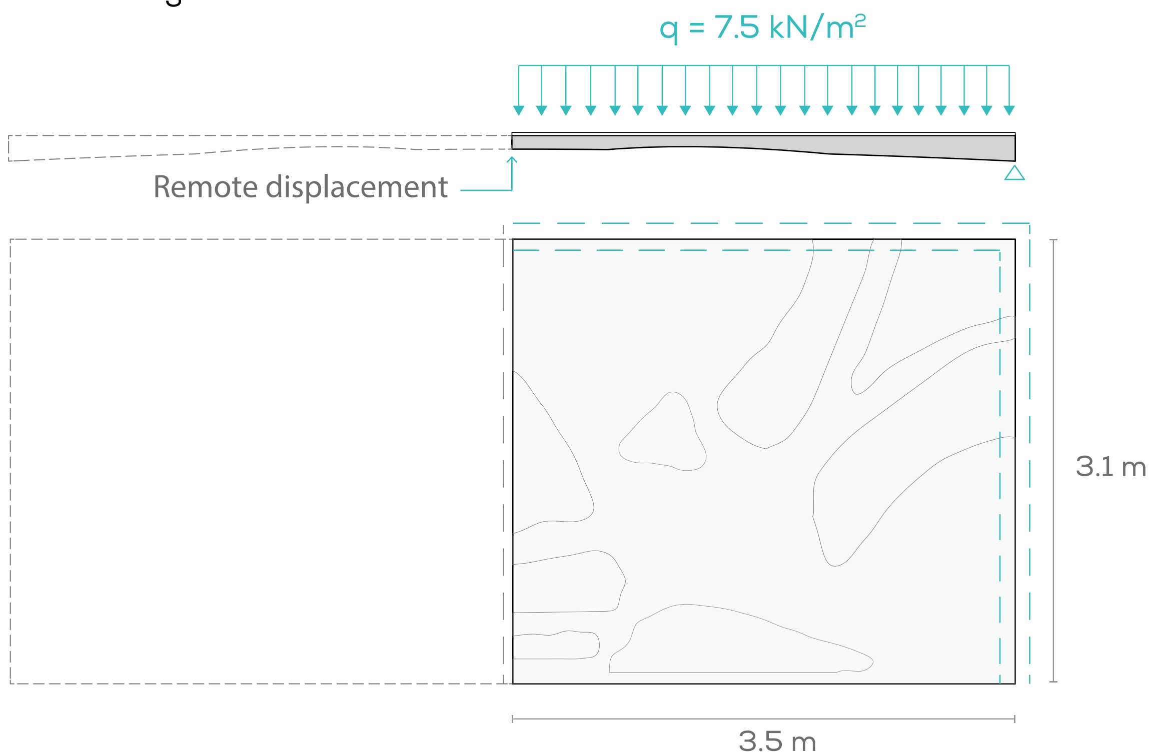

Figure 66: 2d diagrams showing the supports and load condition of the half slab.

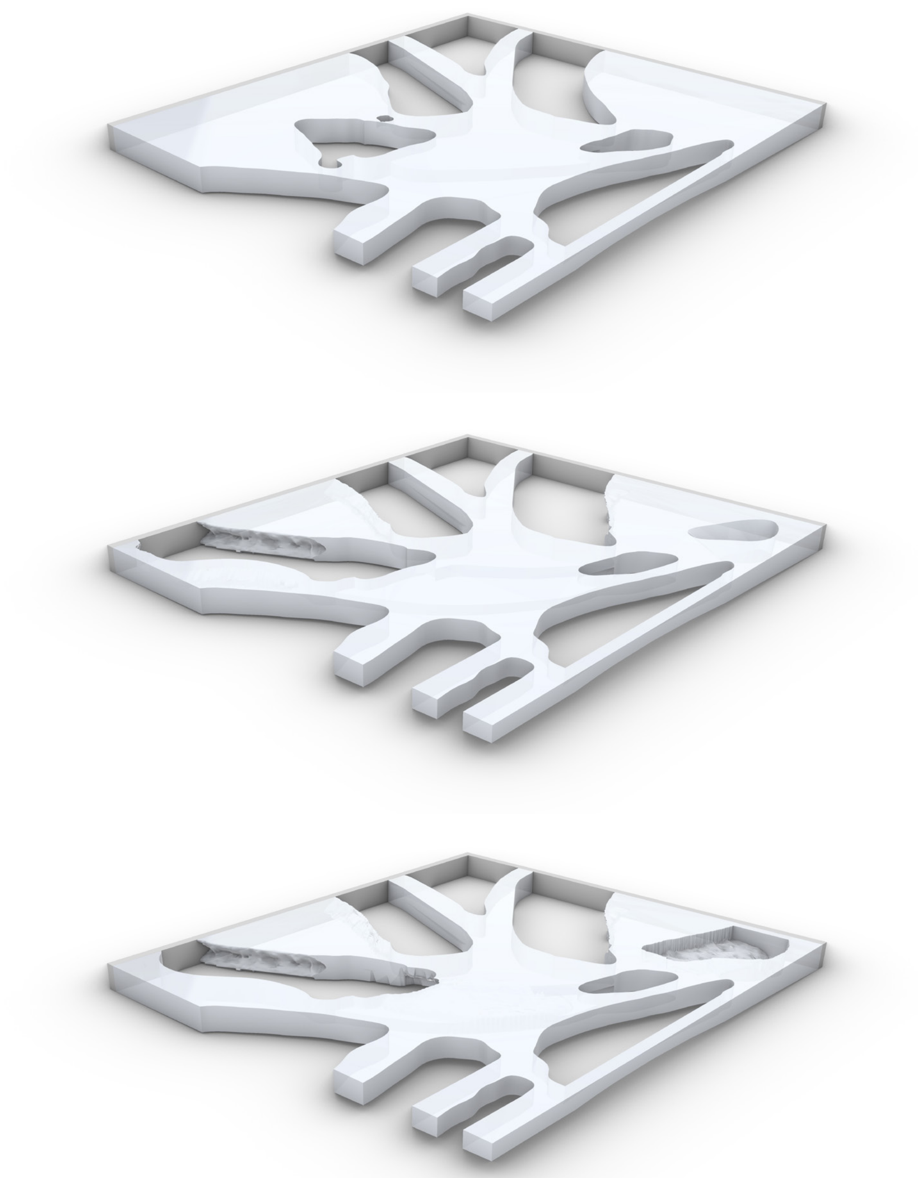

Figure 67: The last three optimizations after splitting in two the slab.

	Units	Opt5	Opt6	Opt7
Mesh size	mm	16	14	14
Mass reduction	-	37%	48.8%	55.2%
Total deformation	mm	-	-	4.780
Max tensile stress	MPa	12.536	13.462	16.503
Max compressive stress	MPa	-12.728	-13.245	-16.838

Table 12: A comparative listing of the last 3 optimizations. The deformations of the 5th and 6th optimization were omitted since half geometry was only tested and not the entire slab.

The deduction of all the previous regarding the topology optimization process was a **55.2%** lighter slab with a better distributed mass throughout its initial bounding box. Although the critical structural values were slightly more than doubled until the last optimization, they do not exceed the pre-calculated limits.

Plenty limitations and difficulties were phased during that phase which will be extensively discussed in a following chapter.

5.5. Post processing of the final result

After obtaining the final optimum design, one last process for improving the quality of the surfaces and removing any flaws and sharp edges was required.

For compatibility reasons, the post-processing phase was performed in the ANSYS environment, in Spaceclaim. The Ansys Discovery SpaceClaim is a 3d modeling application with a variety of tools for fixing geometry problems, repairing and simplifying it.

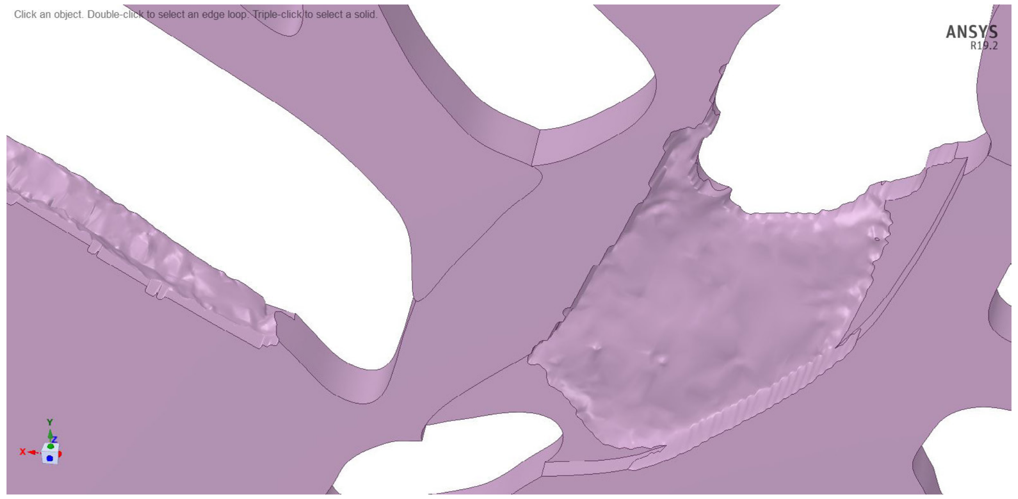

The rough result of the final optimization with sharp and irregular surfaces which consists an inappropriate model for glass casting.

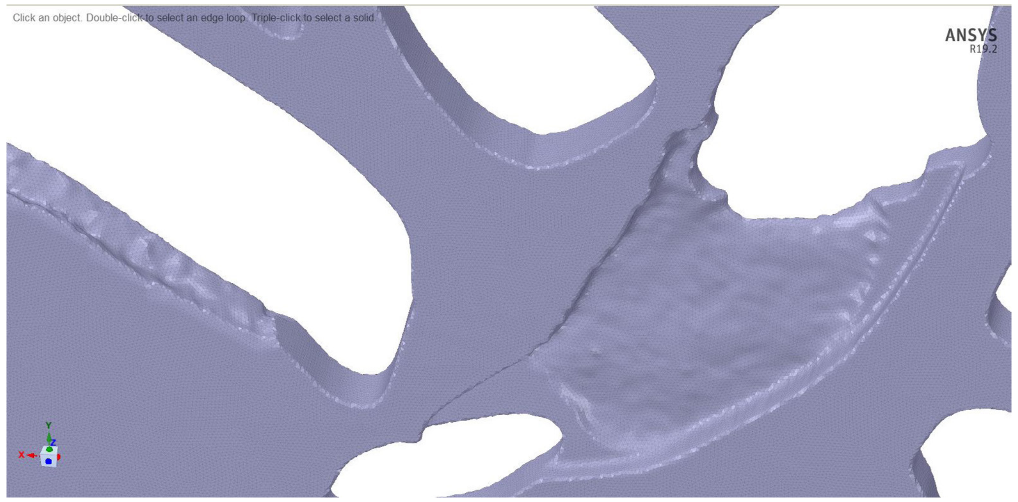

This picture represents the better quality surface after using the *shrinkwrap* tool. The function of this tool is based on draping a triangular mesh around the model and envelops it with the chosen tolerance of detailing to be determined from the mesh subdivision degree.

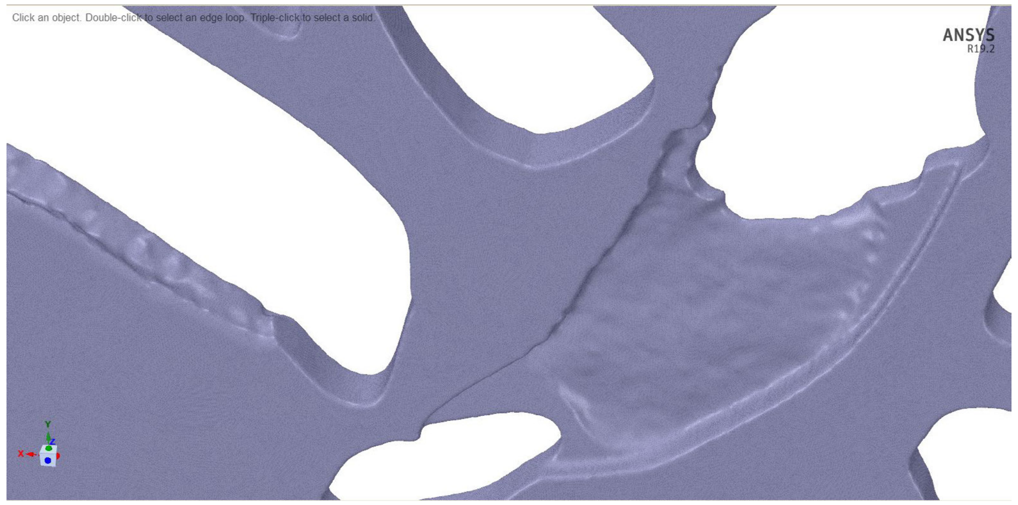

The final post processing step is to smooth the *shrinkwrap* facet using the namesake tool which offers a local or approximate choice. For this project both choices were used to heal the complicated problematic model.

6. Fabrication and assembly

Once the final design is obtained, it is time to study in detail how the slab system could be produced and integrated into the museum.

6.1. Slabs connections

All the optimization and structural simulations were performed including only the linear circumferential supports of the slab, allowing free movement and rotation in the edges where the slab is split. However, for practical reasons a connection between the two pieces seems to be necessary.

The necessity is demonstrated in Figure 68, while from a structural analysis of the unconnected pieces with load applied only in one half, a step of almost 1 cm is created between the two pieces. This step can be dangerous for the visitors as well as for the glass elements. The visitors could trip over on the step making the motion on the slab unpleasant while the edges of the glass, float and cast, can be exposed with high risk of damage, for example from a cleaning machine.

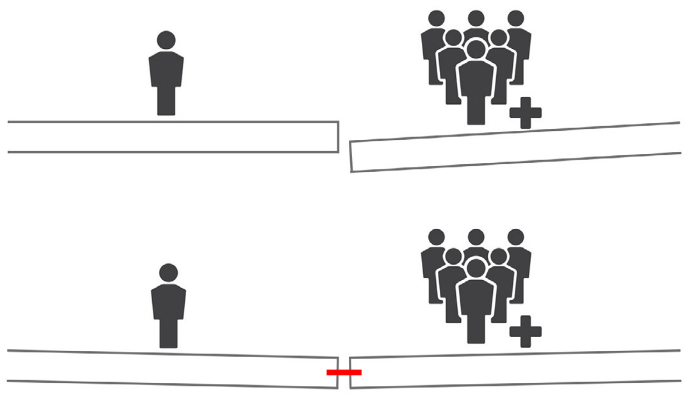

Figure 68: The step between the two slabs caused from different distribution of the live load can be normalized with the use of a connection.

The use of adhesive in the connection was rejected in order to facilitate possible disassemble and replacement half of the slab in emergency case of breakage or failure. Instead, a solution which allows the disassembly of the slabs was searched. Several designs were generated and tested, as Figure 69 presents, until ending up with the best solution.

The first design, which was inspired from the literature, is not appropriate for a glass body, after all, since the stresses in the area of the connection can break the bumps.

Then an external metal element was decided to connect the two slabs, like the second image, but the type of the connection demanded a horizontal assembly of the slabs which is impossible in that case as the slabs need to be sink into an existing cavity of the building.

Finally, after converting the connecting elements to be compatible with the need for vertical assembly of the slabs, the elements that initially designed were too complicated to be connected on site while they will be pre-laminated on each piece.

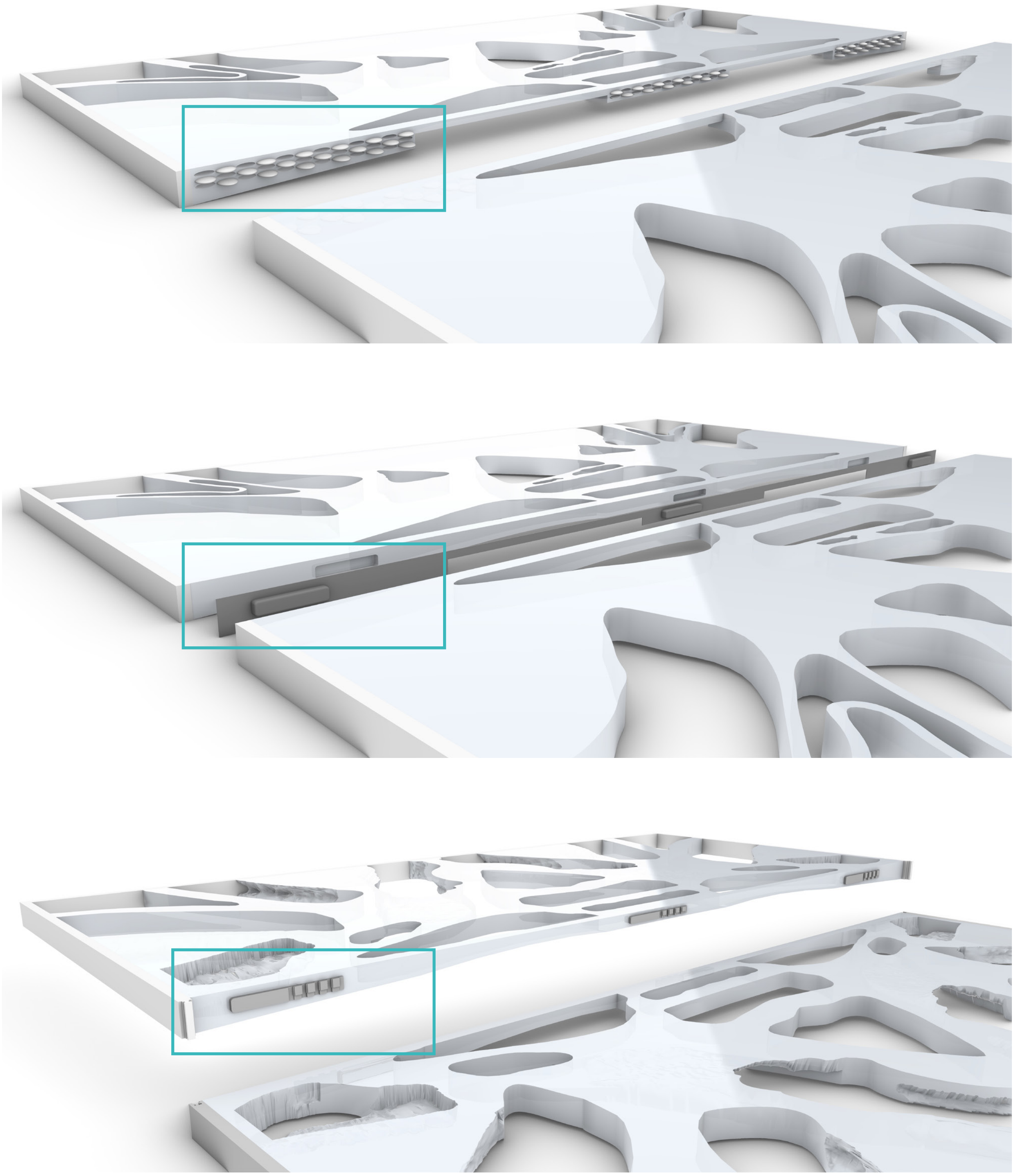

Figure 69: The evolution of the connection design.

Therefore, for the final design, an easy to be assembled connection was designed as the next figures show.

In the fourth design, three connecting positions found to be the most appropriate in order to distribute the load evenly. The connections are based in a simple system of interlocking elements, while a series of nuts and bolts secures them.

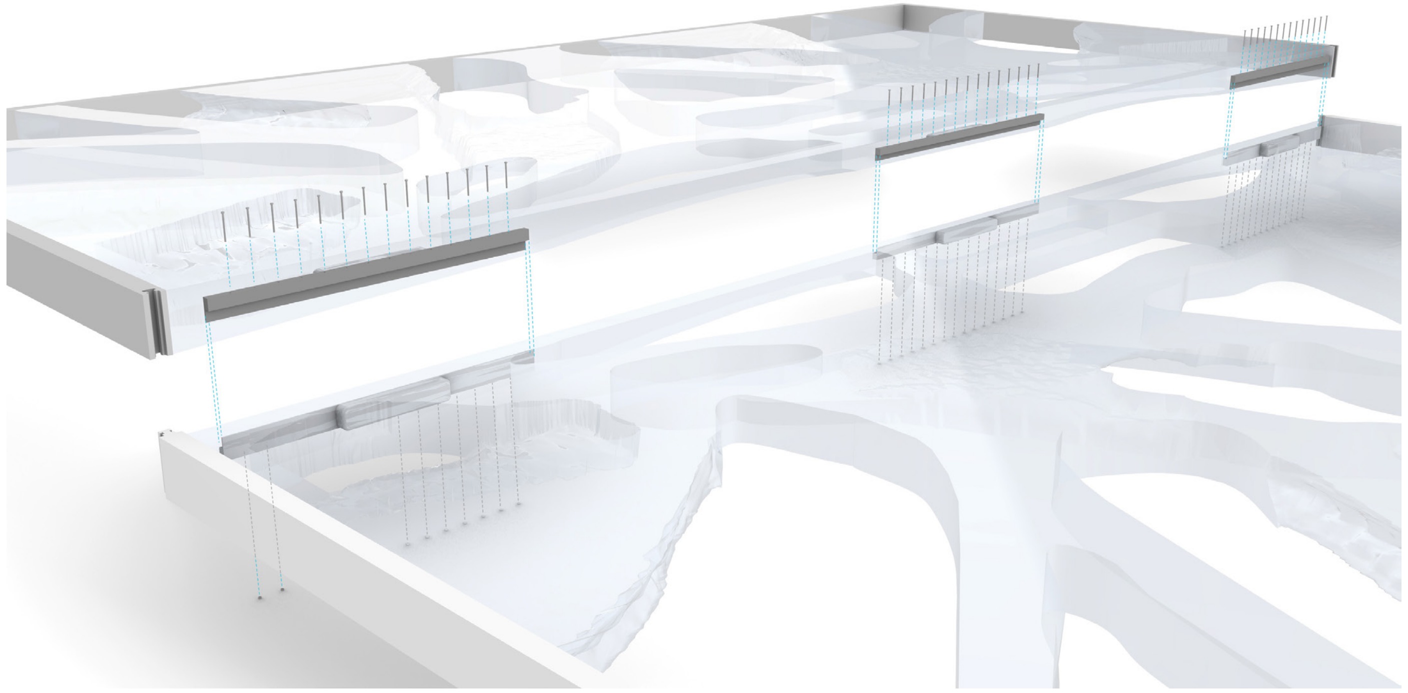

Figure 70: Axonometric exploded view of the final connection design where the 3 pairs of interlocking components are displayed, along with the bolts and the nuts that secure them.

As the top view in figure 71 and the cross section in figure 72 illustrate, a part of 5*38 cm from each element is laminated inside the slabs in cavities that are generated during the casting. The external parts of the connections are extended in both directions, while a neoprene layer separates the glass and the metal connections, absorbing any vibrations and accommodating the tolerances. M10 bolts are fastened from the top of the slabs and nuts secure them from the bottom. The gap that the connections create is a 4 cm cavity that needs to be covered with a spacer block to protect the bolt heads and secured with an aluminum covering. Silicon seal layers protect the contact between the above parts.

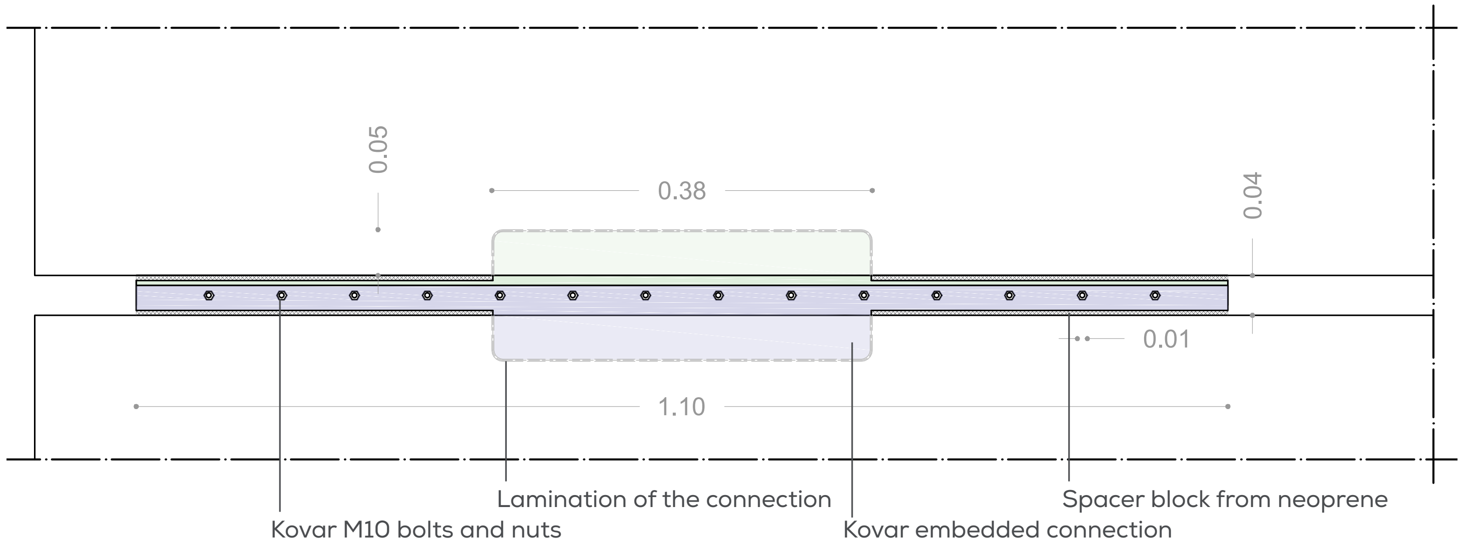

Figure 71: A top view drawing of one of the three connecting points.

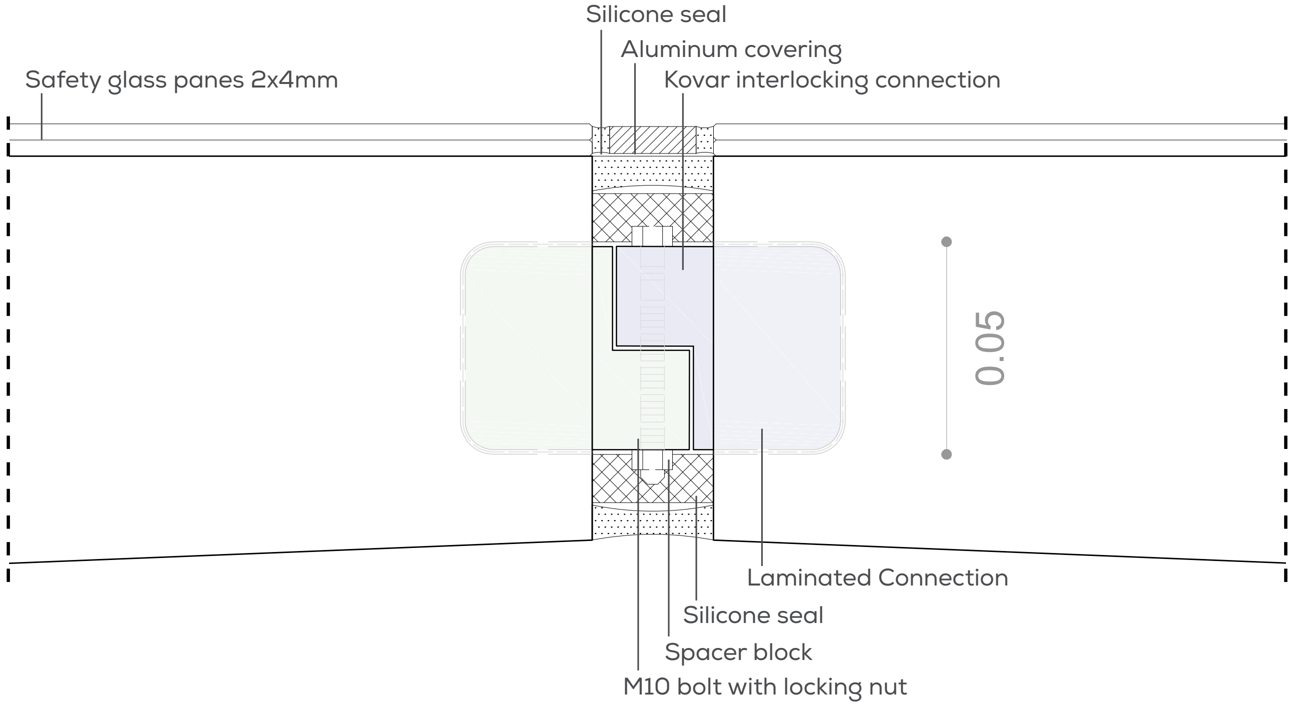

Figure 72: The cross section of the connection of the two slabs with the peripheral layers.

The embedded connection consists of kovar while a softer rubber, like neoprene, acts as an interlayer between the connection and the glass.
The purpose of using kovar here originates on the similar thermal expansion coefficients of the two materials, borosilicate and kovar, the properties of which can be seen in Table 13 and Appendix D.
In the embedded part of the metal components, the spacing between them and the glass is so thin that cannot accommodate differences in thermal expansion. Therefore, the bodies need

to change similarly and kovar is one of the best choices among the other metals. However, a soft interlayer from rubber or silicone is always essential when glass and metal materials are in contact in order to protect glass from localized stresses.

	Unit	**Kovar**
Density	Kg/m^3	8320-8400
Young's modulus	GPa	135-141
Tensile strength	MPa	517-621
Compressive strength	MPa	345-410
Poisson's ratio	-	0.312-0.322
Thermal expansion coefficient	μstrain/°C	4.6-5.5

Table 13: Mechanical and thermal properties of the chosen metal for the connection-Kovar. (CES Edupack, 2019)

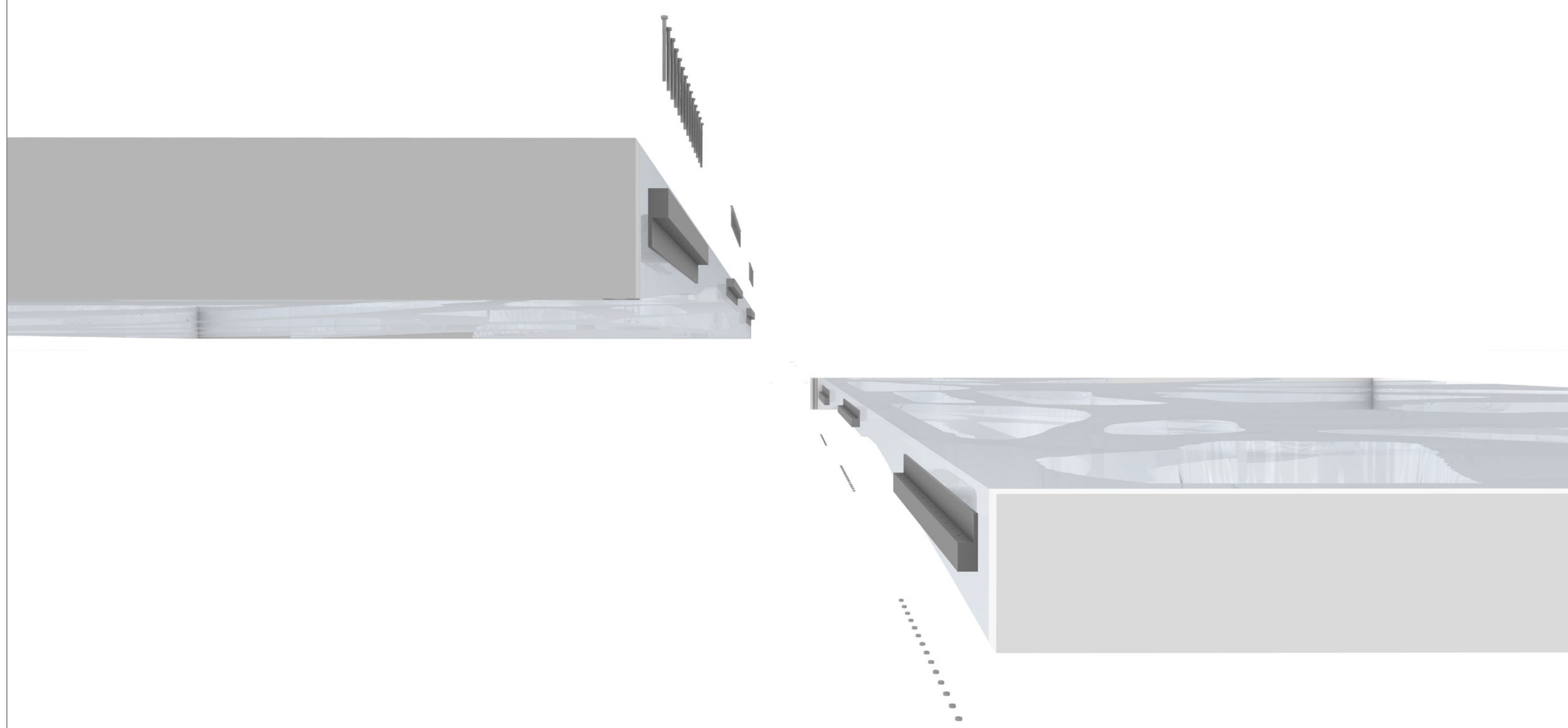

All alternative connections were structurally analyzed in Ansys and can be found in Table 13 and Appendix E. All alternatives were tested under two load cases. In the Load Case 1 (LC1), the two slabs are under a uniformly distributed load. However, in the Load Case 2 (LC2), only the one slab carries the 7.5 kN/m2 live load, while the other has only its dead load.
Since the models contain several elements, the academic license and the numerous contacting surfaces complicate the analysis and lead to results that may differ from the reality. Physical prototyping experiments are suggested as further development, which could demonstrate the results. For the current project, the analysis results for connecting the two slabs are employed comparatively.

	Units	Connection 1		Connection 2		Connection 3		Connection 4		Connection 4a	
		LC1	LC2	LC1	LC2	LC1	LC2	LC1	LC2	LC1	LC2
Total deformation	mm	1.92	1.23	1.94	1.24	4.27	2.26	3.82	2.05	4.23	2.44
Max tensile stress	MPa	34.4	27.1	12.7	8.6	69.8	50.3	106.3	165.1	42.3	22.9
Max compressive stress	MPa	-16.6	-10.3	-12.9	-9.8	-104.6	-54.9	-114.8	-191.1	-46.7	-25.2

Table 14: The important structural values of all alternative connections, each under two different load cases.

As the above table demonstrates, although the fourth connection presents a more convenient assembly, the tensile stresses that are generated under the live load can be very high. Despite the fact that these stresses are concentrated in the metal connections, which can resist them, they can also transferred to the glass and cause failure.

For this reason, the middle hole, right behind the middle connection, which is the one that concentrates the most stresses due to higher deflection, was closed, Figure 73. In addition, the interlayer between glass and kovar was imported in the simulation and an attempt of minimizing the amount of elements, provided with a finer mesh.
The results after this improvements were much lower than the previous and can be acceptable considering the limitations of a digital simulation, as the Table 14 shows.

Figure 73: The critical holes that closed in order to increase the material and therefore the stiffness around the middle connection.

6.2. Slabs fabrication

For the fabrication of the slabs three phases can be considered. The first is the fabrication of the mould. This stage starts with the printing of the mould pieces, then the assembling of them and the preparation for the furnace. Afterwards the glass is placed on the mould cavity and the whole system is ready for the kiln-casting process. The next important stage concerns the annealing process of the products.
If this stage is successfully completed, the lamination of the safety float glass sheets and the framing of the slabs can take place before the two slabs are transferred to the building.

6.2.1. Mould fabrication

Mould separation

According to the Chapter 4.2, the 3d printed sand moulds considered the optimum solution for the current project. However, even these moulds present a significant limitation, which generally needs to be overcome aiming to a quicker integration in the building environment. The printers of sand moulds have restricted dimensions, with the largest one not exceeding a 4*2*1 m building platform.
Therefore, since the studied slabs' maximum dimensions are 7*3.1*0.18 m the mould needs to be printed in segments. In order to decide the division points, multiple factors were taken into account.

The main aspect that was considered for the separation was an almost equal volume for each piece, in order to facilitate their transfer. According to the company Voxeljet, a mean density of the sand printings is 1.4 kg/L. Therefore it has been calculated that each piece range between 130-200 kg. For their transfer into the furnace setting, a combination of human force and small machine, like a mini crane, will be employed. That way, a careful and delicate treatment will protect any failure of the brittle sand moulds.

Apart from equality in pieces weight, it was important to split the pieces in areas that will not expose and endanger small and very thin elements of the mould. In addition, the size of the pieces should be small for easy transportation but at the same time large enough to eliminate the joints in between them.

Infill-shell

A significant aspect when it comes to 3d printing, especially in large scale products, is the efficient treatment of the solid areas. Printing an element with 100% density can be highly time-consuming and at the same time increases the cost of the printing.

A solution when these areas are big is usually an infill structure that replaces these solid areas. The infill structure can have any pattern, with more frequent honeycomb, grid, triangular, rectangular, concentric structure, etc. In addition, the density of the infill can vary depending the functionality of the element and the required strength. The most common infill densities range within 20-25%, balancing between strength and time reduction. A lower infill can be suitable when time-cost minimization is the main concern, while a higher density provides a stronger, functional component.

Less strength	Usual density 20%	Functional element
Cost effective		Time-consuming

As figure 74 highlights with the lighter color, the mould for the obtained slab contains plenty of these solid areas, in between the mould cavity, which should be replaced with an infill pattern. As a common practice, a shell of consistent thickness surrounds the mould cavity in the entire mould, while the rest unused solid parts are replaced by the chosen pattern. The importance of this equal-thickness wall around the cavity considers both the mould stability and the glass uniform annealing.

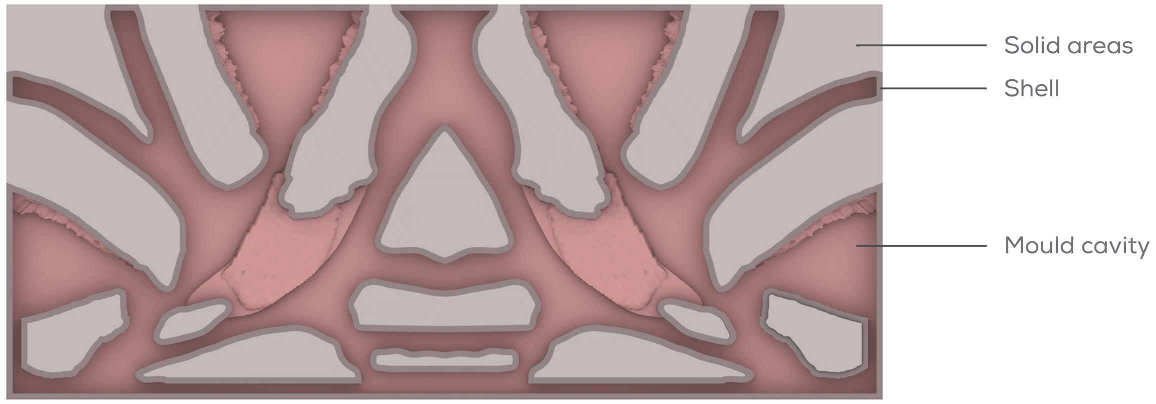

Figure 74: The solid areas which need replacement and the mould cavity in which the glass will be formed.

In order to estimate the required thickness of the shell, a calculation of the hydrostatic pressure that is generated during the glass melting, was conducted. The maximum pressure that the shell should be able to resist is 4414.5 N/m^2 and the analytical calculations can be found in Appendix F.
For a more valid result, the wall of the mould cavity contacting the biggest amount of glass was examined. Also, the bending strength of the sand mix, 220 N/cm^2 was included in the calculations.

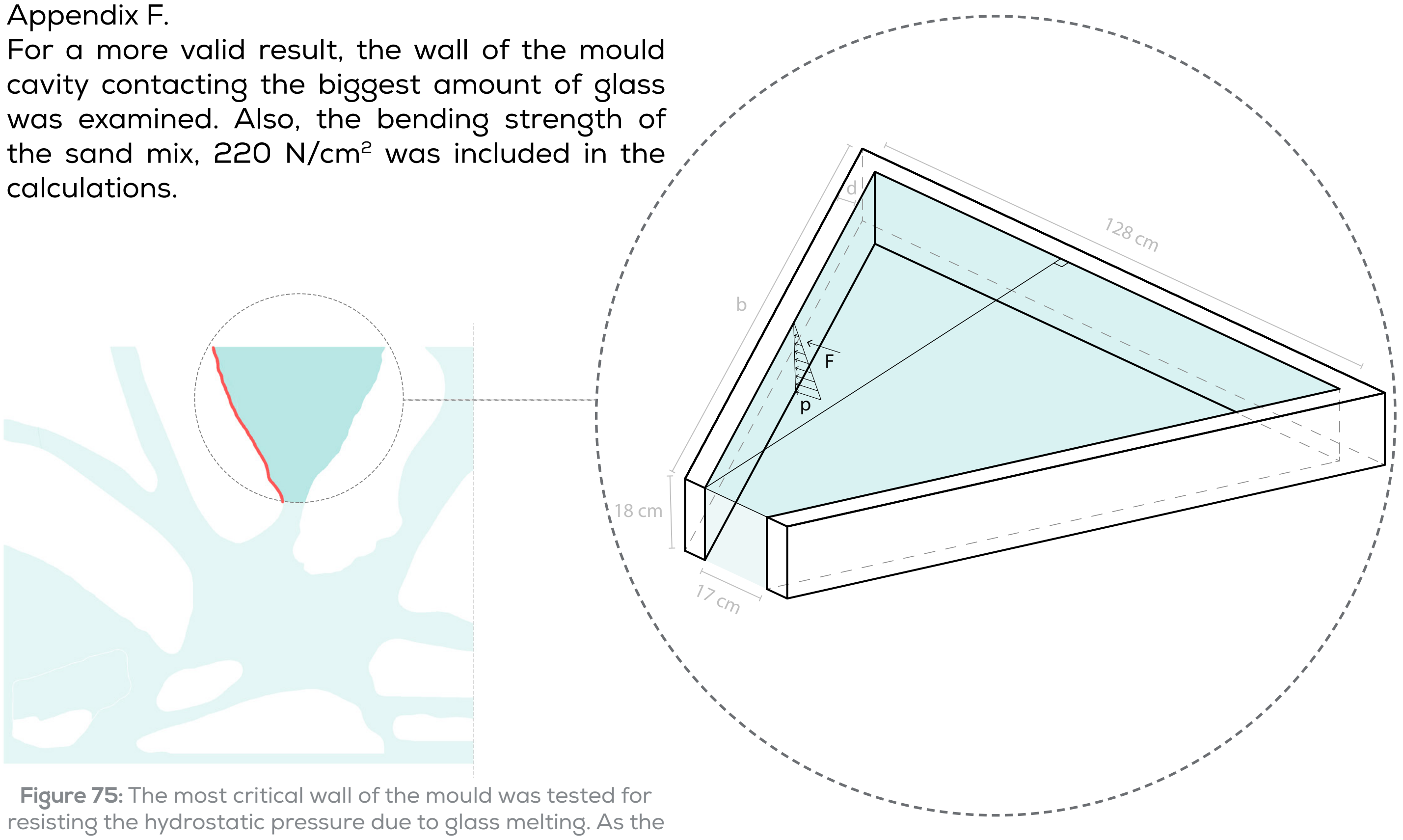

Figure 75: The most critical wall of the mould was tested for resisting the hydrostatic pressure due to glass melting. As the pressure is proportional to the depth, the bottom part of the wall accepts the highest pressure.

The required thickness that resulted from the calculations is 2 cm. However, since the values are theoretical and in reality situations the materials probably cannot reach their full strength capacity, an increase of that value was considered.

Before design the shell and infill alternatives, specific criteria were considered as an outcome from all the above.

- Consistent thickness of shell
- Similar amount of material on each side of the mould cavity (outside of the shell)
- Stronger on the bottom-lighter on top (following the hydrostatic pressure magnitude)
- Resist pressure p ≤ **4414.5 N/m^2**
- Accommodate connections of the pieces
- Lightweight (around **20-25% density**)
- Minimize printing time
- Minimum thickness **4 mm**

Two alternative proposals were designed regarding the optimum shell shape. As figure 76 illustrates, a buttress-shaped shell of a uniform thickness range 3-6 is proposed inspired from the dam walls' structural system. The other solution integrates a honeycomb structure of a 30% density, as it is a functional element, in between of two thin solid layers.

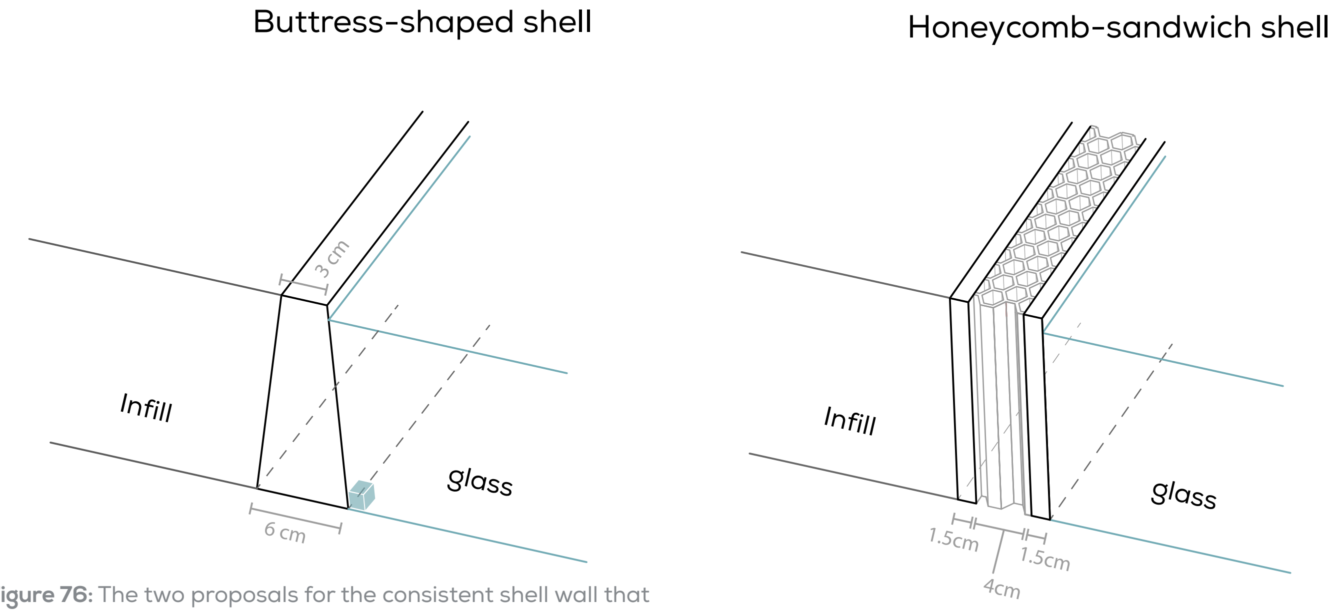

Figure 76: The two proposals for the consistent shell wall that surrounds the glass.

Regarding the infill structure, four alternatives were designed and evaluated according to the weight reduction and, therefore, the time and cost minimization.

The first solution regards letting the unused areas hollow and filling them with the loose sand that will already cover that parts in the sand bed, Figure 77. That way, the mould pieces will be compacted and stable during the glass melting and annealing process.

Another option was an infill from honeycomb structure in order to stabilize the mould pieces but at the same time provide a more lightweight component. The density of the honeycomb is 20%, the common infill density that balance strength with time and cost minimization.
Under the same method the third option refers to a grid structure of higher density, as figure 79 illustrates.

Finally, an alternative similar with the first shell proposal, is presented in figure 80. The buttresses are placed in every 15cm and they will be surrounded by unconsolidated sand, as the first option.

Option 1: Loose sand

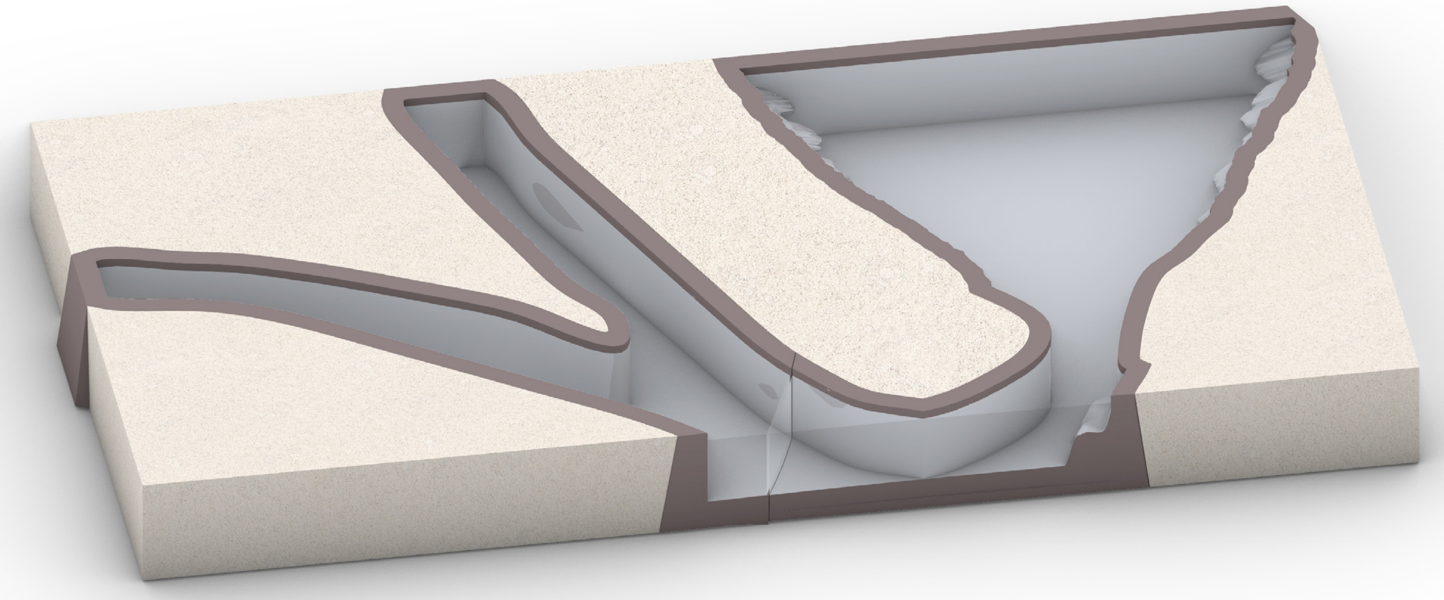

Figure 77: Unconsolidated sand filling the unused areas of the mould and compacting the pieces.

Option 2: Honeycomb 20%

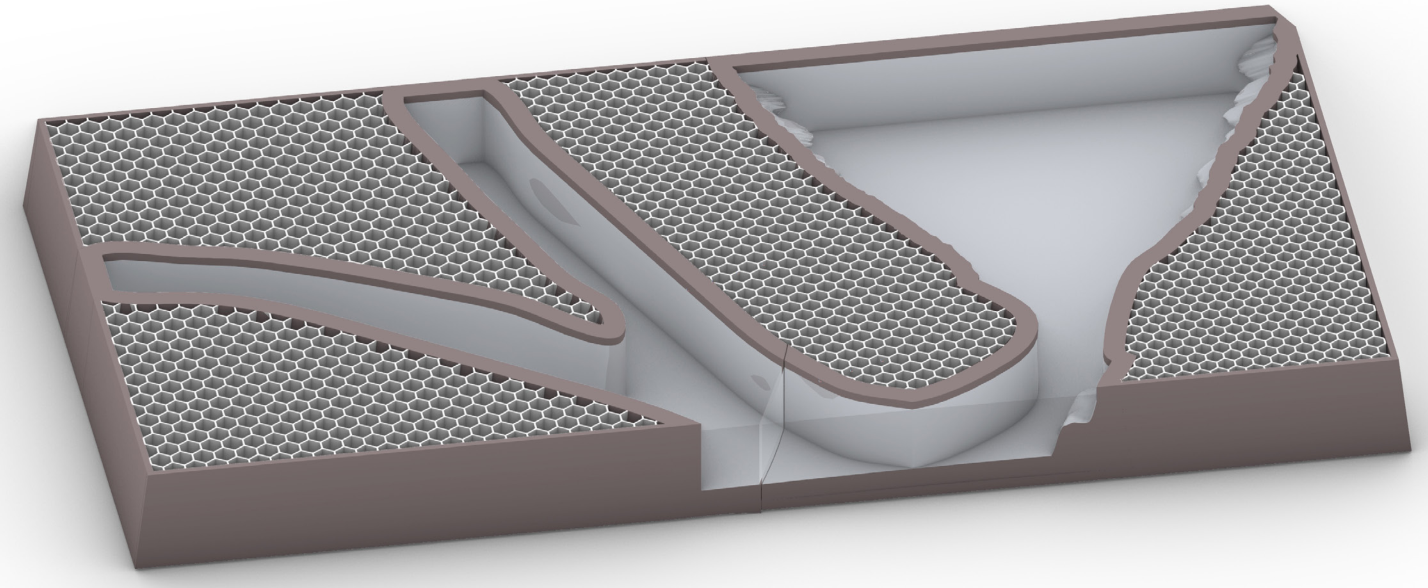

Figure 78: An infill structure from honeycomb of 20% density.

Option 3: Grid 25%

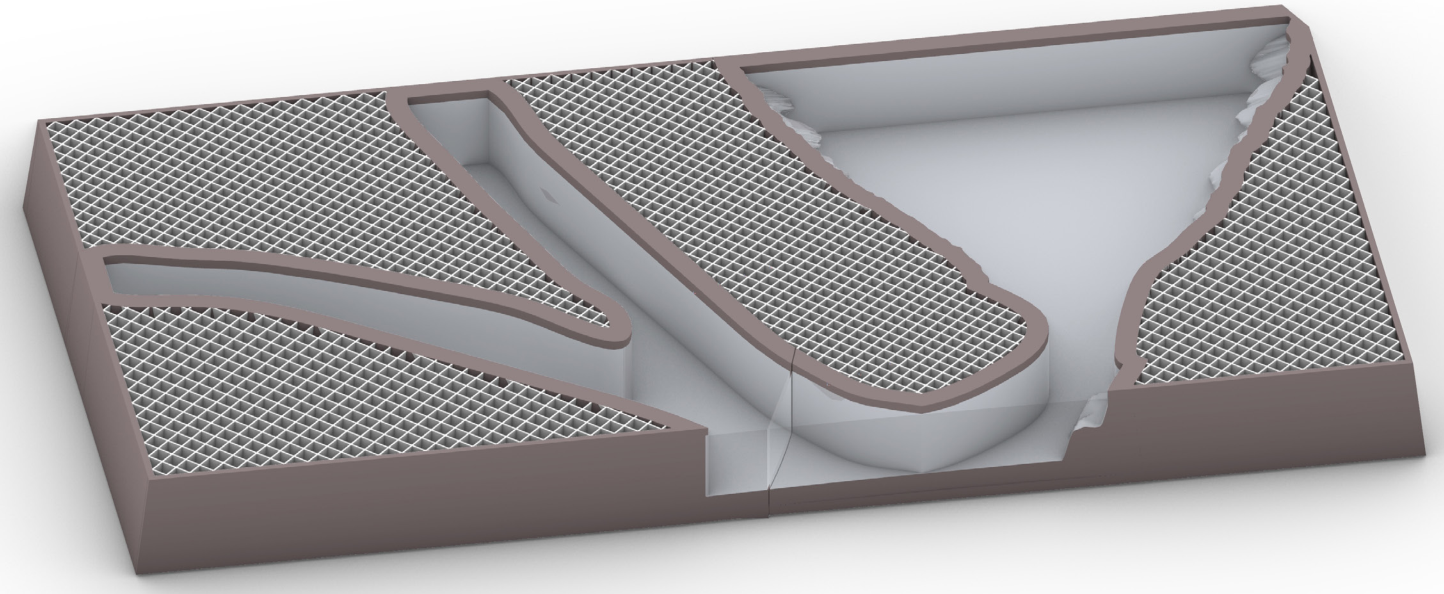

Figure 79: A grid infill structure of 25% density.

Option 4: Buttresses

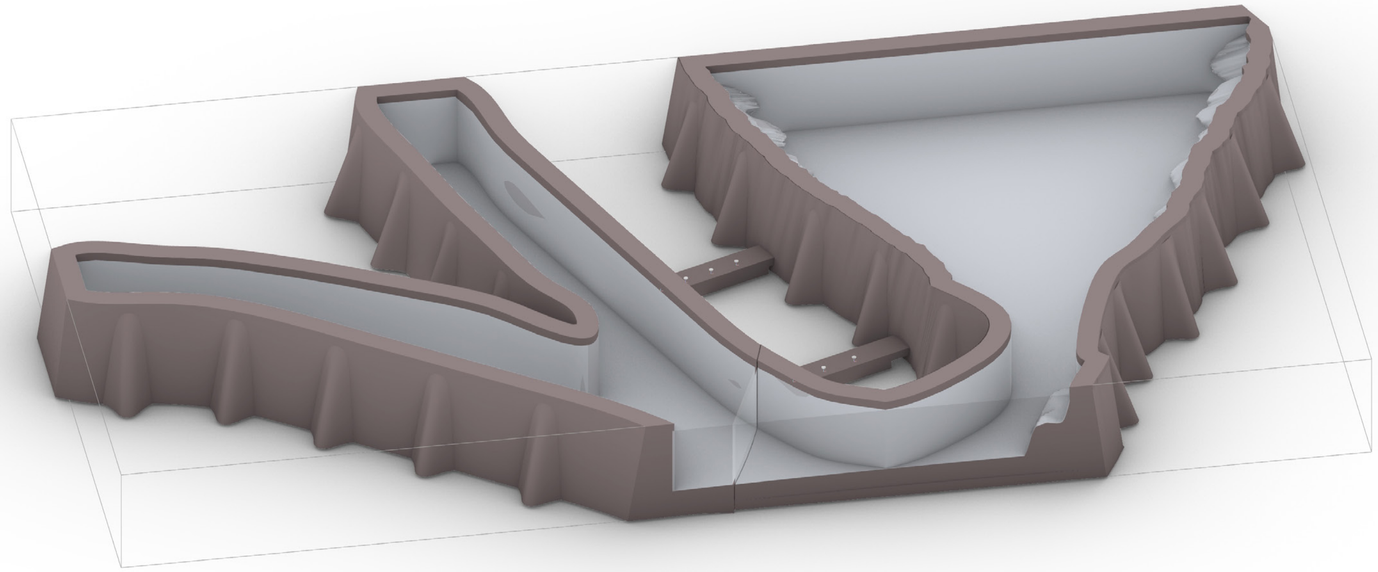

Figure 80: Last proposal from integrated buttresses supporting the shell. The rest area could be filled with loose sand as option 1.

According to the Table 15, where the two shell proposals were compare with a solid rectangular shell of 6 cm, the optimum design is the one that consists of the honeycomb sandwich.

	Volume percentage in comparison with rectangular shell of 6cm
Buttress-shaped shell	74%
Honeycomb sandwich	69%

Table 15: Assessment of the shell alternatives in terms of volume.

In addition, in order to evaluate the four infill proposals the Table 16 was created. An assessment of the infill alternatives is conducted regarding the volume percentage of each, in comparison with an 100% infill. For the current project, since the strength requirements are fulfilled by the shell itself, the first alternative was chosen as the quickest with the lower manufacturing costs.

	Volume percentage in comparison with the 100% solid infill
Hollow filled with loose sand	0%
Honeycomb infill	20%
Grid infill	25%
Buttresses	21%

Table 16: Comparison table between the four infill proposals in terms of volume.

Pieces connectivity

A usual problem that mould pieces present is possible leakages of the glass in the seam of two pieces, which have been proven extremely dangerous for the final result. Owing to the fact of the hydrostatic pressure that is released during the glass melting, the moulds can be deformed and even break if the glass surrounds them.

Therefore, an interlocking connection system, with extensions and undercuts and frequent nodes securing the seam between two pieces was designed, as it is shown in Figure 81, with In addition, some extra plate elements were designed in between the pieces to stabilize them.

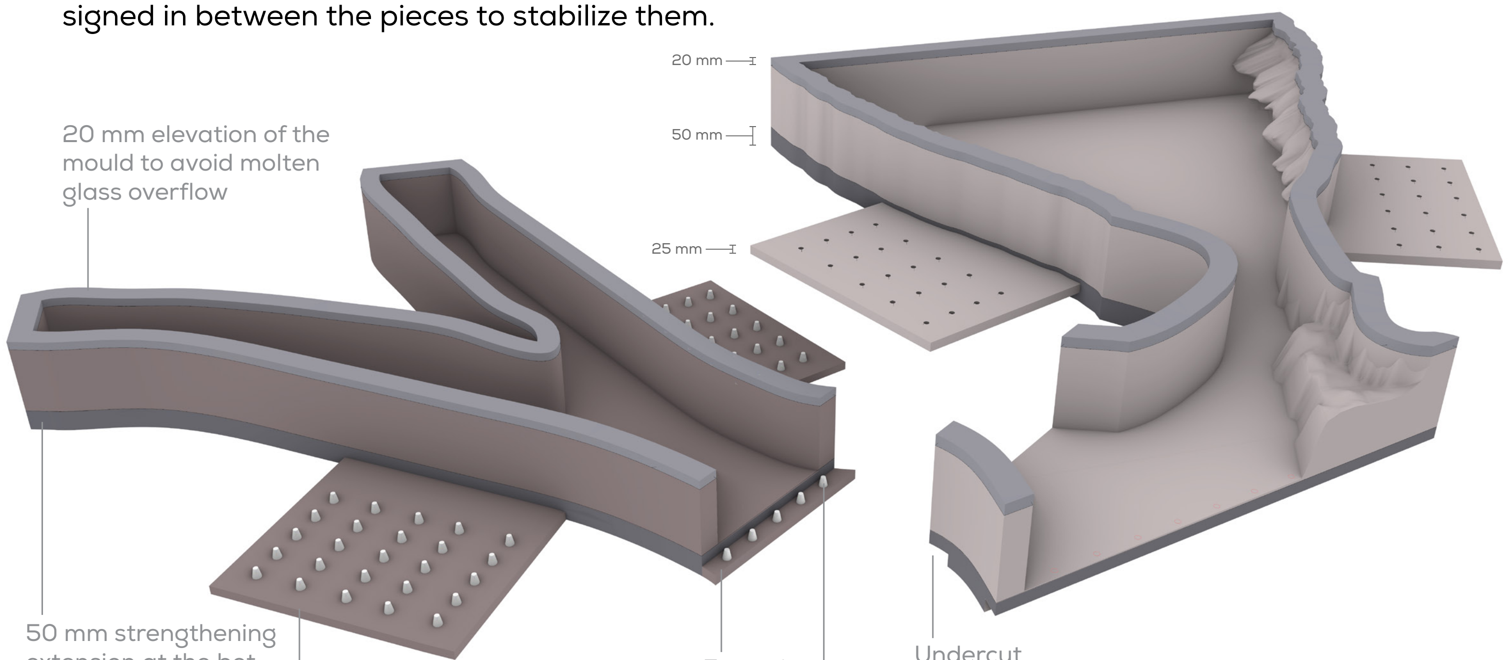

Figure 81: The connectivity system between the mould pieces.

Mould overview

Therefore, the final mould system was completed, as Figure 83 presents, while the mould as a whole before the separation is illustrated in Figure 82.

The moulds are colored according to the order they can be placed, starting from the darker to the lighter.

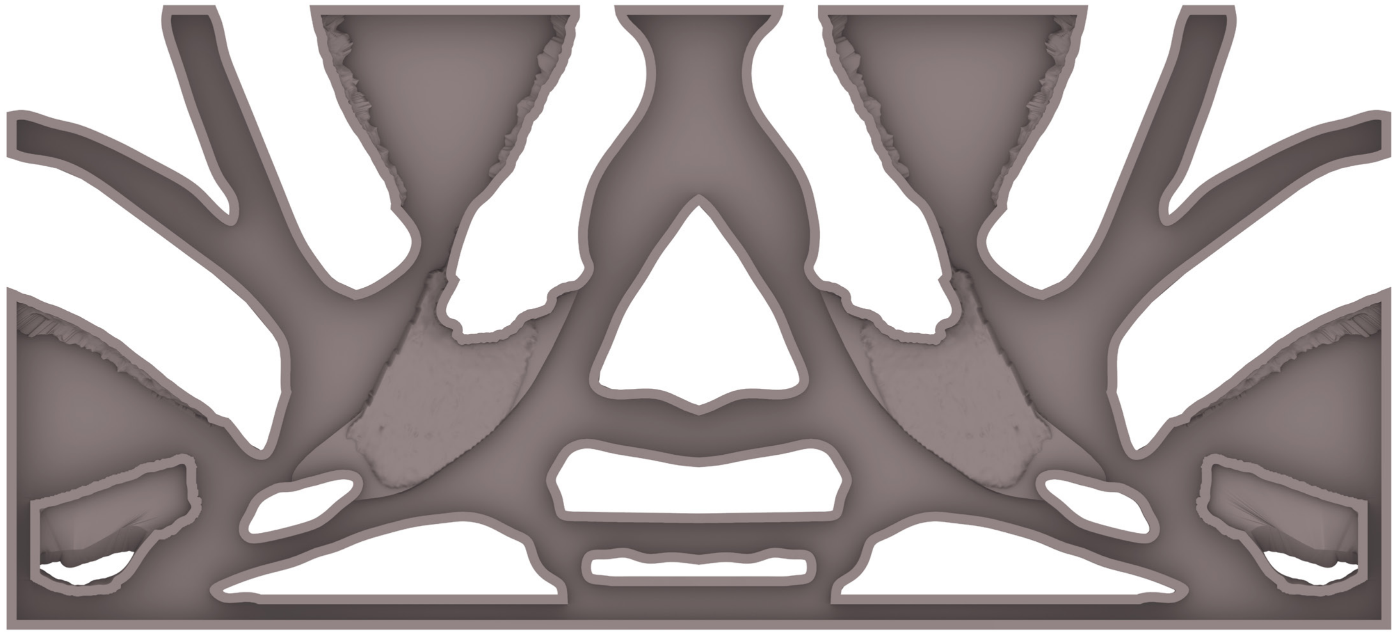

Figure 82: The initial mould before the separation due to the size limitations of the printer.

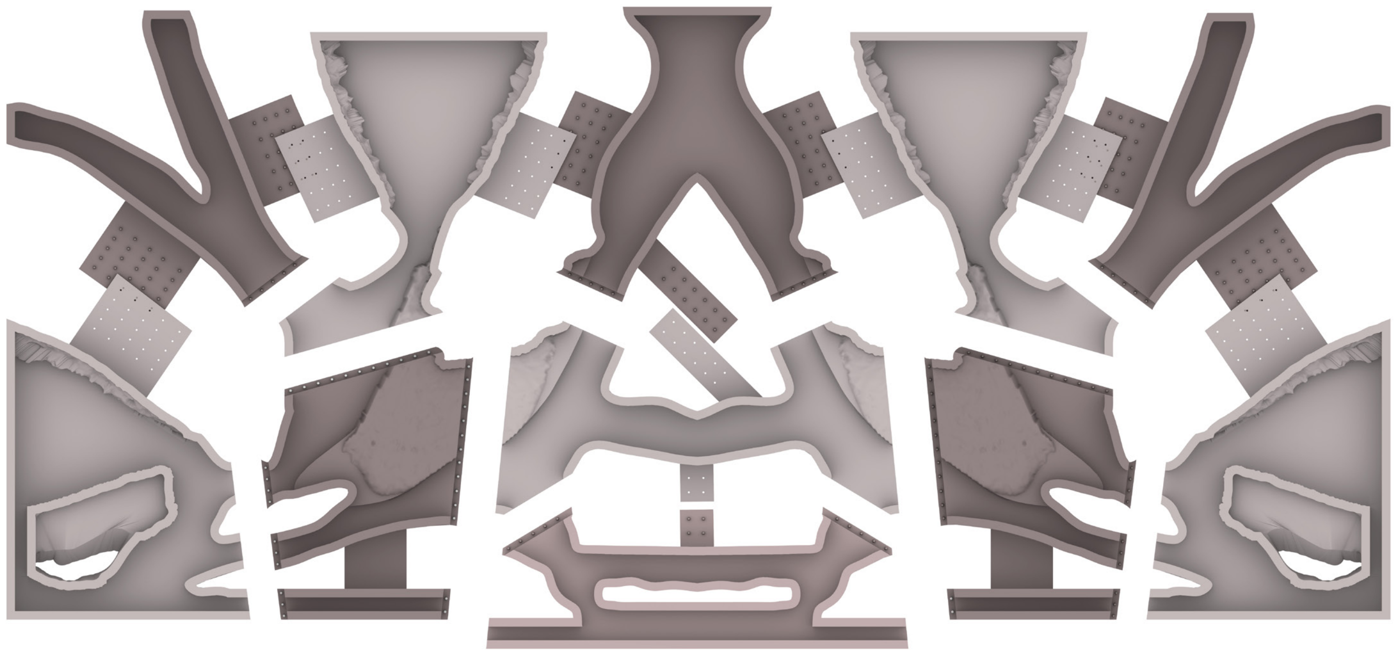

Figure 83: The equally weighing mould pieces with smaller dimensions than 4*2*1 m. The different colors show, from the darker to the lighter, the order of assembly, from the first to the latest respectively.

Fabrication sequence

In terms of moulds' order of assembly, both next figures, describe the appropriate sequence. The first step after the mould pieces are printed, is to remove the loose sand from the mould cavity and treat the surfaces with a coating for smoother surface of the glass element, such as Crystal Cast (Bhatia, I., S., 2019).

To begin with, a concrete container will be the base for the entire glass generating procedure. A layer of glass wool blanket is firstly placed inside the container to accommodate the different thermal expansion coefficients of the two contacting materials, concrete and sand. A layer of coarse sand could have the same function, however, the blanket is preferred as it can be applied quicker.

On top of the glass wool, the mould pieces are placed in three groups. First the ones with the extensions and the nodes. Then, the central piece which contains both connection systems, extensions and undercuts, is placed. The last pieces are the ones with the undercuts that will lock with the rest and stabilize the system.

After all pieces are placed into the concrete container, unconsolidated sand that was removed after the printing fills the open areas outside the shell. That way, it fixes the moulds inside the concrete base by cover and compact any gap.

Finally, big pieces of pre-formed solid glass are spread inside the mould cavity and the preset heating program for glass melting and annealing can begin.

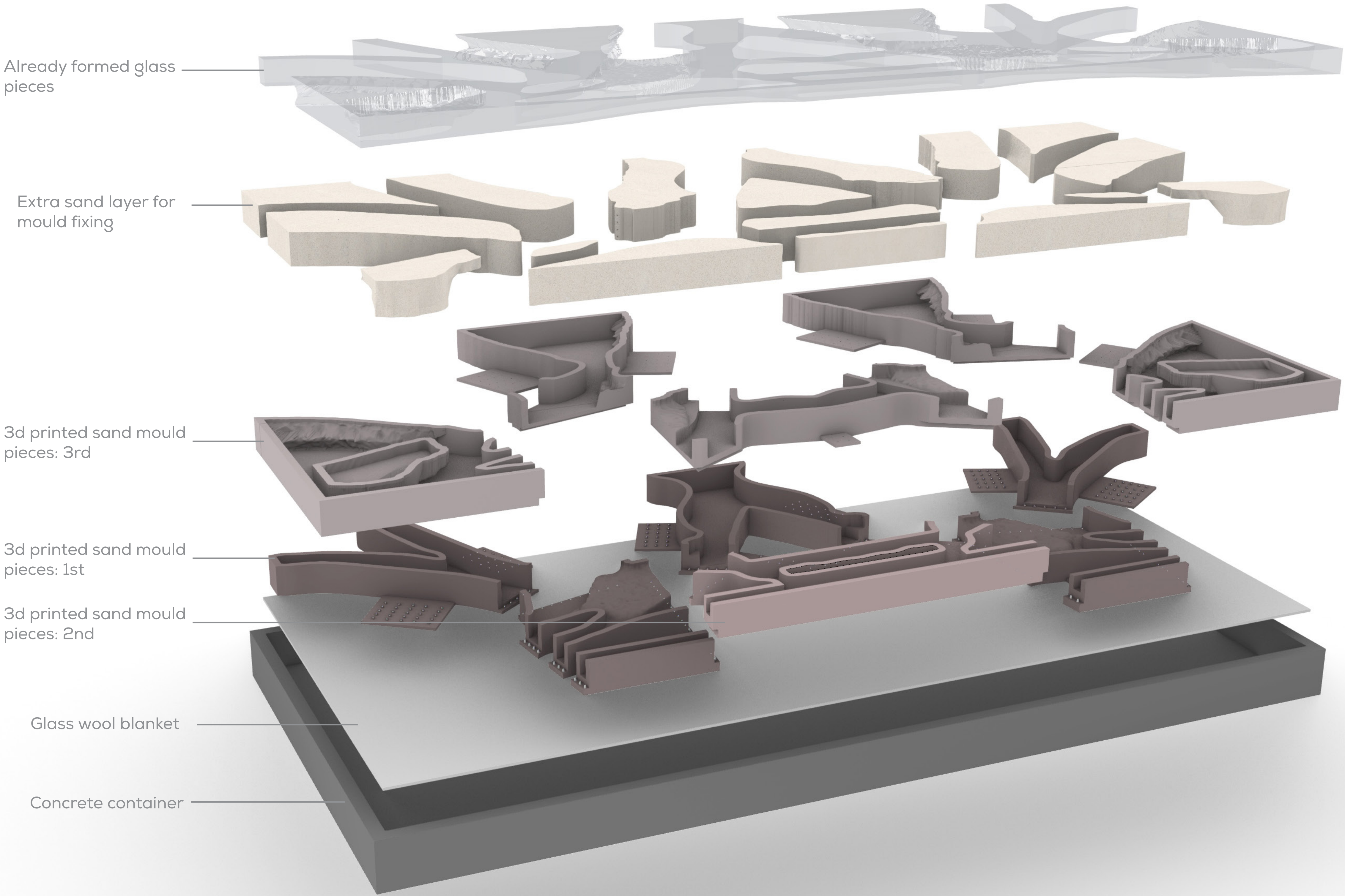
Already formed glass pieces
Extra sand layer for mould fixing
3d printed sand mould pieces: 3rd
3d printed sand mould pieces: 1st
3d printed sand mould pieces: 2nd
Glass wool blanket
Concrete container

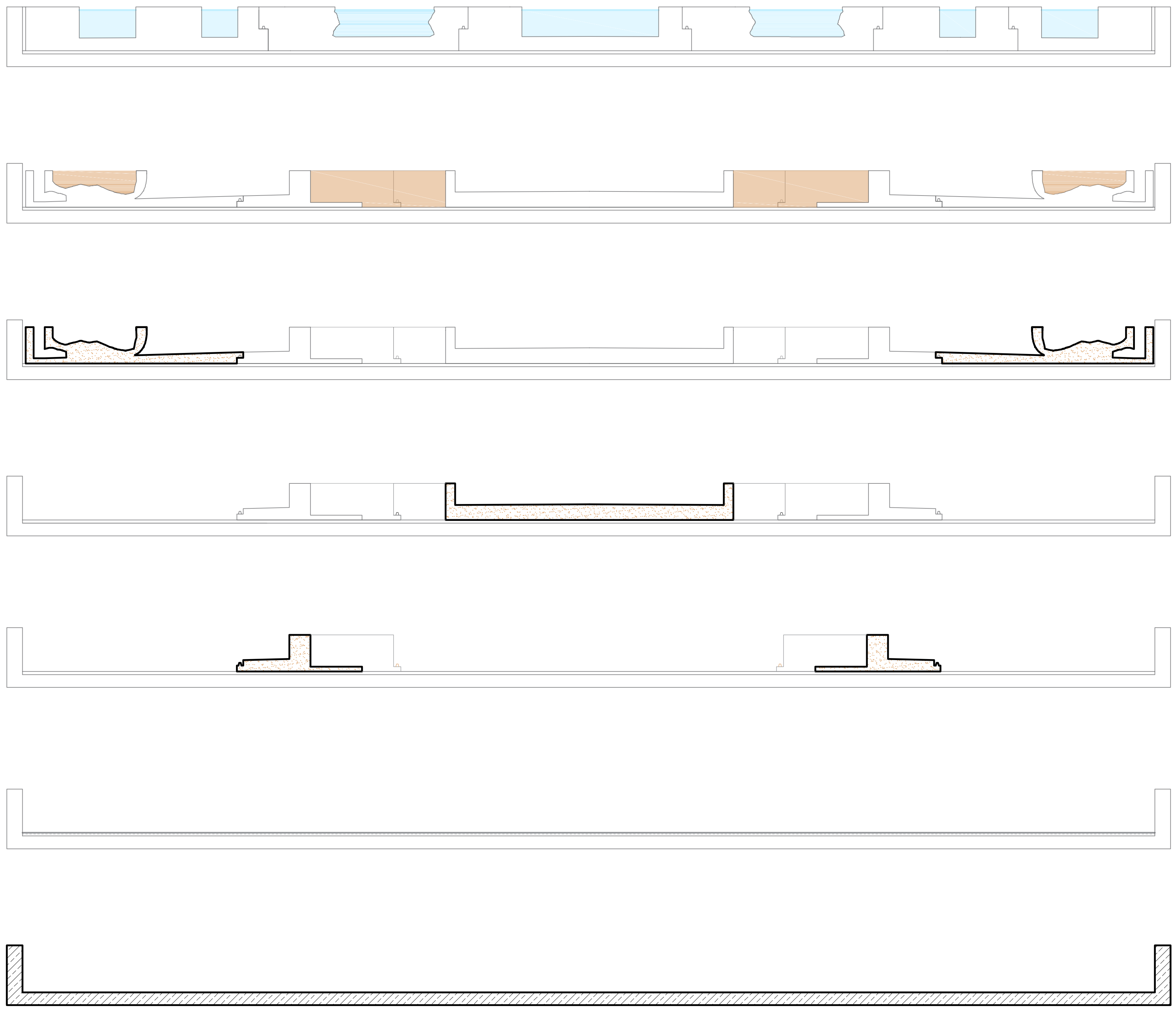

7

The required volume of glass is placed in small pieces of pre-formed-glass into the mould.

6

The gaps are filled with unconsolidated sand to compact and fix the pieces from horizontal and vertical movement.

5

The final group of pieces with the undercuts lock the rest, generating a stable mould system.

4

Next, the middle piece with the combination of extensions and undercuts is located.

3

The first group of pieces with the extensions are placed.

2

A layer of 2cm glass wool is added at the bottom of the container to accommodate the different expansions of concrete and sand mould.

1

A concrete container is generated as the mould base.

6.2.2. Annealing time

If we go back to the problem statement, which was emerged after studying realized projects from cast glass, an attempt of estimating the annealing time that the optimized slab will require, could not be missing from this thesis.

To do so, an overview of the thickness range that the optimized slab elements present is necessary. Therefore, a thickness analysis was performed in Autodesk Meshmixer. According to the analysis, the majority of the elements vary between **100-180 mm**.
Although the max-min thickness that were set as a constraint during the last optimization ranged within 150-170 mm, the thicknesses has changed. That happened since the model was redesigned in Rhinoceros, in order to avoid very weak elements at the connection areas, and, afterwards, smoothened in Spaceclaim to minimize irregularities.
Figure 84 shows with red color the elements that range within the 100-180 thickness limits.

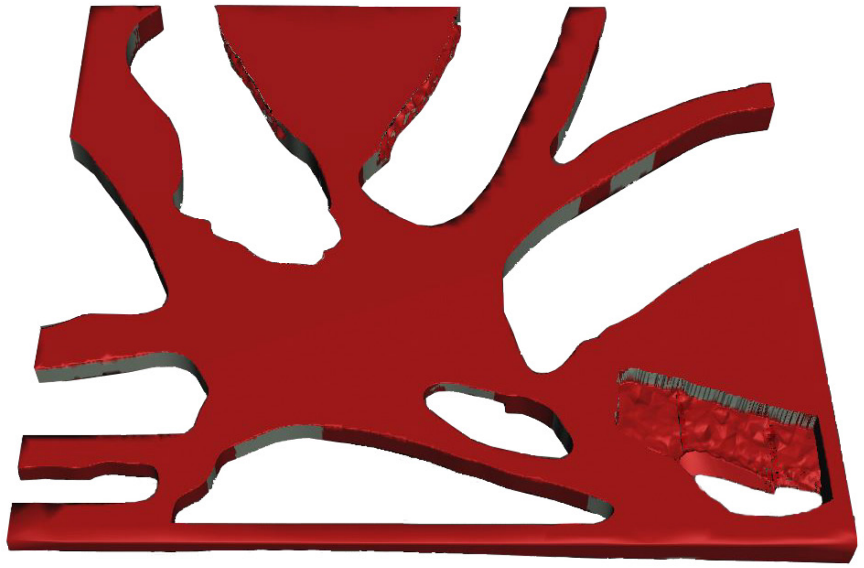

Figure 84: Thickness analysis result from Autodesk Meshmixer. The red color indicates the elements that range between 100-180 mm.

To estimate now the annealing time of the slabs, an annealing chart for the kiln-casting of a thick slab from Bullseye glass was used. The chart can be seen in Table 17 and Appendix G and it refers to flat slabs of uniform thickness which can be evenly cooled from top and bottom. Although the thesis slab does not belong in that category a rough estimation can still be obtained from the table. The optimized slab contains plenty of holes into the general bounding box and, thus, it will cool down from more surfaces than the top and the bottom. Therefore, an annealing

time for a middle value of 150 mm thickness will be preferred than the higher element thickness 18mm that contains.

According to the company, Bullseye glass is a soda lime glass, whereas for this project a borosilicate glass is used. As already mentioned in previous chapter, the thermal expansion coefficient of the borosilicate glass, 3.2–4*10-6/K, is way lower than soda lime's one, 9.1–9.5*10-6/K. From the theory, lower thermal expansion coefficient provides a shorter annealing process. To estimate the percentage of the different annealing times the two types of glass present, a review of the Table 3, Chapter 4.1.2., is necessary. In that table a comparison between the Atocha Memorial, from borosilicate, and the Crystal Houses facade, from soda lime glass, is conducted. Both projects consist of cast glass blocks of different dimensions. The 8.4 kg block of the Atocha Memorial was ready after 20 h of annealing, while the 7.2 kg block of the Crystal Houses facade needed 36-38 h.

Therefore, based on the obtained data from the two realized projects, a component from borosilicate glass requires almost **1/2** of the annealing time a soda lime component needs.

THICKNESS	RATE	TEMP	HOLD/ ANNEAL SOAK TIME	1ST COOLING TIME	TEMP	HOLD	RATE/2ND COOLING RATE	TEMP	HOLD	RATE/FINAL COOLING RATE	TEMP	HOLD	TOTAL MINIMUM TIME
6mm	AFAP	482	1:00	0:40	427	:00	0:22	371	:00	0:42	21	:00	˜3:00
12mm	AFAP	482	2:00	1:00	427	:00	0:33	371	:00	1:03	21	:00	˜5:00
19mm	AFAP	482	3:00	2:13	427	:00	1:14	371	:00	2:20	21	:00	˜9:00
25mm	AFAP	482	4:00	3:42	427	:00	2:02	371	:00	3:53	21	:00	˜14:00
38mm	AFAP	482	6:00	8:20	427	:00	4:32	371	:00	8:45	21	:00	˜28:00
50mm	AFAP	482	8:00	14:42	427	:00	8:20	371	:00	15:22	21	:00	˜47:00
62mm	AFAP	482	10:00	25:15	427	:00	12:30	371	:00	24:14	21	:00	˜70:00
75mm	AFAP	482	12:00	33:20	427	:00	18:30	371	:00	35:00	21	:00	˜99:00
100mm	AFAP	482	16:00	58:49	427	:00	32:15	371	:00	63:00	21	:00	˜170:00
150mm	AFAP	482	24:00	133:20	427	:00	76:55	371	:00	140:00	21	:00	˜375:00
200mm	AFAP	482	32:00	238:05	427	:00	131:34	371	:00	252:00	21	:00	˜654:00

Table 17: Annealing chart for thick slabs from © 2018 Bullseye Glass Co.

From the table and the previous assumptions that we made, the optimized slab that this thesis generated, would require

375*1/2 h = **176 h** ≈ 1 week

A prototyping test could give more information and probably more reliable results, but since it could not be done a theoretical estimation give the general impression which proves that the optimization part worked. A slab of two pieces with maximum dimensions 7 * 6.2 m can be casted and annealed in one week!

6.2.3. Final stage before transportation

After completing the fabrication of the slab, a few more steps remain so that the slab system is ready to be transfered to the museum and be installed.

The first step refers to the lamination of the connecting elements inside the holes which are already created during the casting. Another laminating process that needs to be completed under factory conditions is the one of the top safety float glass panes.

When the lamination stage is done, a framing of the slab with three components from kovar is conducted so that the slab system is ready to be installed. The framing also protects the slab edges during the transportation.

The sequence of the slab system assembly is shown in Figures 85-88.

1.

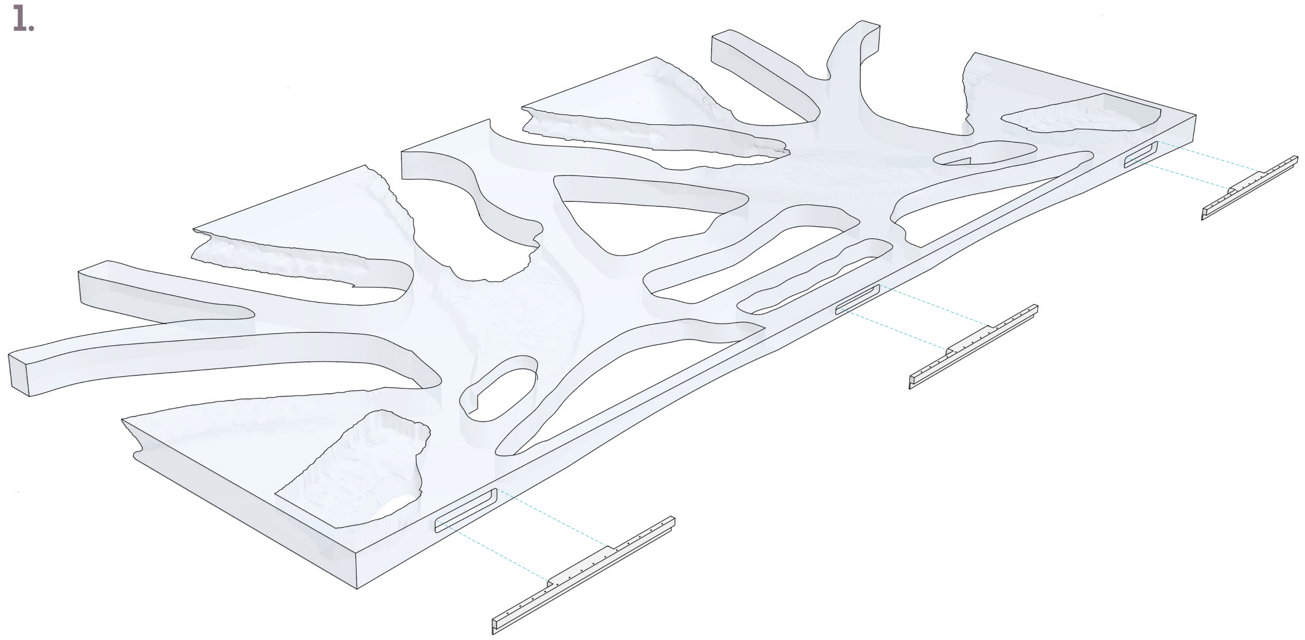

Figure 85: Lamination of the three connecting components.

2.

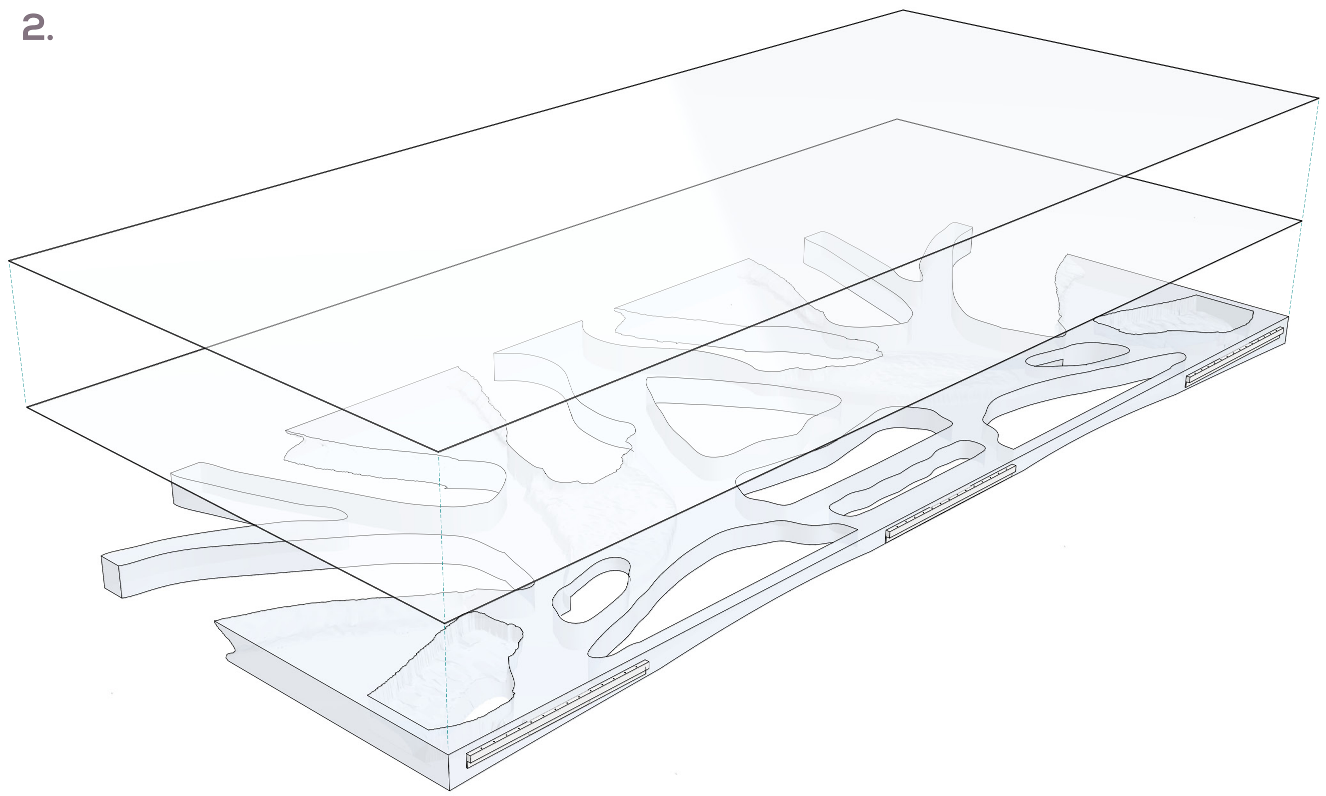

Figure 86: Lamination of the two 4 mm float glass panes on top surface.

3.

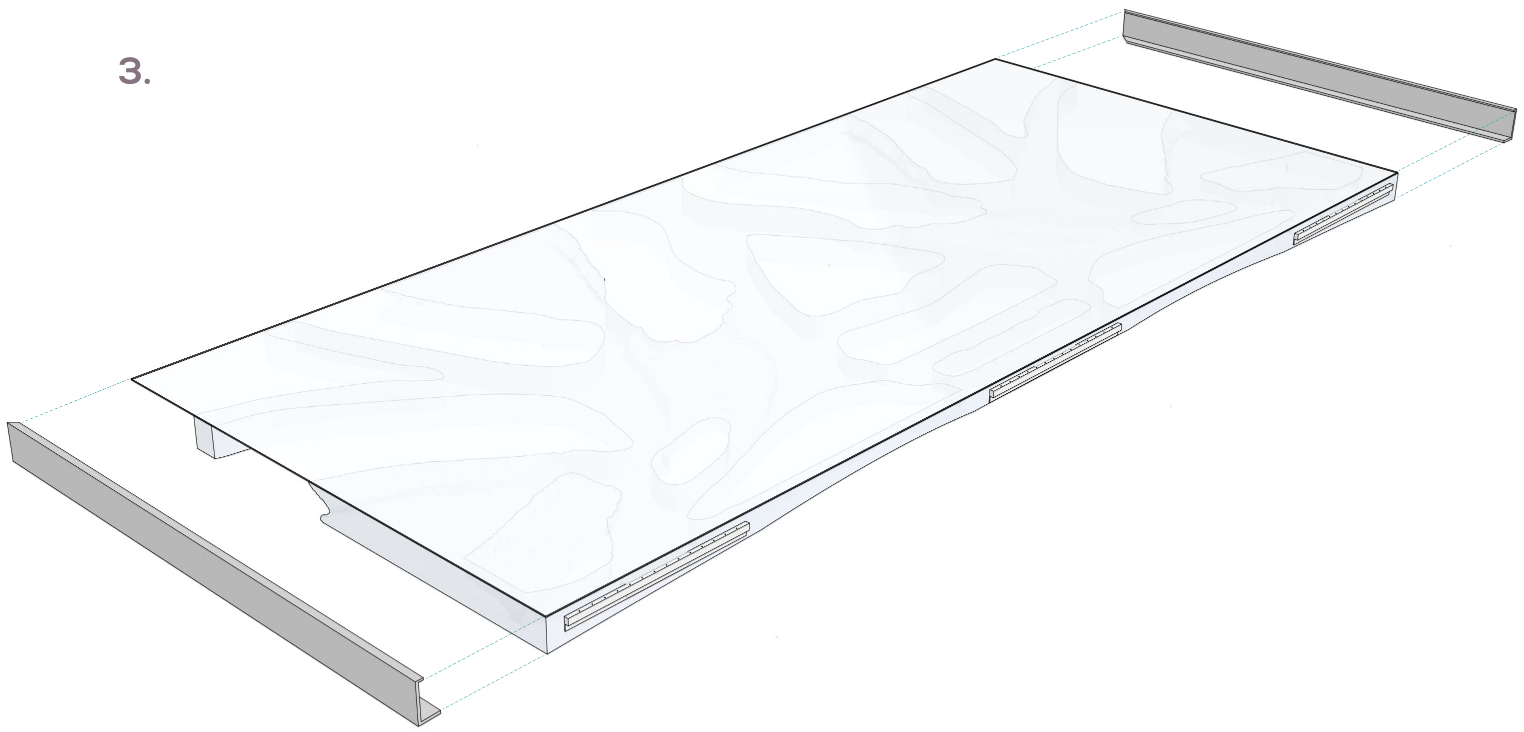

Figure 87: Installation of the two lateral framing components.

4.

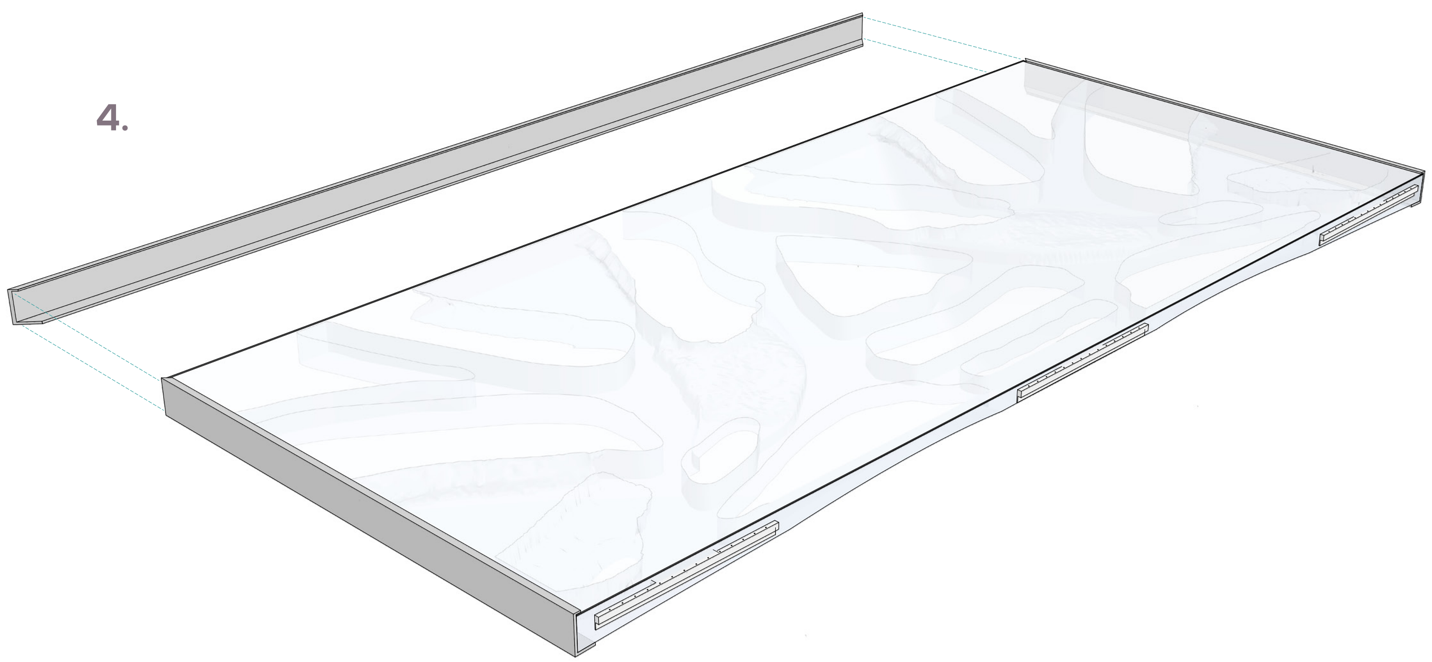

Figure 88: The last step under the factory condition when the final framing piece is placed and secures the whole system.

6.3. Building integration

After the glass is casted and annealed it is time to be transformed in the building and installed. As mentioned in Chapter 5.1., the slab is divided from the beginning in two pieces to facilitate the transportation, according to the allowable truck dimensioning. The assembly of the slabs into the building is described in this chapter.

First of all, as Figure's 89 floor plans illustrate, we can see the comparison between the new optimized slab in relation with the existing floor system. The improvement of the current situation, in which the view is restricted by the thick concrete beams and the metal frames, is obvious.

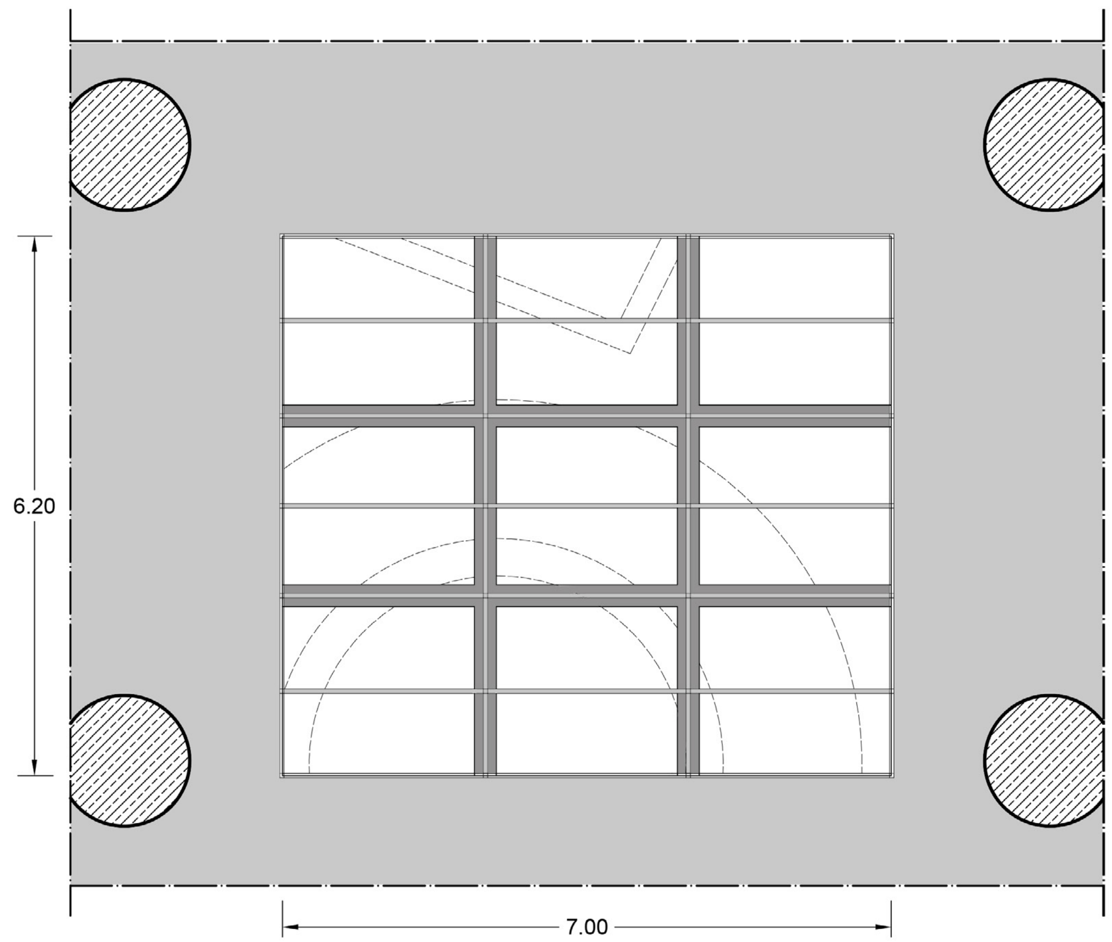

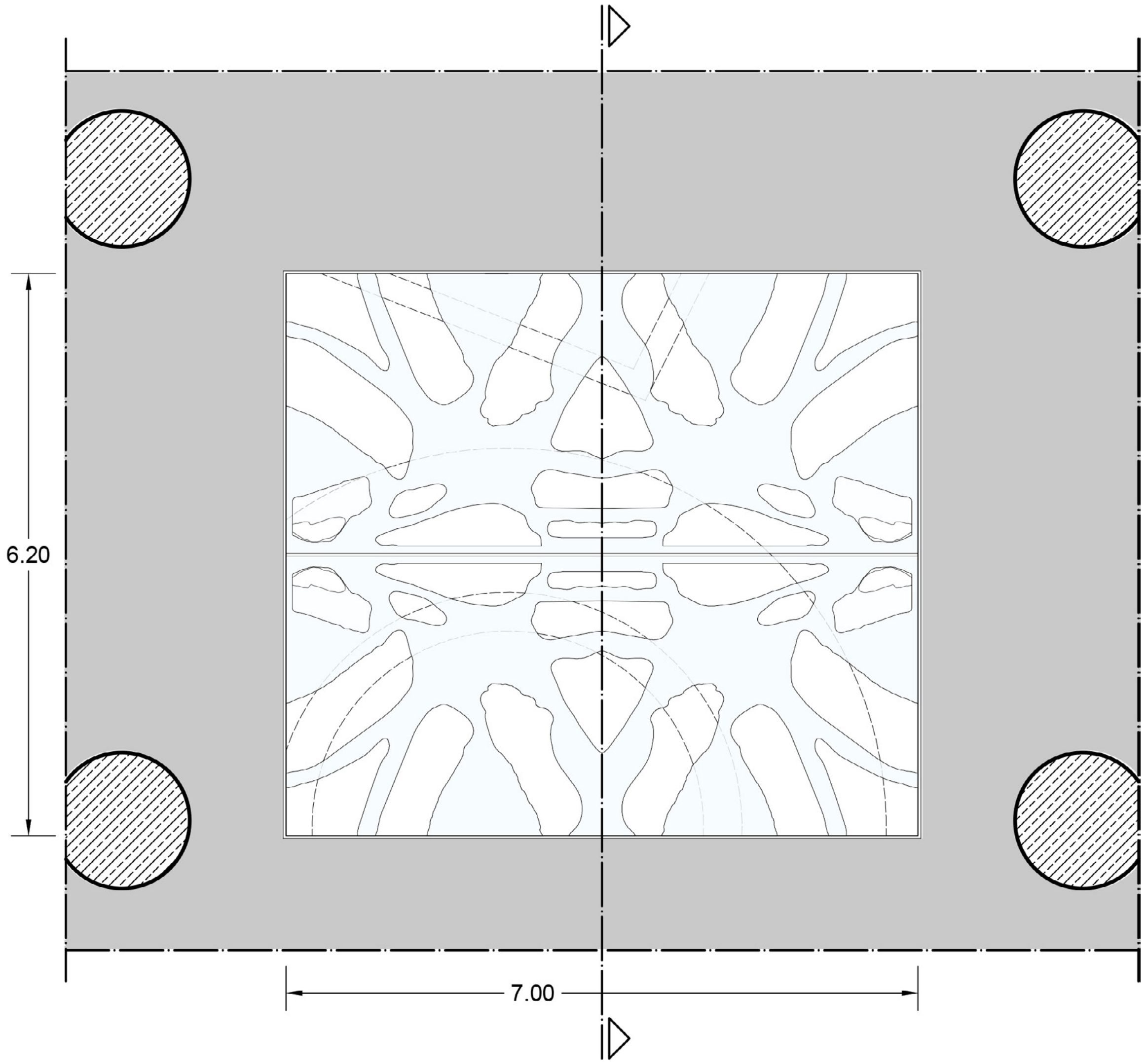

Figure 89: Up: The existing slab structure with the 25*55cm concrete beams obstructing the view of the underneath archeological findings. **Down:** The optimized slab exclusively consists of cast glass increasing the viewing freedom of the audience and presents architectural interest.

In Figure 90, a perpendicular to the connection of the two slabs section, the important points of assembly are illustrated. The installation of the slab to the concrete beams and the connection of the slabs need to be completed after the slab transportation.

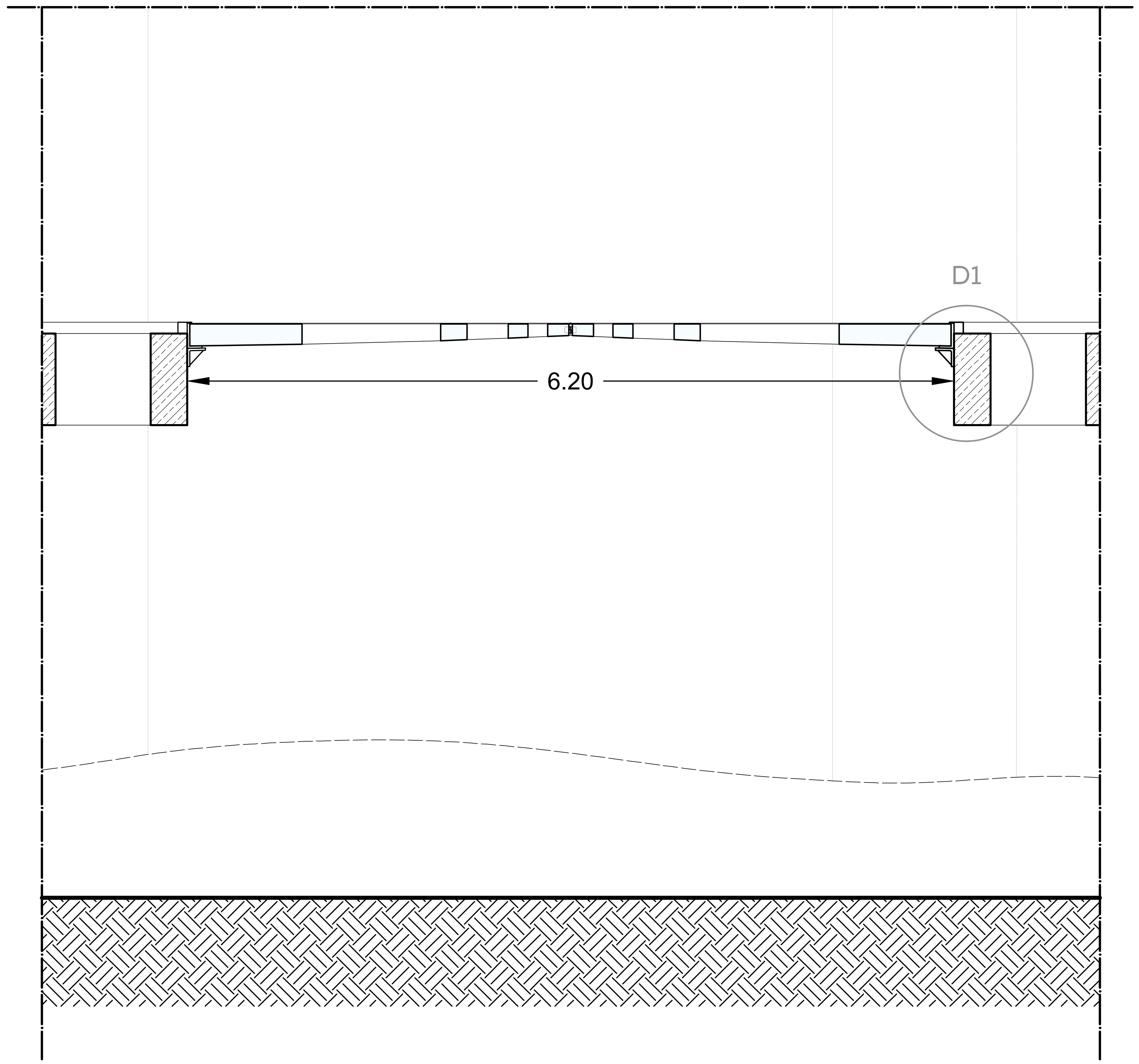

Figure 90: Section of the optimized slab integrated in the existing structural system of the museum. The detail of the slab attachment on the existing concrete beams are remarked on the drawing, as D2.

As it was decided from the beginning of the design development, in the structural simulations, the linear circumferential supports prevent the movement in every axis, as well as the rotation around z axis, while the rotation around x and y axes is allowed. This condition was applied in order to minimize the stress concentrations of a fixed support type in the glass. More specifically, a slab naturally tends to present deformation due to the live load, especially in a museum with crowds of people moving and standing on it. By applying a support that restricts all 6 degrees of freedom that a body may present, in a non-elastic material as glass, the element becomes severely prone to breakage.

The following three different designs are attempts of translating the desired support condition and structural performance of the slab to practical supporting installation. The 3rd design is the final and best solution which was chosen for satisfying both the structural behavior and the assembling feasibility of the slab integration.

The first two designs were rejected since both are clamped connections which restrict the free rotation of the slab around the horizontal axes. Apart from that, in terms of assembly, the first design required horizontal adjustment of the slabs, which was feasible only for the first piece's placement.

Therefore, after searching for a solution of vertical placement, the second design emerged. The vertical installation of both slab pieces was possible here, due to the customized metal bar and the accessible bolt fasteners. However, the metal component that was needed for this solution has a complex customized geometry which requires simplification for fabrication facilitation. Thus, a third solution was designed, as it is displayed in Figure 92.

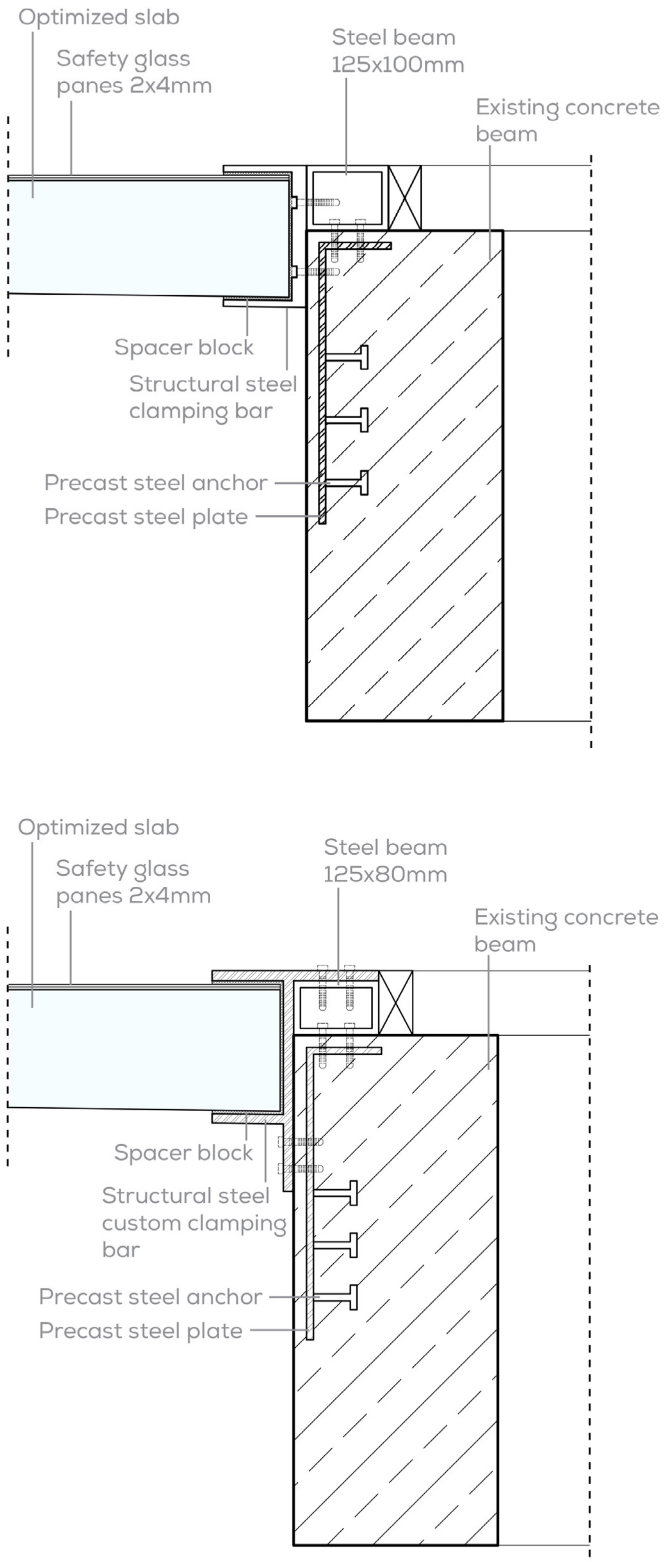

Figure 91: The preliminary designs for the detail D2, the slab integration with the building.

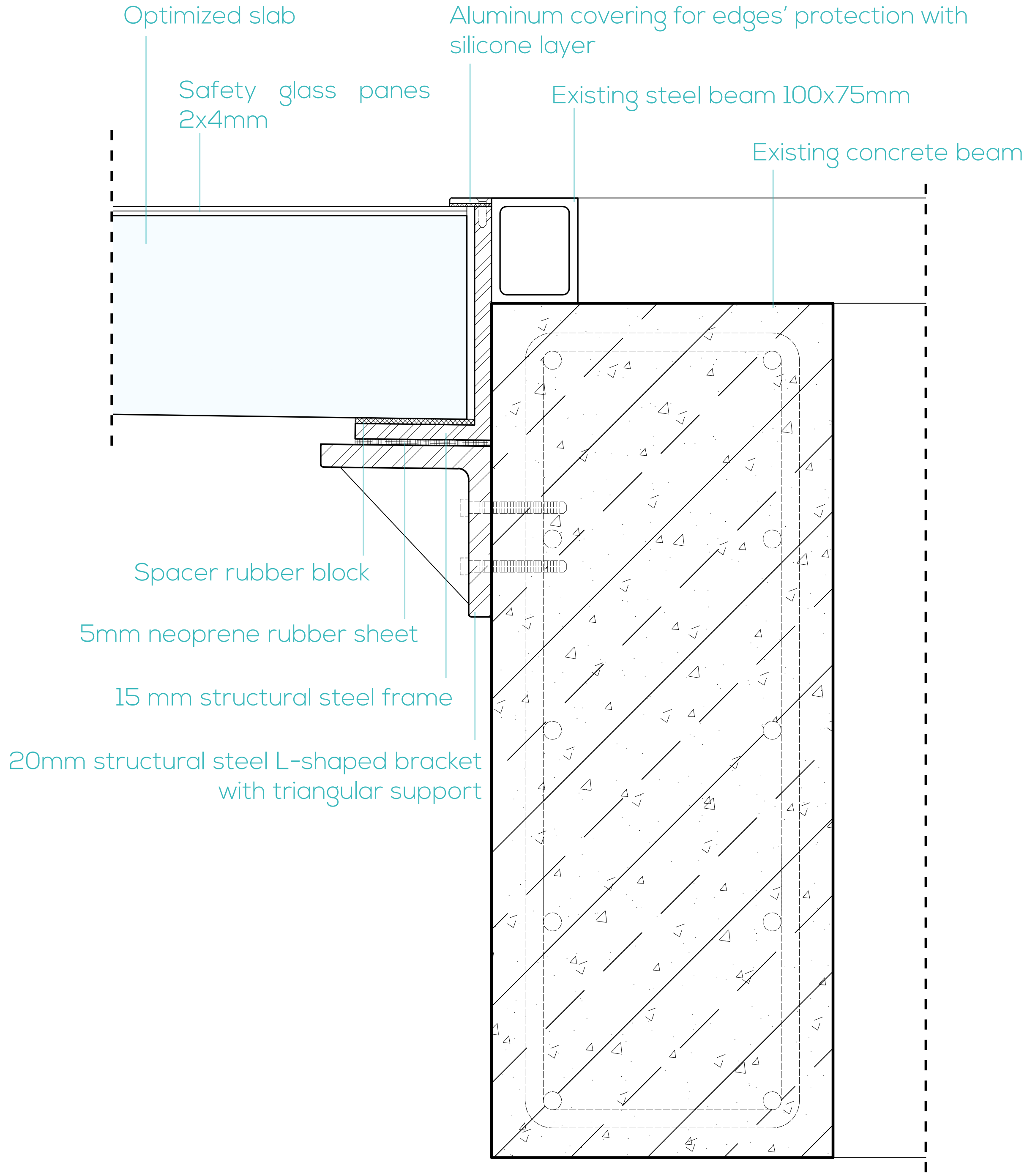

Figure 92: The selected design for the detail D2 of the system which connects the slab with the existing structure of the building.

The final installation system basically consists of two separate parts, the one of which is pre-assembled in the factory and the other on site, as already mentioned in Chapter 6.2.3. The 15mm thickness frame is adjusted around the slab pieces under factory conditions having as a result the protection of the slab edges during the transportation.

After the 20mm L-shaped bracket is fastened on the concrete beam's reinforcement, the slab-frame system is pulled down and rest on top of it. The stiffness of the L-shaped bracket is secured from the welded 10mm triangular plates. Between the slab frame and the steel bracket a 5mm rubber layer, from neoprene, exists in order to accommodate tolerances and vibrations.

Finally, an aluminum covering with an underneath silicone layer is fastened on top of the slab joint to protect the seam from water and dust.

Regarding the assembly sequence of the slab system into the building, there are six steps that need to be followed. Figures 93-98 illustrate the order of these steps, one by one. Since the slab system is crucial to be vertically located into the floor hole, the whole assembling procedure needs to agree with that principle.

More specifically, the assembly starts with the L-shaped brackets adjustment with bolts on each surrounding concrete beam. The slab with the bottom-extended connecting elements is firstly placed on top of the brackets. Then, the second slab rests on top of them, the bolts are screwed from the top and the nuts can be placed under the slab, securing the connection. That way, the slabs behave as an entire system. To finish the installation, the middle and circumferential coverings are adjusted.

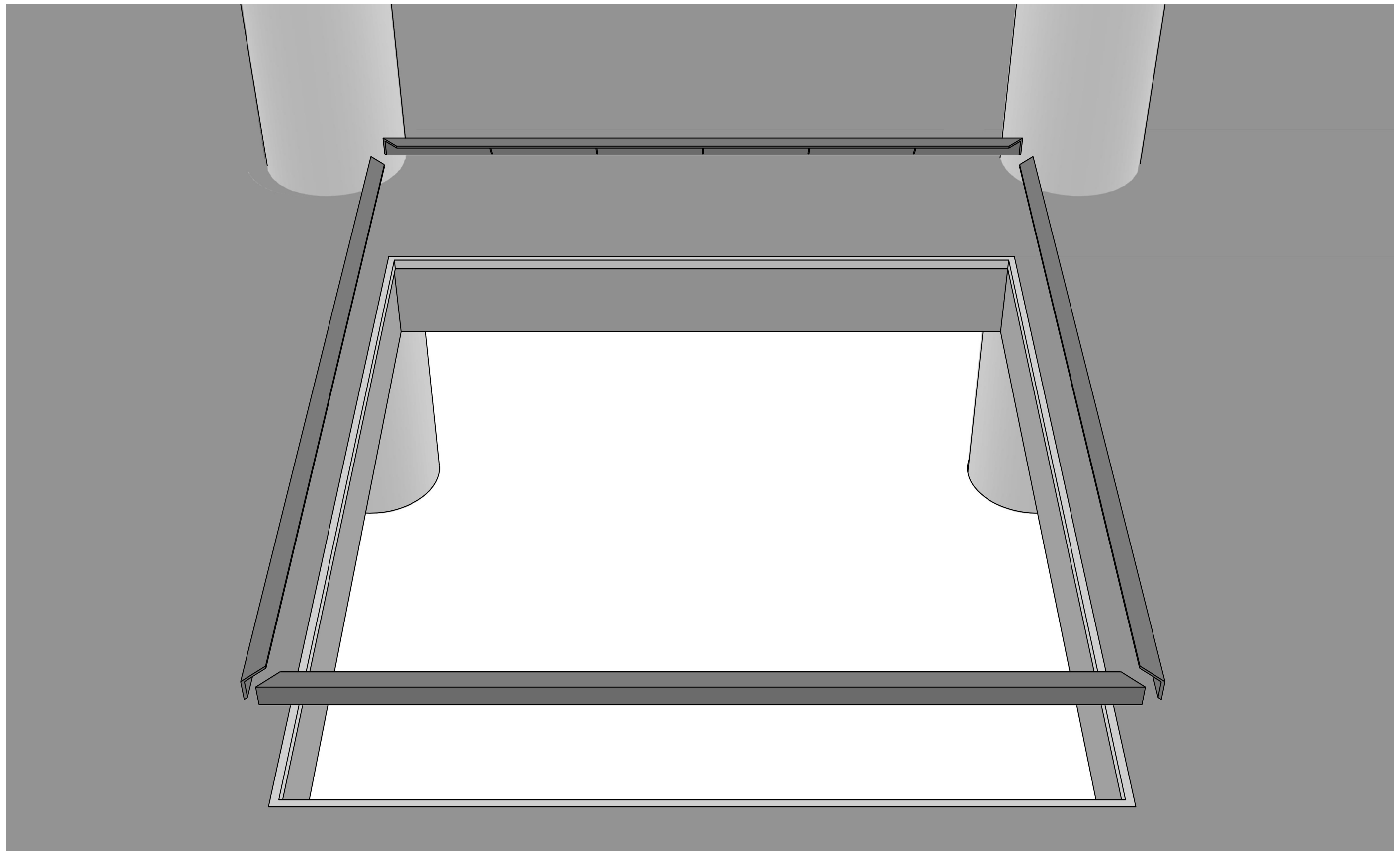

Figure 93: The L-shaped brackets are adjusted on the concrete beams.

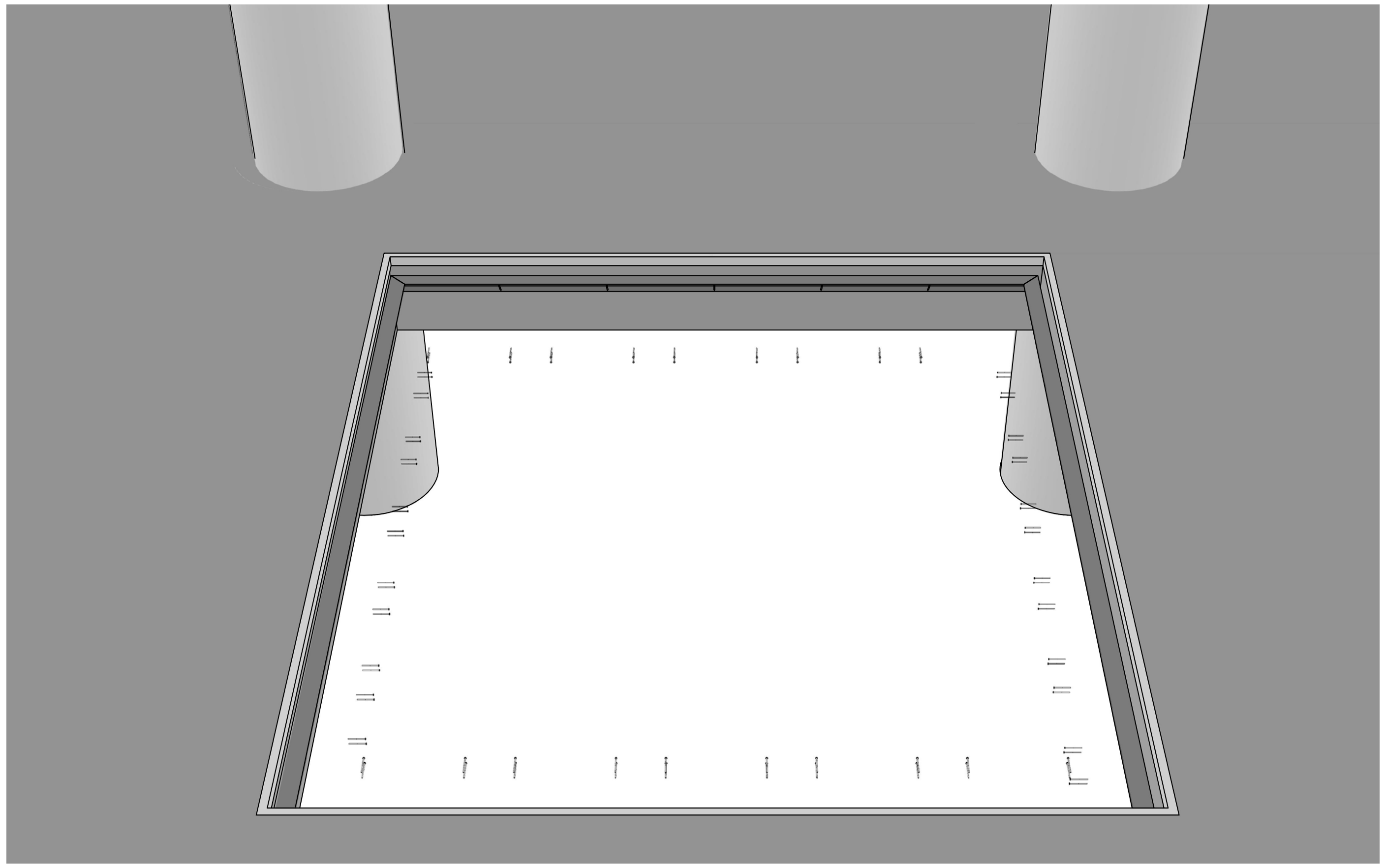

Figure 94: Two rows of bolts secure each bracket.

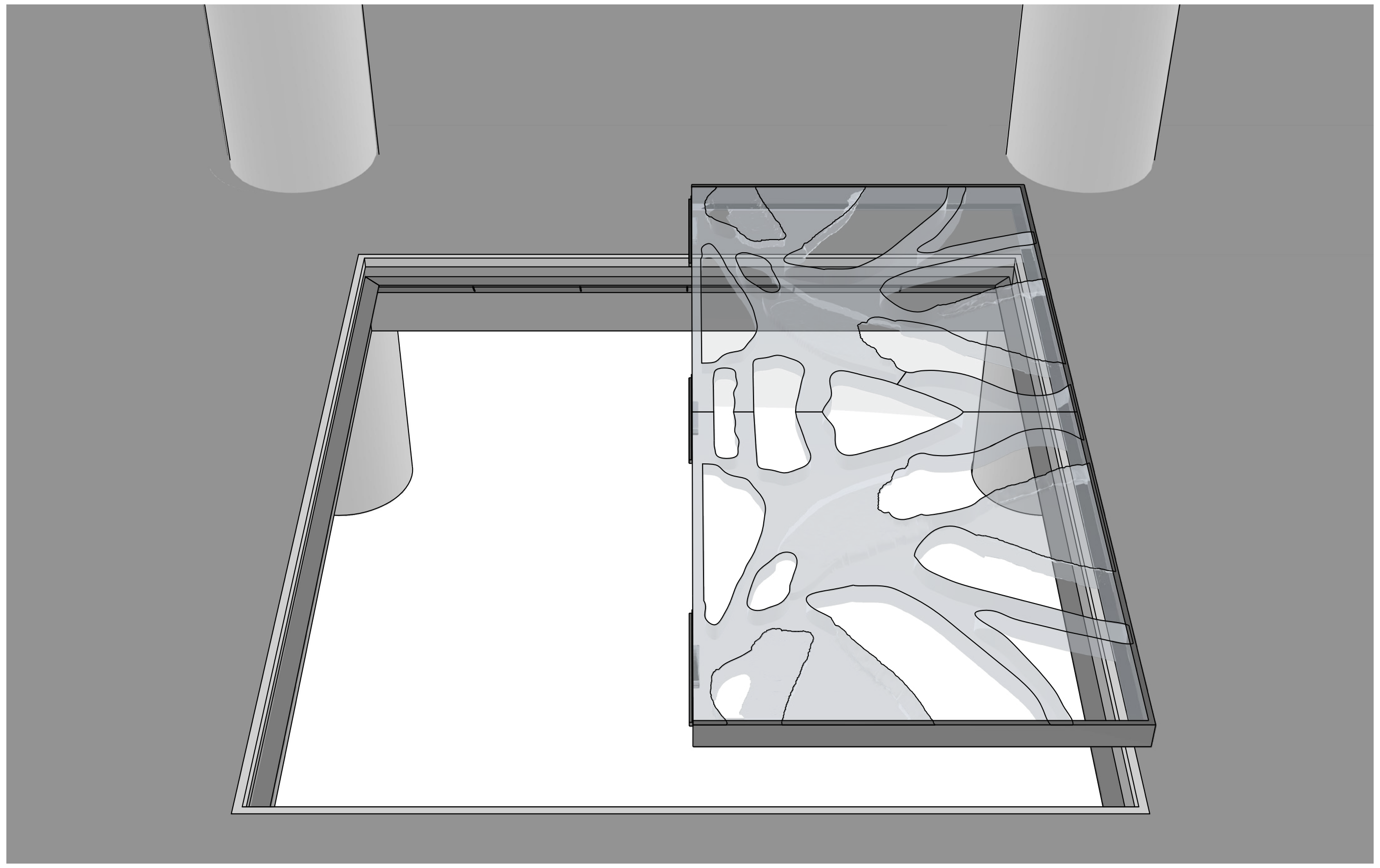

Figure 95: The first slab system with the laminated components and the framing is placed.

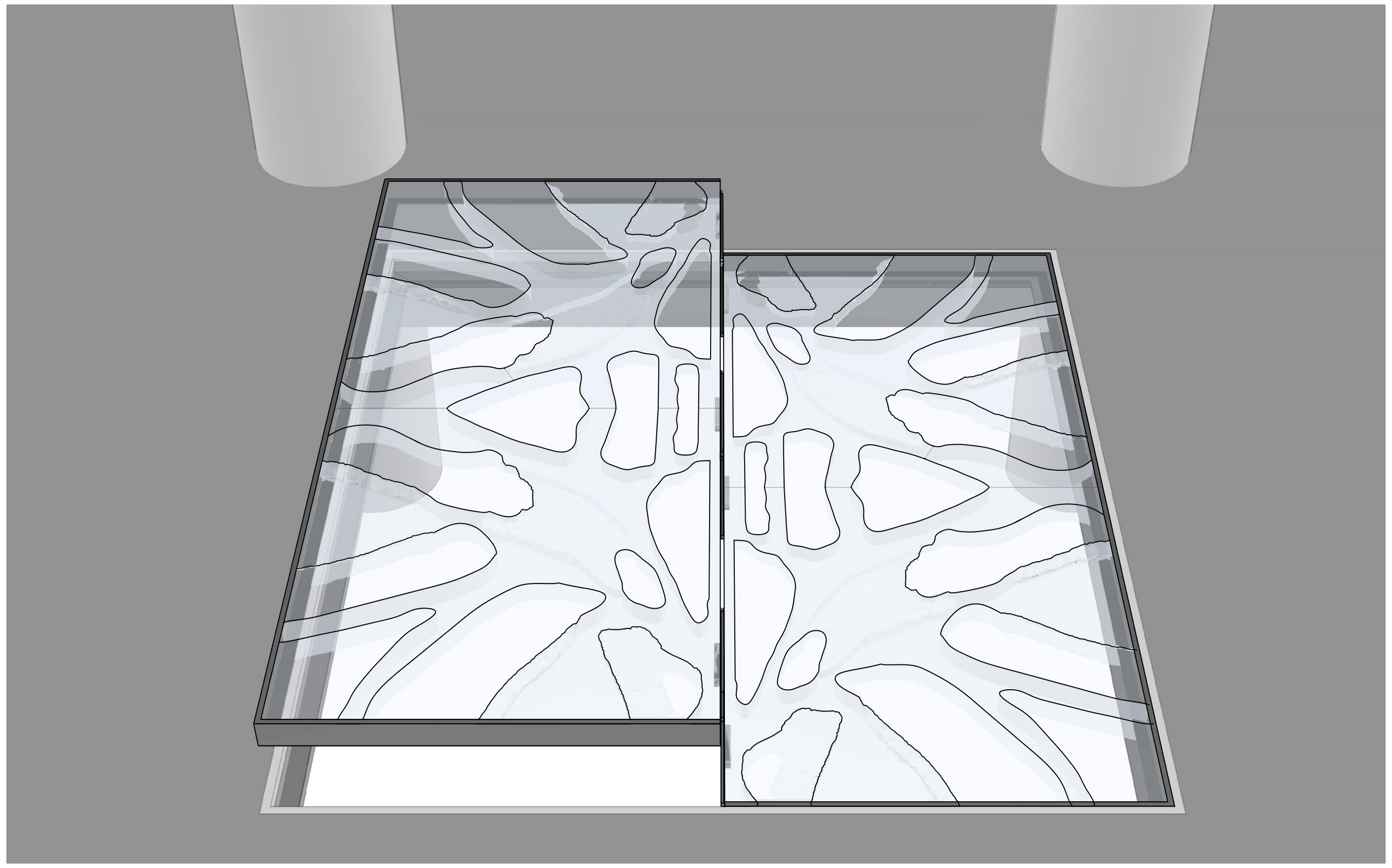

Figure 96: The second slab is installed and the middle connecting elements adjust.

Figure 97: The bolts and nuts secure the connecting system.

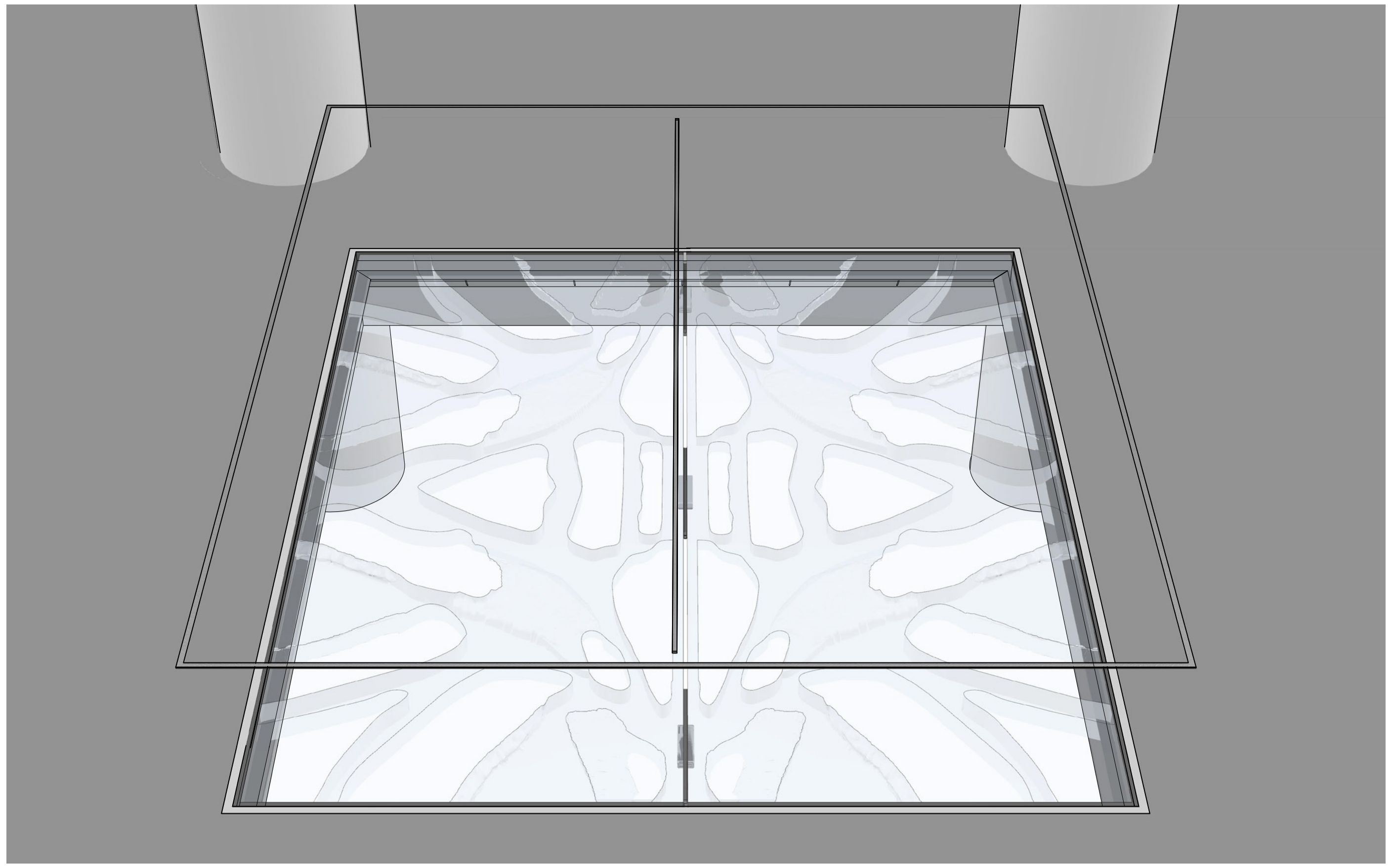

Figure 98: The final covering parts finish the whole system.

As an overall overview of the project, a comparison between the initial floor system and its restrictions, with the thesis proposal, can be acquired from the observation of the two systems illustrations. In Figures 99 and 100, the current floor of the museum is presented in a real photograph and a 3d visualization. Figure 101 shows how the optimized floor system would fit in the museum and improve the artworks overview.

Figure 99: The slab with the concrete sub-structure that currently exists in the Acropolis museum.

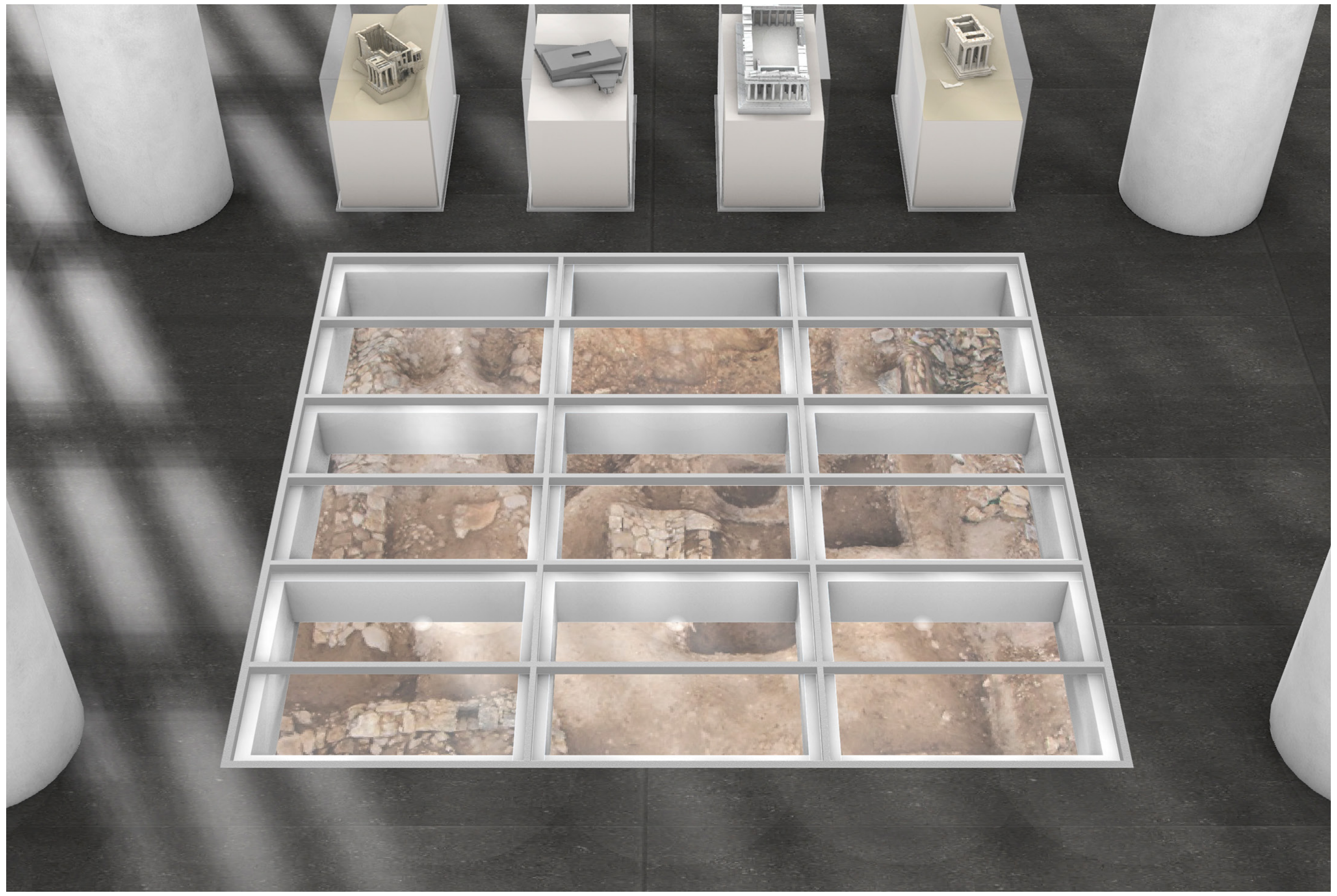

Figure 100: 3d visualization of the existing slab.

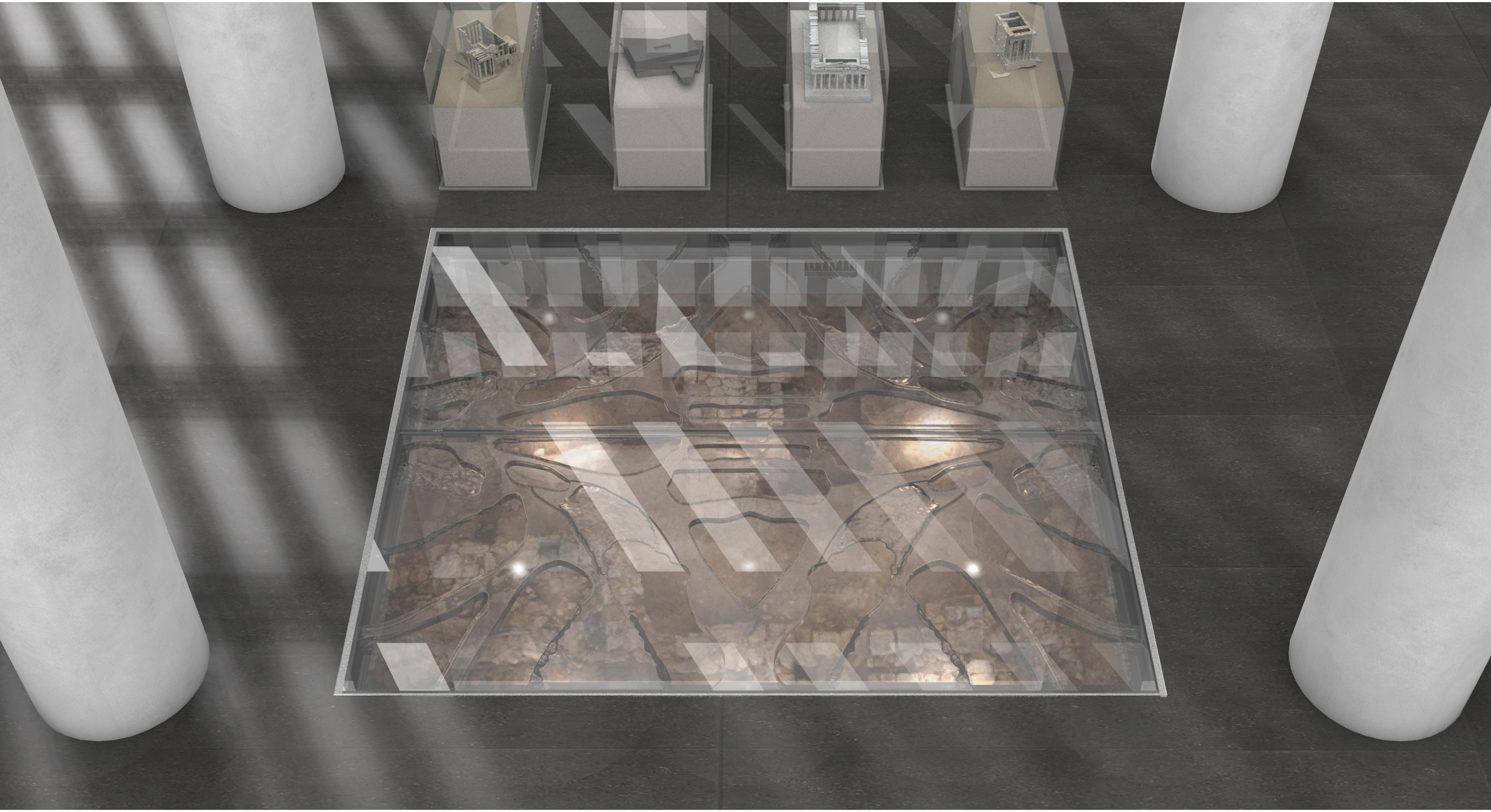

Figure 101: 3D visualization of how the final slab system could look like in the museum.

7. Conclusions

By answering the initial research questions, an overall concluding overview of the thesis project is presented.

From the beginning of the thesis, the main inquiry was the possibility of producing a large-scale monolithic structural cast glass component using the topology optimization method as a designing technique and the 3d printing sand moulds for fabricating it.

The main problem the thesis tackles, while exploring the aforementioned potential, is the solution of the annealing time problem of large-scale elements, the minimization of their weight and material consumption and the investigation of the fabrication technique. In particular, the casting of a complex component which exceeds the available printing dimensions into 3d printed sand moulds.

Therefore, the main research question has been formed as follows:

What are the potential and the limitations of using Topology Optimization as a design tool and 3d printed sand moulds as a manufacturing method to produce massive structural cast glass components of reduced annealing time and volume?

Let's see how this thesis answers the main research question by responding to the segmental sub-questions:

• Which is the objective function for a TO of a cast glass slab?

According to the literature review regarding the topology optimization method in structural elements, the most widespread algorithms are the Von Mises stress-based and the compliance based optimization. The main difference of the two algorithms is the structural constraint, which the optimization respects and tries to retain. The Von Mises stress is represented by a single value without a distinction between tensile and compressive stresses. Since the objective of the thesis is a slab from cast glass and according to the mechanical properties of glass, using the V.M. stress-based algorithm is impossible to control the magnitude and the location of the tensile stresses that can endanger the whole structure.

The most appropriate solution would be principal stresses based algorithm which currently is not that developed and since there is no available software, could not be chosen.

The **compliance based** optimization was ended up to be the most suitable for a slab project. The strain and the stiffness of the model are respected, while optimizing the initial design which allows keeping low values of deflection, the most critical structural value for a slab. The limitation of this particular algorithm is a necessity for structural analysis of the model after each optimization to test for tensile concentrations. By using Ansys for the TO, it was demonstrated that this limitation can be easily overcome, since the Ansys Workbench operates the topology optimization integrated into the structural analysis function. Therefore, a structural analysis before and after the optimization is provided naturally, encouraging the user to check the model's structural behavior immediately.

• Which design constrains derive from structural, glass casting and manufacturing demands of a massive cast glass slab?

The main design principles which derived from the literature research focus on structural, cast glass and manufacturing requirements that the final design is expected to follow.

Starting from the structural demands, the allowable limits for the two more crucial structural values for a glass slab, the deflection and the tensile stress, were set. Indeed, the deflection of the final design, which is **4.78 mm**, does not exceed the **24.8 mm** deflection limit. Also, the **17.5 MPa** of maximum tensile stress allowable were not surpassed in any optimized model, with the final one reaching **16.5 MPa** max tensile stress.

Another important design criterion was the optimization, conducted with the use of a compliance-based algorithm following the requirement for structural validation of the results. Indeed, as mentioned above, the software environment structural analysis is an integrated function of the optimization process.

Finally, the evaluation of the structural behavior of the safety float glass, which can affect the optimization as an extra constraint, was required. During the design development, the optimization results was regularly tested so that they would not exceed the preset design principles, maximum voids' area **A = 1.17 m²** and maximum **span = 1.65 m.** When the fourth optimization exceeded the limits and endangered the stiffness of the float glass layer, additional elements were designed in order to minimize the particular cavities.

In terms of the cast glass demands, the uniform mass distribution was aimed during the whole optimization process. The member size function of the Ansys TO did not always work correctly for the current project. It was creating plenty of irregular inner holes, because of the coarse meshing. Thus, the replication of those holes was difficult due to the redesigning in rhino method which was followed. In addition, the algorithm method that Ansys use, SIMP method, do not provide a function of adding back material. Therefore, when the TO was removing some elements, which could be crucial from a non-structural point of view, they manually had to added back, changing the preset thickness range.
However, by excluding elements or faces in the TO region, strengthening weak thin components and "forcing" the software to further optimize specific areas led to a more uniform material distribution into the model. The thickness range of the final model vary within **100-180mm** and the mass reduction **55.2%** of the same solid slab.

The manufacturing constraint regarding the feasible transportation of the slab was adapted from the beginning of the design development process, during which the slab was split in two identical pieces, optimized and analyzed as separate.
The rest requirements such as the smooth surfaces and round edges as well as the minimum thickness limit of the manufacturing demands were accommodated during the post-processing.

• How can a monolithic massive cast glass slab be fabricated with 3d sand moulds? How can smaller pieces of moulds be assembled in order to produce one giant monolithic piece of cast glass?

Regarding the 3d printed sand moulds as a fabrication technique, several aspects needed intense consideration. These aspects concern the separation of the mould, the shell and infill structures, the pieces connectivity and finally the fabrication sequence.

Starting with the mould separation, although 3d printing has been already established in the building industry the past few years, strong restrictions are still presented. Specifically, the sand printers with the binder jetting method have not developed a flexible sizing for large-scale building components yet. Therefore, a separation of the required mould for the glass casting was inevitable here.

Since the sand printers allow the freedom of almost infinite design choices the mould separation method had to rely on specific factors. The main aspects focused on the low and even mass of the pieces, but at the same time on minimizing the joints. Splitting the mould in areas and shapes that will not generate fragile, prone to failure elements was concerned.

According to the topologically optimized geometry that was obtained, plenty of holes are existed in the slab, revealing several solid parts of the mould that do not contribute in its function. Therefore, after studying the topology optimization for the cast glass slab, an optimization of the mould itself could not be left out. By introducing an infill structure of less density than the solid one, the total weight of the mould is reduced, the printing time is by far decreased and the manufacturing costs drop. A shell wall of consistent thickness surrounds the mould cavity, protecting the mould from failure that the hydrostatic pressure during glass melting can cause. Two alternative designs of shell where proposed, one buttress-shaped and one honeycomb sandwich wall. According to the volume assessment the second choice was preferred, since the maximum thickness value is almost the same but the honeycomb sandwich presents 5% less volume.

Therefore, four infill alternatives where generated and assessed in terms of volume, one with hollow infill, a 20% honeycomb pattern, a 25% grid pattern and a buttresses-system infill. Since the shell structure was demonstrated enough for the hydrostatic pressure, the hollow infill was chosen, filled with unconsolidated sand

in order to fix and compact the mould pieces.

In terms of connectivity, extensions and undercuts were generated in the mould pieces, interlocking with integrated dense nodes. Some additional elements in the hollow infill were created, in order to stabilize the whole system.

For the assembly of the pieces, it was important that the placement of the mould pieces inside a concrete container, which works as a ring beam around them, restricts any horizontal movements. After the placement of a glass wool blanket to accommodate the different expansions of glass and concrete, the pieces are adjusted inside in three stages, according to their type of connection. Finally, the loose sand fills the hollow parts, ensuring also that the pieces will not move upwards in case of a glass leakage.

• How this optimized glass slab will be integrated into the building? (connections, details etc)

The integration of the two slab pieces into the building is conducted in two phases, the first one under factory conditions and the second one on-site. In general, the most important aspect was the necessity for vertical placement of the new slab into the cavity in which the replaced floor currently exists.

Starting from the factory phase, the lamination part of the connecting elements and the float glass panes need to be completed before the framing of the three supported faces of the slab. Then, the slab system can be transferred to the building.
In the museum, four L-shaped brackets have already been fastened in the existing concrete beams. The slab with the bottom connection is placed first and rests on top of the brackets. Then the next slab is applied and the connection is fastened with nuts and bolts while the surface coverings finish the result.
All contact surfaces of glass and steel or kovar are protected with the appropriate interlayer each time, varying from silicone and POM to neoprene, so as to avoid cracks due to stress concentrations.

As an overall conclusion, a lightweight slab with minimized and proper annealing time, due to the material distribution, was designed and solved. Starting from the fabrication part with 3d printed sand moulds, the transportation in pieces, until the integration into the Acropolis museum.

The optimized slab highlights the contrast between the ancient and the new-age architecture, blending the different eras harmoniously. The transparency and the light diffusion into the building makes the visitor to feel like hovering between past and future.

8. Limitations

Plenty limitations were faced during working on the project. Some were unsolvable and never overcome, while others were solved with adaptive solutions.

The main problem that could not be defeated was the impact of the Covid-19 outbreak in this thesis. Since the lockdown of the university and most services of the country taking place a bit earlier than P3 presentation, prototyping, glass casting and validation structural tests were doomed. Therefore, all relative conclusions were based on theoretical background, on the valuable mentors' contribution and literature findings.

Another factor which created several difficulties in the optimization part of the thesis was the limitation regarding the elements' and nodes' magnitude allowable for the optimization and structural analysis functions due to the academic license. With obtaining several results, the one after the other, and remeshing them, this problem overcame. However, the result with a professional license would be worth to be checked as well.

Many difficulties can emerge while working with topology optimization results for structural evaluation. The optimized geometry can get quite rough and irregular that importing it for another simulation can be impossible or extremely time-consuming. That is why each obtained geometry was firstly edited in other 3d modeling software and then was imported in Ansys. In addition, although the final model was smoothened during post-processing, the acquired geometry was not feasible to be obtained as a solid body. Therefore, using it for the following operations was impossible, except from the 3d visualization.

Finally, another limitation regarding the topology optimization and the used software was that the SIMP method that Ansys algorithm employs is restricted in terms of adding back elements which can contribute to the structural performance of the model. In contrast with BESO algorithms, with this method only the less contributing material is recognized, classified and due to the penalization factor is eliminated. Therefore, the designer needs to interfere with the software to obtain the optimum outcome.

9. Discussion and recommendations

A recommendation for a future development is the integration of an additional constraint during the optimization, such as aesthetic criteria. Considering that below the proposed slab is important archeological excavation, the optimization design could be developed in way to highlight them appropriately. For example, the slab elements could perform sparser on top of significant artworks, following their shape, and denser on top of the intermediate areas. Therefore, the slab could be perfectly blended with the environment but always considering as the first priority the structural constraints.

Another recommendation for further study would be to check the optimizing result of the entire slab before splitting, in case the license limitations allow, in order to test if the design remains the same. In addition, from an architectural point of view, while considering topology optimization as an interesting design method with unique results, an experimentation of applying different boundary conditions in the two slabs could end up with fascinating asymmetrical results.

The automization of the design process, for making topologically optimized cast glass slabs more feasible and affordable on a wider production with applications in every case, would be a useful further development. Although in this thesis the optimization part was quite time-consuming, in a commercial scenario the professional license and the strongest computing environment will give access to more options and finer meshing. This way, it will lead to a simplification of the procedure and an avoidance of many steps, occurred using the student license.

More specifically, as broader applications that the current thesis could have, two categories can be proposed. The first is the most realistic and straightforward outcomes of this thesis, while the second one contains ambitious, more challenging, out-of-the-box applications in which plenty of changes should be made in the current parameters.

In the first category, we could see other glass floor systems that any architect could desire with the maximum transparency that an exclusively cast glass structure provides. By adjusting the load and the support conditions in each case, the result of this research could be easily applied in every slab, dome vault or arch has high transparency demands and require less manufacturing time, weight and material consumption. The designing method, with the compliance-based optimization, and the fabrication technique, with the 3d printed sand mould system could be applied in this cases.
Particularly, some fascinating applications could be in a bridge floor,or a skyscraper balcony that one could enjoy the breathtaking view. Also a topologically optimized cast glass dome ceiling of a stadium could serve the largest, amazing cast glass application.

In the category where more parameters should be reconsidered, different geometrical types are proposed, such as an underwater tunnel that would allow the users to admire the sea during their journey. For that kind of applications the extra load of the water pressure and ultimate airtightness should be taken as extra constraints during the topology optimization.

References

Beghini, L.L., Beghini, A., Katz, N., Baker, W.F., Paulino, G.H., (2014), *Connecting architecture and engineering through structural topology optimization*, Engineering Structures, 59, pp.716-726.

Bendsoe, M.P., Sigmund, O., (2003) *Topology Optimisation: Theory, Methods and Applications.* Springer-Verlag, Berlin/Heidelberg, Germany.

Bhatia, I., S., (2019), *Shaping transparent sand in sand,* Master Thesis, TU Delft BK.

Corning, Nuclear Glass Blocks, (2018), (https://www.corning.com/worldwide/en/products/advanced-optics/product-materials/specialty-glass-and-glass-ceramics/radiation-shielding-glass/corning-med-x-glass.html)

Corning Museum of Glass, (2008), Meet the artist: Karen LaMonte,
(https://www.cmog.org/transcript/meet-artist-karen-lamonte)

Corning Museum of Glass, (1999), *Reflections on glass: Telescope mirrors, Innovations in Glass*, pp. 30–31. (https://www.cmog.org/article/reflections-glass-telescope-mirrors)

Cruz, P., J., S., (2016), *Structures and Architecture: Beyond their Limits*, CRC Press.

Damen, W., (2019), *Topologically optimized cast glass grid shell nodes,* Master Thesis, TU Delft BK.

Flygt, E., RISE Glas, (2018), *Utveckling av 3D-Printade sandformar for glasgjutning.*, GLAS. vol. 4-2018, p. 3. Stockholm.

Galjaard, S., Hofman, S., Perry, N., Ren, S., (2015), *Optimizing Structural Building Elements in Metal by using Additive Manufacturing,* IASS Symposium 2015, Amsterdam.

Gebisa, A.W., Lemu, H.G., (2017), *A case study on topology optimized design for additive manufacturing,* Materials Science and Engineering. Stavanger, Norway.

Goppert, K., Paech, C., Arbos, F., Teixidor, C., (2008), Innovative glass joints - the 11 march memorial in Madrid, in: C. Louter, F. Bos, F. Veer (Eds.), Challenging Glass: Conference on Architectural and Structural Applications of Glass, IOS Press, Delft, The Netherlands, pp. 111–118.

Hailu S.G., Dereje E.W., Fakhruldin M.H., (2017), *A comparative study on stress and compliance based structural topology optimization,* IOP Conference Series: Materials Science and Engineering 241.

Huang, X., Xie, Y.M., (2010), *Evolutionary topology optimization of continuum structures with an additional displacement constraint.* Structural and Multidisciplinary Optimisation, 40, 409-416.

Jewett, J., Carstensen, J. (2019), *Topology-optimized design, construction and experimental evaluation of concrete beams.* Automation in Construction 102, 59-67.

Jipa, A., Meibodi, M.A., Bernhart, M., Dillenburger, B., (2016), *3D-Printed Stay-in-Place Formwork for Topology Optimised Concrete Slab*, TxA Emerging Design + Technology Conference, San Antonio, Texas, USA.

Liew, A., López López, D., Van Mele, T., Block, P., (2017), *Design, fabrication and testing of a prototype, thin-vaulted, unreinforced concrete floor,* Engineering Structures 137, pp. 323-335.

Lundgren, J., Palmqvist, C., (2012) *Structural Form Optimisation; Methods of numerical optimization and applications on civil engineering structures.* Master Thesis, Department of Civil and Environmental Engineering, Chalmers University of Technology, Göteborg, Sweden.

Niehe, P, (2017), *Sand Printing Makes Complex Casted Structural Parts Affordable,*
(https://www.arup.com/news-and-events/news/sand-printing-makes-complexcasted-structural-parts-affordable).

Nijsse, R., (2003), *Glass in Structures: elements, concepts, designs,* Birkhäuser.

Oikonomopoulou, F., Bristogianni, L., Veer, F.A., Nijsse, R., (2017), *The construction of the Crystal Houses façade: challenges and innovations,* Glass Structures and Engineering, 3, pp. 87-108.

Oikonomopoulou, F., Bristogianni, T., Barou, L., Veer, F.A., Nijsse, R., (2018), *The potential of cast glass in structural applications,* Journal of Building Engineering 20, pp. 213-234.

Oikonomopoulou, F., (2019), Unveiling the third dimension of glass, Dissertation, TU Delft BK, Sirene Ontwerpers, Rotterdam.

Oikonomopoulou, F, Bhatia, I., S., Weijst, F., Damen, W., Bristogianni, T., (2020), *Rethinking the Cast Glass Mould. An Exploration on Novel Techniques for generating Complex and Customized Geometries,* Challenging Glass 7, Conference on Architectural and Structural Applications of Glass, Ghent University.

Rozvany, G., (2009), *A critical review of established methods of structural topology optimization, Structural Multidisciplinary Optimization*, 37, 217-237.

Shand, E.B., Armistead, W.H., (1958) *Glass Engineering Handbook,* McGraw-Hill Book Company, New York, 1958.

Vitalis, D., (2017), *Glass Sandwich Panel: Exploring the potential of glass sandwich structures for relatively lightweight planar elements with high stiffness and controlled transparency*, Msc thesis, TU Delft BK.

Wang, M.Y., Wang, X., Guo, D. (2003) *A level set method for structural topology optimization,* Computer methods in applied mechanics and engineering, 192, pp. 227-246.

Wurm, J., (2007), *Glass structures: Design and construction of self-supporting skins*, Birkhäuser, pp. 175-179.

Appendices

Appendix A
KG33 glass properties

CES 2019 EDUPACK

Borosilicate - KG33

General information
Designation

KG33

Typical uses

Laboratory ware,

Composition overview
Compositional summary

81% SiO2/2% Al2O3/13% B2O3/4% Na2O/4.5% MgO

Material family	Glass
Base material	Oxide

Composition detail (metals, ceramics and glasses)

Al2O3 (alumina)		2			%
B2O3 (boric oxide)		13			%
MgO (magnesia)		0	-	4,5	%
Na2O (sodium oxide)		0	-	4	%
SiO2 (silica)		81			%

Price

Price	*	3,55	-	5,33	EUR/kg
Price per unit volume	*	7,82e3	-	1,2e4	EUR/m^3

Physical properties

Density		2,2e3	-	2,25e3	kg/m^3
Porosity (closed)		0			%
Porosity (open)		0			%

Mechanical properties

Young's modulus	*	61	-	65	GPa
Specific stiffness	*	27,4	-	29,3	MN.m/kg
Yield strength (elastic limit)	*	28,6	-	31,6	MPa
Tensile strength		28,6	-	31,6	MPa
Specific strength	*	12,8	-	14,2	kN.m/kg
Elongation	*	0,04	-	0,05	% strain
Compressive strength	*	286	-	316	MPa
Flexural modulus	*	61	-	65	GPa
Flexural strength (modulus of rupture)	*	37,2	-	41,1	MPa
Shear modulus	*	25,5	-	27,1	GPa
Bulk modulus	*	33,3	-	35,5	GPa
Poisson's ratio	*	0,19	-	0,2	
Shape factor		15			
Hardness - Vickers	*	85,7	-	94,7	HV

Values marked * are estimates.
No warranty is given for the accuracy of this data

CES 2019 EDUPACK

Borosilicate - KG33

Elastic stored energy (springs)		6,48	-	7,95	kJ/m^3
Fatigue strength at 10^7 cycles	*	27,1	-	30	MPa

Impact & fracture properties

Fracture toughness	*	0,6	-	0,62	MPa.m^0.5
Toughness (G)	*	0,00565	-	0,00618	kJ/m^2

Thermal properties

Glass temperature		488	-	648	°C
Maximum service temperature	*	244	-	518	°C
Minimum service temperature		-273			°C
Thermal conductivity	*	1,1	-	1,2	W/m.°C
Specific heat capacity	*	760	-	800	J/kg.°C
Thermal expansion coefficient		3,13	-	3,26	µstrain/°C
Thermal shock resistance	*	140	-	159	°C
Thermal distortion resistance	*	0,343	-	0,377	MW/m

Electrical properties

Electrical resistivity	*	1e22	-	1e24	µohm.cm
Electrical conductivity		1,72e-22	-	1,72e-20	%IACS
Dielectric constant (relative permittivity)		4,4	-	4,7	
Dissipation factor (dielectric loss tangent)		0,0196	-	0,0218	
Dielectric strength (dielectric breakdown)	*	12	-	14	MV/m

Magnetic properties

Magnetic type	Non-magnetic

Optical, aesthetic and acoustic properties

Color		Clear			
Refractive index		1,46	-	1,48	
Transparency		Transparent			
Acoustic velocity	*	5,23e3	-	5,41e3	m/s
Mechanical loss coefficient (tan delta)		4,6e-5	-	6,2e-5	

Critical materials risk

Contains >5wt% critical elements?	No

Durability

Water (fresh)	Excellent
Water (salt)	Excellent
Weak acids	Excellent
Strong acids	Excellent
Weak alkalis	Excellent
Strong alkalis	Acceptable
Organic solvents	Excellent
Oxidation at 500C	Excellent

Values marked * are estimates.
No warranty is given for the accuracy of this data

CES 2019 EDUPACK

Borosilicate - KG33

UV radiation (sunlight)	Excellent
Halogens	Acceptable
Metals	Acceptable
Flammability	Non-flammable

Primary production energy, CO2 and water

Embodied energy, primary production	*	21,4	-	23,7	MJ/kg
CO2 footprint, primary production	*	1,33	-	1,47	kg/kg
Water usage	*	10,2	-	11,3	l/kg

Processing energy, CO2 footprint & water

Glass molding energy	*	8,27	-	9,14	MJ/kg
Glass molding CO2	*	0,662	-	0,731	kg/kg
Glass molding water	*	2,46	-	3,69	l/kg
Grinding energy (per unit wt removed)	*	26,1	-	28,9	MJ/kg
Grinding CO2 (per unit wt removed)	*	1,96	-	2,17	kg/kg

Recycling and end of life

Recycle		✓			
Embodied energy, recycling	*	17,5	-	19,4	MJ/kg
CO2 footprint, recycling	*	0,93	-	1,03	kg/kg
Recycle fraction in current supply		22,7	-	25,1	%
Downcycle		✓			
Combust for energy recovery		✗			
Landfill		✓			
Biodegrade		✗			

Notes

Other notes

The borosilicates have a better environmental performance when given appropriate heat treatments

Links

ProcessUniverse

Producers

Reference

Shape

Values marked * are estimates.
No warranty is given for the accuracy of this data

Appendix B

Holes limitations due to float glass deflection

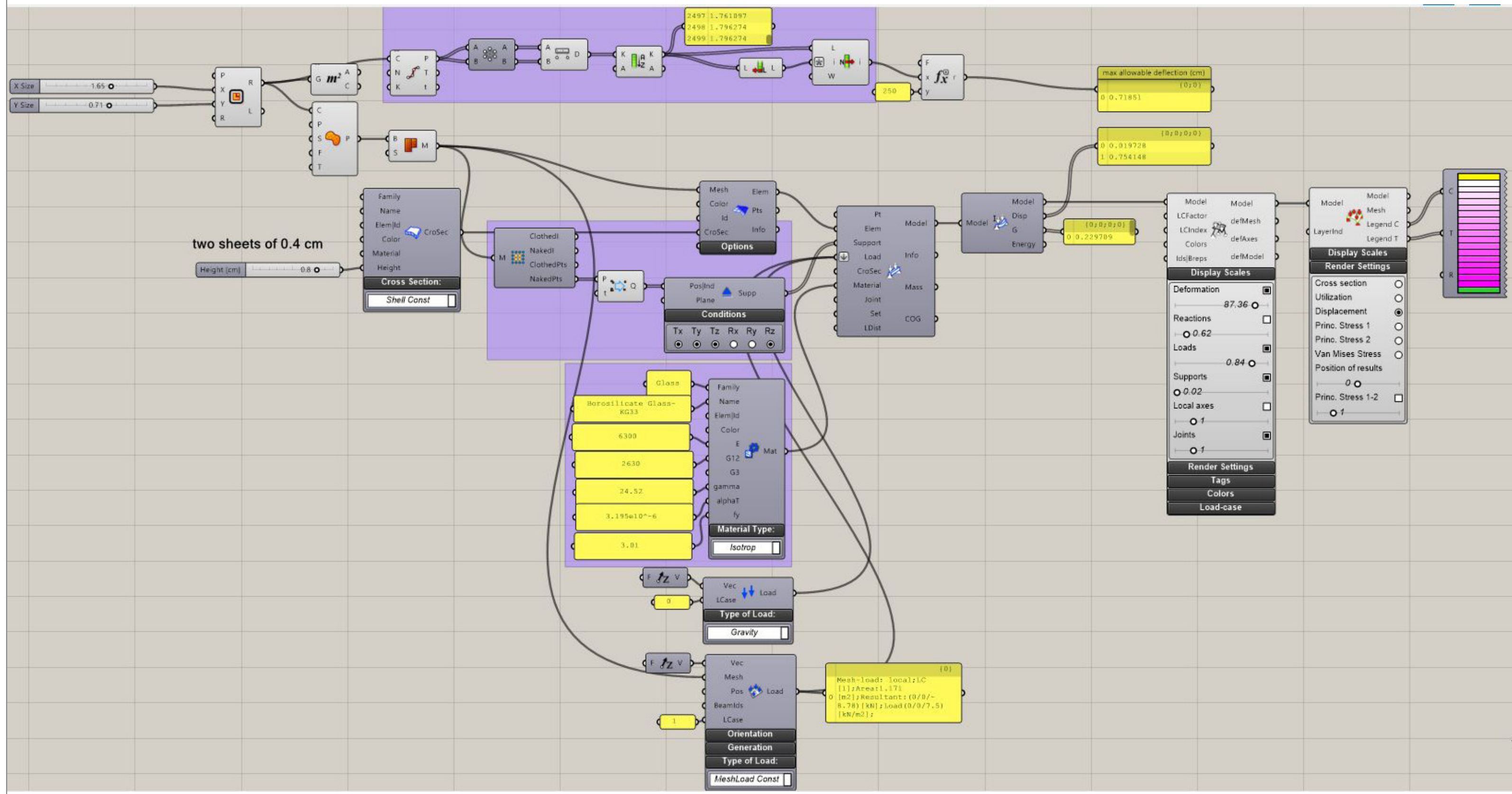

Appendix C

Optimization 0

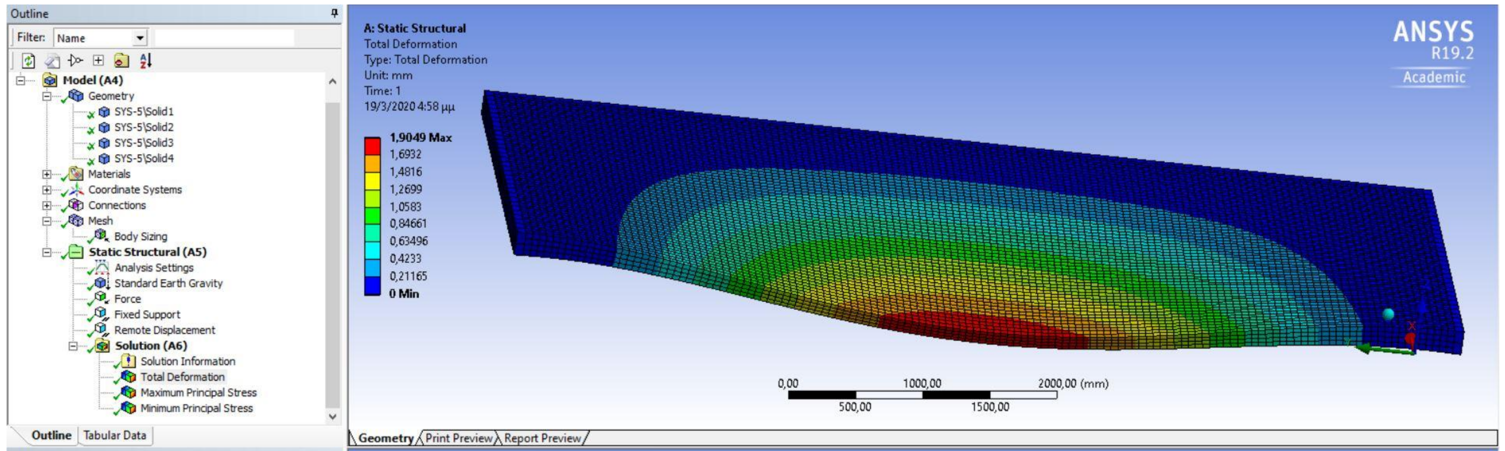

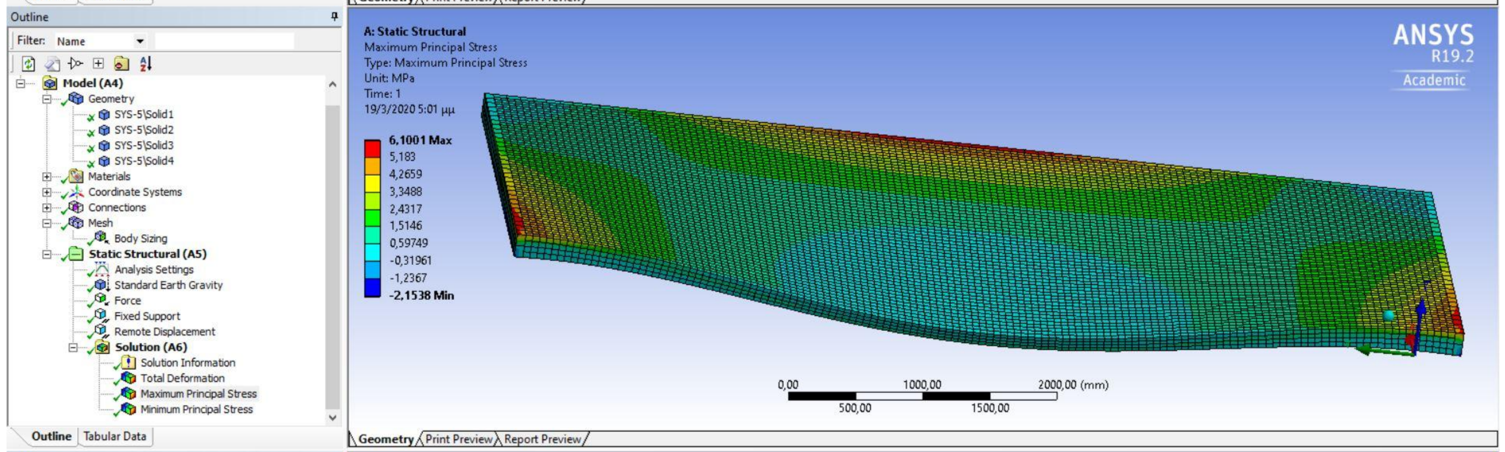

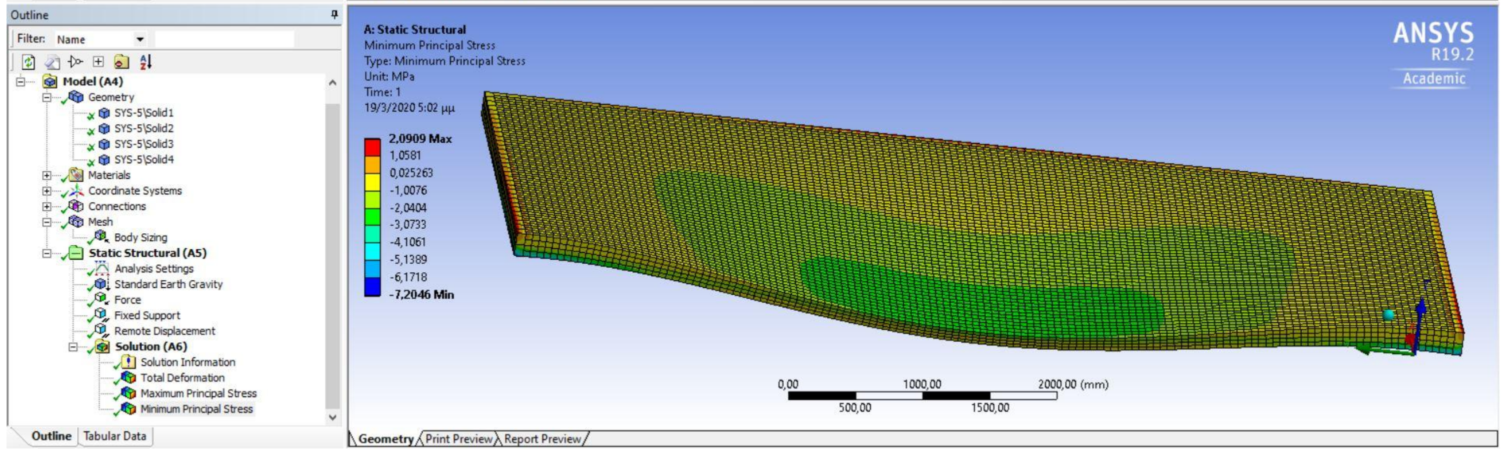

Optimization 1

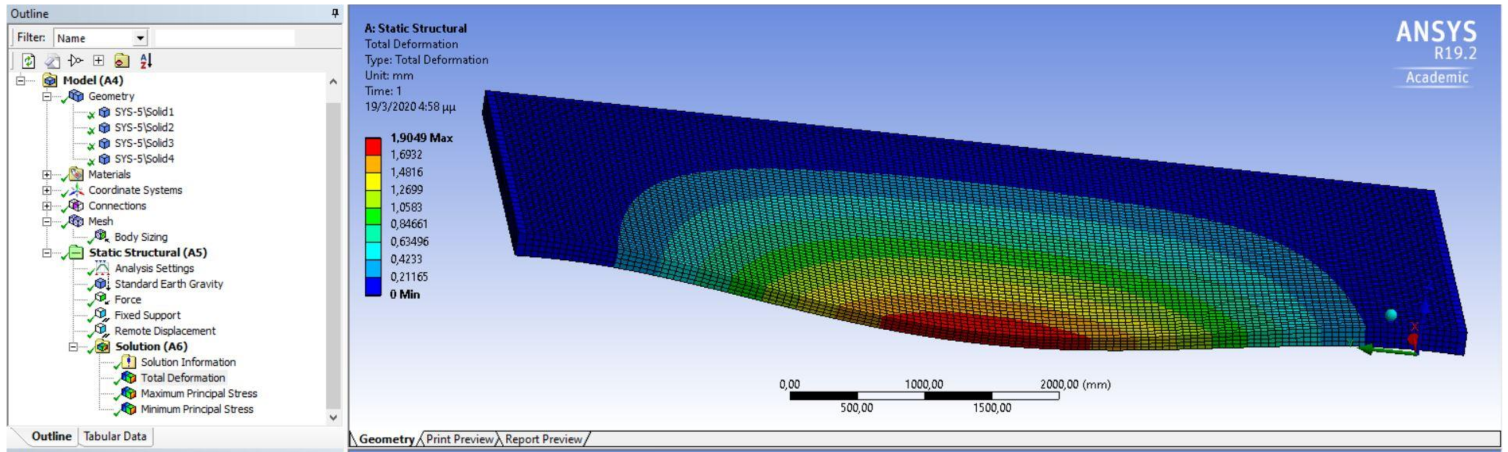

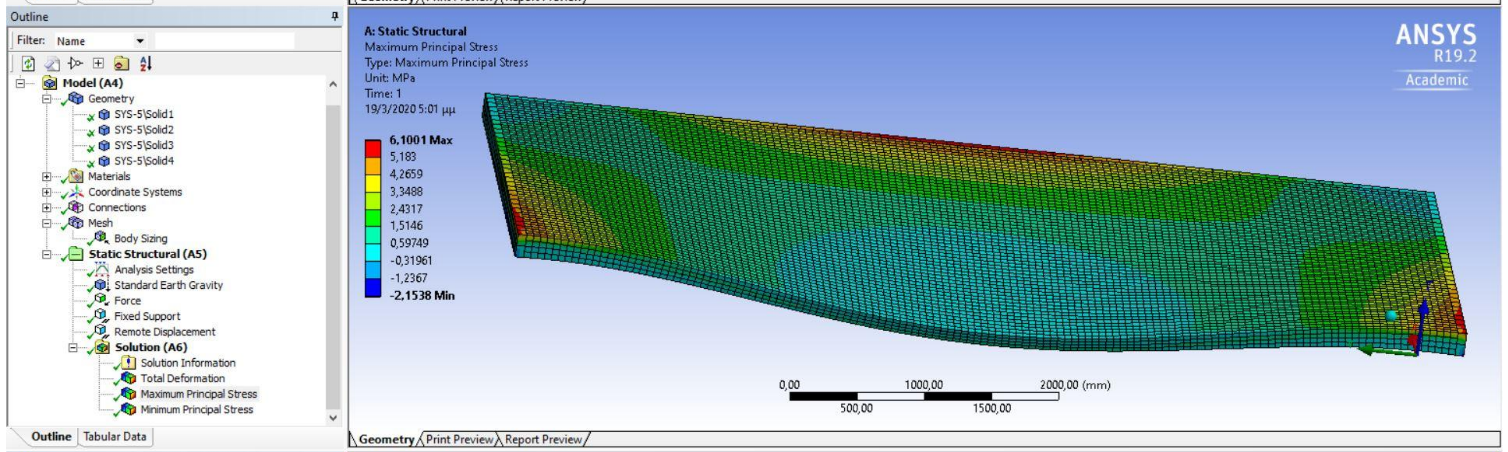

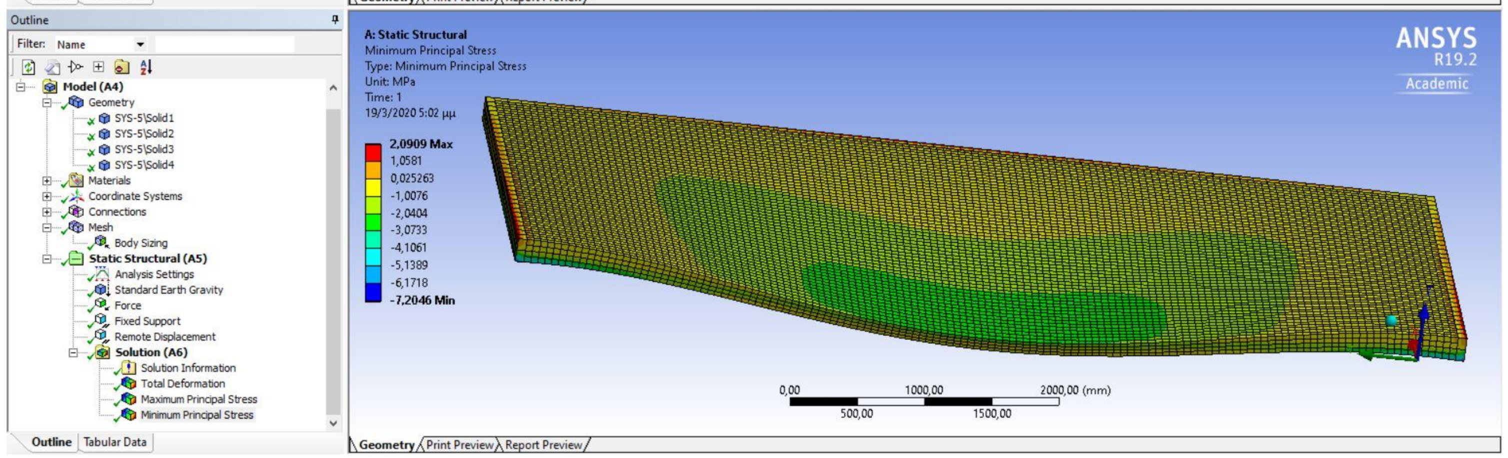

Optimization 2

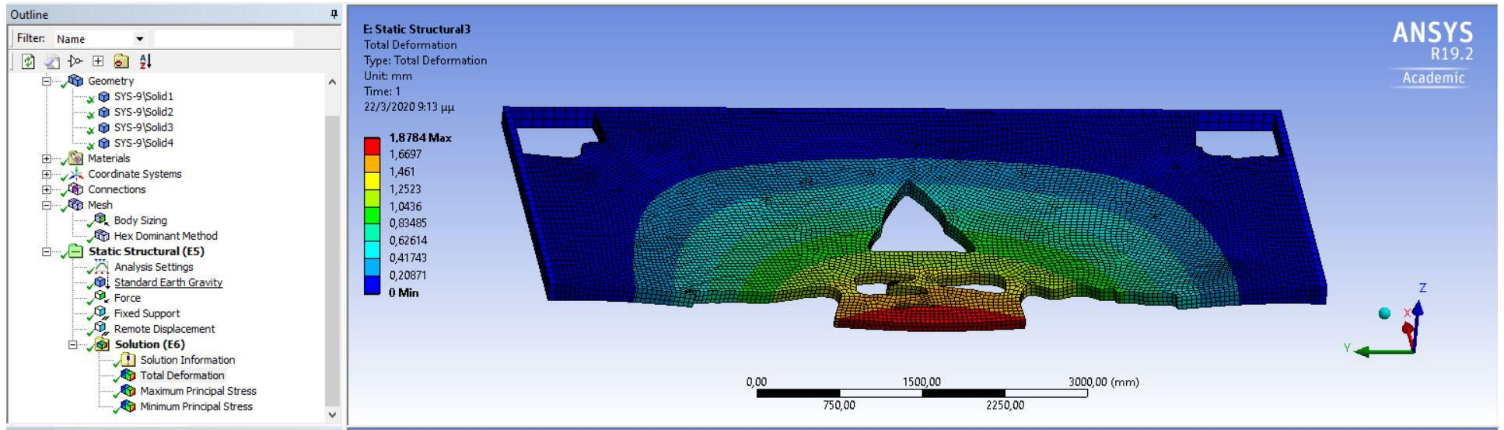

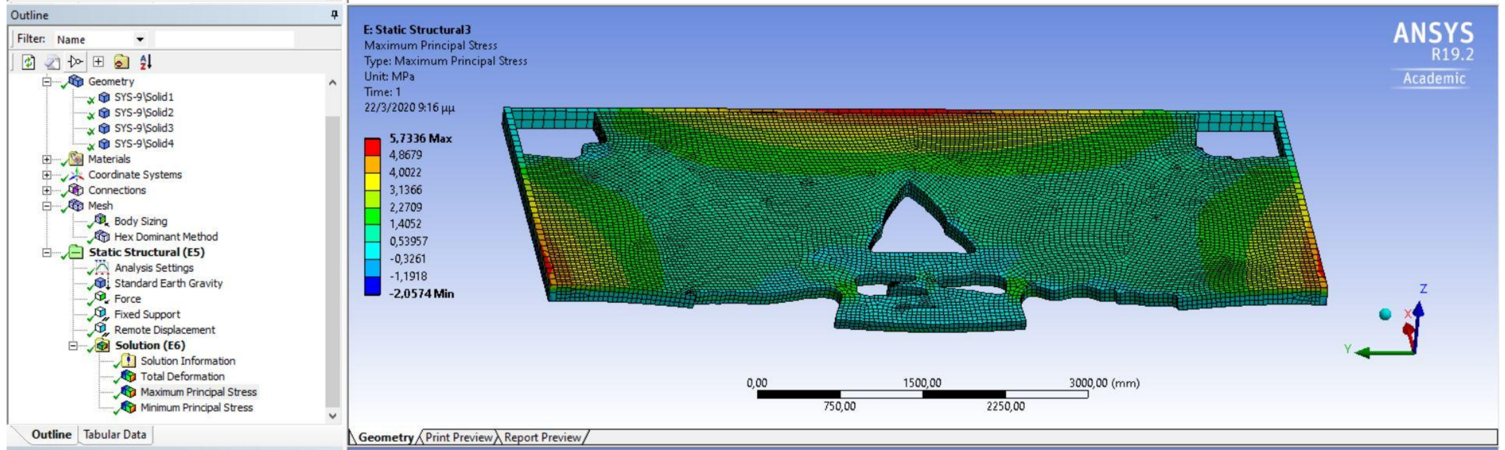

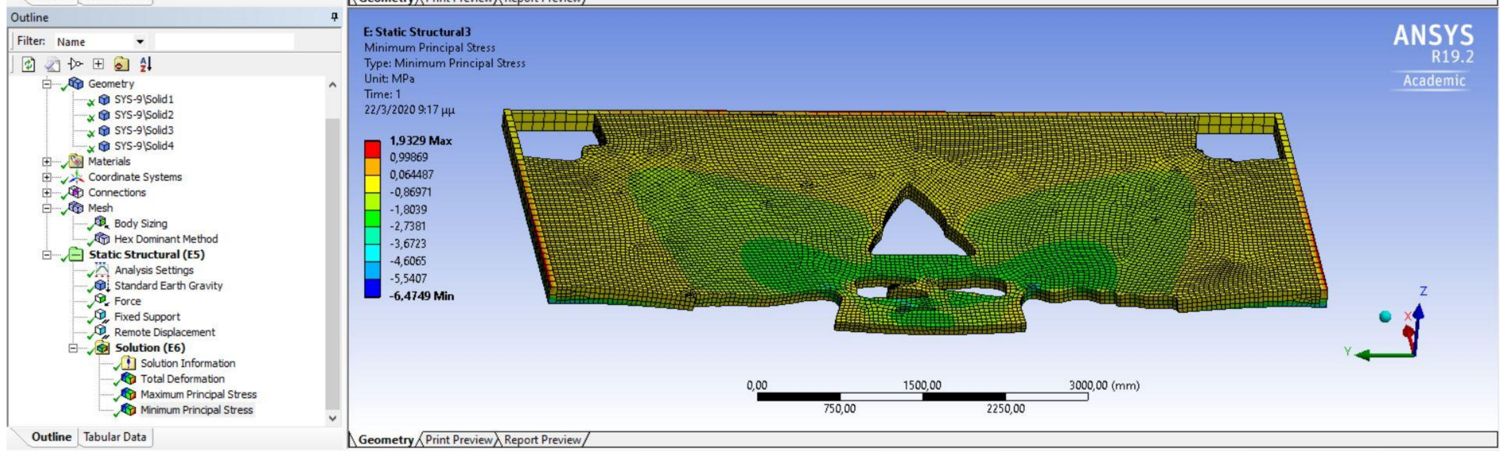

Optimization 3

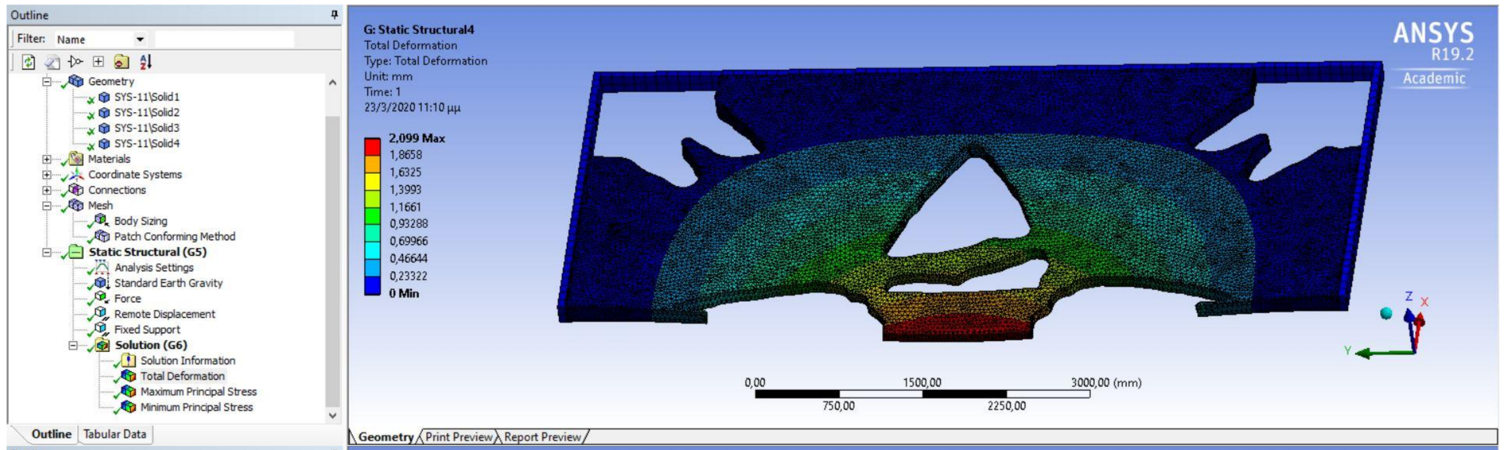

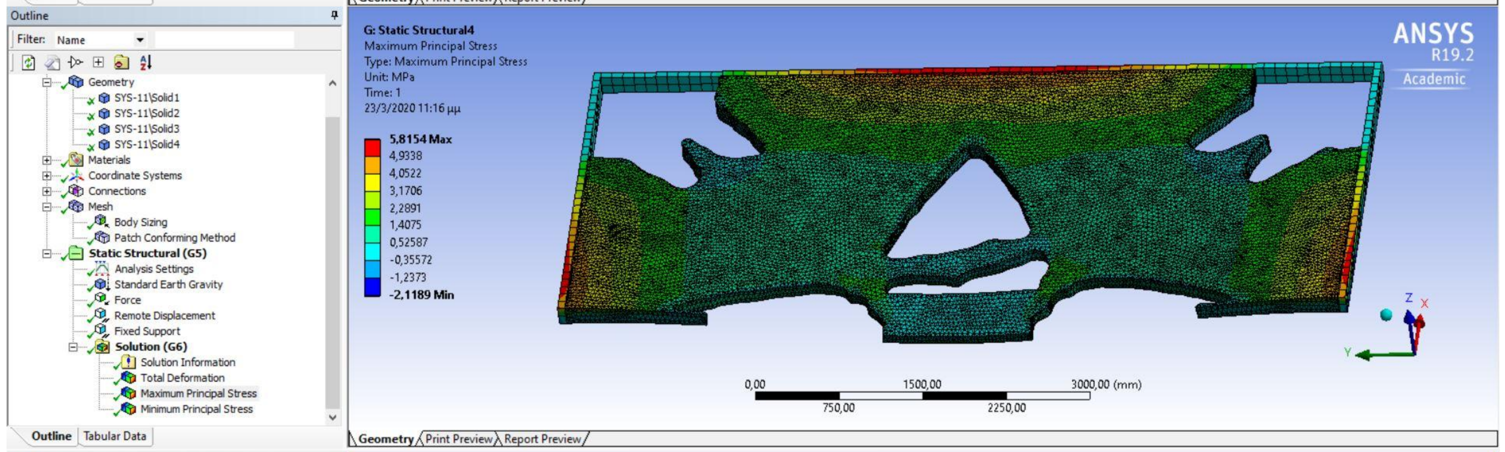

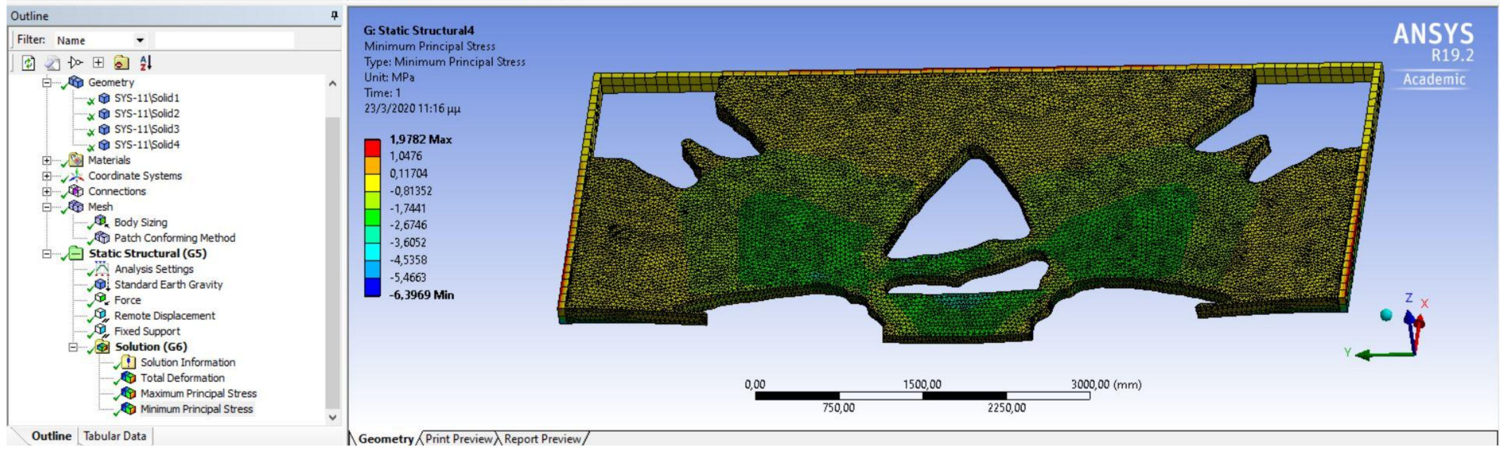

Optimization 4

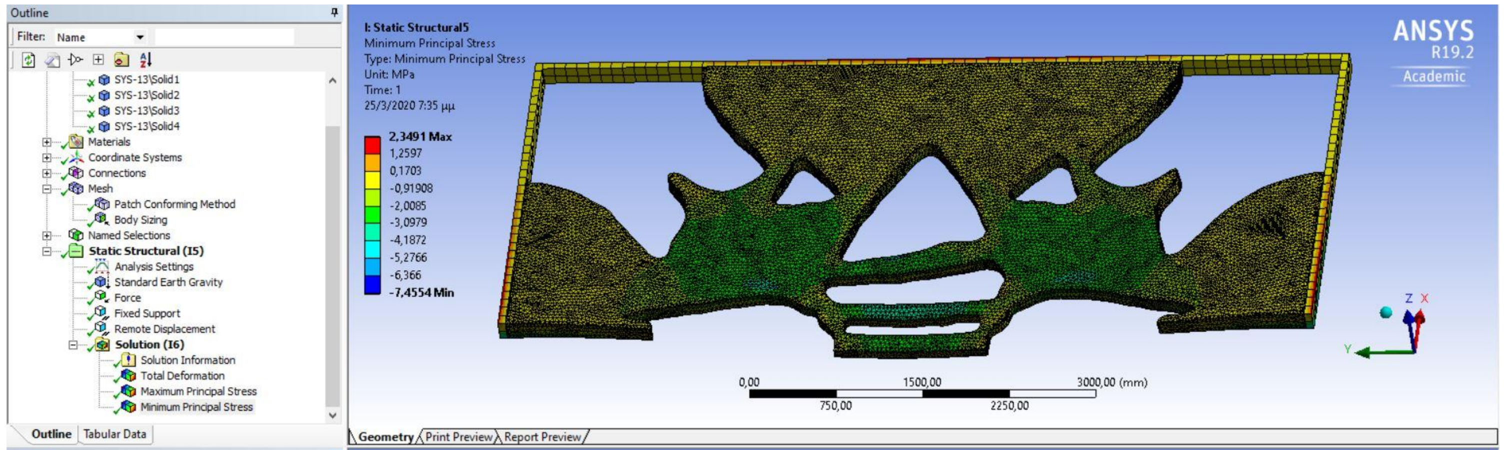

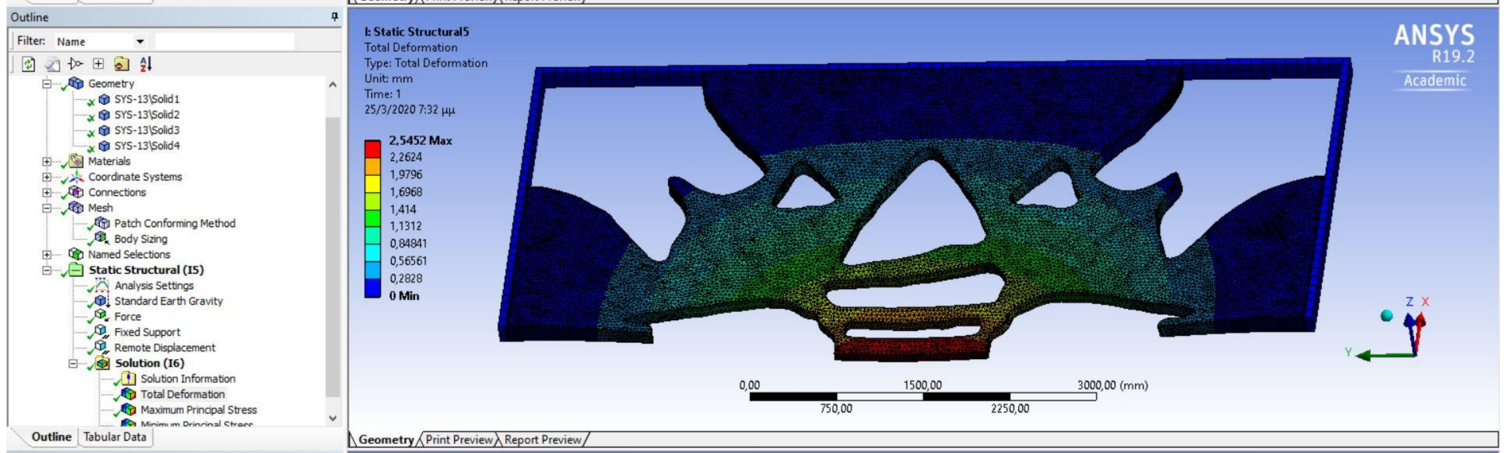

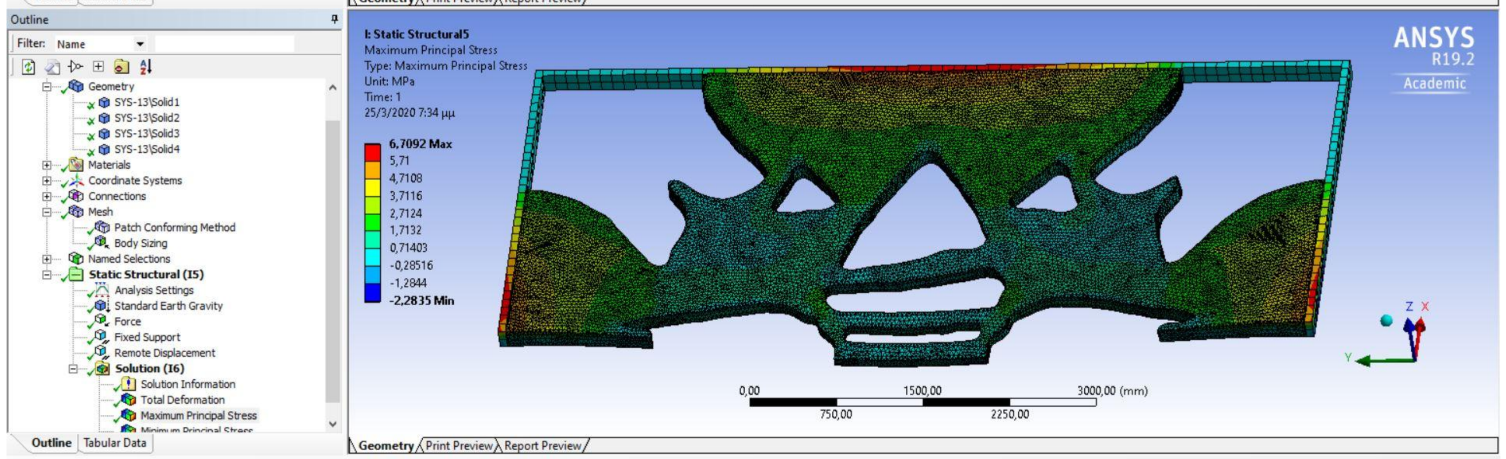

Optimization 4 - alternative

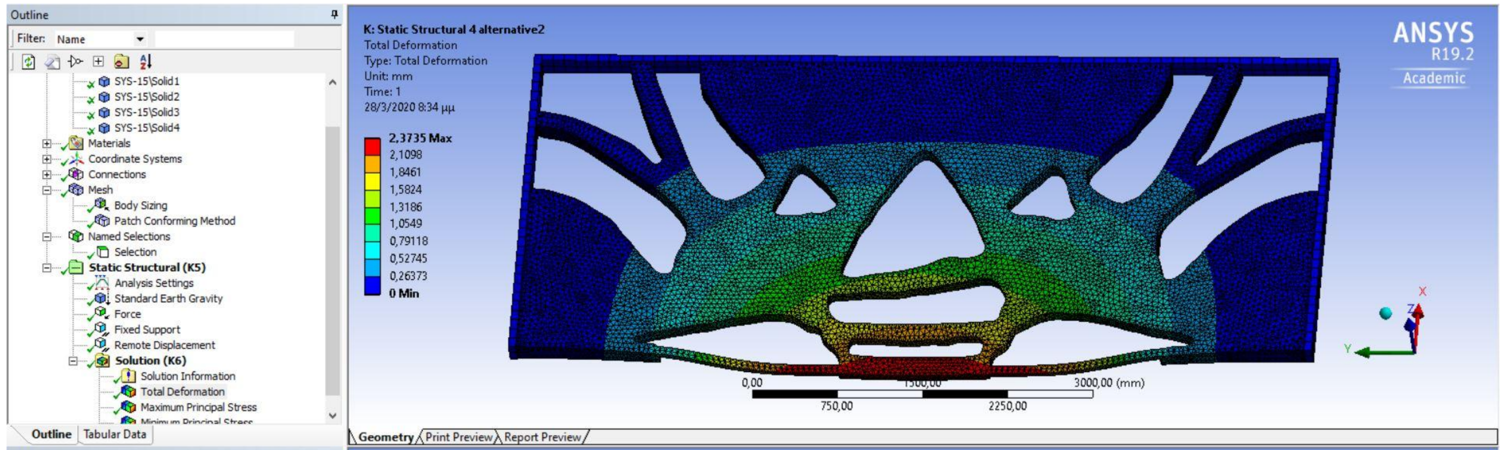

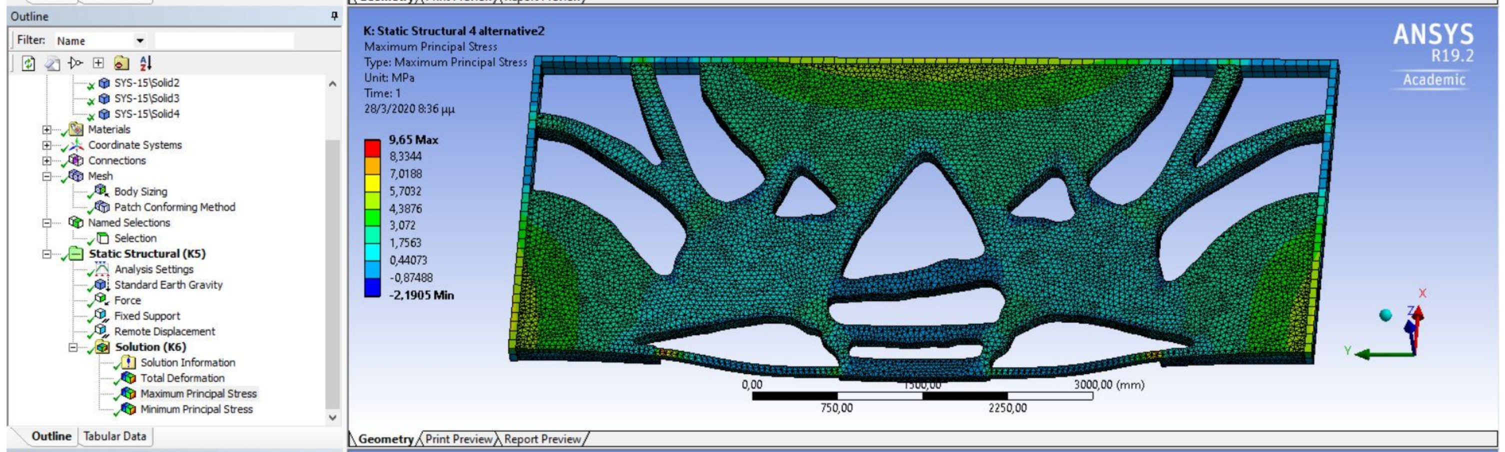

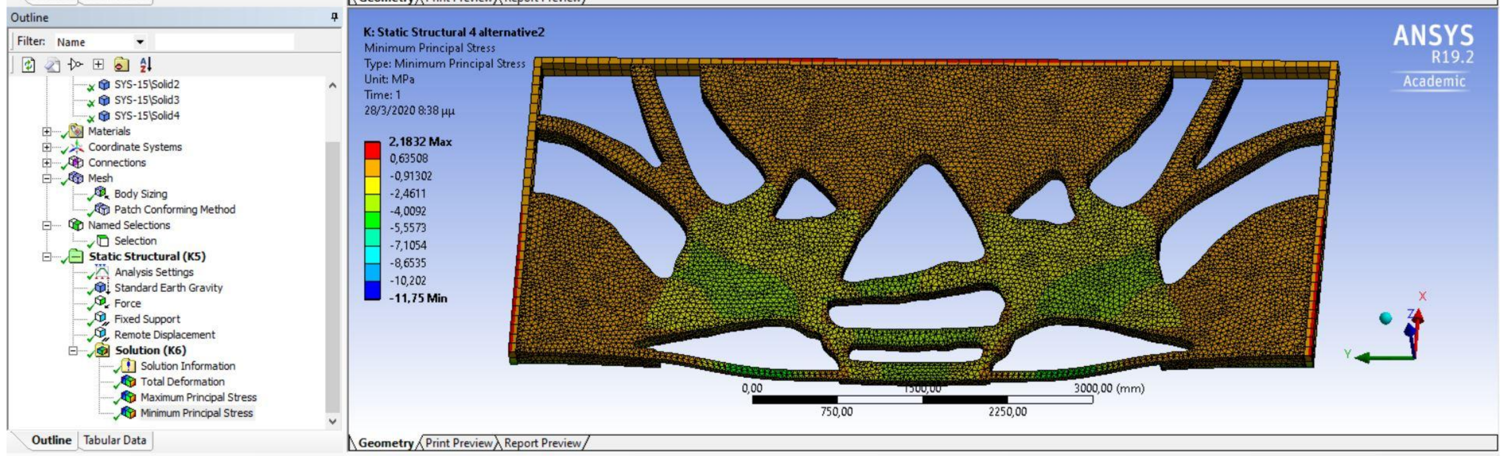

Optimization 5

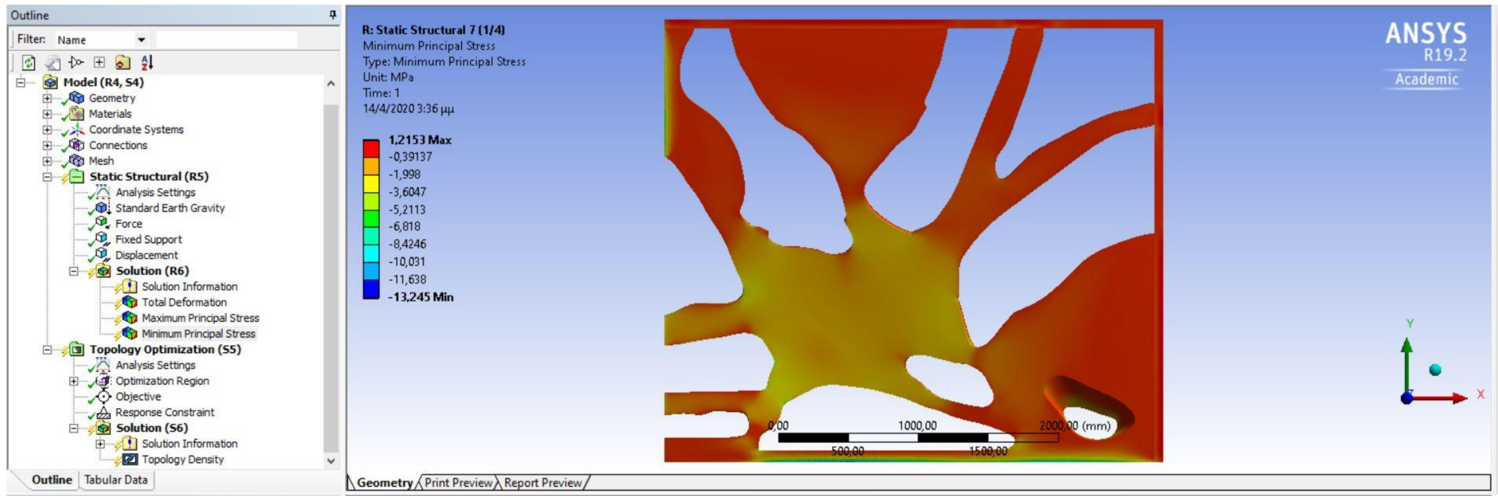

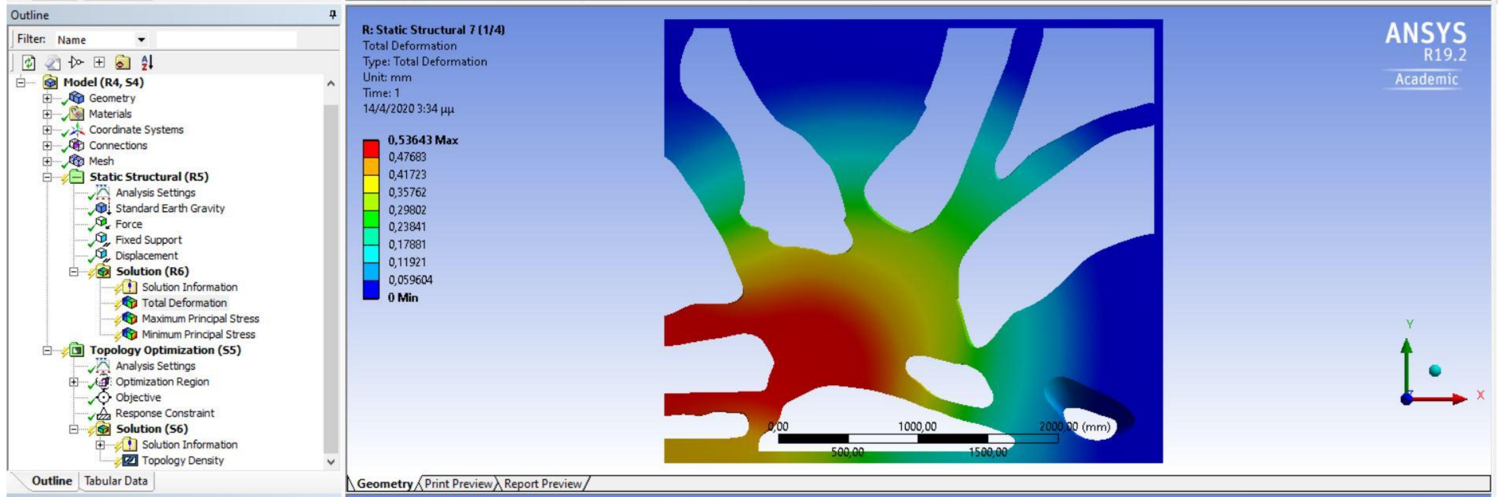

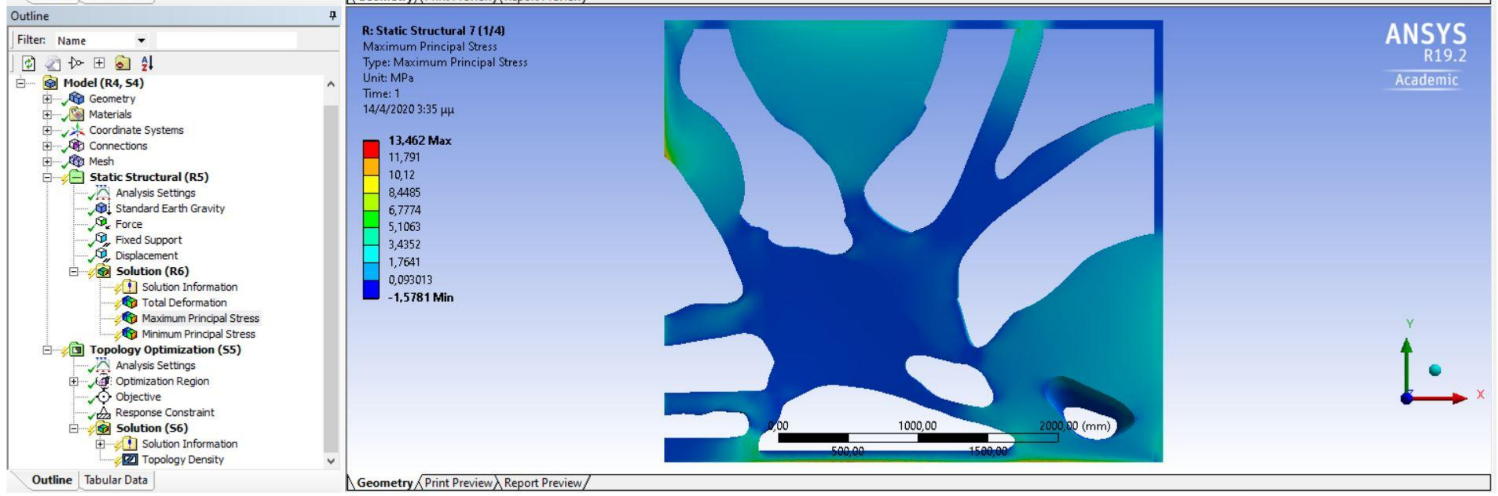

Optimization 6

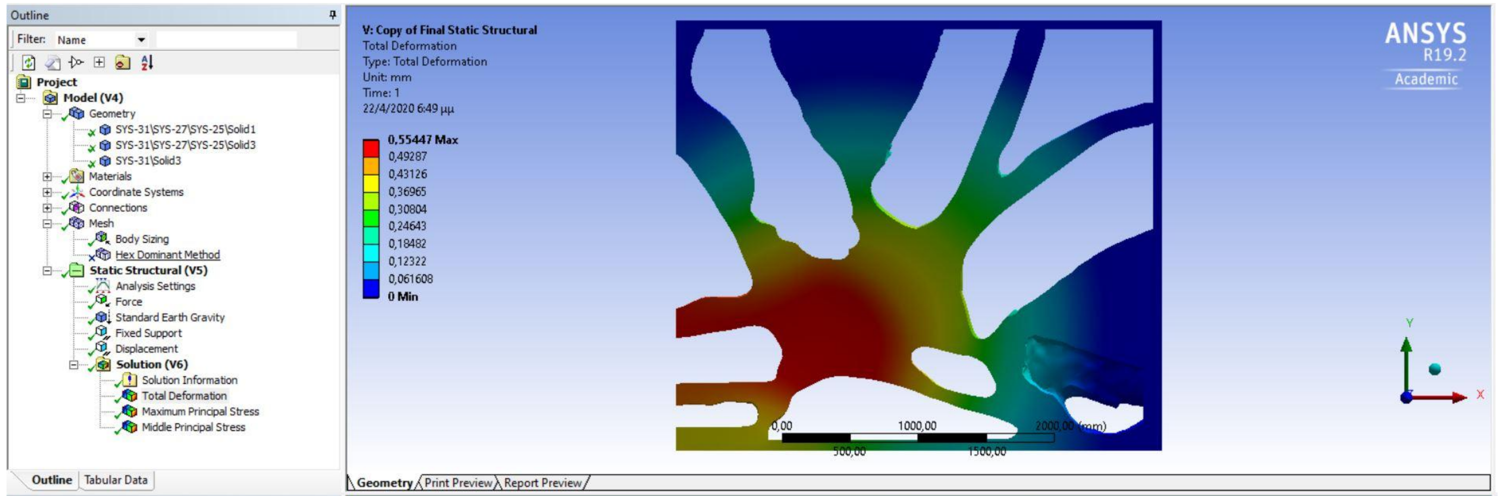

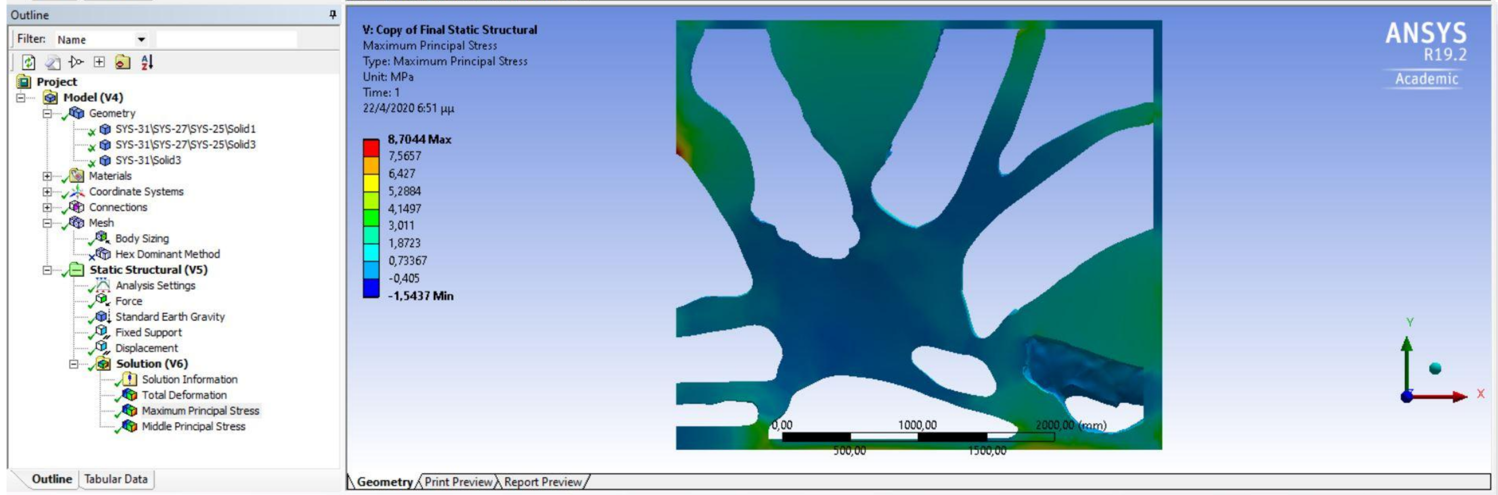

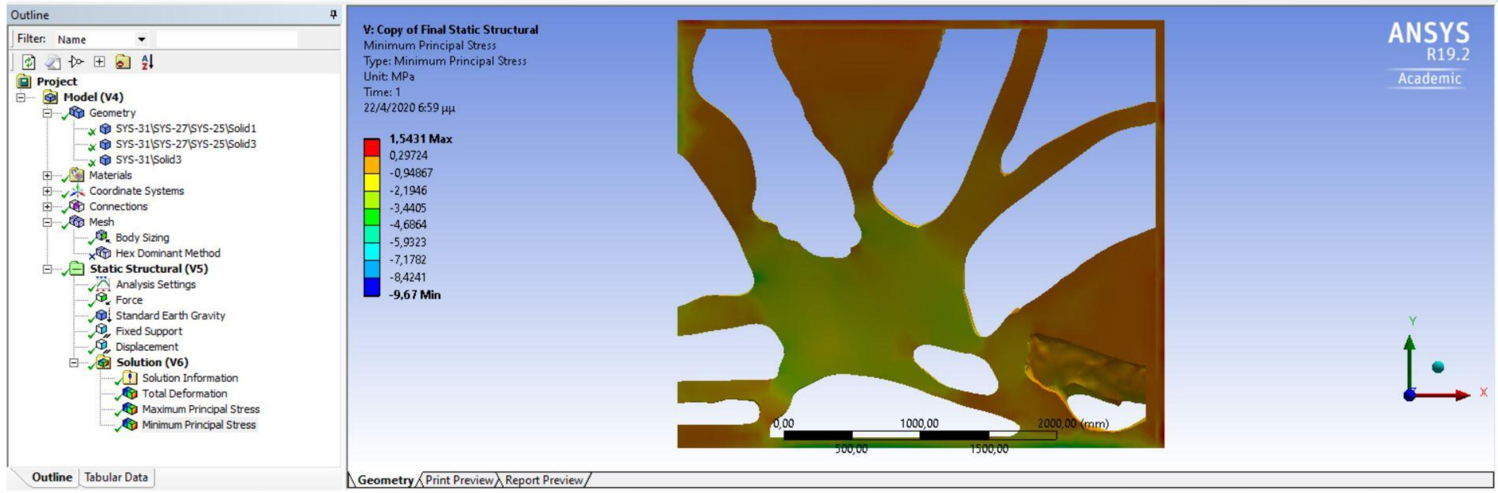

High alloy steel, Kovar, annealed

General information

Designation

Kovar, wrought

Condition	Annealed
UNS number	K94610
US name	AMS 7726 (wire), AMS 7727 (bars & forgings) , AMS 7728 (sheet strip plate), ASTM F15
EN name	DIN 17745 - SEW 385, GX3NiCo29-17, X3NiCo29-18, NiCo 29-18, BS ISO 19960
EN number	1.3981

Tradenames

CINSEAL, DILVER P, FENICOLOY, HAI-373, KOVAR, NICOSEAL, NICOSEL, NICOVAR, NILO ALLOY K, PERNIFER 2918, PFIZER SEAL VAR TM, PRP-GSA, RODAR, RODSEAL 29-17, SEALVAC A, SEALVAR, SIVAR 48, TECHALLOY GLASSEAL 29-17, TELCOSEAL, TELCOSEAL 1, THERLO, ULBRAVAR 29-17, VACON 10

Typical uses

Metal to glass or ceramic sealing, eg. cathode ray tubes, light bulbs, photoetching, thermal shock resisting

Composition overview

Compositional summary

Fe50-56 / Ni28-30 / Co16-18 (impurities: Mn<0.5, Cr<0.2, Cu<0.2, Mo<0.2, Si<0.2, C<0.05, P<0.03, S<0.03, Al,Mg,Ti,Zr<0.01)

Material family	Metal (ferrous)
Base material	Fe (Iron)

Composition detail (metals, ceramics and glasses)

Al (aluminum)	0	-	0,01	%
C (carbon)	0	-	0,05	%
Co (cobalt)	16	-	18	%
Cr (chromium)	0	-	0,2	%
Cu (copper)	0	-	0,2	%
Fe (iron)	* 50,5	-	56	%
Mg (magnesium)	0	-	0,01	%
Mn (manganese)	0	-	0,5	%
Mo (molybdenum)	0	-	0,2	%
Ni (nickel)	28	-	30	%
P (phosphorus)	0	-	0,03	%
S (sulfur)	0	-	0,03	%
Si (silicon)	0	-	0,2	%
Ti (titanium)	0	-	0,01	%
Zr (zirconium)	0	-	0,01	%

Price

Price	* 15,1	-	19,4	EUR/kg

High alloy steel, Kovar, annealed

Price per unit volume	* 1,25e5	-	1,63e5	EUR/m^3

Physical properties

Density	8,32e3	-	8,4e3	kg/m^3

Mechanical properties

Young's modulus	135	-	141	GPa
Specific stiffness	16,1	-	16,9	MN.m/kg
Yield strength (elastic limit)	345	-	410	MPa
Tensile strength	517	-	621	MPa
Specific strength	41,3	-	49,1	kN.m/kg
Elongation	25	-	42	% strain
Compressive modulus	* 135	-	141	GPa
Compressive strength	* 345	-	410	MPa
Flexural modulus	* 135	-	141	GPa
Flexural strength (modulus of rupture)	* 321	-	385	MPa
Shear modulus	50,4	-	53	GPa
Shear strength	* 388	-	466	MPa
Bulk modulus	* 123	-	129	GPa
Poisson's ratio	0,312	-	0,322	
Shape factor	43			
Hardness - Vickers	* 127	-	180	HV
Hardness - Rockwell B	68	-	82	HRB
Hardness - Brinell	120	-	170	HB
Elastic stored energy (springs)	434	-	606	kJ/m^3
Fatigue strength at 10^7 cycles	* 267	-	311	MPa
Fatigue strength model (stress range)	* 235	-	354	MPa

Parameters: Stress Ratio = -1, Number of Cycles = 1e7cycles

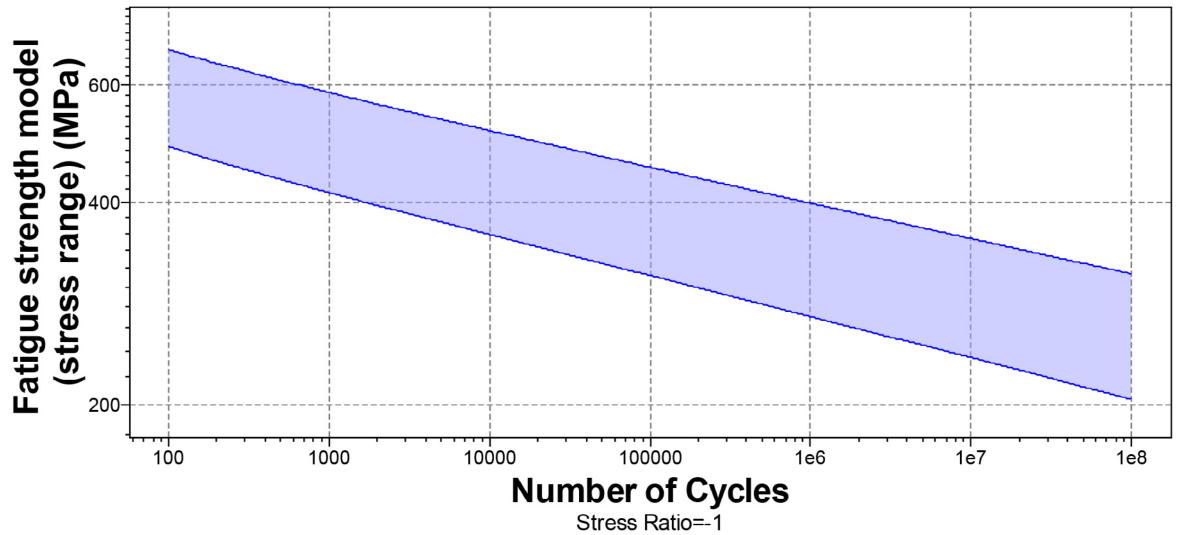

Impact & fracture properties

Fracture toughness	*	307	-	371	MPa.m^0.5
Toughness (G)		688	-	990	kJ/m^2

Thermal properties

Melting point		1,44e3	-	1,46e3	°C
Maximum service temperature	*	468	-	488	°C
Minimum service temperature		-273			°C
Thermal conductivity		17	-	17,6	W/m.°C
Specific heat capacity		431	-	448	J/kg.°C
Thermal expansion coefficient		4,6	-	5,5	µstrain/°C
Thermal shock resistance		479	-	613	°C
Thermal distortion resistance	*	3,14	-	3,77	MW/m
Latent heat of fusion		268			kJ/kg

Electrical properties

Electrical resistivity		46,7	-	51,4	µohm.cm
Electrical conductivity		3,35	-	3,69	%IACS
Galvanic potential	*	-0,47	-	-0,39	V

Magnetic properties

Magnetic type	Magnetic

Optical, aesthetic and acoustic properties

Transparency		Opaque			
Acoustic velocity		4,02e3	-	4,11e3	m/s
Mechanical loss coefficient (tan delta)	*	3e-4	-	5e-4	

Critical materials risk

Contains >5wt% critical elements?	Yes

Processing properties

Metal casting	Unsuitable	
Metal cold forming	Excellent	
Metal hot forming	Excellent	
Metal press forming	Excellent	
Metal deep drawing	Unsuitable	
Machining speed	8,23	m/min
Weldability	Excellent	
Notes	Preheating and post weld heat treatments may be required	

Durability

Water (fresh)	Excellent
Water (salt)	Excellent
Weak acids	Excellent
Strong acids	Acceptable

Weak alkalis	Excellent
Strong alkalis	Excellent
Organic solvents	Excellent
Oxidation at 500C	Excellent
UV radiation (sunlight)	Excellent
Galling resistance (adhesive wear)	Limited use
Flammability	Non-flammable

Corrosion resistance of metals

Pitting and crevice corrosion resistance	Low (<20)
Stress corrosion cracking	Slightly susceptible
Notes	Rated in chloride; Other susceptible environments: Hydrogen sulfide

Primary production energy, CO2 and water

Embodied energy, primary production	*	79,6	-	87,8	MJ/kg
CO2 footprint, primary production	*	5,77	-	6,36	kg/kg
Water usage	*	107	-	119	l/kg

Processing energy, CO2 footprint & water

Roll forming, forging energy	*	3,1	-	3,5	MJ/kg
Roll forming, forging CO2	*	0,24	-	0,26	kg/kg
Roll forming, forging water	*	2,9	-	4,3	l/kg
Extrusion, foil rolling energy	*	6	-	6,6	MJ/kg
Extrusion, foil rolling CO2	*	0,45	-	0,5	kg/kg
Extrusion, foil rolling water	*	6,1	-	6,4	l/kg
Wire drawing energy	*	22	-	24	MJ/kg
Wire drawing CO2	*	1,64	-	1,81	kg/kg
Wire drawing water	*	8,2	-	12,3	l/kg
Metal powder forming energy	*	35,9	-	39,6	MJ/kg
Metal powder forming CO2	*	2,69	-	2,97	kg/kg
Metal powder forming water	*	39,1	-	58,6	l/kg
Vaporization energy	*	1,07e4	-	1,18e4	MJ/kg
Vaporization CO2	*	804	-	886	kg/kg
Vaporization water	*	4,46e3	-	6,69e3	l/kg
Coarse machining energy (per unit wt removed)	*	0,9	-	1	MJ/kg
Coarse machining CO2 (per unit wt removed)	*	0,068	-	0,075	kg/kg
Fine machining energy (per unit wt removed)	*	4,8	-	5,2	MJ/kg
Fine machining CO2 (per unit wt removed)	*	0,36	-	0,39	kg/kg
Grinding energy (per unit wt removed)	*	9	-	10	MJ/kg
Grinding CO2 (per unit wt removed)	*	0,68	-	0,75	kg/kg
Non-conventional machining energy (per unit wt removed)	*	107	-	118	MJ/kg
Non-conventional machining CO2 (per unit wt removed)	*	8,04	-	8,86	kg/kg

Recycling and end of life

Recycle	✓			
Embodied energy, recycling	* 15,5	-	17,1	MJ/kg
CO2 footprint, recycling	* 1,22	-	1,34	kg/kg
Recycle fraction in current supply	* 28,9	-	31,9	%
Downcycle	✓			
Combust for energy recovery	✗			
Landfill	✗			
Biodegrade	✗			

Notes

Standards with similar compositions

Kovar, wrought, N94630, KOVAR, PERNIFER, ULBRAVAR, NICOSEL, RODAR, FENICOLOY, 1.3981

Links

ProcessUniverse

Producers

Reference

Appendix E

Connection 1 - LC1

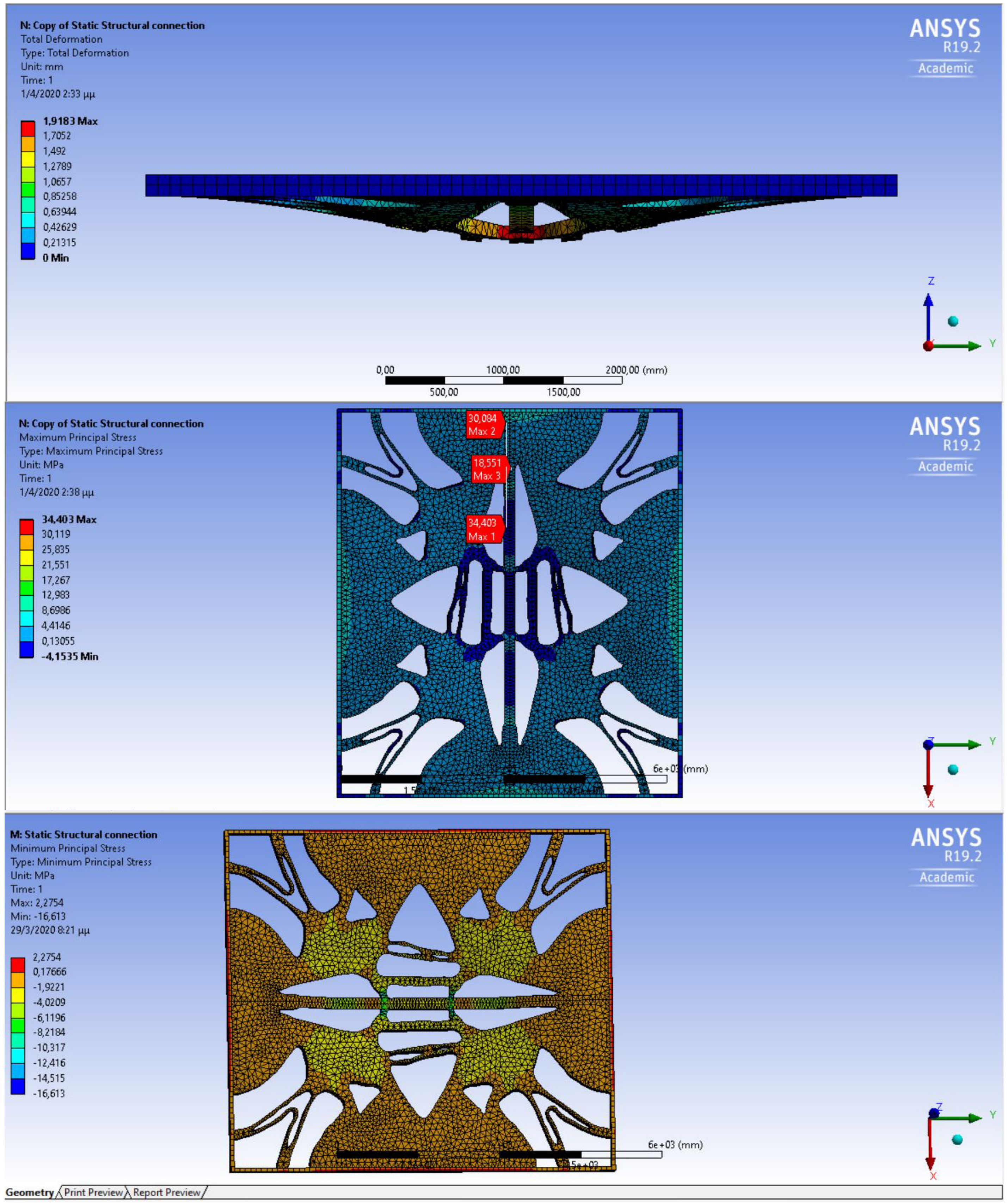

Connection 1 - LC2

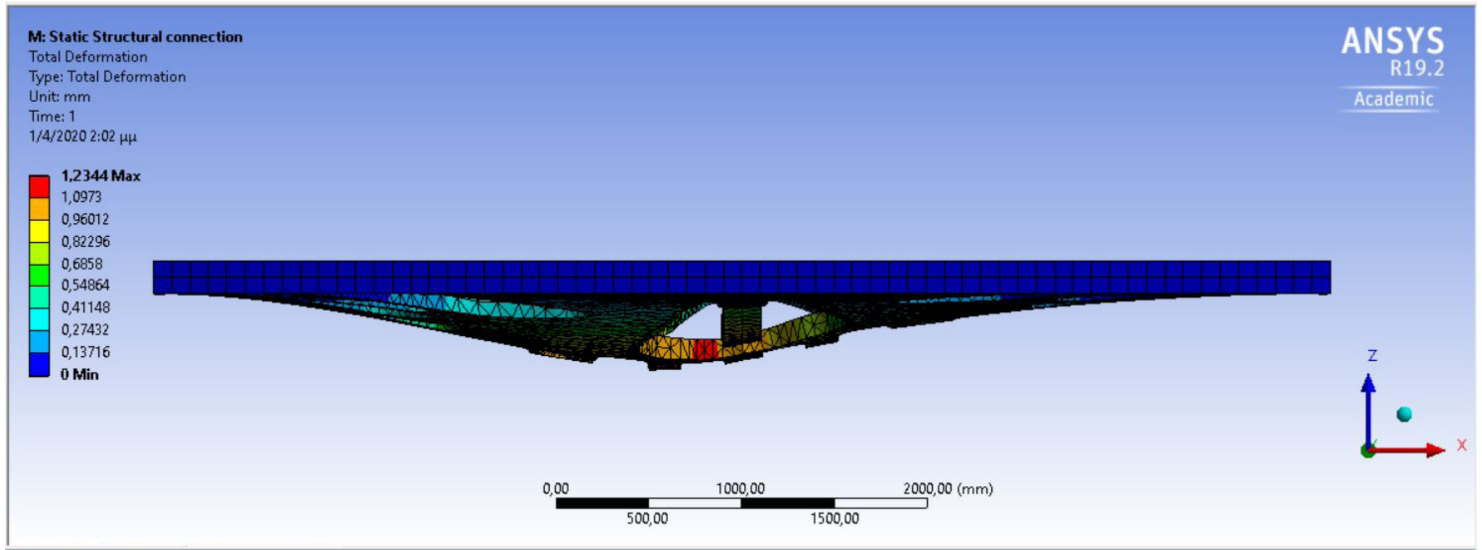

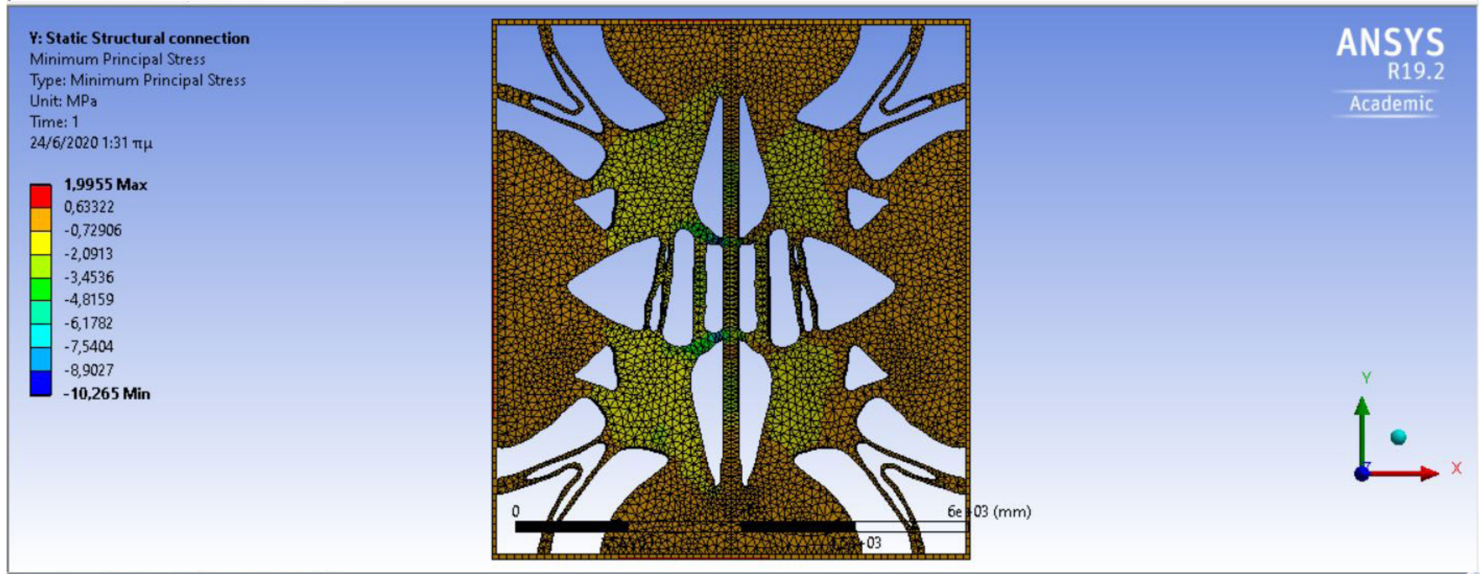

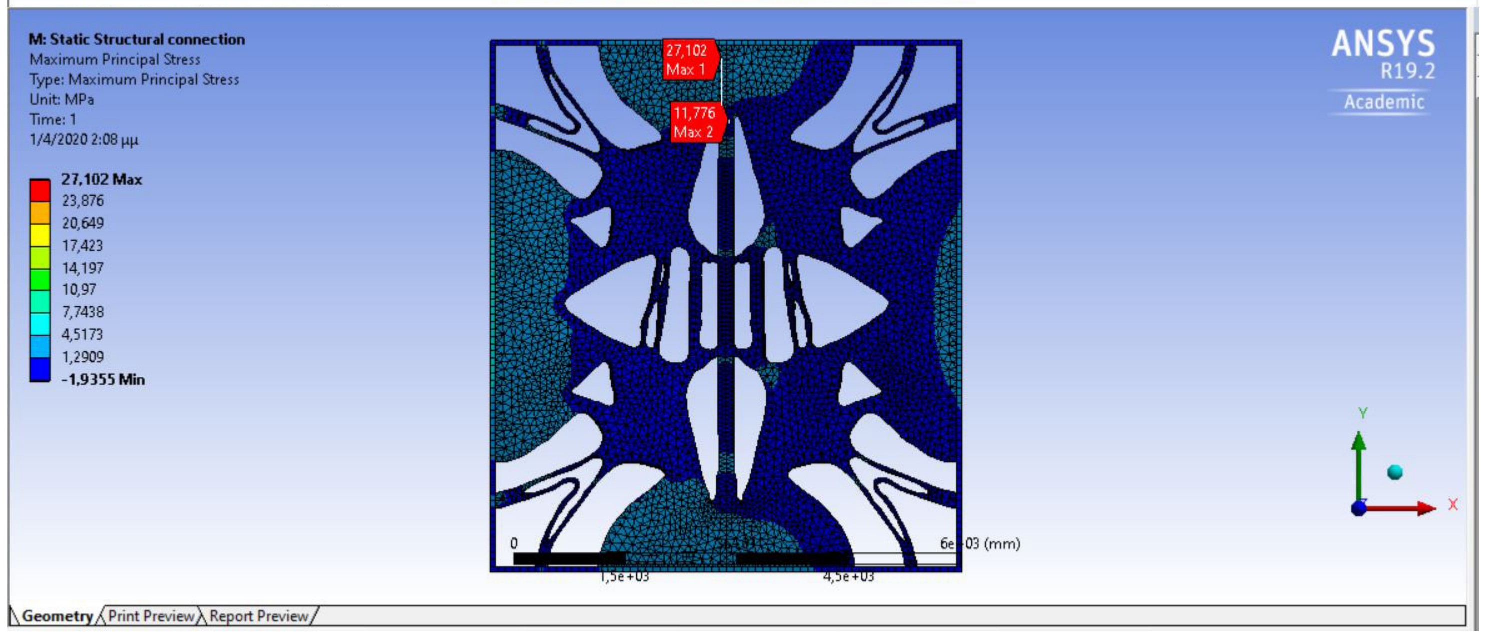

Connection 2 - LC1

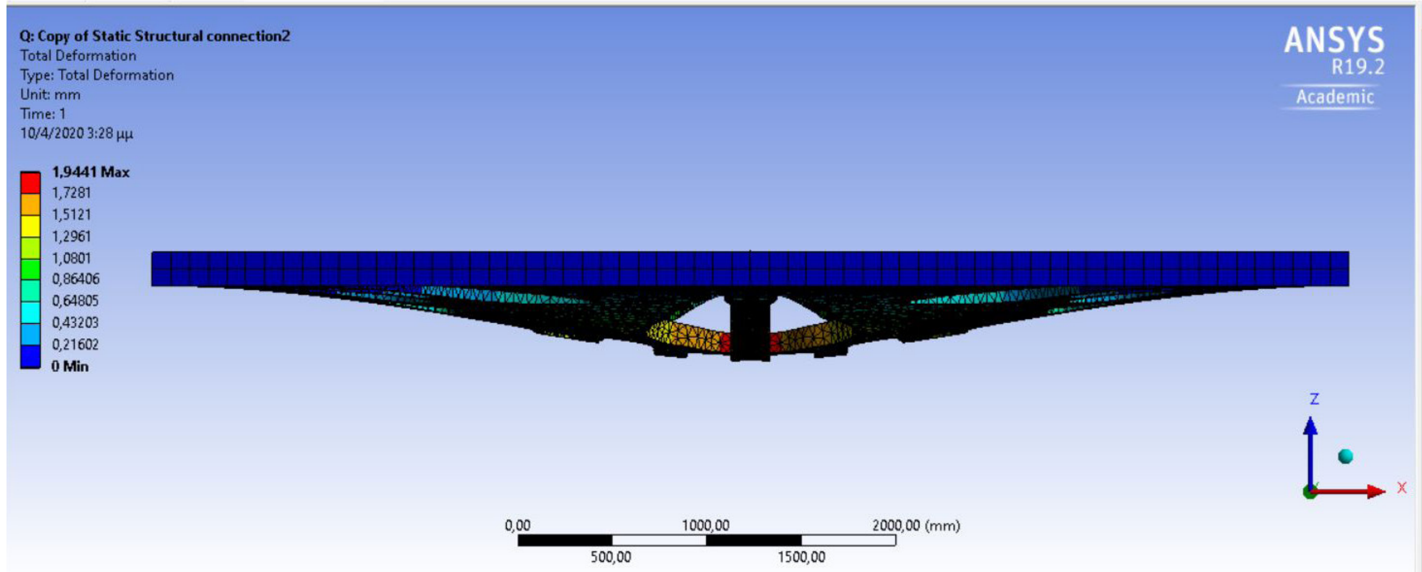

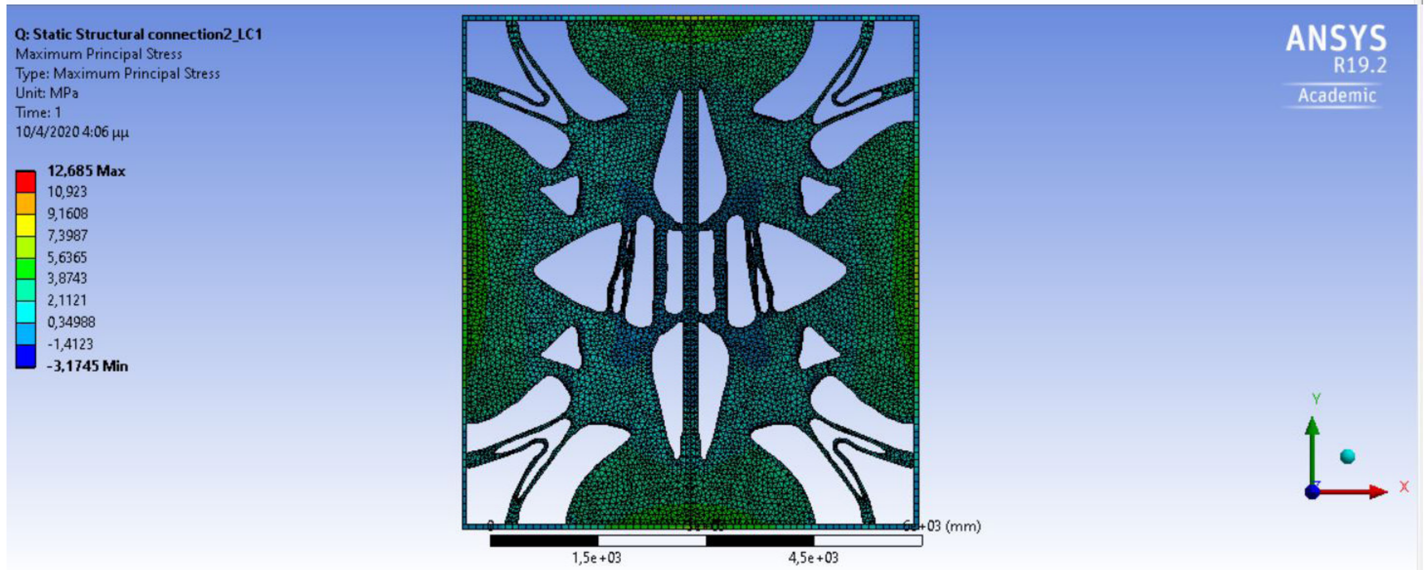

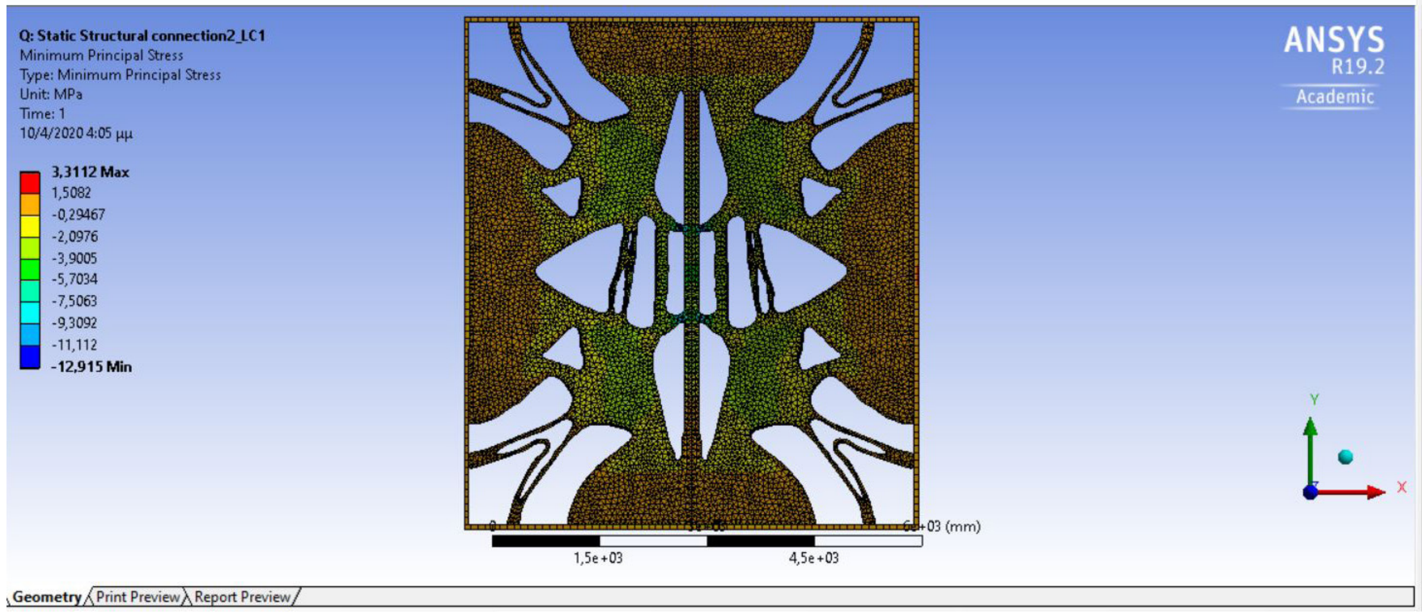

Connection 2 - LC2

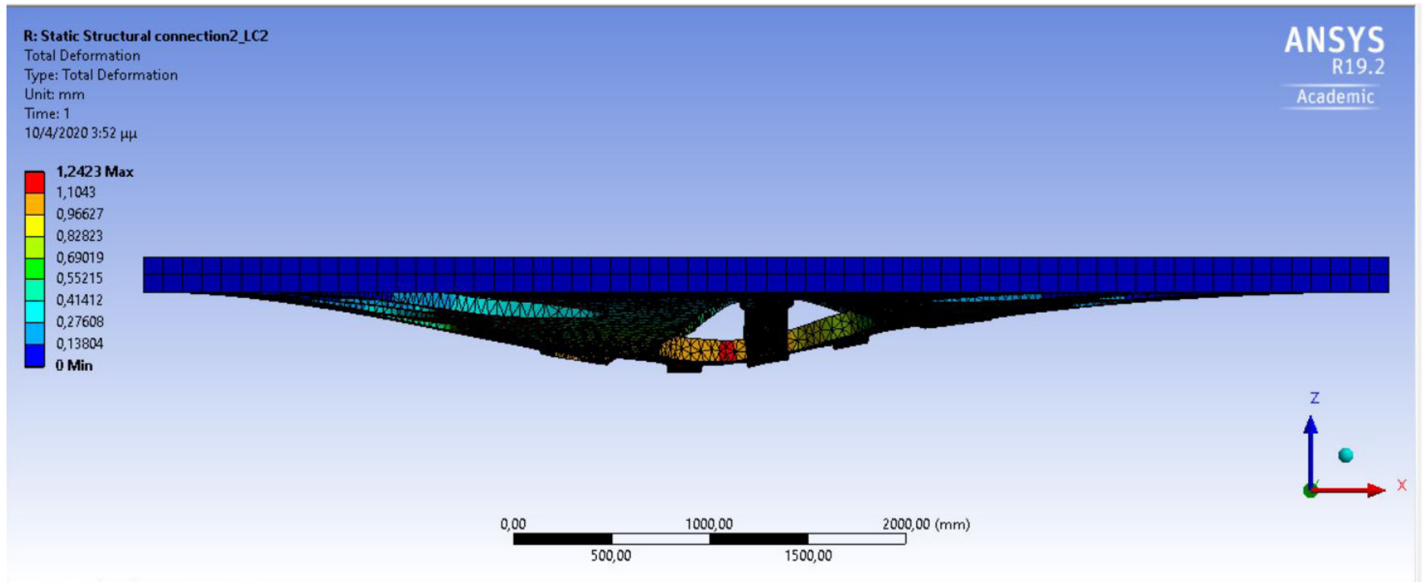

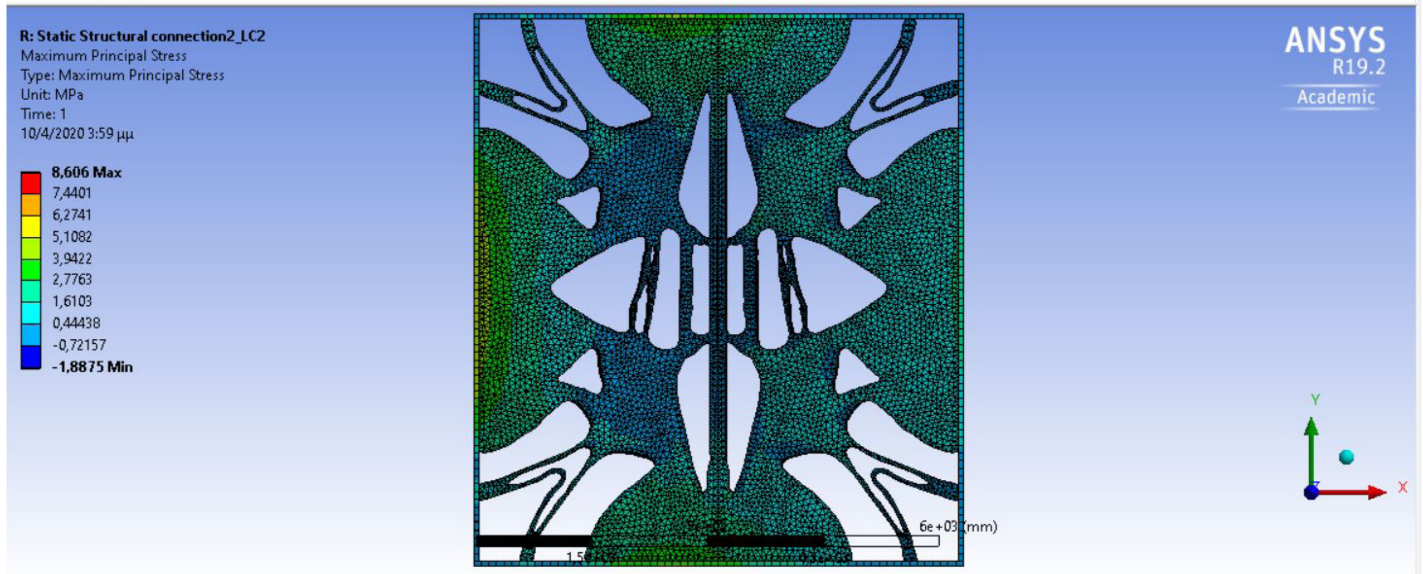

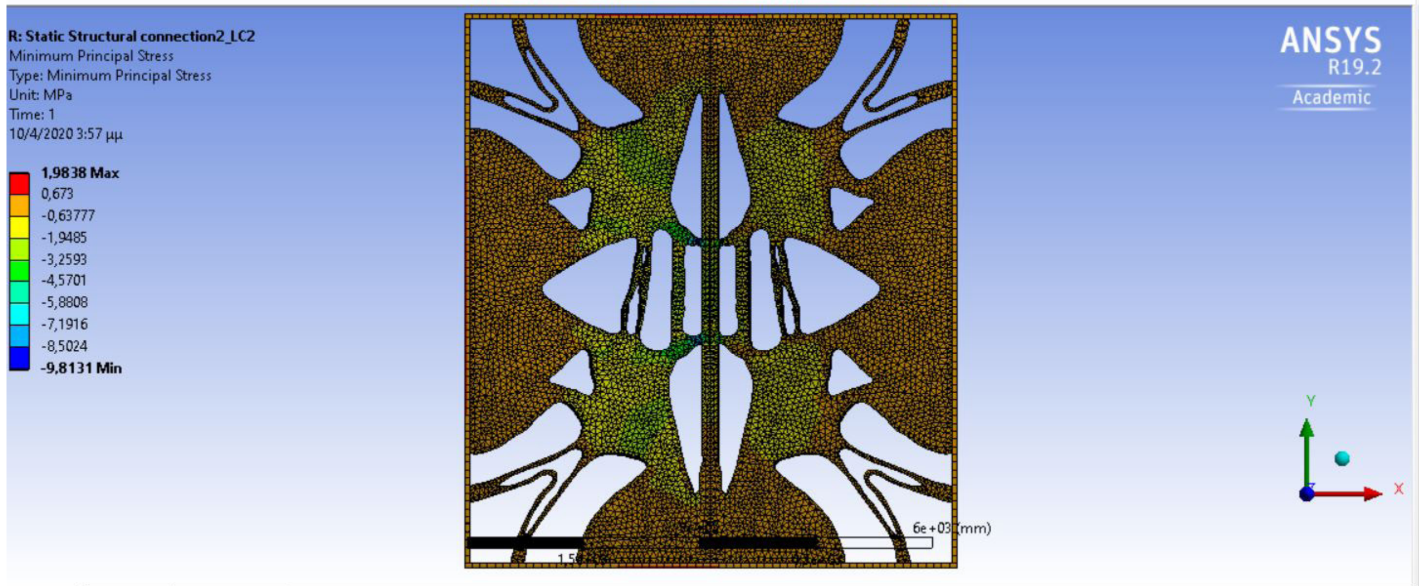

Connection 3 - LC1

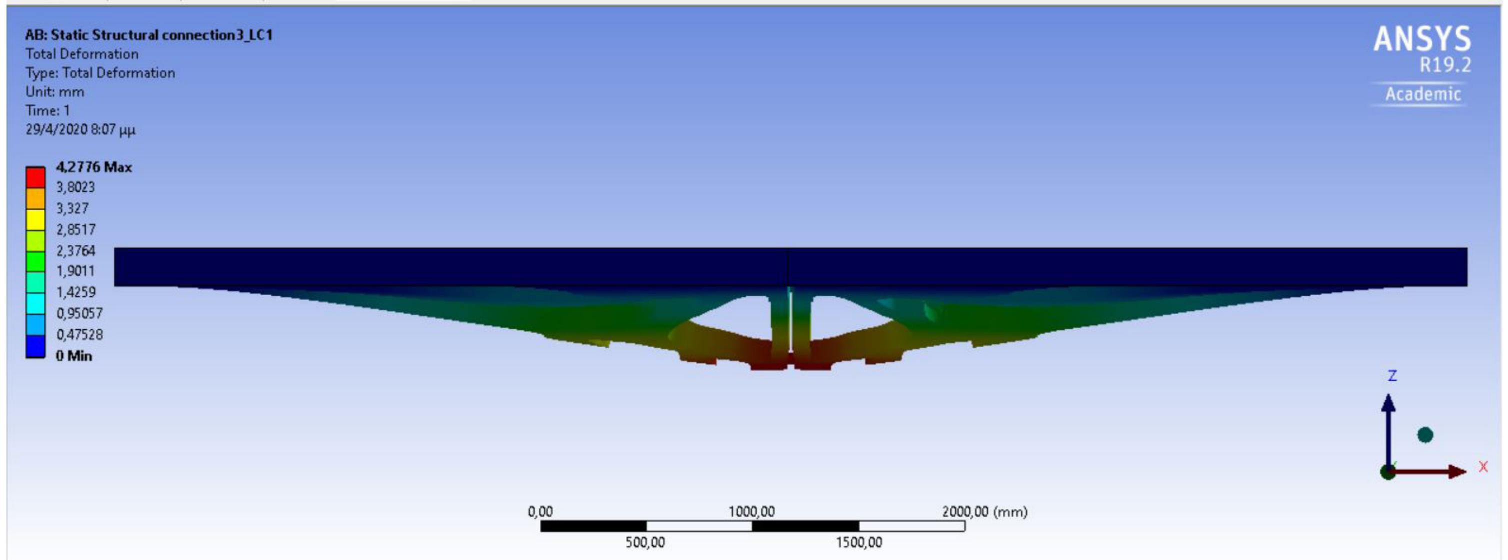

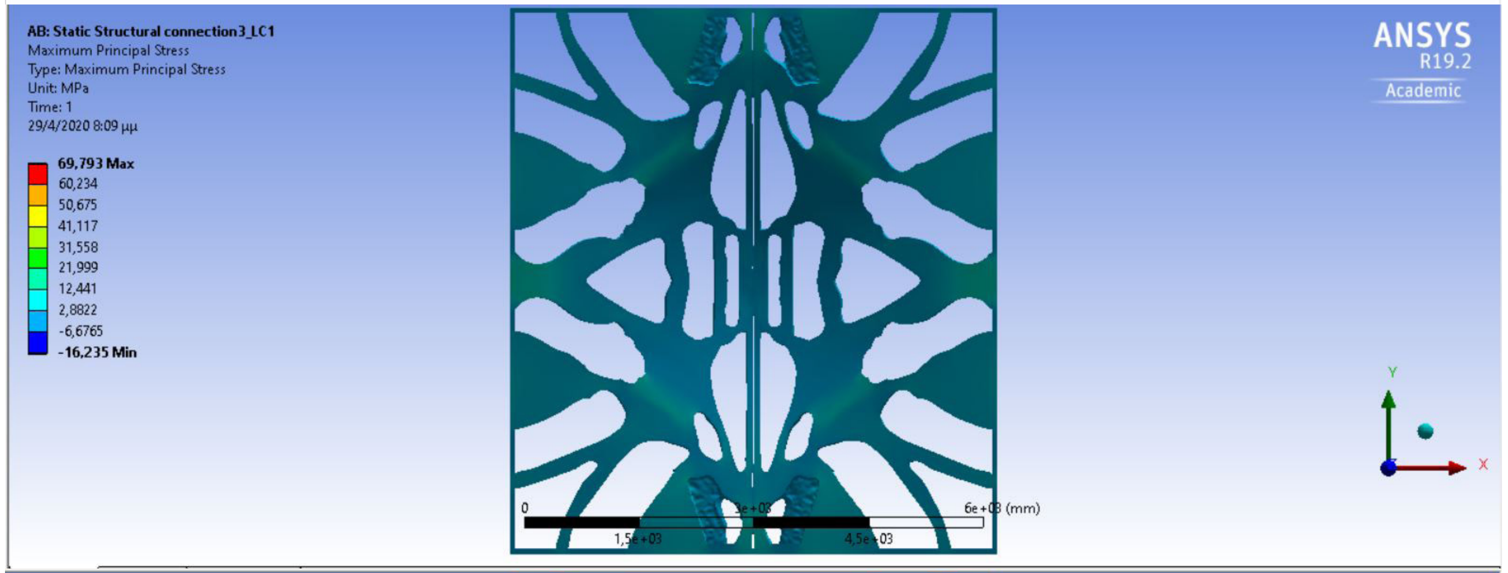

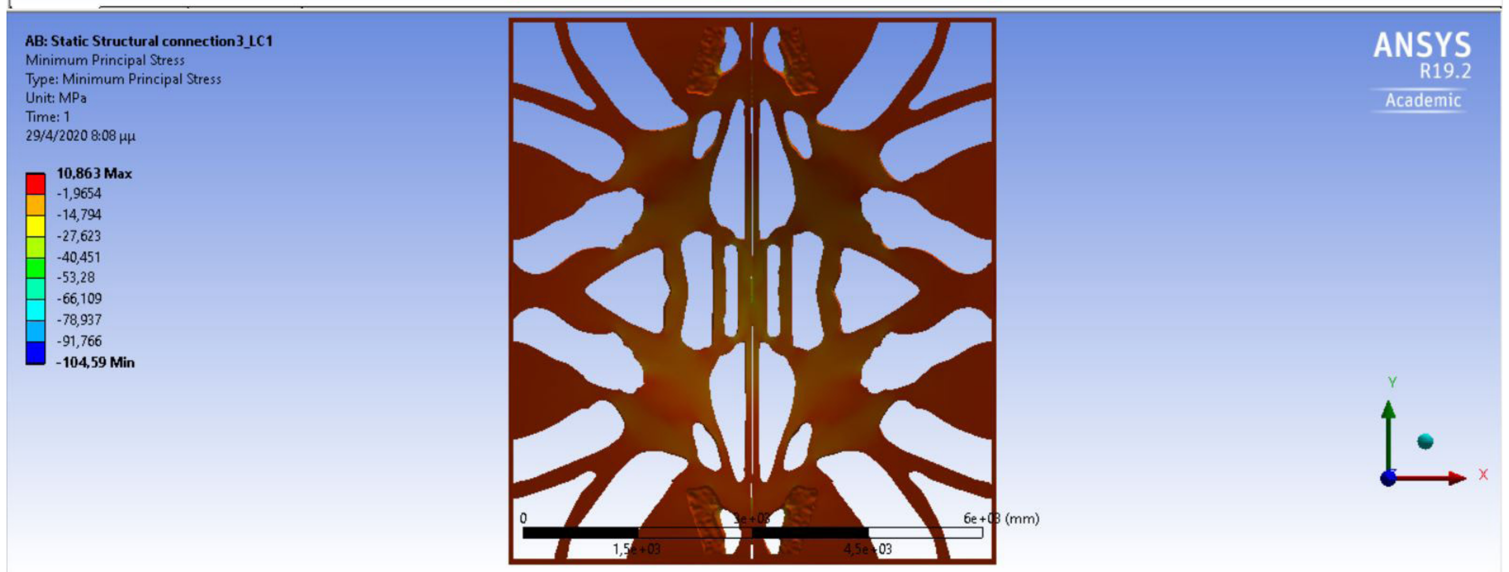

Connection 3 - LC2

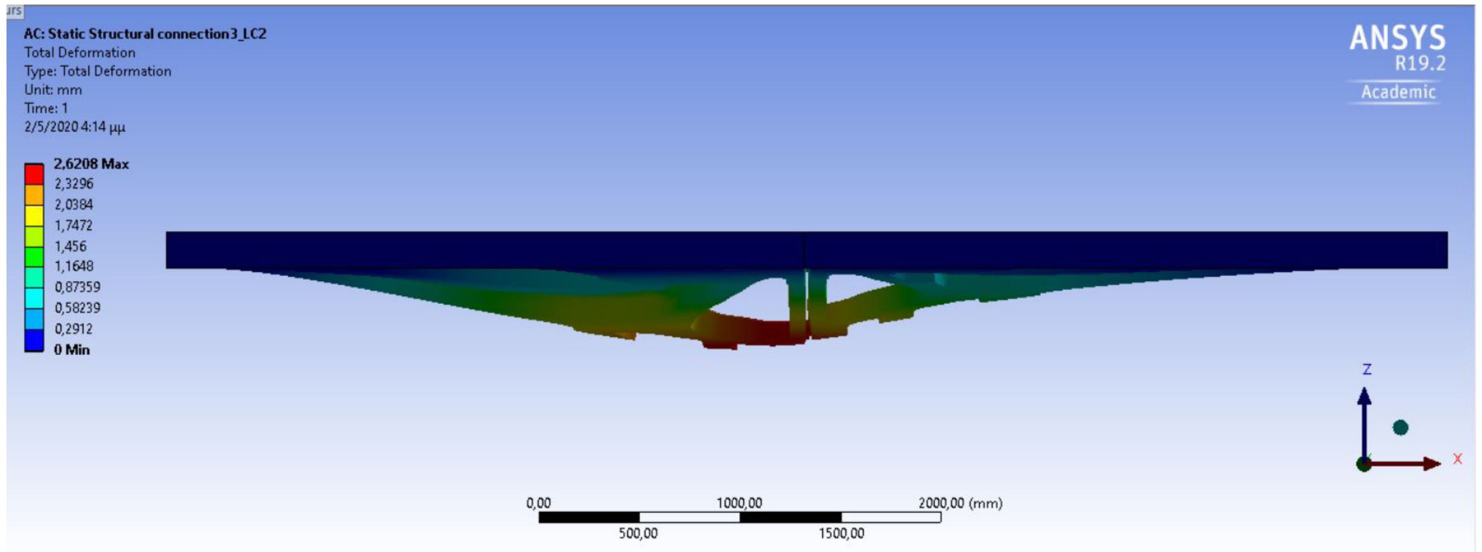

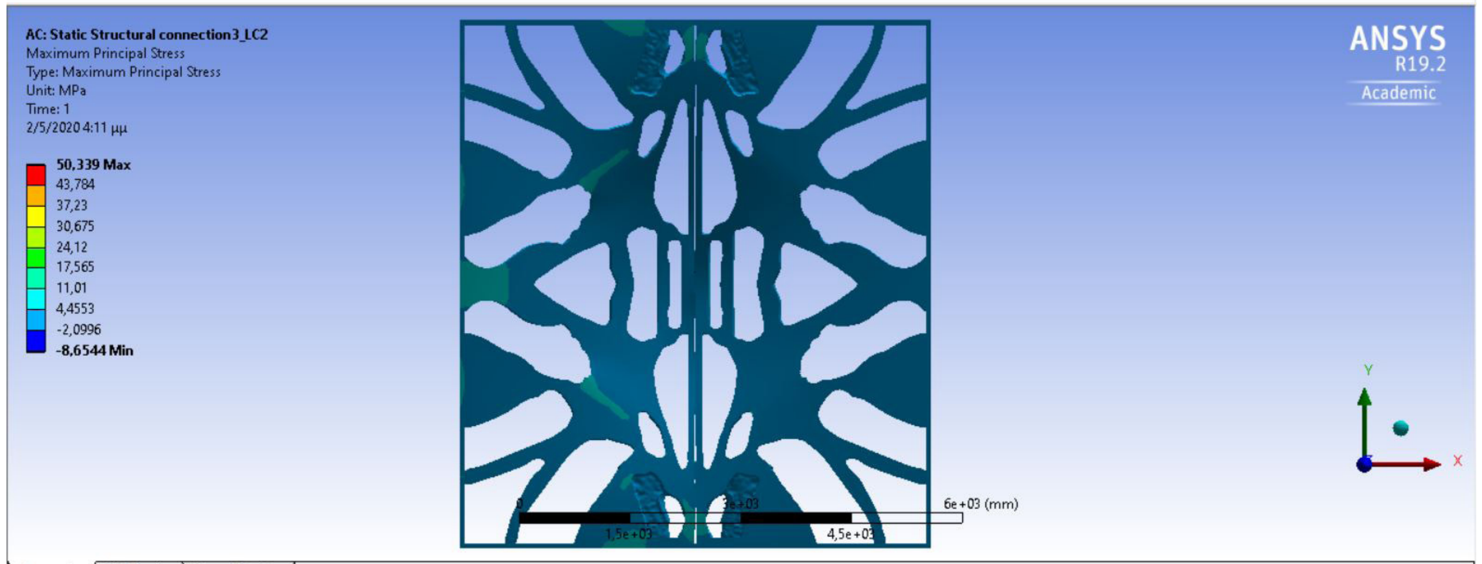

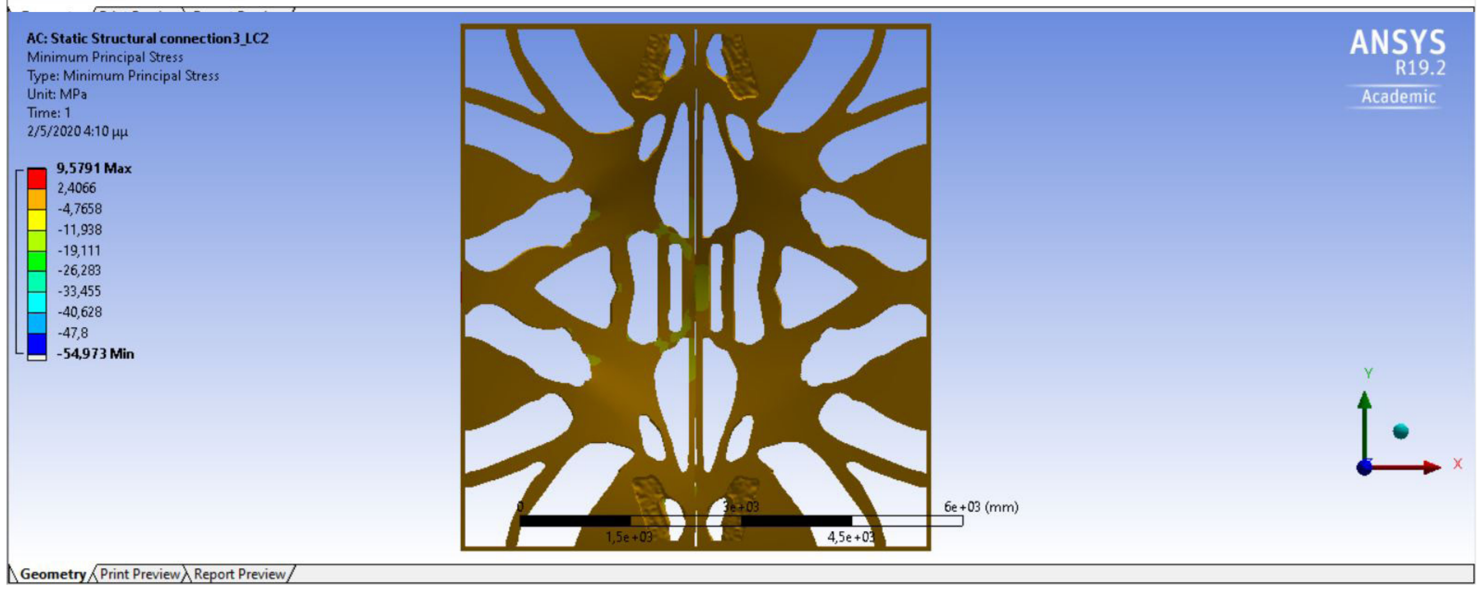

Connection 4 - LC1

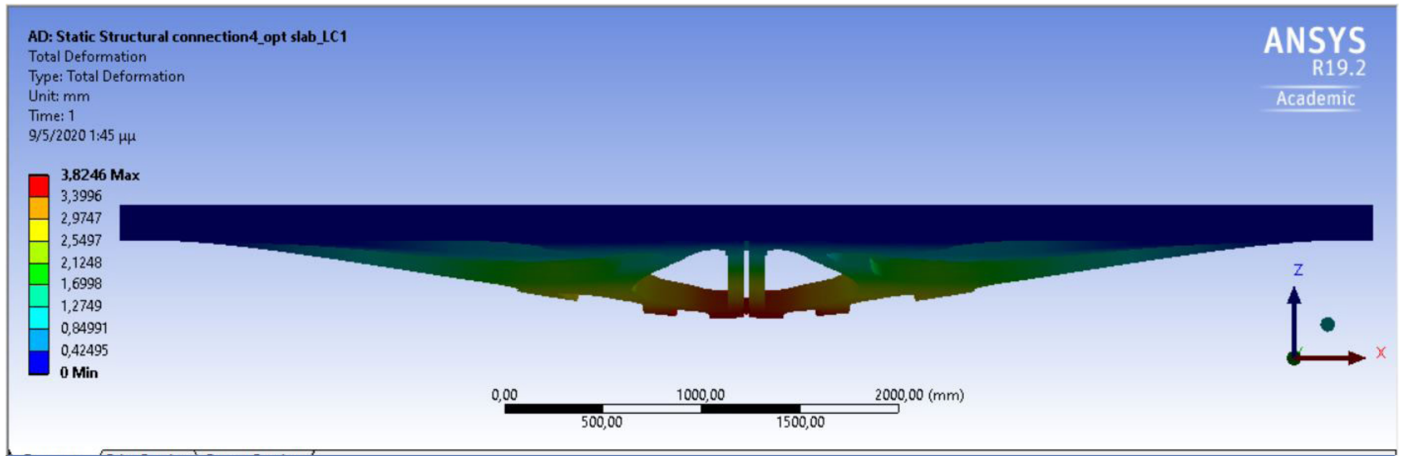

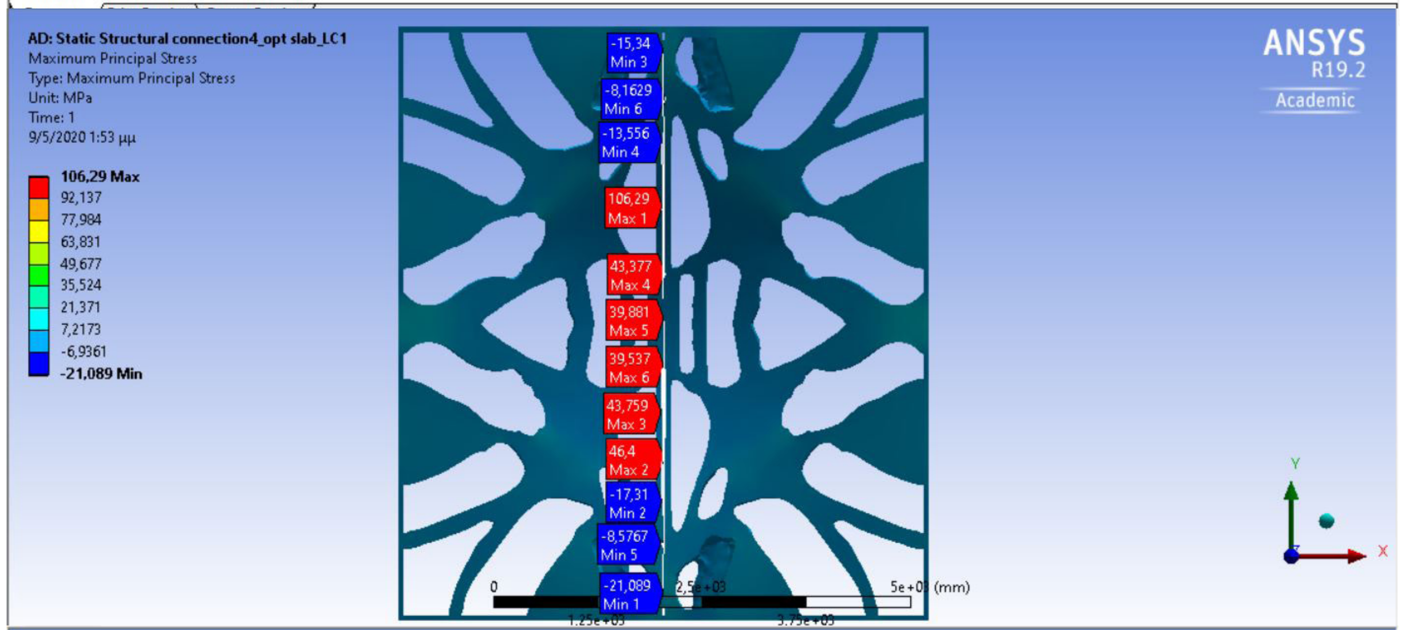

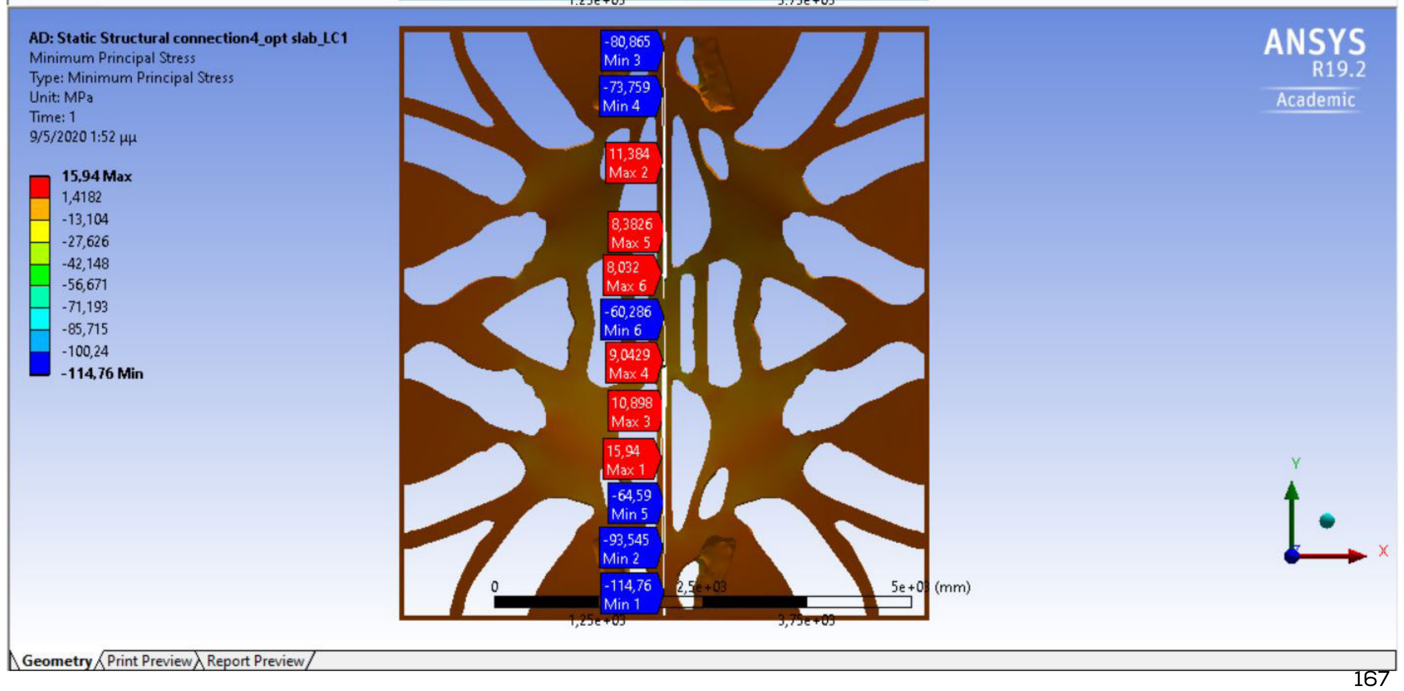

Connection 4 - LC2

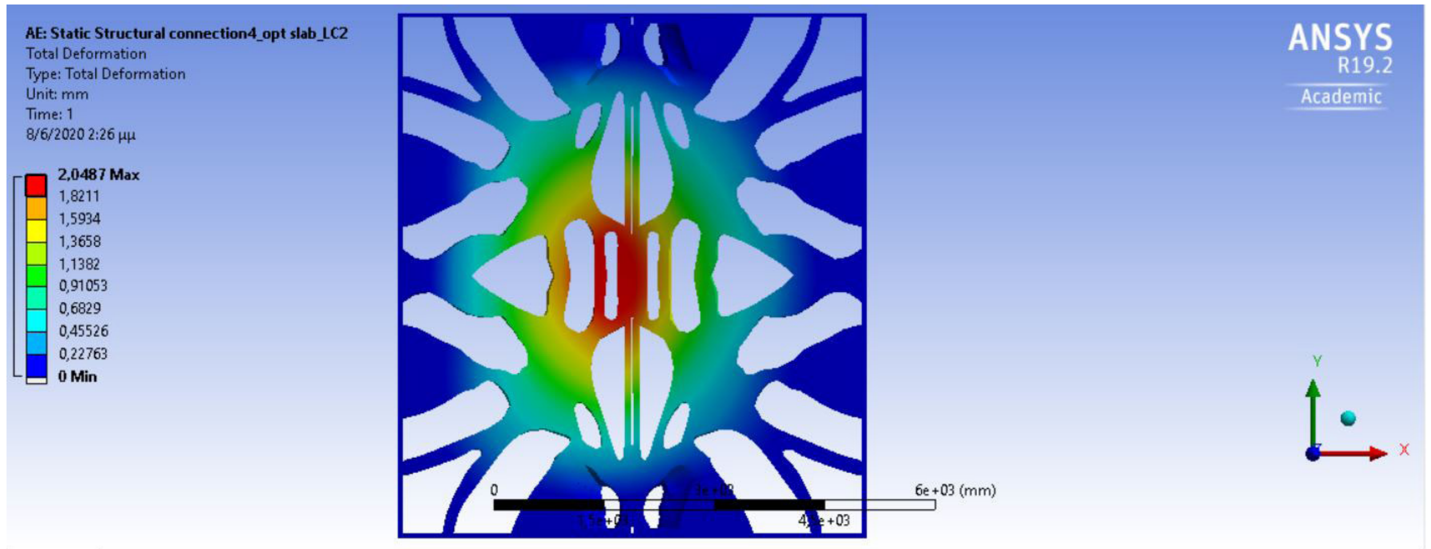

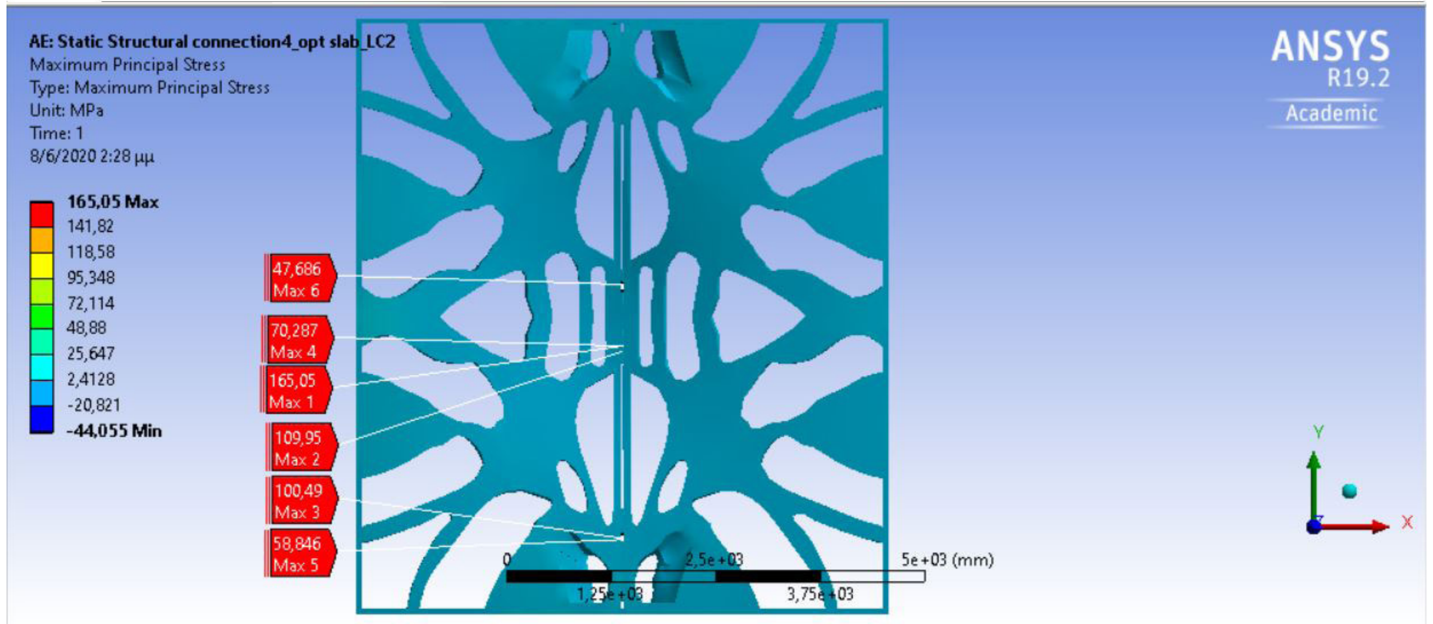

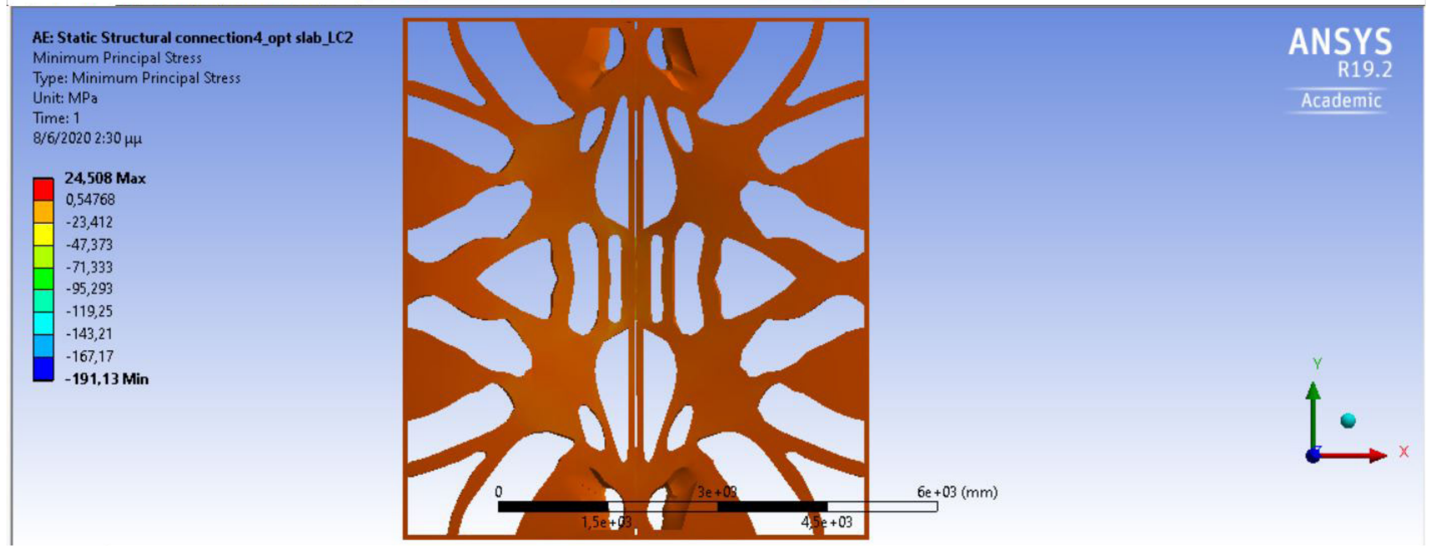

Connection 4 with closed hole - LC1

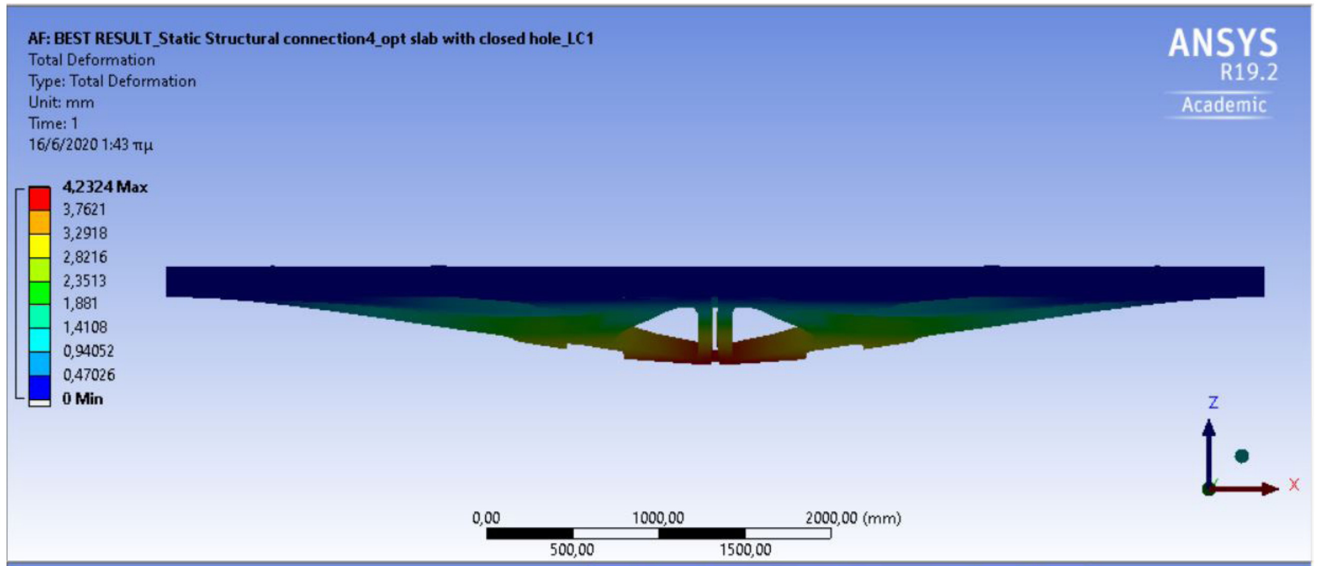

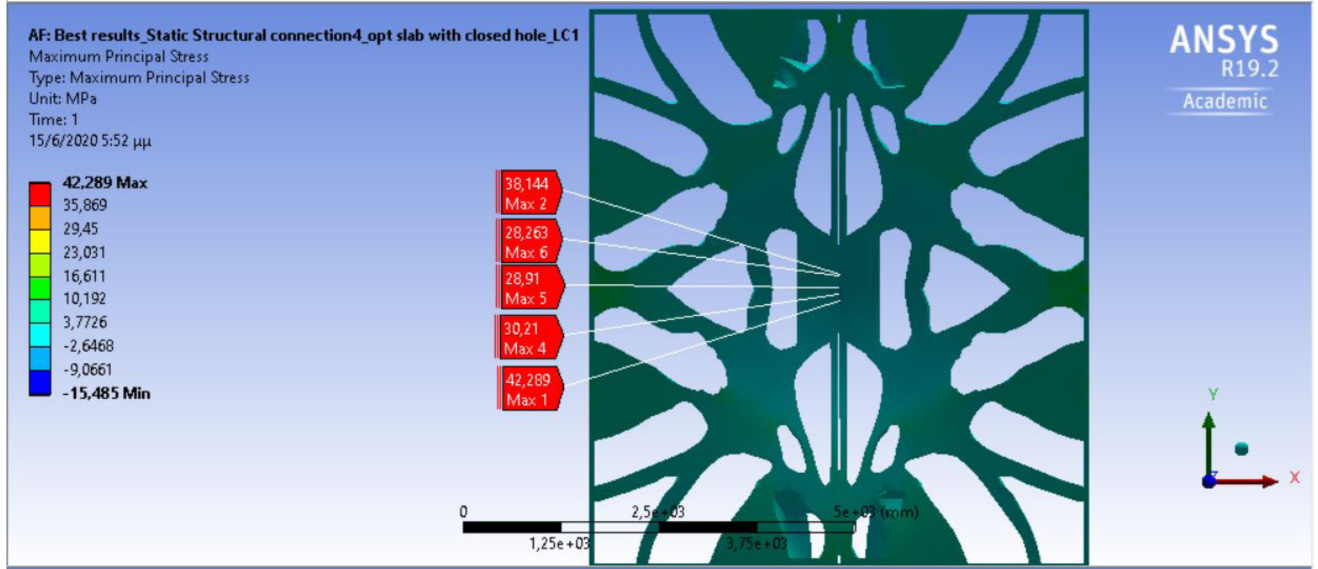

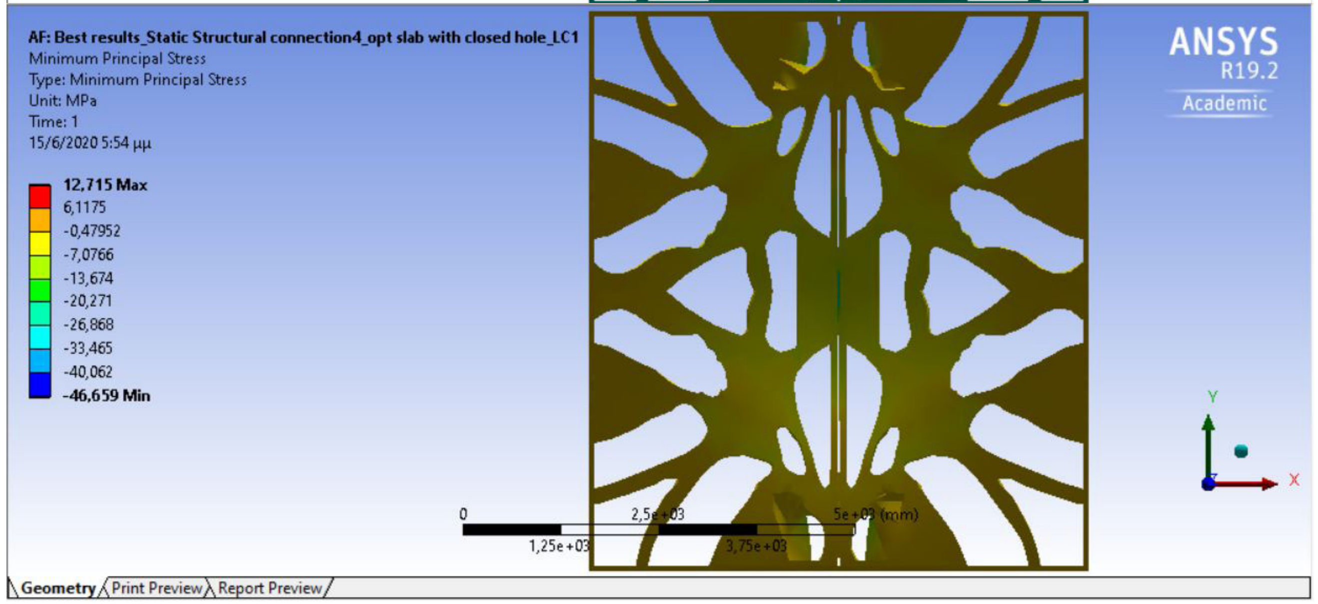

Connection 4 with closed hole - LC2

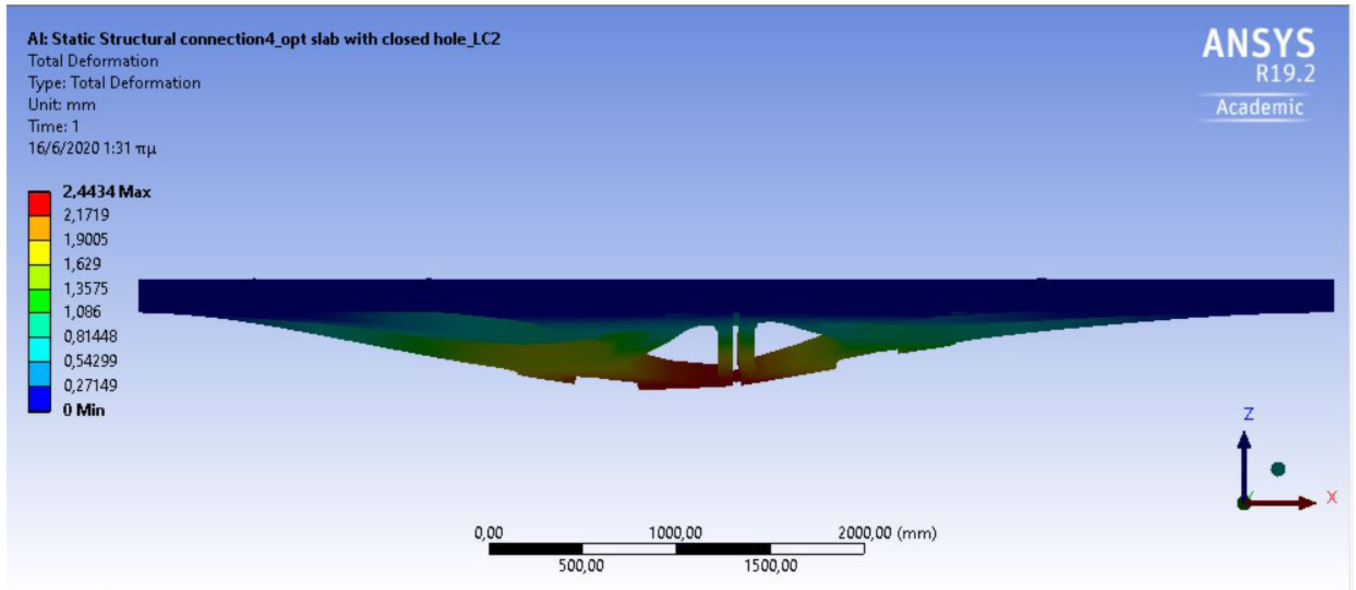

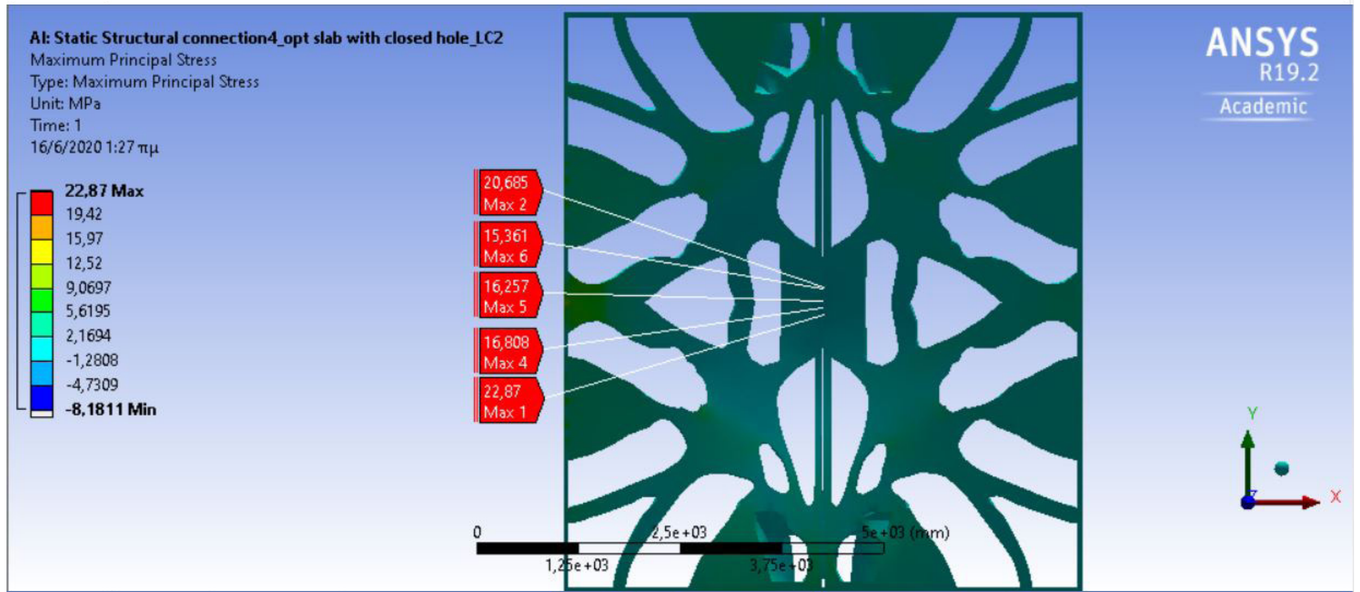

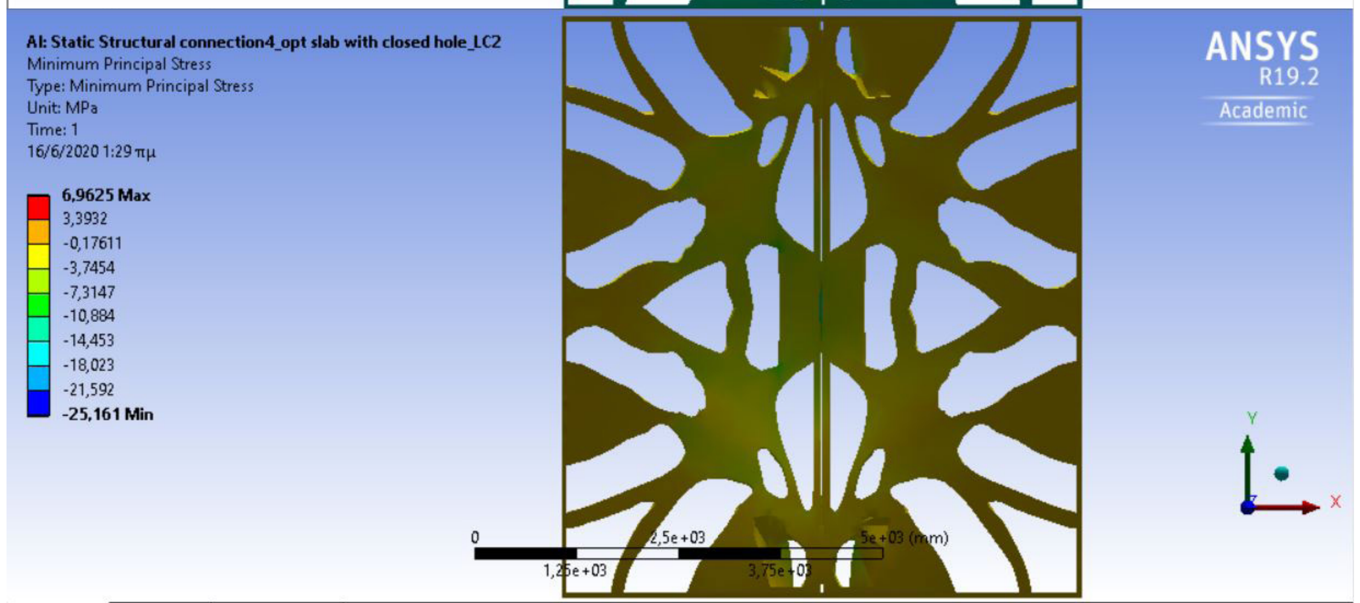

Appendix F
Shell thickness calculations

According to the formula of the hydrostatic pressure:

$$p = \rho * g * h$$

where
p = pressure in liquid (N/m^2)
ρ = density of liquid (kg/m^3)
g = acceleration of gravity (9.81 m/s^2)
h = depth in the fluid where pressure is measured (m)

$$p_{max} = \rho * g * h_{max}$$
$$= 2500 \text{ kg/m}^3 * 9.81 \text{ m/s}^2 * 0.18 \text{ m}$$
$$= 4414.5 \text{ N/m}^2$$

The hydrostatic force acting on a surface of the mould, which is in contact with the glass, can be calculated as:

$$F = p_a A$$
$$= \rho * g * h_a * A$$

where
F_A = thrust force (N)
p_a = average pressure on the surface (P_a)
A = area of submerged surface (m^2)
h_a = average depth (m)

$$F_A = \rho * g * h_a * A_{trapezoid}$$
$$= 2500 \text{ kg/m}^3 * 9.81 \text{ m/s}^2 * 0.09 \text{ m} * (\frac{1.28 + 0.17}{2} 1.15)$$
$$= 1840.3 \text{ N}$$

If we consider the shell wall of the mould as a cantilever beam with a force acting on A:

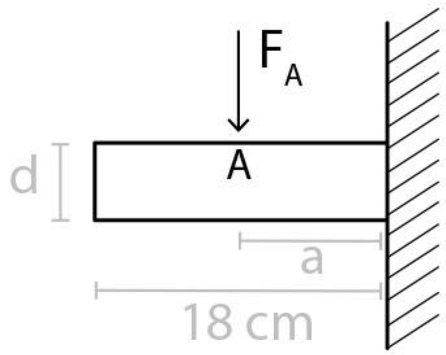

$$M_{max} = F_A * a$$
$$= 1840.3 \text{ N} * 0.09 \text{ m}$$
$$= 165.6 \text{ Nm}$$

From the company Voxeljet, moulds' bending strength range 220-300 N/cm^2 is given. It is known that

$$\boldsymbol{\sigma}_{\mathbf{bend}} = \frac{\mathrm{My}}{\mathrm{I}}$$

$$= \frac{\mathrm{M*d/2}}{\frac{1}{12}\mathrm{bd}^3} = \frac{6*\mathrm{M}}{\mathrm{b*d}^2}$$

By choosing the worse scenario of 220 N/cm^2, the allowable thickness of the shell is:

$$\mathbf{d} = \sqrt{\frac{6*M}{\sigma_{bend} *b}}$$

$$= \sqrt{\frac{6*165.6\ Nm}{220*10^4\frac{N}{m^2}*1.26\ m}}$$

$$= 0.02 \text{ m}$$

$$= 2 \text{ cm}$$